LBNL-41027
UC-000

ERNEST ORLANDO LAWRENCE
BERKELEY NATIONAL LABORATORY

Hydrological and Geochemical Investigations of Selenium Behavior at Kesterson Reservoir

Progress Report
October 1, 1994 through September 30, 1996

Peter T. Zawislanski, Tetsu K. Tokunaga,
Sally M. Benson, H. Scott Mountford, Tobin C. Sears,
Hau Wong, Dorian King, and Joan Oldfather

Earth Sciences Division

October 1997

DISCLAIMER

LBNL-41027
UC-000

HYDROLOGICAL AND GEOCHEMICAL INVESTIGATIONS OF SELENIUM BEHAVIOR AT KESTERSON RESERVOIR

Progress Report

October 1, 1994 through September 30, 1996

Peter T. Zawislanski, Tetsu K. Tokunaga, Sally M. Benson, H. Scott Mountford, Tobin C. Sears, Hau Wong, Dorian King, and Joan Oldfather

Earth Sciences Division
Lawrence Berkeley National Laboratory
University of California
Berkeley, CA 94720

October 1997

This work was supported by the U.S. Bureau of Reclamation, under U.S. Department of Interior Interagency Agreement 9-AA-20-20, through U.S. Department of Energy Contract No. DE-AC03-76SF00098

Table of Contents

List of Figures

List of Tables

Acknowledgments

We thank Mike Delamore and Bill Greer of the U.S. Bureau of Reclamation for their continued support. We also thank the Kesterson Field Office personnel for facilitation of field activities; Nigel Quinn of LBNL for a review of this text; Gamani Jayaweera of UC Davis for assistance in sample collection in Pond 2; Chris Green of CH2MHill for help in Reservoir-wide sample collection; and Sue Chau and Annette Brownfield of LBNL for field assistance. We thank Steve Rodriguez for help in editing the document, and Sherry Seybold for secretarial support.

This work was carried out under U.S. Department of Energy Contract No. DE-AC03-76SF00098.

1 Executive Summary

This report describes research relevant to selenium (Se) speciation, fractionation, physical redistribution, reduction and oxidation, and spatial distribution as related to Kesterson Reservoir. The work was carried out by scientists and engineers from the Earth Sciences Division of the Lawrence Berkeley Laboratory over a two year period from October 1994 to September 1996. Much of the focus of this research was on long-term, Reservoir-wide changes in Se concentrations and distribution; estimation and prediction of the physical extent ephemeral pools; and the quantification and prediction of Se levels in ephemeral pools waters and underlying sediments.

Chapter 2 contains descriptions of field monitoring of soil processes. In **Section 2.1**, elevated Se concentrations observed in groundwater in the northern part of Pond 9 are investigated. The past removal of the original surface soil in the northern Pond 9 area resulted in the enhancement of Se transport into the shallow groundwater in this area. Removal of the most organic-rich surface soil horizon left the remaining profile with a lower capacity to generate and sustain reducing conditions needed to immobilize Se. Furthermore, removal of the lower permeability surface soil left the remaining profile more hydraulically conductive since sands are encountered at fairly shallow depths. These conditions result in Se remaining oxidized down to the 2.00 m depth throughout the year.

Reservoir-wide monitoring of Se is described in **Section 2.2**. Unlike in previous years, the data was carefully analyzed by habitat. The absence of any statistically-significant changes in the total Se measured in the surface soils of the Fill habitat is evidence for a lack of net enrichment of the fill soils with Se which may be moving upward in the profile due to evapotranspirative fluxes. Similarly, year-to-year changes in Se concentrations in the Grassland habitat are minor, with no long-term trends emerging. Open habitat total Se values seem to fluctuate much more than in the other habitats, although the reason for this is not clear. It is possible that the number of samples collected each year within this habitat is not large enough to adequately describe the statistical distribution of soil Se concentrations. With this caveat in mind, there are no consistent trends in total Se concentrations in the Open habitat.

The formation of ephemeral pools, temporal and spatial distributions of Se therein, and predictions of both the physical formation of and Se levels in these pools are examined in **Chapter 3**. In **Section 3.1**, field observations of Se and salt concentrations in ephemeral pools are described. Major features of trends in Kesterson Reservoir ephemeral pool Se concentrations have been identified. Initial pool Se concentrations can be extremely high (100's to 1,000's

ppb). The extremely high Se concentrations diminish quickly. However, pools typically maintain lower Se concentrations over long periods of time which are usually still significantly above surface water quality goals. A model for the prediction of ephemeral pool formation is presented in **Section 3.2**. It is shown that the timing of major rainfall events during the wet season is the primary determinant of the formation and duration of large-scale ponding. Ponding is more likely following early rains, due to the relatively lower potential evaporation rates. The formation of ephemeral pools in local depressions, however, cannot be predicted using this model, as it is dependent on local topography, soil texture, and depth of the water table. The results of a laboratory microcosm experiments on Se transfer between ephemeral pool waters and underlying sediments are presented in **Section 3.3**. Volatile losses of Se were found to be of secondary importance, while 80% to 95% of the initial pool Se inventory was transferred into the sediments over the course of approximately 24 days of ponding.

Results of soil and soil-water monitoring in the Pond 2 Microbial Volatilization Pilot-Scale plot are presented in **Chapter 4**. By integrating Se mass over a depth of 0.60 m, the influence of Se leaching out of the soil profile was minimized, though it is clear that some Se transport in solution occurs below that depth. Se data collected over a period of 7 years shows the effects of rainfall-infiltration-induced fluctuations in near-surface concentrations, but an absence of net Se losses, suggesting that the effect of microbial volatilization on the Se inventory in Pond 2 is minor. This conclusion agrees with the results of direct Se emission measurements.

The ongoing analytical quality control program is described in **Chapter 5**. This includes the methods for monitoring the performance of both the analytical instrument and the analyst, through the use of blanks, standards, spikes, and duplicates. Selenium standard statistics are presented.

In addition to this report, the following related articles have been either published or submitted for publication over the past two years:

- Tokunaga, T.K., I.J. Pickering, and G.E. Brown, Jr. 1996. X-ray absorption spectroscopy studies of selenium transformations in ponded sediments. *Soil Sci. Soc. Am. J.* 60:785-790.
- Zawislanski, P.T. and M. Zavarin. 1996. Nature and rates of selenium transformations: A laboratory study of Kesterson Reservoir soils. *Soil Sci. Soc. Am. J.* 60:791-800.
- Zawislanski, P.T., and A.E. McGrath, in press. Selenium cycling in estuarine wetlands: Overview and new results from the San Francisco Bay, *in*, Environmental Chemistry of Selenium, W.T. Frankenberger and R.A. Engberg, editors, Marcel Dekker, New York.
- Benson, S.M., in press. Influence of nitrate on the mobility and reduction kinetics of selenium in groundwater systems, *in*, Environmental Chemistry of Selenium, W.T. Frankenberger and R.A. Engberg, editors, Marcel Dekker, New York.

1.1 Recommendations

Given the results of field and laboratory research, a number of recommendations regarding the future management and further investigations of Kesterson Reservoir are presented below.

- Given that the results of Reservoir-wide monitoring of soil Se concentrations do not show year-to-year changes, it is recommended that such sampling should occur on a two-year interval.

- Areas underlain by high-conductivity soils, in which groundwater has been shown to contain elevated Se concentrations, such as site P9L and certain areas in the northern part of Pond 2, should be filled with lower conductivity soil, or "capped." The existing monitoring equipment should be maintained to allow for future monitoring of the impact of the filling operation.

- Wildlife impacts of persistent ephemeral pools at Kesterson Reservoir need to be identified, in order to evaluate the need for developing site management strategies during high rainfall years.

- If wildlife impacts of persistent ephemeral pools warrant changes in site management, alternative strategies need to be identified, evaluated, and implemented.

- The remaining open areas which are susceptible to ponding by water table rise should be filled in. These areas are primarily former soil profile monitoring and research sites. If possible, monitoring equipment at these sites should be maintained for future use.

- Long-term monitoring of the Se inventory at site P2VS has shown that microbial volatilization of Se from soils is not very effective under passive or near-passive management. Although future monitoring of this site may be useful in that it will document changes in soluble Se concentrations, it is not likely that continued soil monitoring of the kind performed to date will shed any further light on rates of and variables affecting microbial volatilization of Se in the field setting. Therefore, the discontinuation of this experiment is recommended. However, given the high degree of characterization of this site, it is recommended that at least some portion of it be preserved for potential future tests of emerging remediation technologies.

2 Vadose Zone Monitoring

The following sections describe efforts in soil monitoring at previously established field sites. Although in the past monitoring results from sites in Pond 5, Pond 8, and Pond 11 were reported on, this report focuses on findings from Pond 9 and Reservoir-wide monitoring of near-surface soils and soil water. General layout of monitoring sites is shown in Fig. 2.0.1.

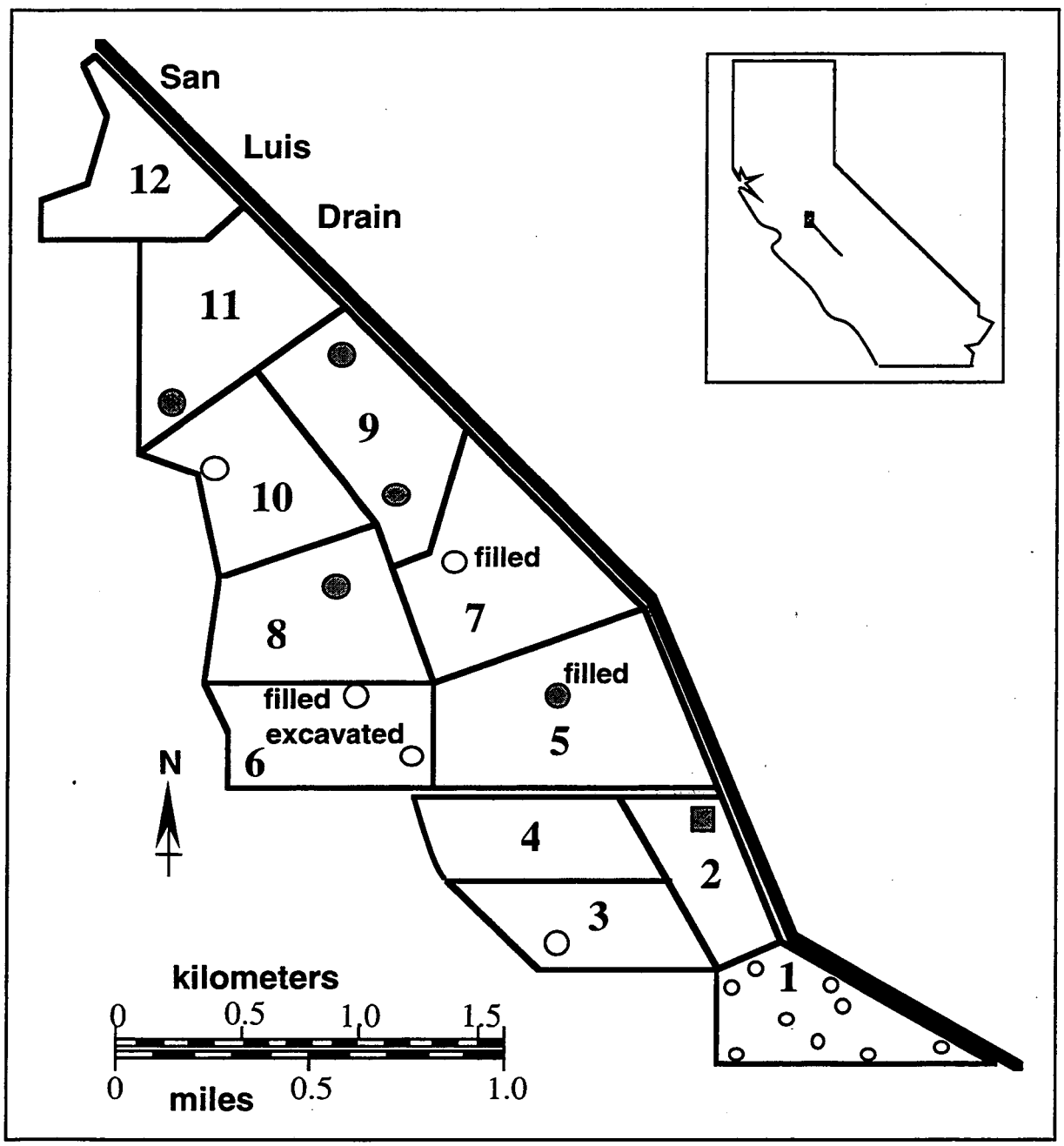

Figure 2.0.1. Distribution of monitoring sites at Kesterson Reservoir.

2.1 Deeper Soil Pore Waters from the Northern Pond 9 Monitoring Area

Tetsu Tokunaga
Earth Sciences Division
Lawrence Berkeley National Laboratory

Groundwater quality monitoring wells continue to provide water samples with low Se concentrations (< 5 ppb) from all sites immediately adjacent to Kesterson Reservoir (USBR, 1996). Although most monitoring wells within Kesterson Reservoir also have yielded groundwater with low Se concentration, wells in three interior areas have shown elevated levels of Se. These areas are located in the northern portion of Pond 9, at the intersection of Ponds 2, 3, and 4, and at the southeast corner of Pond 1. It is likely that these areas of shallow groundwater contamination result from rapid leaching of seleniferous waters through higher permeability soil profiles since the first 2 of these 3 areas coincide with regions mapped as having only a thin surficial layer of "clayey material" (USBR, 1986). A deep soil profile monitoring site in the northern section of Pond 9 was installed in late 1993, motivated by the importance of understanding Se transport through deep soil profiles. The initial data on soluble Se and salinity distributions along a 3.25 m deep profile were reported previously (Zawislanski et al., 1995). An update to that initial report is provided in this section.

2.1.1 Site Description

Soil profile monitoring in a former playa environment in the northern portion of Pond 9 began in February of 1987, about one year after this area last received drainage waters. Locations of LBL soil profile monitoring sites and USBR shallow groundwater monitoring wells (DH9 series) in this area are shown in Fig. 2.1.1. The northern Pond 9 study area has recently been supplemented with additional instrumentation to provide information on deeper soil profile and shallow groundwater Se concentrations. A new monitoring site, P9L, provides soil water and shallow groundwater samples at approximately 0.50 m depth intervals down to 3.25 m below the soil surface (Figure 2.1.2). It is located directly between the DH9-5 and DH9-8 wells, which have yielded the highest shallow groundwater Se concentrations from the northern Pond 9 area. The soil is mapped as a Turlock sandy loam (Albic Natraqualf) by the Soil Conservation Service (Nazar, 1990). Particle-size analysis for this monitoring site showed that surface horizons consist of loam textures (primarily loam, with sandy loam to clay loam) down to the 1.30 m depth, below which sands (loamy sands to sands) were encountered (Fig. 2.1.2). Site P9L contains two sets of soil water samplers and tensiometers, denoted P9L1 and P9L2. The primary set of pore water data at this site comes from the P9L2 set of samplers, which consists of soil water samplers at depths of 0.50, 1.00, 1.50, and 2.00 m, and drive point shallow groundwater samplers at 2.25,

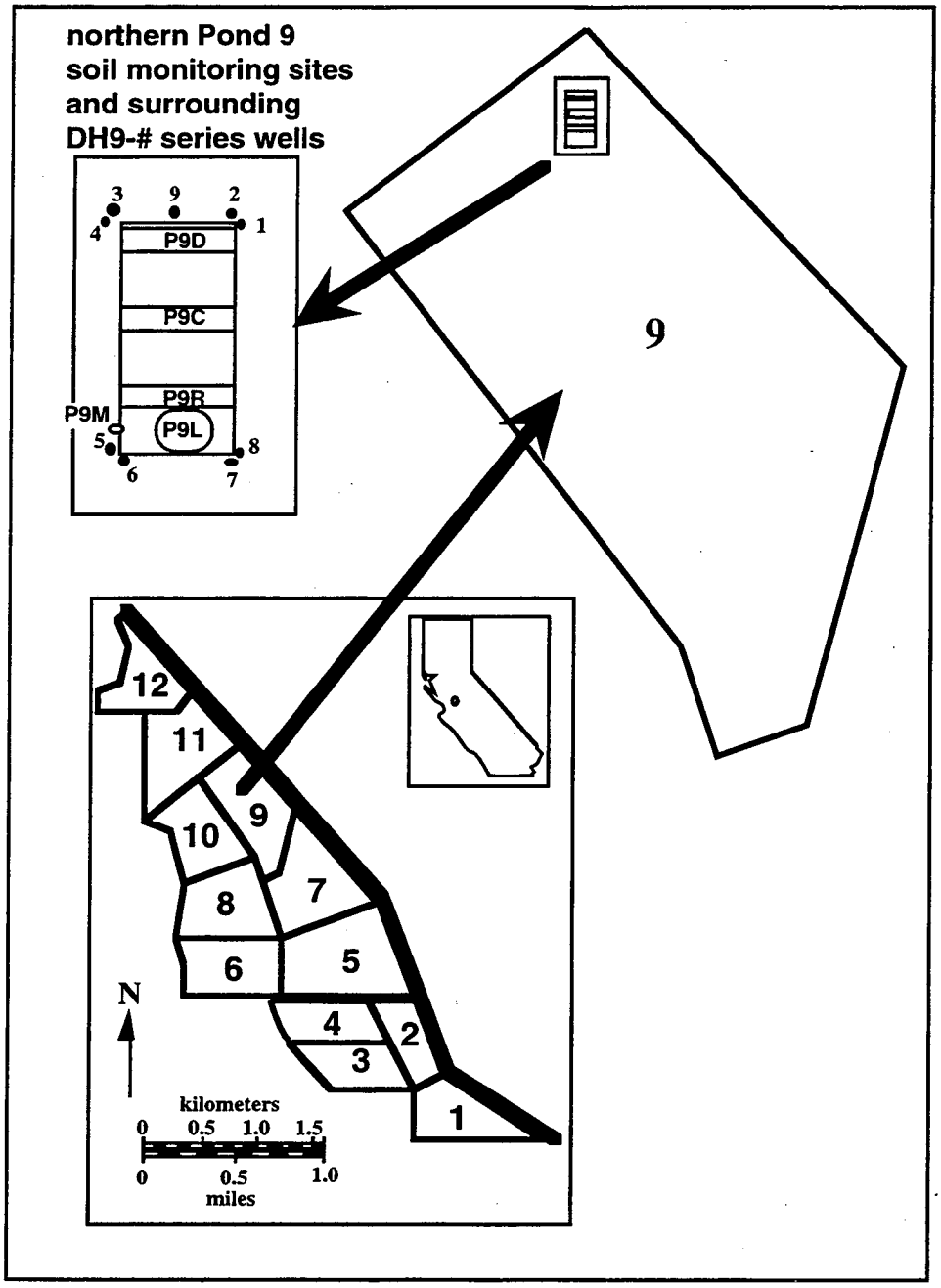

Figure 2.1.1. Locations of northern Pond 9 monitoring sites and shallow monitoring wells.

2.75, and 3.25 m. Locations of the soil water samplers and shallowest drive point sampler are shown in the context of the soil particle-size profile in Fig. 2.1.2. Tensiometers are located at depths of 0.25, 0.75, 1.25, and 1.75 m, installed within the same auger hole as the soil water samplers. Hydraulic potential profiles were obtained from both tensiometers and soil water samplers (Tokunaga, 1992). A second set of soil water samplers and tensiometers were installed in location P9L1, at the same depths as noted for P9L2. The two nested sets of samplers and

tensiometers are laterally separated by a distance of 1.0 m. A neutron probe access tube is located 1.0 m from each of the sampler-tensiometer nests.

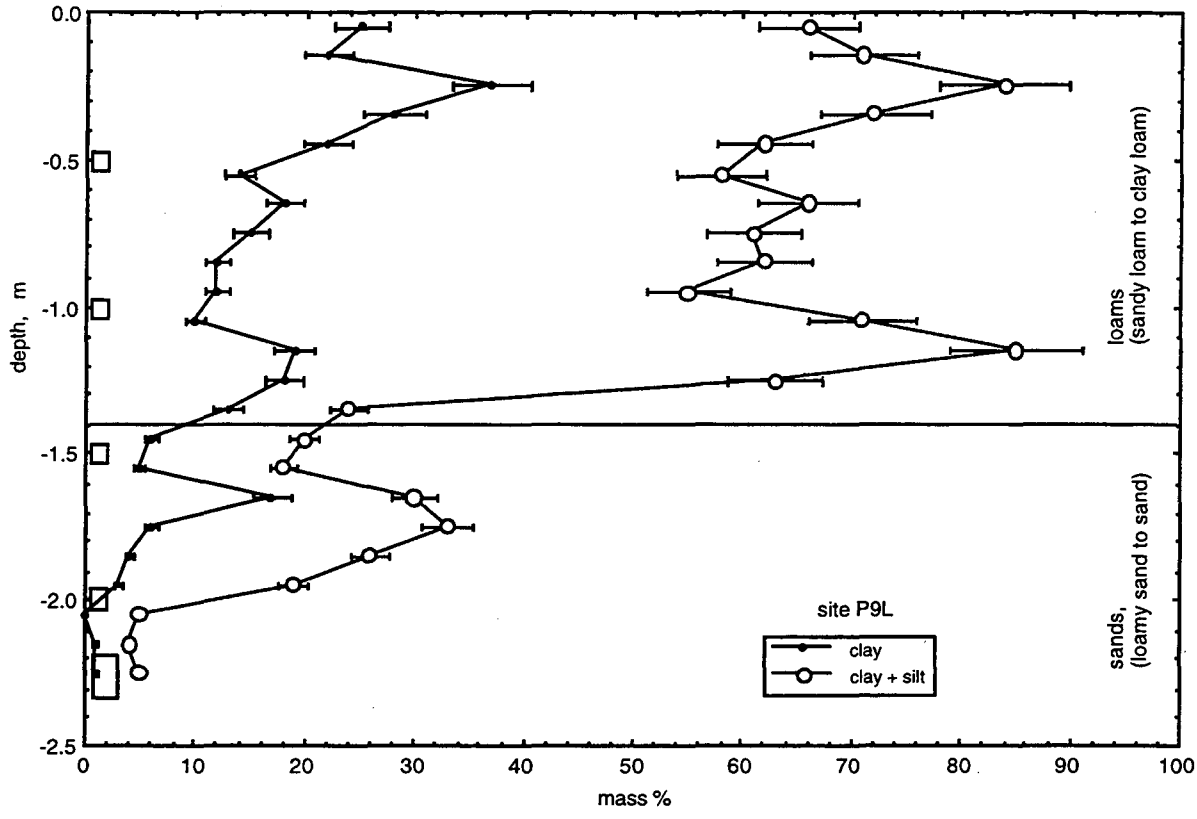

Figure 2.1.2. Soil particle-size profiles for site P9L, based on the USDA definitions (clay ≤2 μm, 2 μm < silt < 50 μm, and 50 μm < sand ≤2 mm). Installation depths for soil water samplers and the shallowest drive-point sampler are shown along the left axis.

2.1.2 Soluble Selenium Profiles and Time Trends at site P9L

Soluble Se profiles are commonly most stable in the late summer to early fall months, since this interval is usually free of rainfall and rapid water table rise, and since several months have elapsed since the last major rainfall events from the previous wet season. Therefore, annual comparisons of soluble Se profiles during these months permit identification of long-term changes. The general shapes of the soluble Se profiles during late summer and early fall months are similar, with maximum solution Se concentrations located around the 1.50 m depth (Fig. 2.1.3a). Maximum solution Se concentrations in the other northern Pond 9 monitoring sites were found at shallower depths shortly after termination of drain water disposal, and drifted downwards in following years (LBL, 1987; Benson et al., 1992). The location of the soluble Se maxima around the 1.50 m depth in late summer-fall months has now persisted for 3 years. The relatively long-term stability of the soluble Se maxima in this depth region is reasonable for

several reasons. Leaching of soluble Se from near-surface soils downwards is limited by reducing conditions encountered deeper in profiles, and Se(VI) can be rapidly reduced and removed from solution in such environments (White et al., 1991). Strongly diffusion-limited supply of oxygen is expected below the water table, which at site P9L always remains within 2.30 m of the surface. The 1.50 m depth is both sufficiently sandy (Fig. 2.1.2) and above the water table during much of the year so that well-aerated conditions are characteristic of this depth. These redox features of site P9L are qualitatively reflected in profiles of the [Se(IV)]:[total soluble Se] ratio shown in Fig. 2B. Note that the relative concentration of the intermediate oxidation state Se(IV) becomes important below the 2.00 m depth, indicating that Se(VI) becomes reduced as it is leached downwards from the usually more aerated surface soils. Note also that the [Se(IV)]:[total soluble Se] ratio is lowest at the 1.50 m depth, indicating an oxidizing environment. Quantitative redox interpretations based on [Se(IV)]:[total soluble Se] or [Se(IV)]:[Se(VI)] ratios in these complex field environments is not possible because of non-equilibrium conditions (Runnells and Lindberg, 1990).

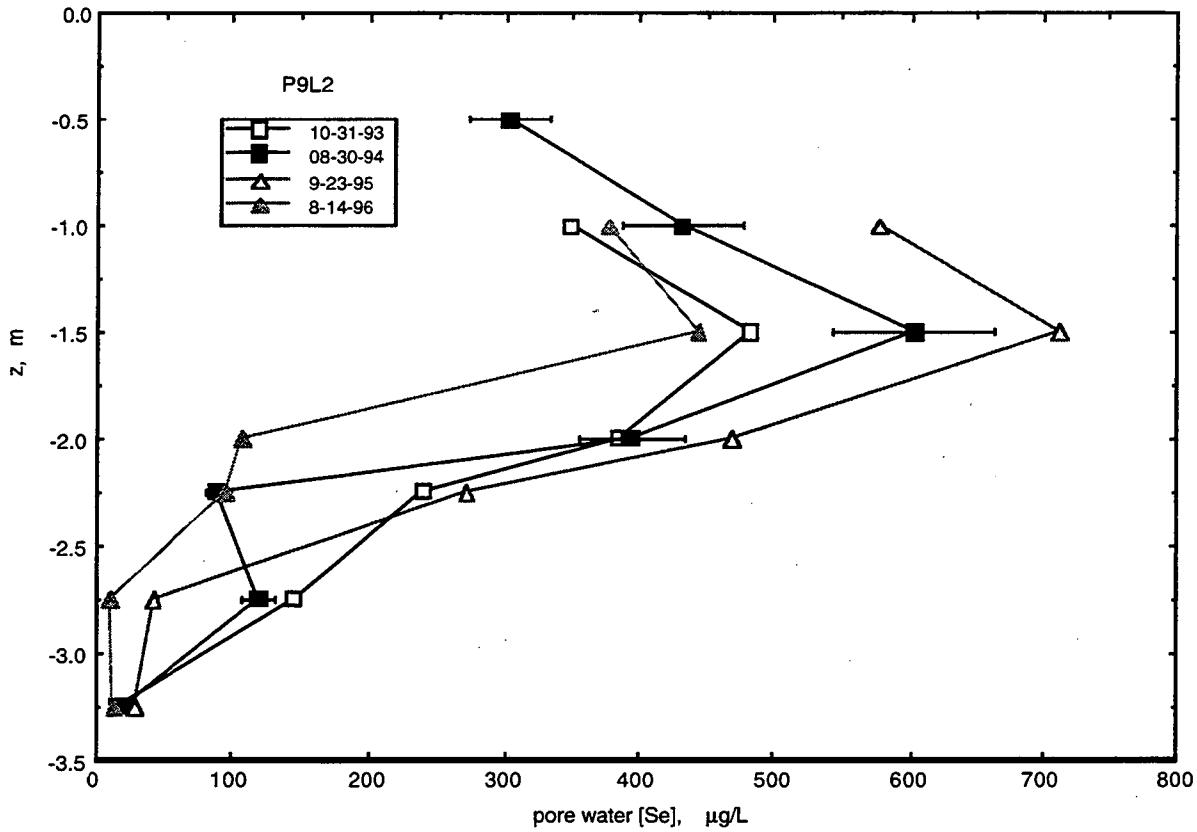

Figure 2.1.3a. Late summer- early fall soluble Se depth profiles at site P9L, 1993 - 1996.

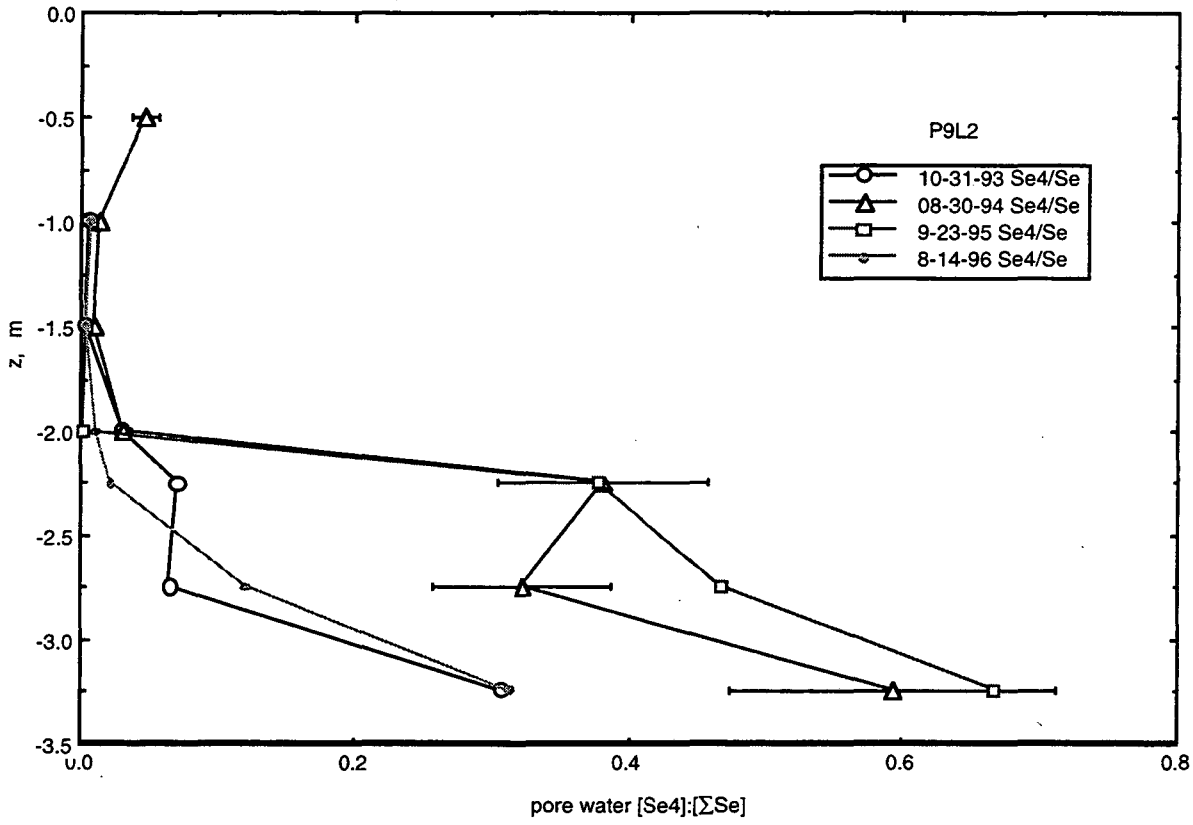

Figure 2.1.3b. Late summer- early fall depth profiles of pore water [Se(IV)]:[total Se] ratios, 1993 - 1996.

Although the late summer to early fall profiles of soluble Se appear relatively stable over the 3 years of monitoring at site P9L, large changes have been observed within individual years during and following the wet season months. The soluble selenium concentration profiles in site P9L are presented sequentially for summer 1994 through summer 1996, in Figs. 2.1.4a to 2.1.4d. Rainfall during the 1994-95 wet season (384 mm) had a much more significant influence on the soluble Se profiles than during the 1995-96 wet season (246 mm), as shown in Figs. 2.1.4a to 2.1.4d, respectively. Soluble Se profiles were relatively stationary from May 1994 through early March 1995 (Fig. 2.1.4a), with significant leaching following the March 9-11, 1995 rain storm (78 mm rainfall) which also resulted in ponding at this site. The soluble Se maxima was displaced from the 1.50 m depth down to the 2.25 m depth during the 2 months following this major storm event. Evapotranspiration-driven Se transport, and Se(VI) reduction at greater depths probably are responsible for bringing the soluble Se profile back to "average" conditions later in the year (Fig. 2.1.4c). As mentioned previously, lower rainfall in the following wet season (1995-1996) prevented significant redistribution of the soluble Se inventory (Fig. 2.1.4d).

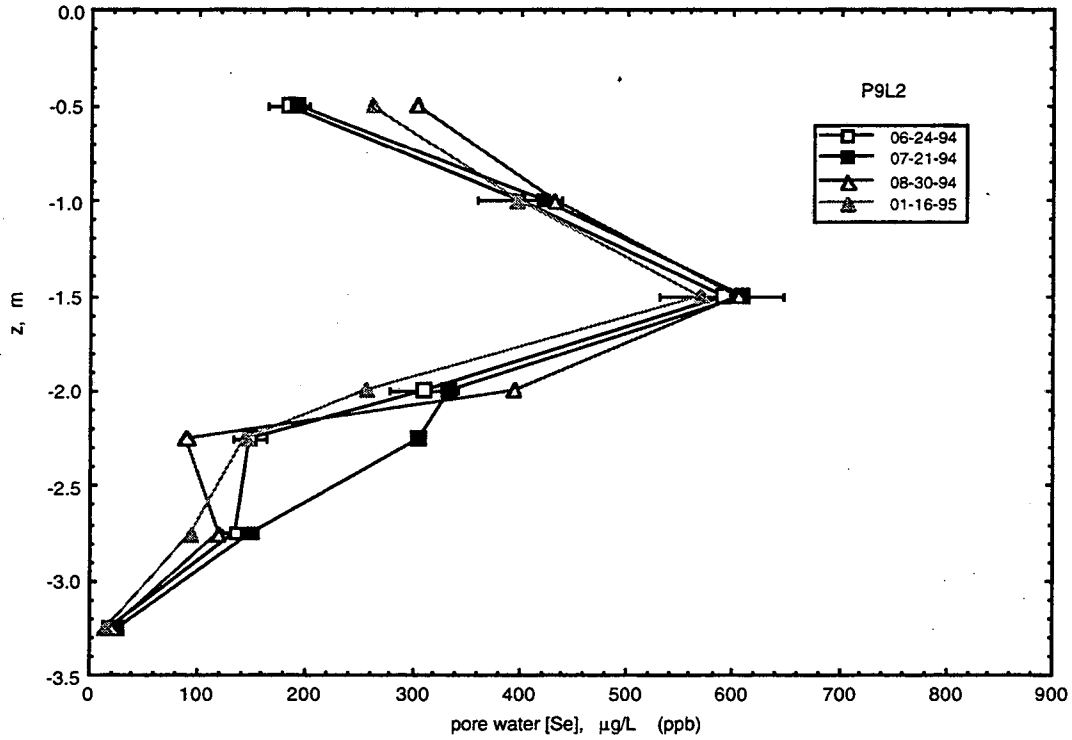

Figure 2.1.4a. Depth profiles of pore water Se concentrates in site P9L, summer 1994 to winter 1995.

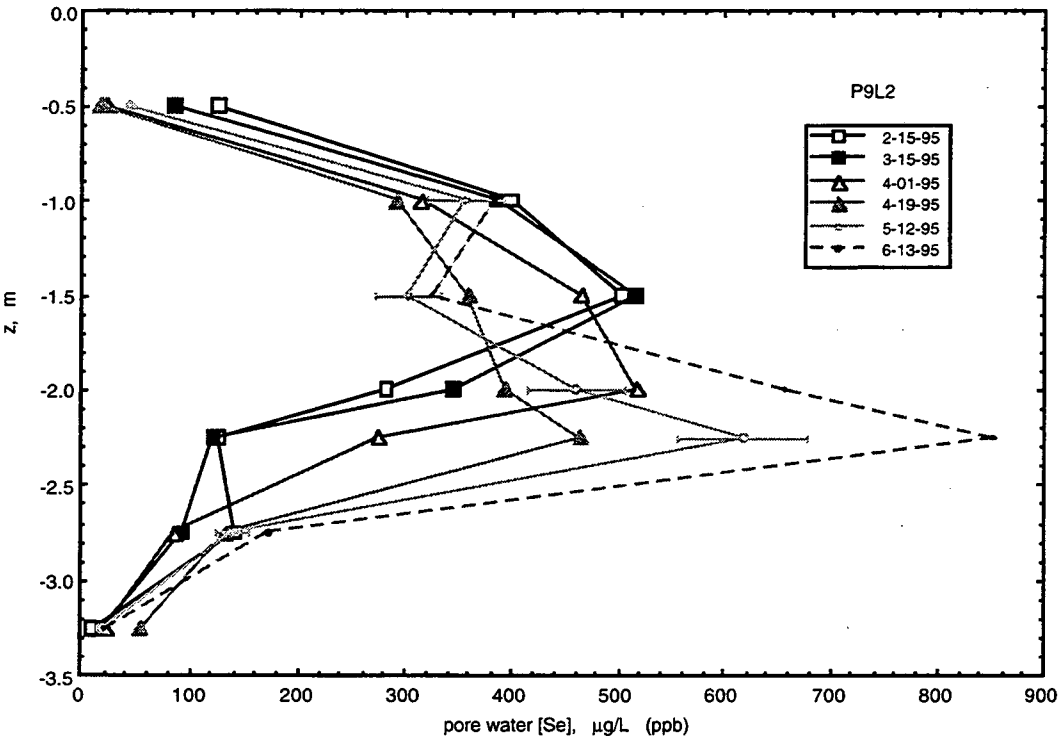

Figure 2.1.4b. Depth profiles of pore water Se concentrations in site P9L, winter 1995 to spring 1995.

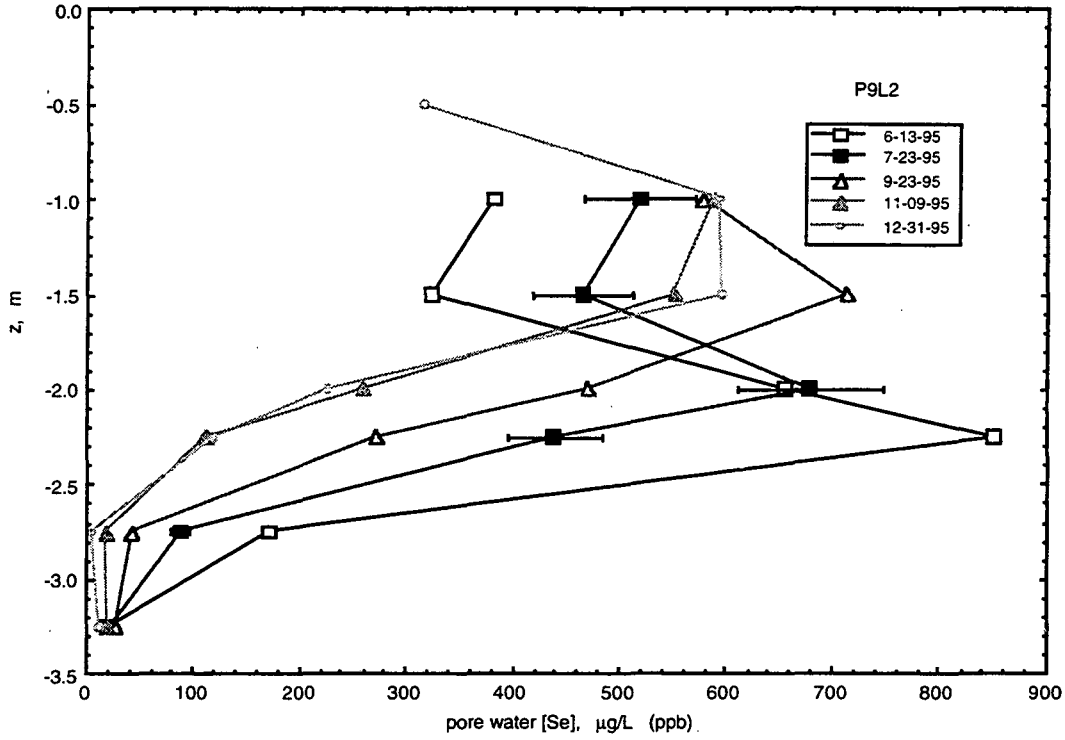

Figure 2.1.4c. Depth profiles of pore water Se concentrations in site P9L, summer 1995 to winter 1996.

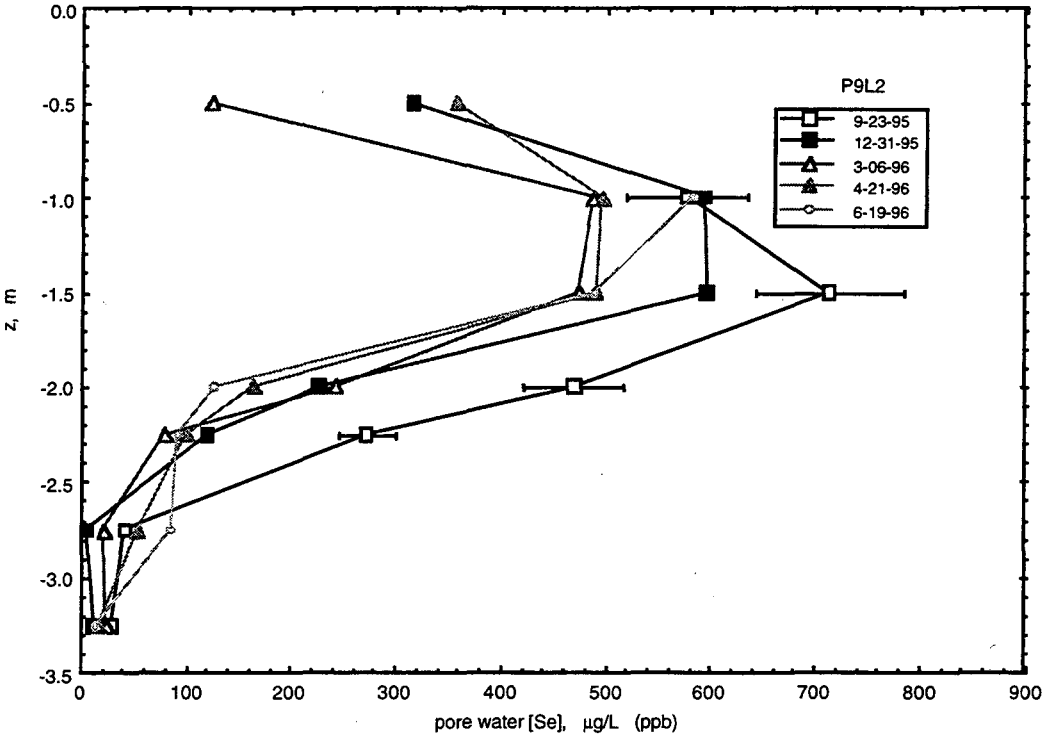

Figure 2.1.4d. Depth profiles of pore water Se concentrations in site P9L, summer 1995 to summer 1996.

The overwhelming influence of the March 1995 rainstorms on soluble Se distributions is illustrated further in time trends. Time trends (Fig. 2.1.5) show large and rapid increases in soluble Se at depths immediately below the 1.50 m region, due to leaching of higher Se concentration waters downwards into these zones. The samplers at and above the 1.50 m zone show decreases in Se concentrations following the storm event, as expected for moving overlying, more dilute waters into these sampling zones. These observations show that advective transport of Se during the wet season largely accounts for its redistribution, and that Se(VI) reduction is a secondary influence. Results presented later show that the P9L soil profile was effectively saturated for about 80 days (late February through April 1995). The lack of significant Se(VI) reduction within the upper 2.0 m of this site is important to recognize. In most soils of Kesterson Reservoir, reductive removal of Se(VI) during ponding was a process of primary importance, leading to the high concentrations of insoluble Se(0) within the upper 0.15 m of profiles (Weres et al., 1989; Pickering et al., 1995), and to low soil water Se concentrations (Long et al., 1990). The inefficient reduction of Se(VI) within the upper, Se-contaminated soil profiles is a necessary condition for deep leaching of Se, and observations of elevated Se concentrations in groundwater monitoring wells. Such conditions have been shown here for the upper 2.0 m of site P9L, and similar observations from other northern Pond 9 soil monitoring sites have been reported in the past.

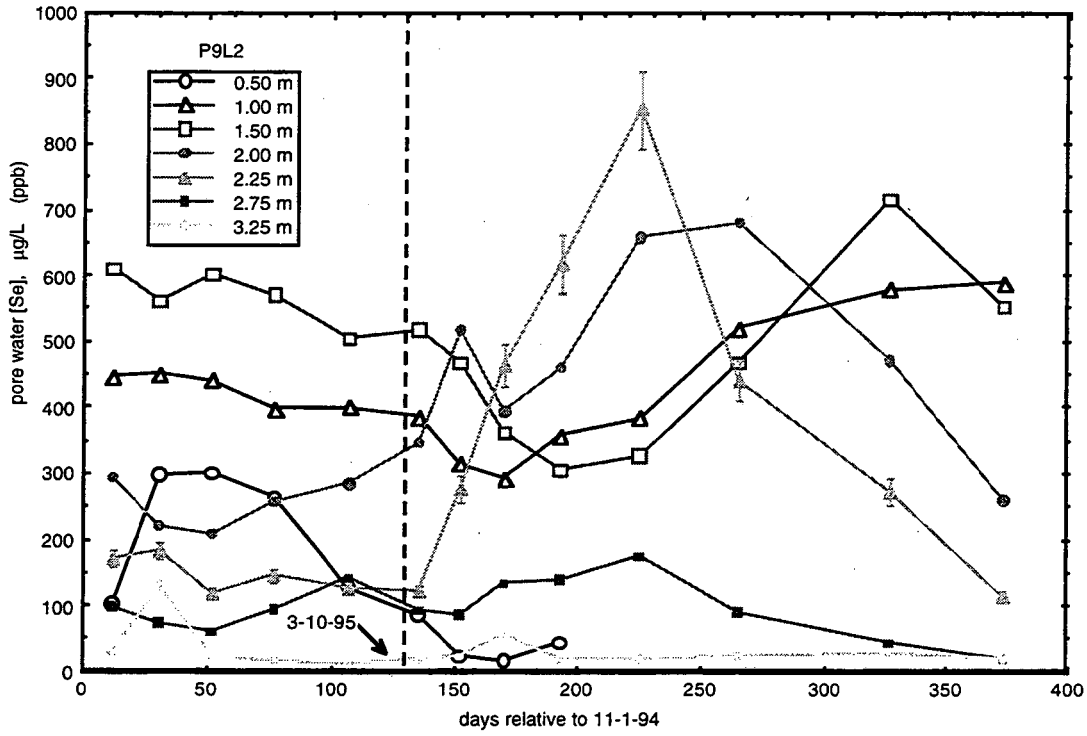

Figure 2.1.5. Time series of pore water Se concentrations at various depths within site P9L, during winter 1994-1995. The major rainfall event took place on March 9-11, 1995 (78 mm).

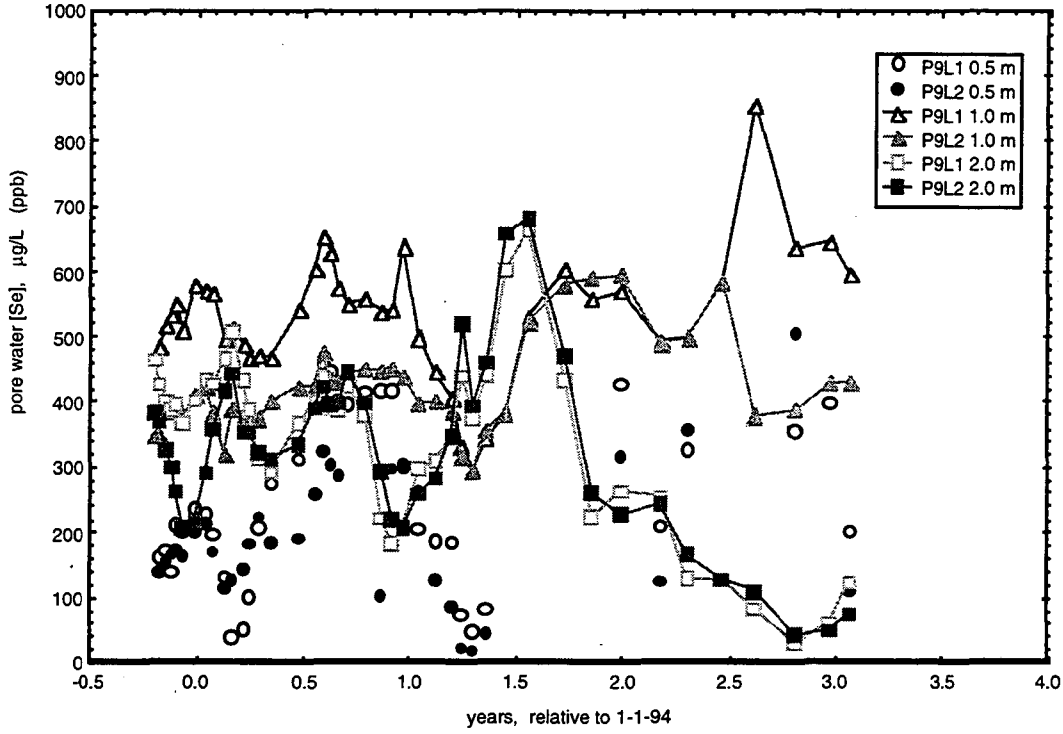

Figure 2.1.6a. Time series for pore water Se concentrations within the 0.50 m to 2.00 m sampling zones at sites P9L1 and P9L2.

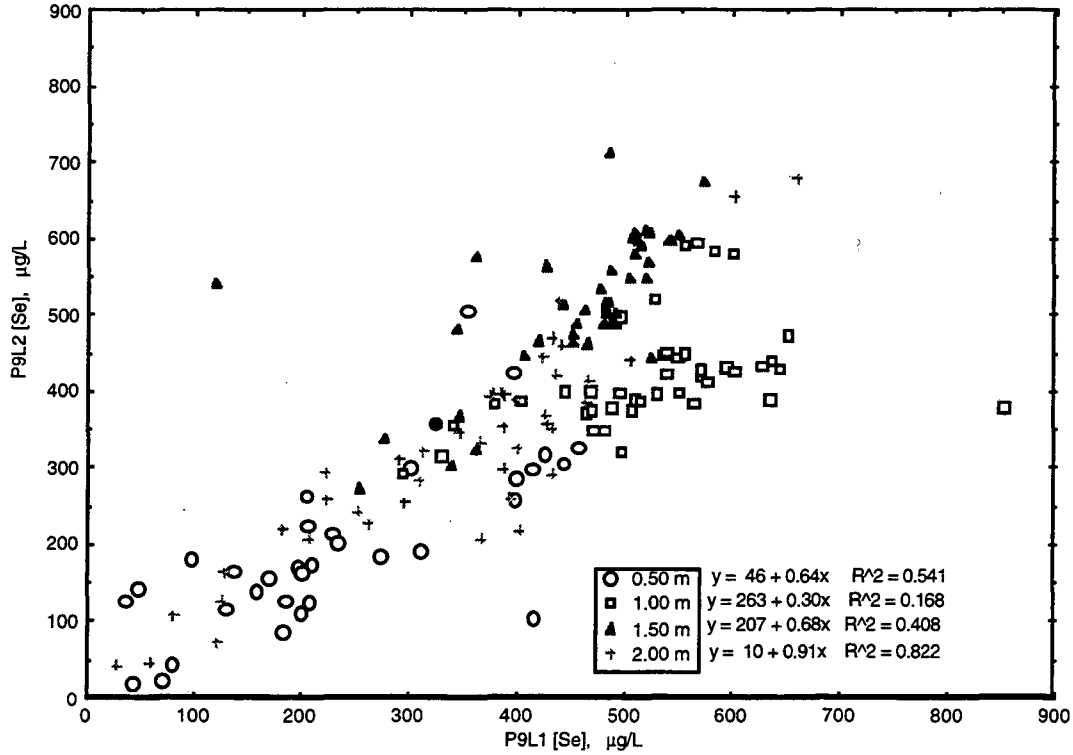

Figure 2.1.6b. Correlation between pore water Se concentrations measured at common depths within site P9L (P9L1 vs. P9L2).

Longer term time trends are considered in the next set of figures. In Fig. 2.1.6a, time trends for soil solution Se concentrations from both profiles P9L1 and P9L2 are shown for comparisons of data obtained from common depths. The correlation between soluble Se concentrations in the two profiles obtained at a given depth are shown in Fig. 2.1.6b. Long term time trends of soluble Se from the deeper soil water samplers and drive point samplers are shown in Fig. 2.1.7.

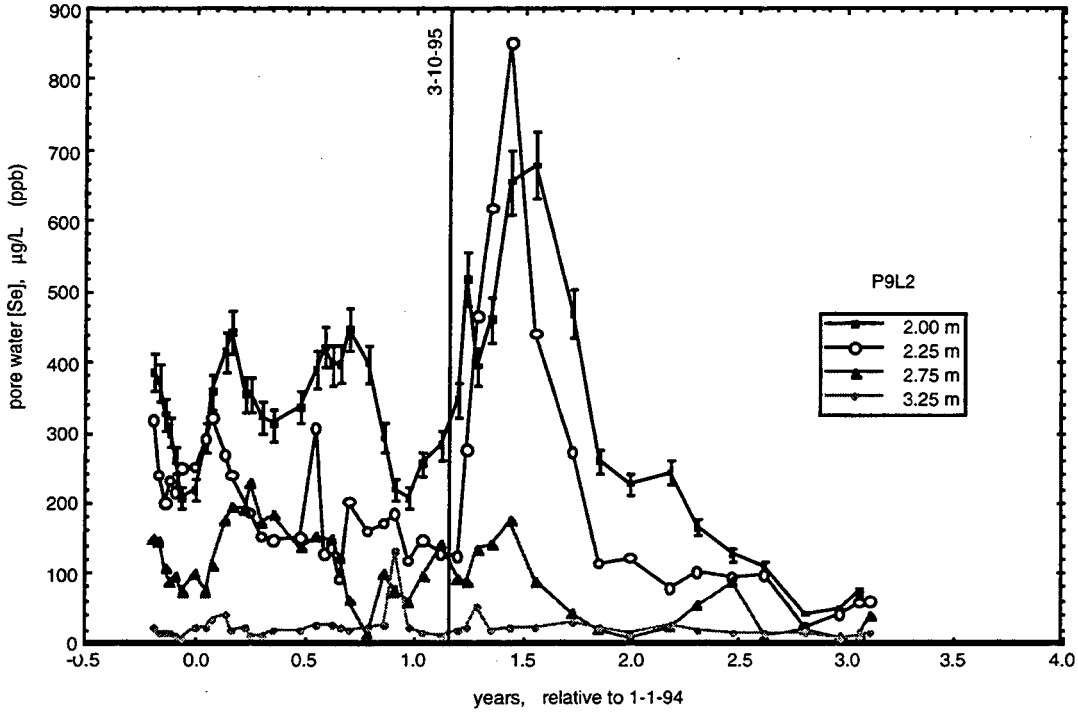

Figure 2.1.7. Long-term time trends in pore water Se concentrations from deeper samplers at site P9L. The major rainfall event within this time interval (fall 1993 to 1996) took place on March 9-11, 1995 (78 mm).

Note that the elevated soluble Se concentrations displaced into the 2.00 and 2.25 m depths after the March 1995 rainfall events are reduced back to pre-storm levels within about 6 months. The fact that the pore water Se concentrations in the 2.75 m and 3.25 m samplers appear relatively un-perturbed following the major rainfall events shows that at this specific site (P9L direct transport of high concentrations of soluble Se to deeper strata does not occur. The long-term time trends of the pore water [Se(IV)]:[total soluble Se] ratios are shown in Fig. 2.1.8. These time trends reveal that (with the exception of some of the 0.50 m data) the upper 2.0 m of pore waters within site P9L maintain low [Se(IV)]:[total soluble Se] ratios, even during flooding events. Thus Se(VI) is being transported through the upper profile without undergoing rapid reduction to insoluble forms. As shown previously, the deepest pore waters (2.75 and 3.25 m) have [Se(IV)]:[total soluble Se] ratios which are typically more reducing, and hence can serve as a sink for Se(VI) transported in from the overlying soil. However, samples obtained from these

depths during much of 1996 (between year 2.2 and 2.9 in Fig. 2.1.8) showed a prolonged period of lower [Se(IV)]:[total soluble Se] ratios, suggesting that oxidizing conditions migrated deeper during that year. More recent samples have had higher [Se(IV)]:[total soluble Se] ratios, more similar to results from earlier years (Fig. 2.1.8). Despite the lower [Se(IV)]:[total soluble Se] ratios obtained in the deepest samplers during 1996, which suggest more oxidizing conditions, total soluble Se concentrations at these depths remained as low or lower than in previous years (Fig. 2.1.7).

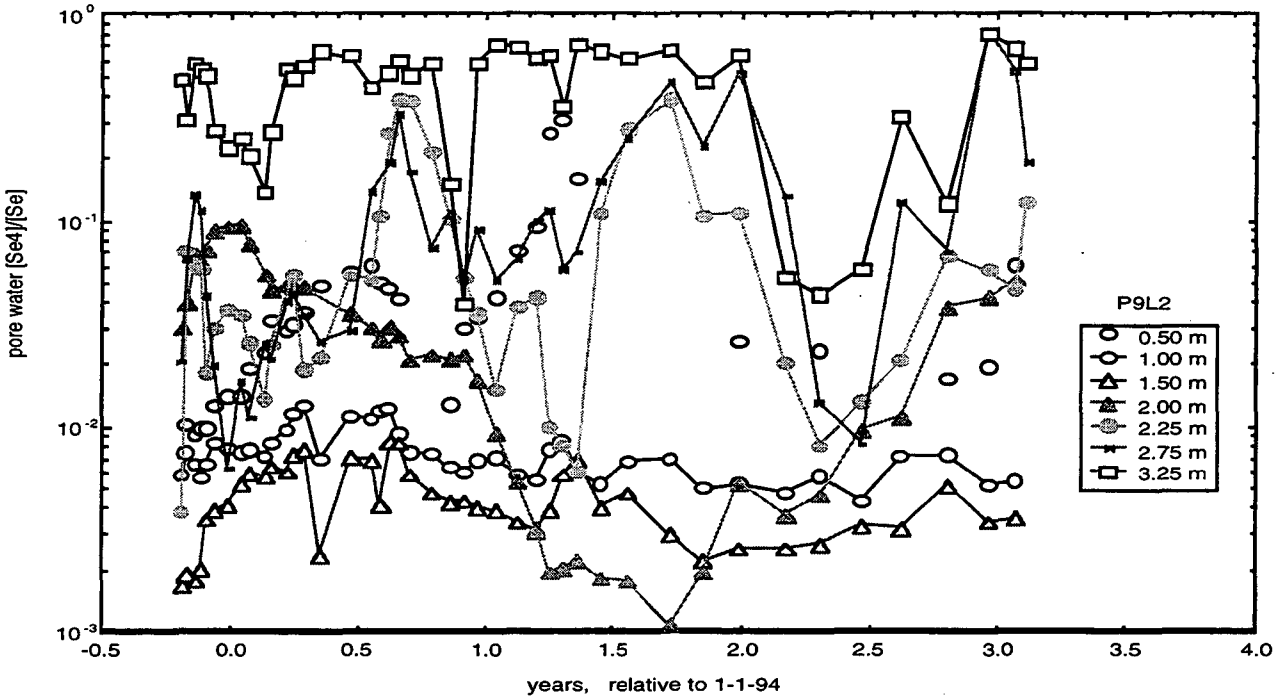

Figure 2.1.8. Time series for pore water [Se(IV):[total Se] ratios at various depths within site P9L.

The hypothesis that consistently low [Se(IV)]:[total soluble Se] ratios in soil solutions are peculiar to regions which have Se-contaminated groundwater (such as northern Pond 9) was partly tested through comparisons with data from other Kesterson Reservoir monitoring sites. Previous results from site P9C (Zawislanski et al., 1995) showed that soil pore waters become more reducing during wet seasons with above-average rainfall and ponding. Since the other soil profile monitoring sites were not intensively sampled during the 1995 wet season, data from the previous major ponding event during the winter of 1992 were used in the following comparison. The [Se(IV)]:[total soluble Se] ratio profiles at P9C and P9L during the winters of 1992 and

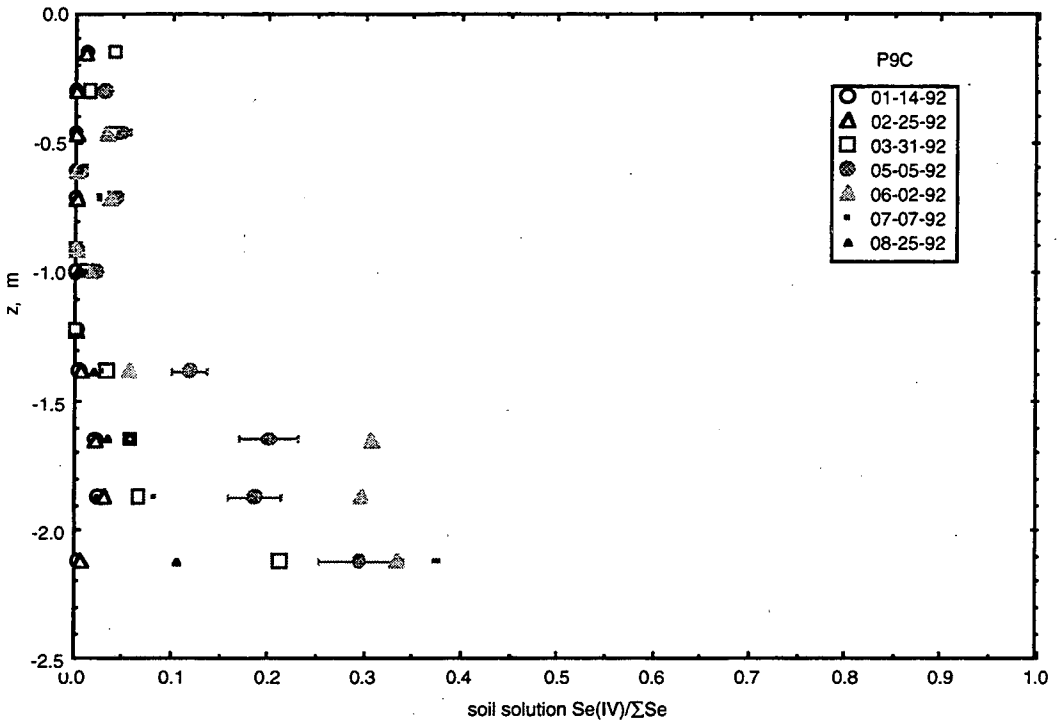

Figure 2.1.9a. Depth profiles of [Se(IV)]:[total dissolved Se] at site P9C during 1992. Flooding occurred on 2-12-92 at this site.

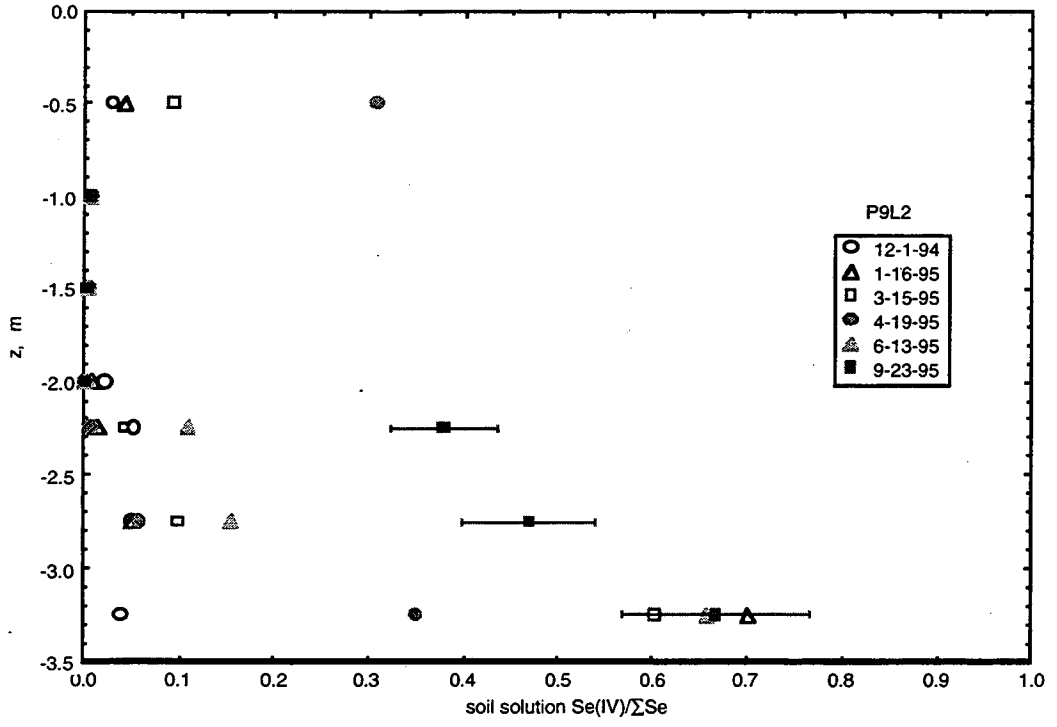

Figure 2.1.9b. Depth profiles of [Se(IV)]:[total dissolved Se] at site P9L during 1995. Flooding occurred on 3-10-95 at this site.

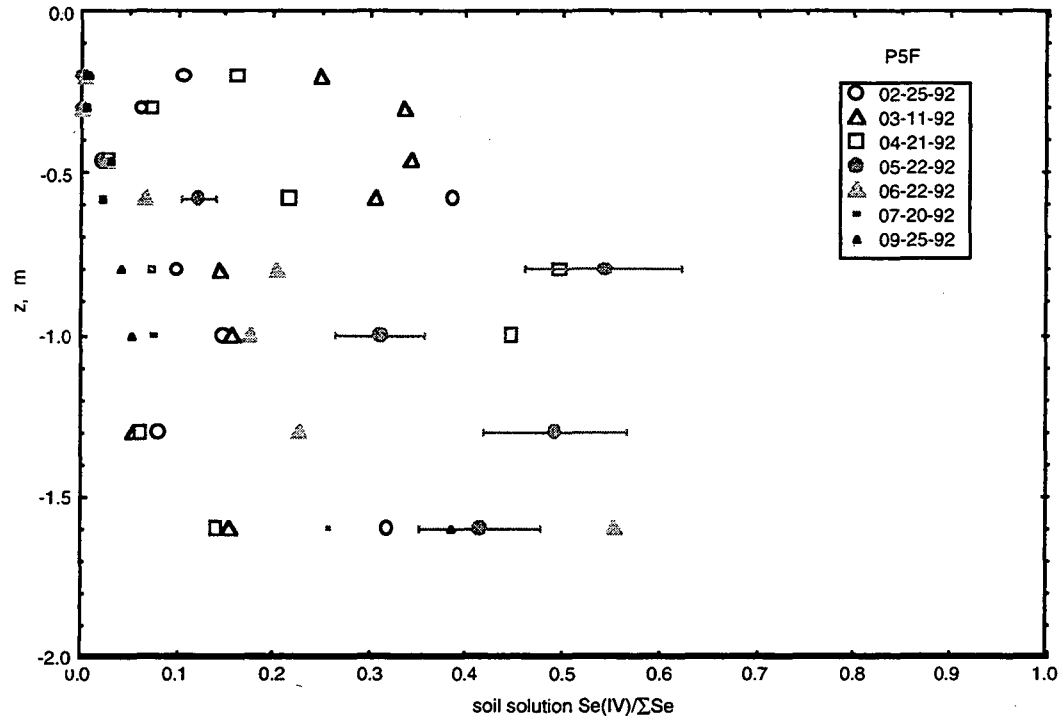

Figure 2.1.9c. Depth profiles of [Se(IV)]:[total dissolved Se] at site P5F during 1992. Flooding occurred on 2-12-92 at this site.

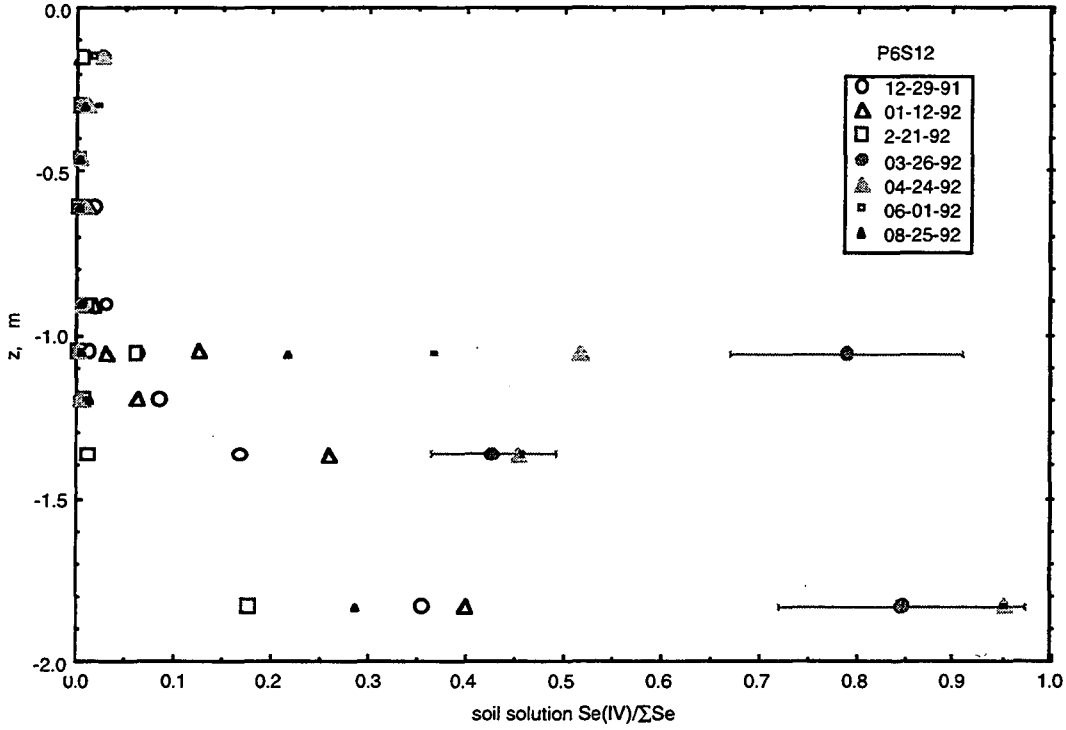

Figure 2.1.9d. Depth profiles of [Se(IV)]:[total dissolved Se] at site P6S12 during 1992. Flooding occurred on 2-12-92 at this site.

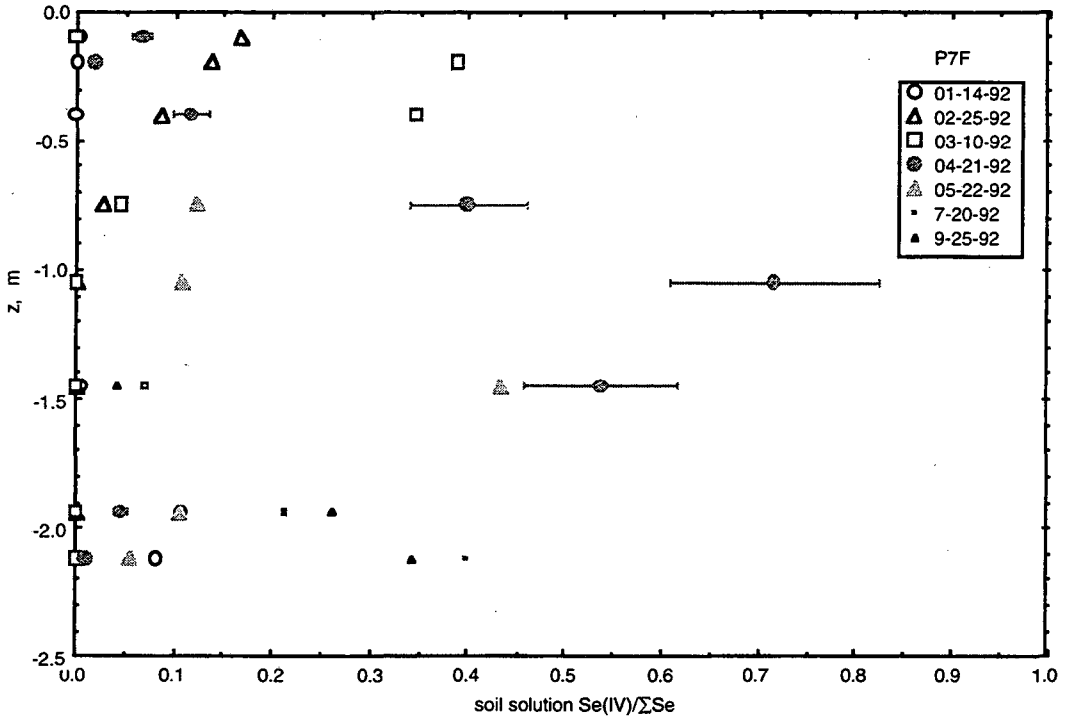

Figure 2.1.9e. Depth profiles of [Se(IV)]:[total dissolved Se] at site P7F during 1992. Flooding occurred on 2-12-92 at this site.

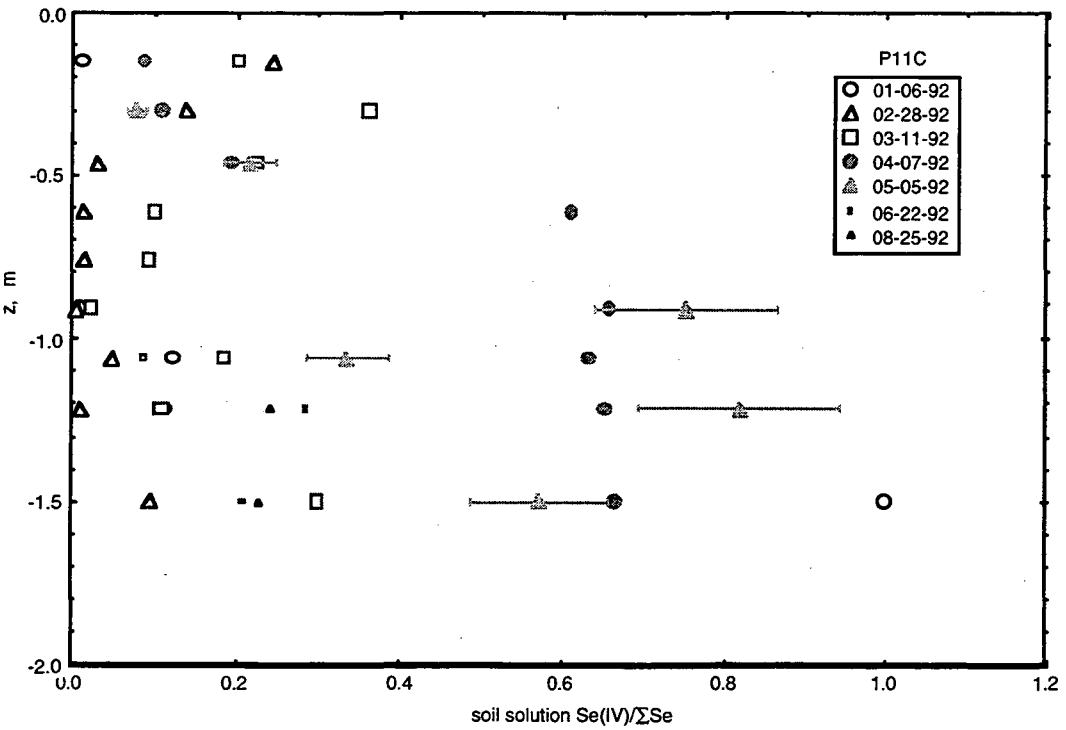

Figure 2.1.9f. Depth profiles of [Se(IV)]:[total dissolved Se] at site P7F during 1992.

1995, respectively, are shown in Figs. 2.1.9a, 2.1.9b. Note that in both of these sites, the [Se(IV)]:[total soluble Se] ratio remains low within the upper 1.5 to 2.0 m (with the exception of data from the 0.5 m depth at P9L during a short period). Profiles of [Se(IV)]:[total soluble Se] ratios from sites P5F, P6S12, P7F, and P11C are shown in Figs. 2.1.9c through 2.1.9f. In the majority of these sites, [Se(IV)]:[total soluble Se] ratios rise significantly following ponding or establishment of high soil profile saturation. The reducing conditions indicated by such observations favor Se adsorption and precipitation, which in turn minimizes deeper Se transport. Among these other sites, only P6S12 maintains low [Se(IV)]:[total soluble Se] ratios within the upper soil profile. This site differs from most other Kesterson Reservoir soils in that the original surface soil was removed, and the soil surface was maintained devegetated. In contrast, sites P5F and P7F are filled sites, in which the original surface soil was covered with imported soil, and which were quickly revegetated. The P11C site was neither filled nor excavated, and is vegetated by a well established growth of salt grass and annual grasses.

The lack of significant Se(VI) reduction within shallow soils of the northern Pond 9 sites and site P6S12 suggest that these two areas have some feature(s) in common. Recall that the only distinguishing feature of site P6S12 is the removal of its original surface (upper 0.3 m) soil. Field observations and aerial photographs of the northern Pond 9 area prior to emplacement of fill soil in areas surrounding the monitoring sites indicate that the surface soil was previously removed here as well, probably for pre-Kesterson surface water management. The surface soil in the northern Pond 9 monitoring area is also devoid of significant visible accumulation of organic matter, in contrast to many other upland and former cattail-vegetated areas of Kesterson Reservoir. Removal of surface soils would have resulted in a significant depletion of organic matter, since its accumulation results from long term build-up of incompletely decomposed plant tissue. Since organic matter content is strongly correlated with Se(VI) reduction in soils (Lakin, 1961; Ylaranta, 1983; Weres et al. 1990), surface soil removal would result in significantly decreased efficiency for Se immobilization within the remaining soil profile.

2.1.3 Pore Water Salinity Trends

Depth profiles of pore water EC at site P9L show that dissolved salt concentrations typically increase with depth below the soil surface, reaching EC values of about 18 dS/m below about 2.00 m (Fig. 2.1.10a). The major ions in solution are dominated by Na, SO_4, and Cl (each typically higher than 10 mM_c), with lower concentrations of Ca and Mg (typically lower that 30 mM_c). Soil water samples from other northern Pond 9 monitoring sites collected during drought years (1987 - 1991) showed that highest pore water salinities were previously associated with the shallower root zone and soil surface (LBL, 1987; Benson et al., 1992). Above average rainfall during most years since then have been effective in leaching soluble salts deeper in soil profiles

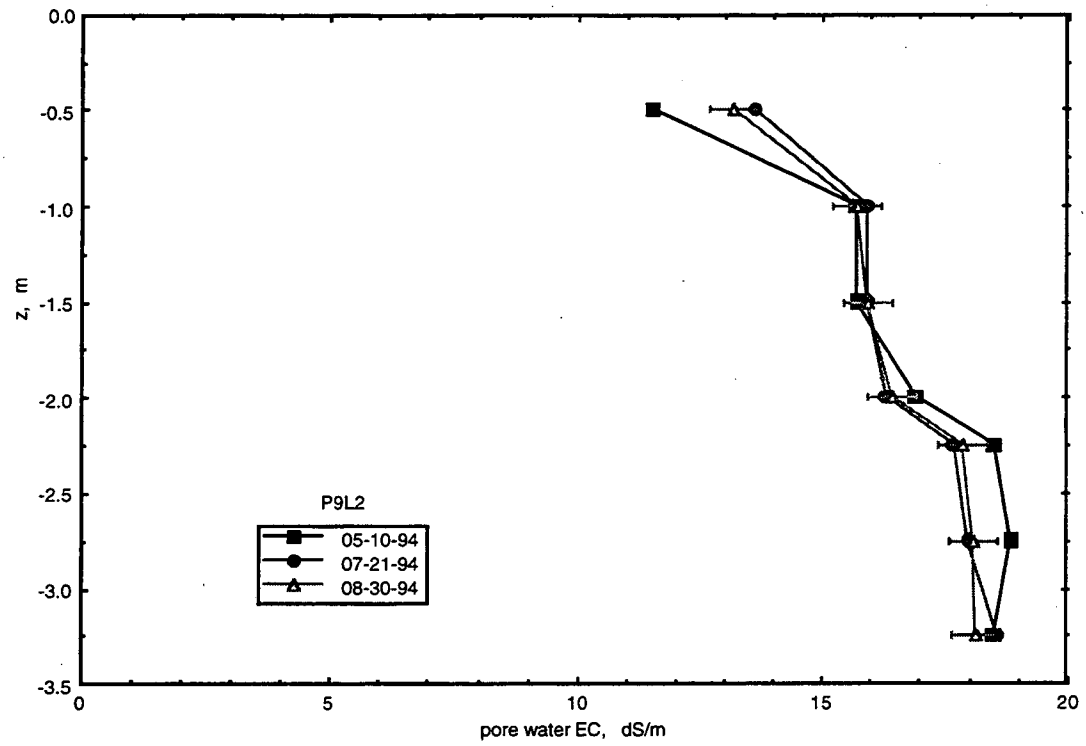

Figure 2.1.10a. Pore water EC profiles at site P9L2, during spring 1994 through summer 1994.

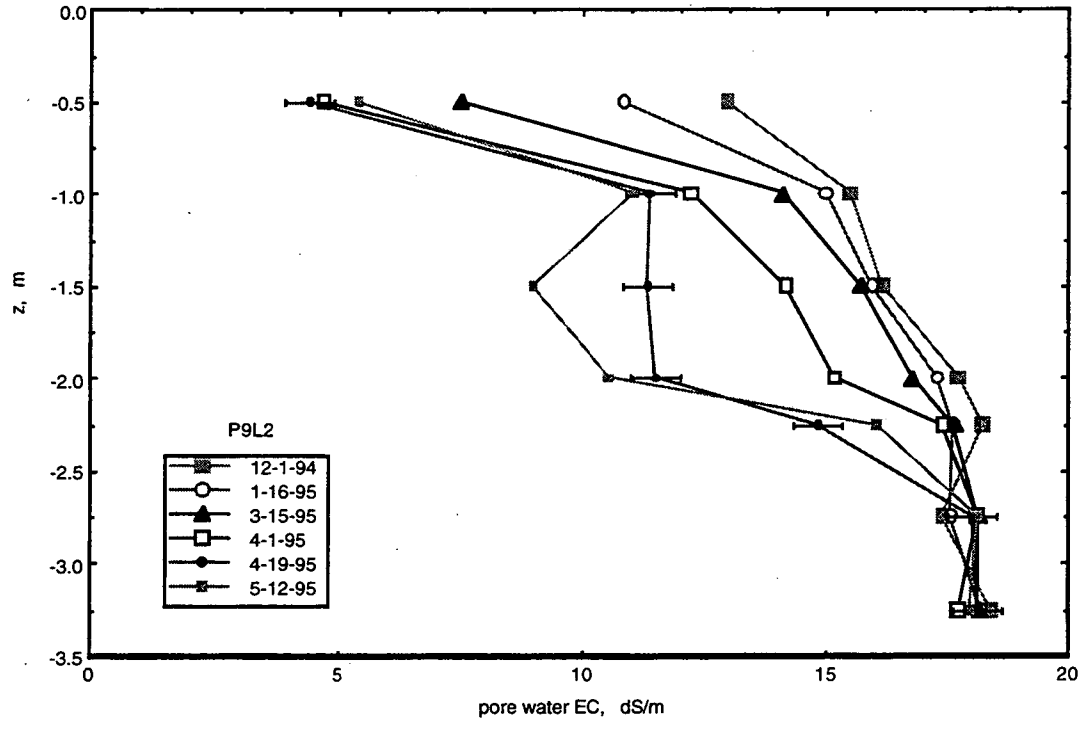

Figure 2.1.10b. Pore water EC profiles at site P9L2 during the 1994-1995 wet season. The major rainfall event took place on March 9-11, 1995 (78 mm).

(Zawislanski et al., 1995). The deeper profile salinities at site P9L are similar and slightly greater than salinities of drainage waters previously ponded at Kesterson Reservoir. Fluctuations in salinity are generally greater towards the soil surface, reflecting rainfall leaching and dilution (Fig. 2.1.10b). Time trends in pore water EC at the various sampling depths in response to the major March 1995 rainfall events roughly followed the expected behavior of lagging and damping of dilution with increased depth (Fig. 2.1.11). The longer term time trend comparisons from soil water samplers in the P9L1 and P9L2 profiles reveal very similar patterns (Fig. 2.1.12a). The March 1995 rainfall events stand out as the strongest influence to date at this site, although salinities have recovered back to pre-storm levels. Direct comparisons between salinities of samples collected at each depth on a given sampling date are presented in Fig. 2.1.12b. Note that, as seen previously for soluble Se, samples collected from the two profiles become better correlated with increased depth. Furthermore, the correlations for salinity at common depths are generally better than for soluble Se, since the soluble inventory of Se is more strongly controlled by redox- and kinetically-controlled reactions involving solid and adsorbed species.

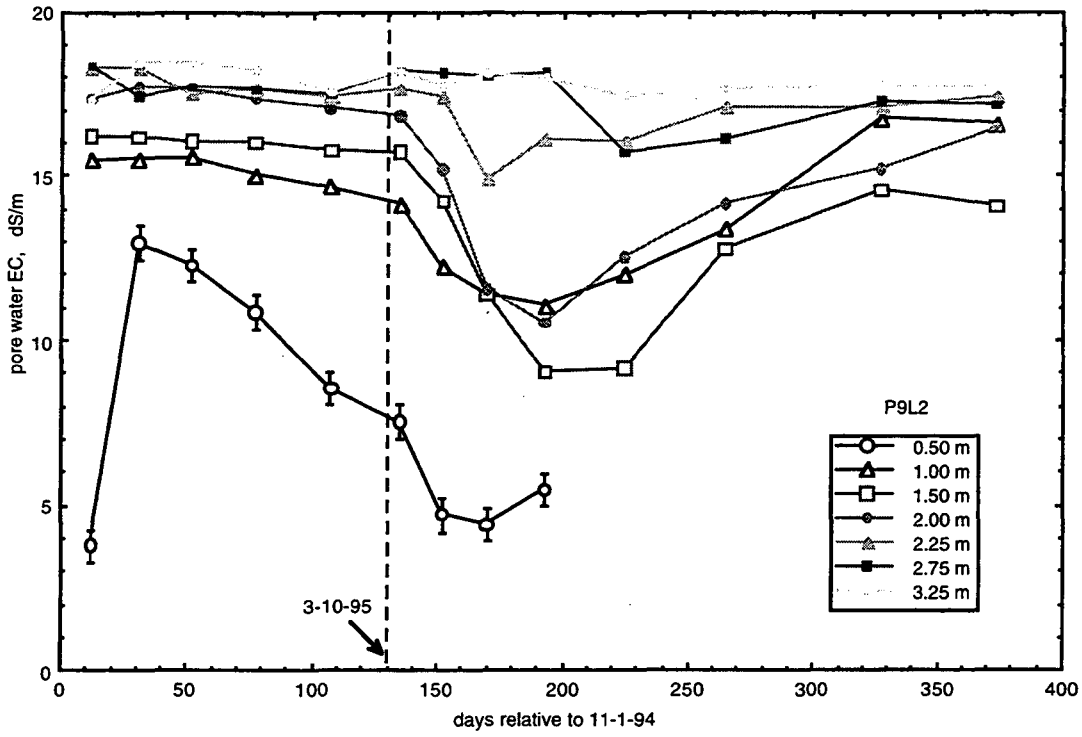

Figure 2.1.11. Pore water EC time series at site P9L2 during the 1994-1995 wet season. The major rainfall event took place on March 9-11, 1995 (78 mm).

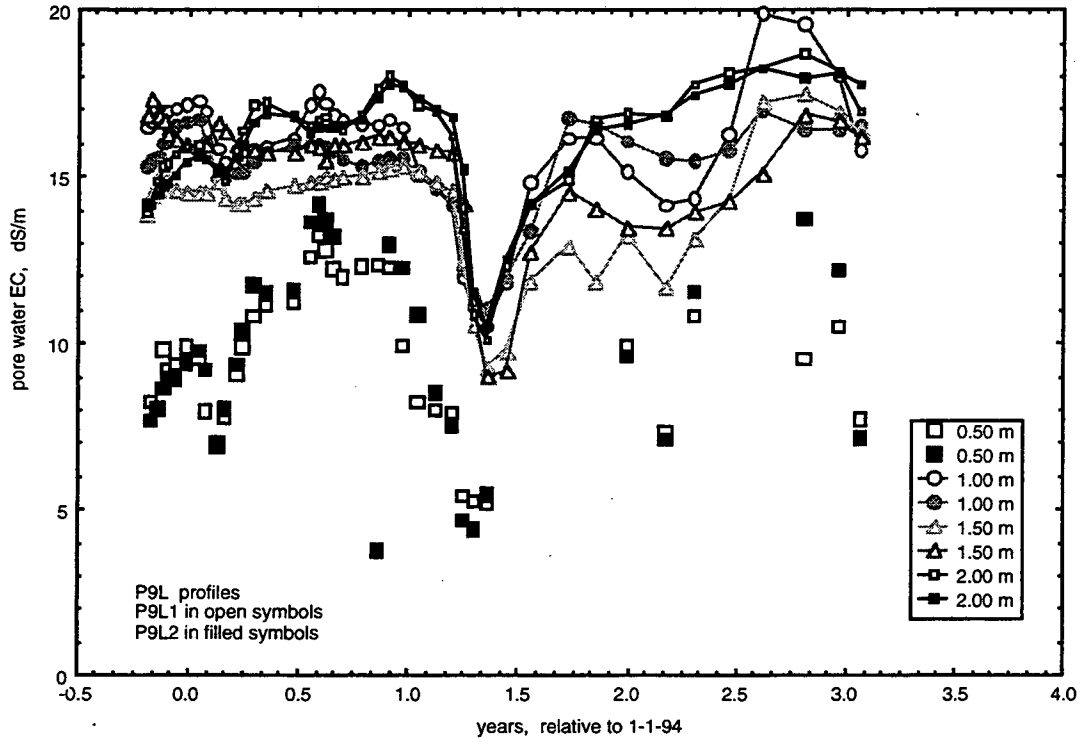

Figure 2.1.12a. Time series of pore water EC from the 0.50 m to 2.00 m depths at sites P9L1 and P9L2.

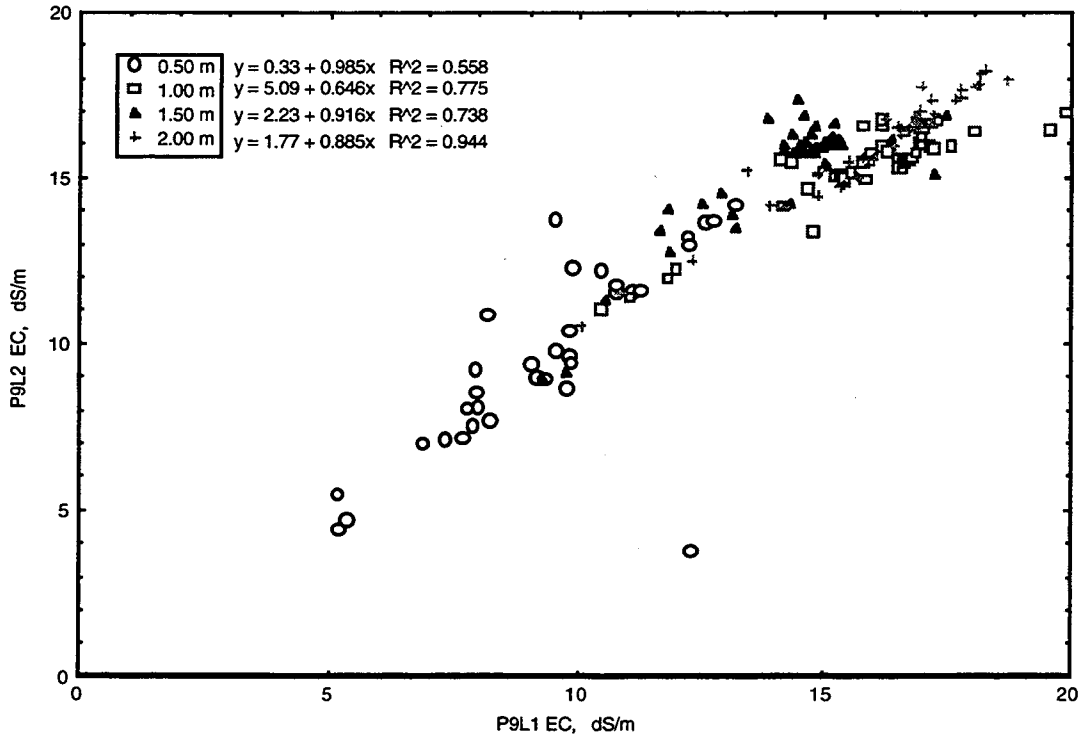

Figure 2.1.12b. Correlation between pore water EC at common depths from sites P9L1 and P9L2.

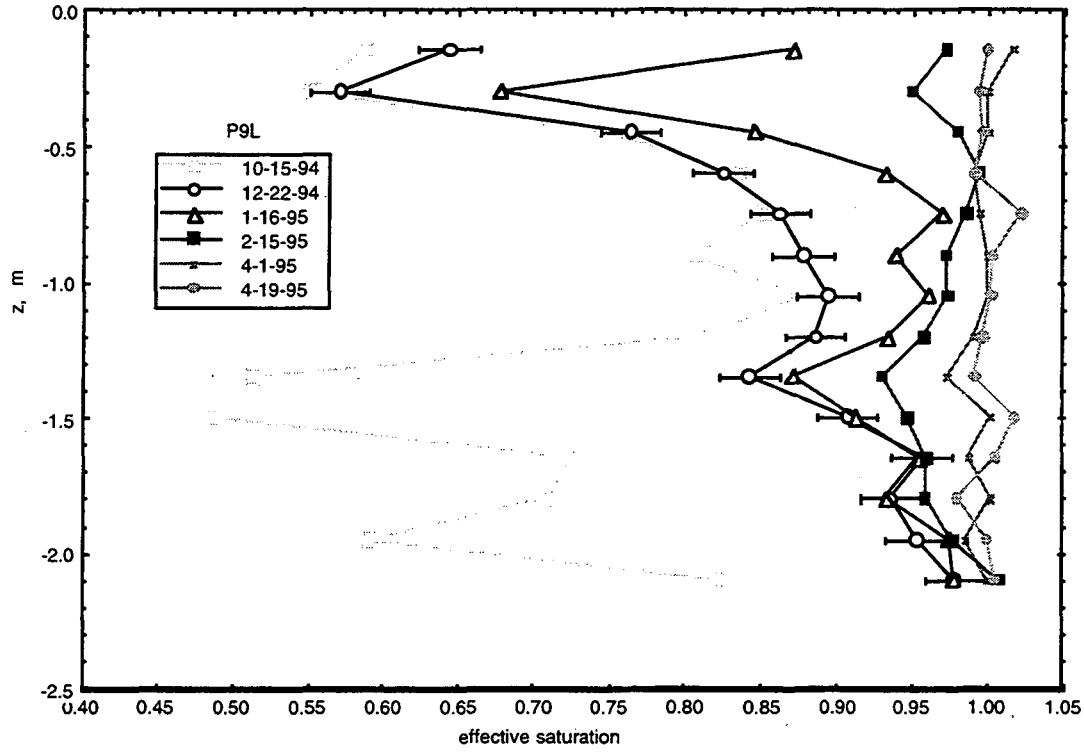

Figure 2.1.13a Depth profiles of effective water saturation during the 1994-1995 wetting cycle at site P9L.

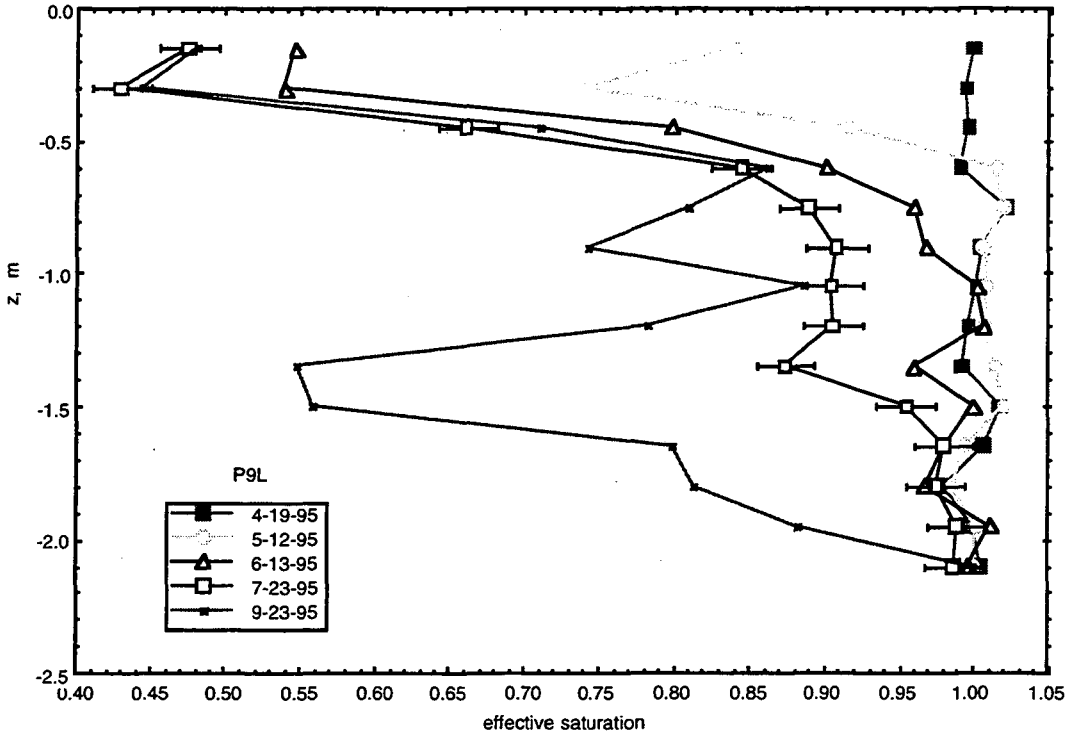

Figure 2.1.13b. Depth profiles of effective water saturation during the 1995 drying cycle at site P9L.

2.1.4 Soil Water Saturation and Hydraulic Potentials

In considering soil profile water contents, it is sometimes more convenient to view data expressed in terms of water saturation rather than in terms of volumetric water content, since the porosity typically varies within profiles. The collective set of neutron probe data from site P9L (Oct. 1993 to June 1996) was evaluated to identify average maximum volumetric moisture contents at each depth. These values of effective porosity ranged from 0.34 to 0.42, and were used to determine effective saturation associated with normalized neutron count rates from specific depths. Saturation profiles during wetting and drying cycles preceding and following the March 1995 rainfall events are shown in Figs. 2.1.13a and 2.1.13b, respectively. Largest changes in saturation occur at the soil surface (greatest evapotranspirative drying), and in the 1.40 - 2.00 m depth interval (sands which seasonally desaturate when the water table drops below this interval). Note that the sandy 1.50 m region undergoes significant desaturation during drying cycles, promoting aerobic conditions which favor low pore water [Se(IV)]:[total solution Se] ratios (recall Fig. 2.1.3b). Time trends of neutron probe measurements within selected regions from the upper P9L profile show that effectively saturated conditions were maintained for about 80 days during the winter-spring months of 1995 (Fig. 2.1.14). Recall that despite this

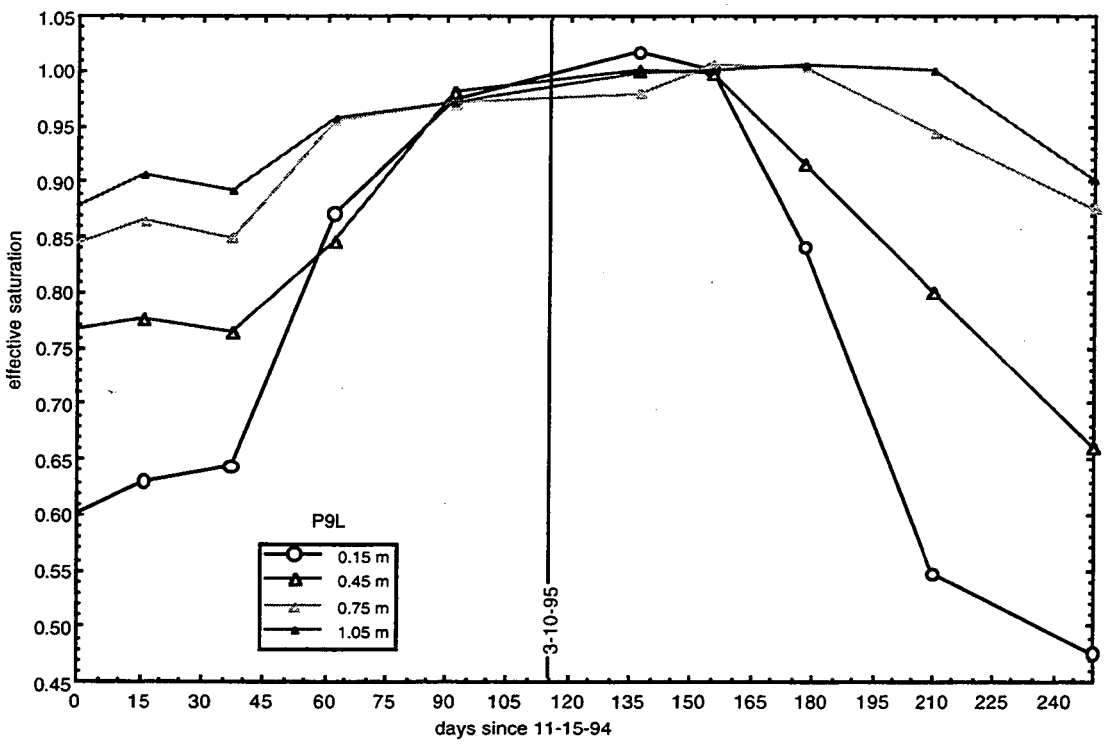

Figure 2.1.14. Time series of effective water saturation within the upper portion of the P9L soil profile, during the 1994-1995 wet season.

prolonged period of effective saturation, the pore water [Se(IV)]:[soluble Se] ratio remained low within the upper 2.00 m of this soil profile (Fig. 2.1.8), and that soluble Se concentration trends during this flooding event strongly reflected influences of advection-dilution rather than Se reduction (Fig. 2.1.5).

Hydraulic potential measurements provide information on the direction of soil water flow (upward or downward in the soil profile) and the depth to the water table. However, quantitative interpretation of hydraulic head profiles can be difficult under flooded or shallow water table environments, as described here. The general seasonal patterns in soil profile hydraulic potentials are similar from year to year, therefore only the wetting and drying cycle from 1994-1995 will be presented here. It differs from some other years primarily in the inclusion of a flooding event. Hydraulic head data obtained from tensiometers and soil water sampler pressure measurements are show in Figs. 2.1.15a and 2.1.15b. Lower regions of soil profiles resaturate by water table rise, as indicated from both the hydraulic head profiles (Fig. 2.1.15a) and neutron probe saturation profiles (Fig. 2.1.13a). The wetting front advance into the profile during the early winter was not recorded since matric potentials within the upper 0.50 m were beyond the functioning range of tensiometers and soil water samplers. Soil profile drying occurs through direct evaporation, evapotranspiration which influences the profile down to about the 1.50 m depth, and the decline of the shallow water table elevation (Fig. 2.1.15b). Apparently hydrostatic conditions develop and persist over much of the wet season. Note that this is the period within which downward displacement of soluble Se occurs (Fig. 2.1.4b). However, upward and downward fluxes can not be distinguished from hydrostatic conditions when the magnitude of the measured hydraulic head gradient is below the limit of quantification, which is about 0.02 m m^{-1} (based on Tensimeter-measured gauge pressures on equilibrated soil water samplers). Since apparent hydrostatic conditions occur during the wet season (Fig. 2.1.15a,b), it is useful to estimate the range of fluxes that could be taking place under such conditions. The lower limit of detectable fluxes can be estimated by combining this limit in hydraulic gradient resolution with values of hydraulic conductivity. In Section 3.2, a summary of available Kesterson soil hydraulic conductivity (under effectively saturated conditions) was provided. A value of 15 mm d^{-1} was suggested for series resistance averaged, saturated Kesterson soil profiles. Thus, in profiles with average saturated soil hydraulic conductivity fluxes lower than 0.3 mm d^{-1} can not be resolved, and apparent hydrostatic conditions are equivalent to fluxes of 0 ± 0.3 mm d^{-1}. The range of possible average pore water velocities under these apparent hydrostatic conditions is obtained by dividing the previous result by the average porosity (0.38), resulting in 0 ± 0.8 mm d^{-1}. However, the soluble Se profiles obtained during this apparent hydrostatic period (Fig. 2.1.4b) show that the region of maximum Se concentration shifts downwards at about 30 mm d^{-1}. If strictly vertical

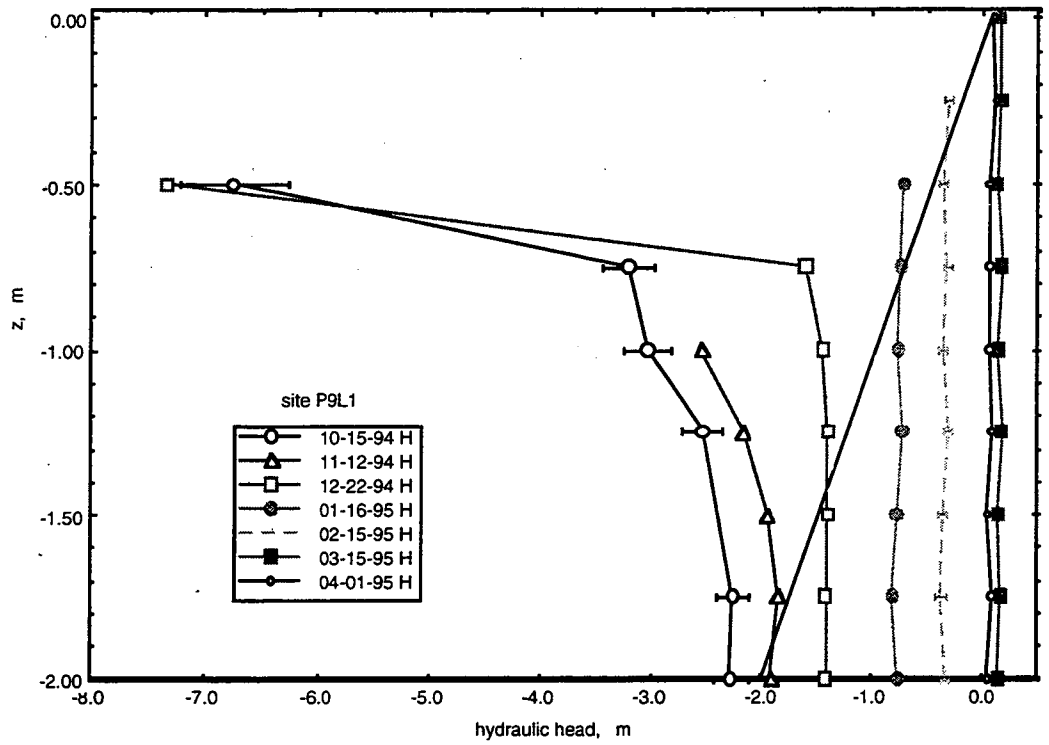

Figure 2.1.15a. Hydraulic head profiles at site P9L during the 1994-1995 wetting cycle. The gravitational head datum is at the soil surface. The diagonal line separates negative (matric) and positive pressure head values.

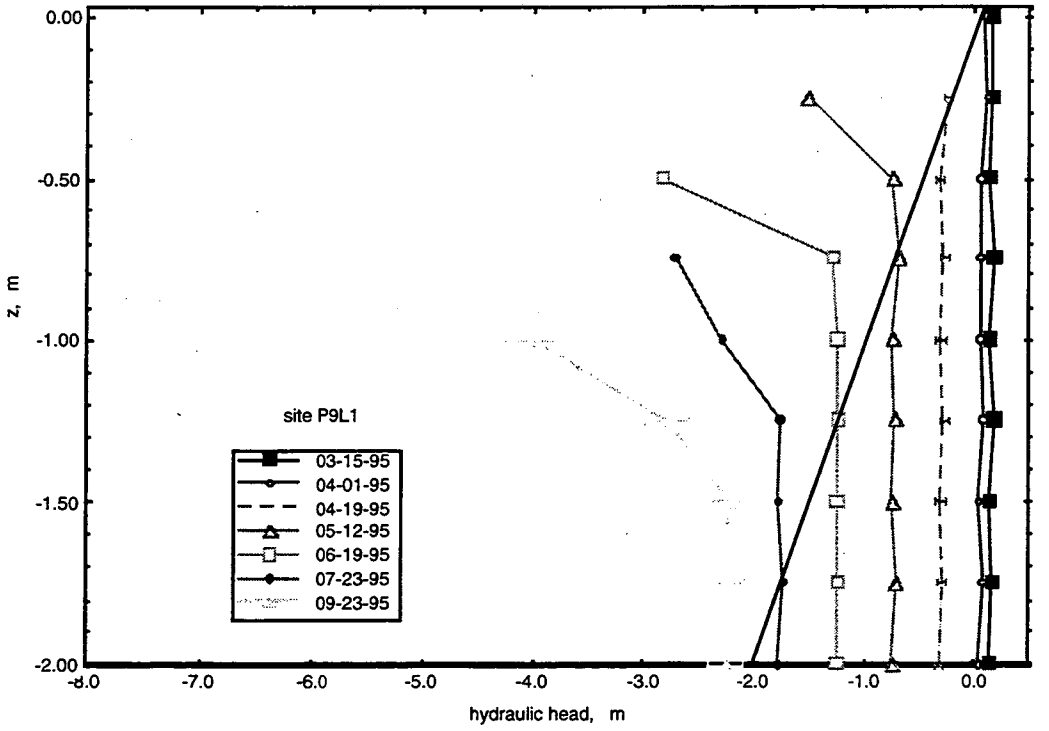

Figure 2.1.15b. Hydraulic head profiles at site P9L during the 1994-1995 wetting cycle. The gravitational head datum is at the soil surface. The diagonal line separates negative (matric) and positive pressure head values.

flow and transport are assumed, this would require that the local soil hydraulic conductivity be in the range of 500 mm d^{-1}. This assumption ignores the influence of lateral flow.

Interpretations of Se transport in these profiles is further complicated by lateral flow of shallow groundwater, which include more of the deeper soil pore waters during the wet season. Typical horizontal gradients in the shallow groundwater underlying site P9L are about 0.6 m km^{-1} (based on water table elevation maps included in USBR, 1996). Combining this with an estimated value of the shallow aquifer hydraulic conductivity of 10 m d^{-1} (selected from a range of values reported in Benson et al., 1991) results in a lateral pore water velocity of 17 mm d^{-1} (using a porosity of 0.35). Thus, the pore waters sampled at and below the 1.50 m depth of P9L are influenced, seasonally, by lateral flow, to a greater degree than by seepage from the immediately overlying soil pore waters. The observed increases in Se concentrations in deeper samplers could therefore originate from more seleniferous, upstream shallow groundwater .

2.1.5 Summary

Deep soil profile monitoring at site P9L was conducted to improve understanding of localized observations of high Se concentrations in the shallow groundwater underlying Kesterson Reservoir. Results show that the Se in soil waters (down to the 2.00 m depth) at this site remains oxidized throughout the year. Downwards displacement of these Se(VI)-dominated waters during the wet season can result in elevated Se concentrations in shallow groundwater when reduction rates are sufficiently slow. The past removal of the original surface soil in the northern Pond 9 area enhances Se transport into the shallow groundwater in two ways. First, removal of the most organic-rich surface soil horizon leaves the remaining profile with a lower capacity to generate and sustain reducing conditions needed to immobilize Se. Second, removal of the lower permeability surface soil leaves the remaining profile more hydraulically conductive since sands are encountered at fairly shallow depths.

2.2 Reservoir-Wide Monitoring of Soil Selenium

Peter Zawislanski and Sally Benson
Earth Sciences Division
Lawrence Berkeley Laboratory

Since 1989, LBNL and CH2M Hill researchers have cooperated to provide a data set on the overall status of the selenium inventory at Kesterson Reservoir. The data presented herein describe and summarize the results of soil sampling and analysis performed by LBNL between 1989 and 1995. Samples collected in 1996 are currently being extracted and the complete data set will be presented in a supplemental report. The details of sample collection site selection and sampling, extraction, and analysis methods have been presented in previous reports (Zawislanski et al., 1995; Wahl et al., 1994) and will be briefly summarized below.

2.2.1 Site Description

Kesterson Reservoir is divided into three distinct habitat types: Fill (F), Grassland (G), Open (O) and three trisections (T1, T2, T3) (Fig. 2.2.1). Fill areas represent areas where the soil surface was previously below the maximum height of the annual groundwater rise. The fill areas were frequently flooded with drain waters. An organic-rich ooze was deposited in the pond bottoms. These areas were filled with non-seleniferous non-native soils in 1988 in order to prevent ephemeral pool formation by water table rise. Fill habitat is presently vegetated with annual vegetation dominated by *Bassia hyssopifolia* and annual grasses. Fill habitat covers about 56 percent of the Reservoir.

Grassland areas, although present in patches throughout the Reservoir, dominate the relatively dry, upland northern ponds and contain large areas covered by saltgrass (*Distichlis spicata*). This habitat normally remained above water most of the year, and a loose deposit of organic detritus accumulated under the canopy of the living vegetation. Grassland sites are dominated by saltgrass and cover 31 percent of the Reservoir.

Open habitats represent areas above high groundwater levels which were flooded during the winter and remained damp during the summer and fall. These areas were dominated by cattails (*Typha sp.*) and were exposed to high levels of selenium. Loose, thick organic deposits of selenium-rich material accumulated and presently remain in these areas. Open areas are former cattail areas that were de-watered and disked in 1988 to eliminate nesting for tri-colored blackbirds. Open sites are sparsely vegetated with *Bassia*, prickly lettuce (*Lactuca serriola*), and clover (*Medicago, Melilotus, Trifolium spp.*). Open habitat covers about 13 percent of the Reservoir (CH2M Hill, 1991).

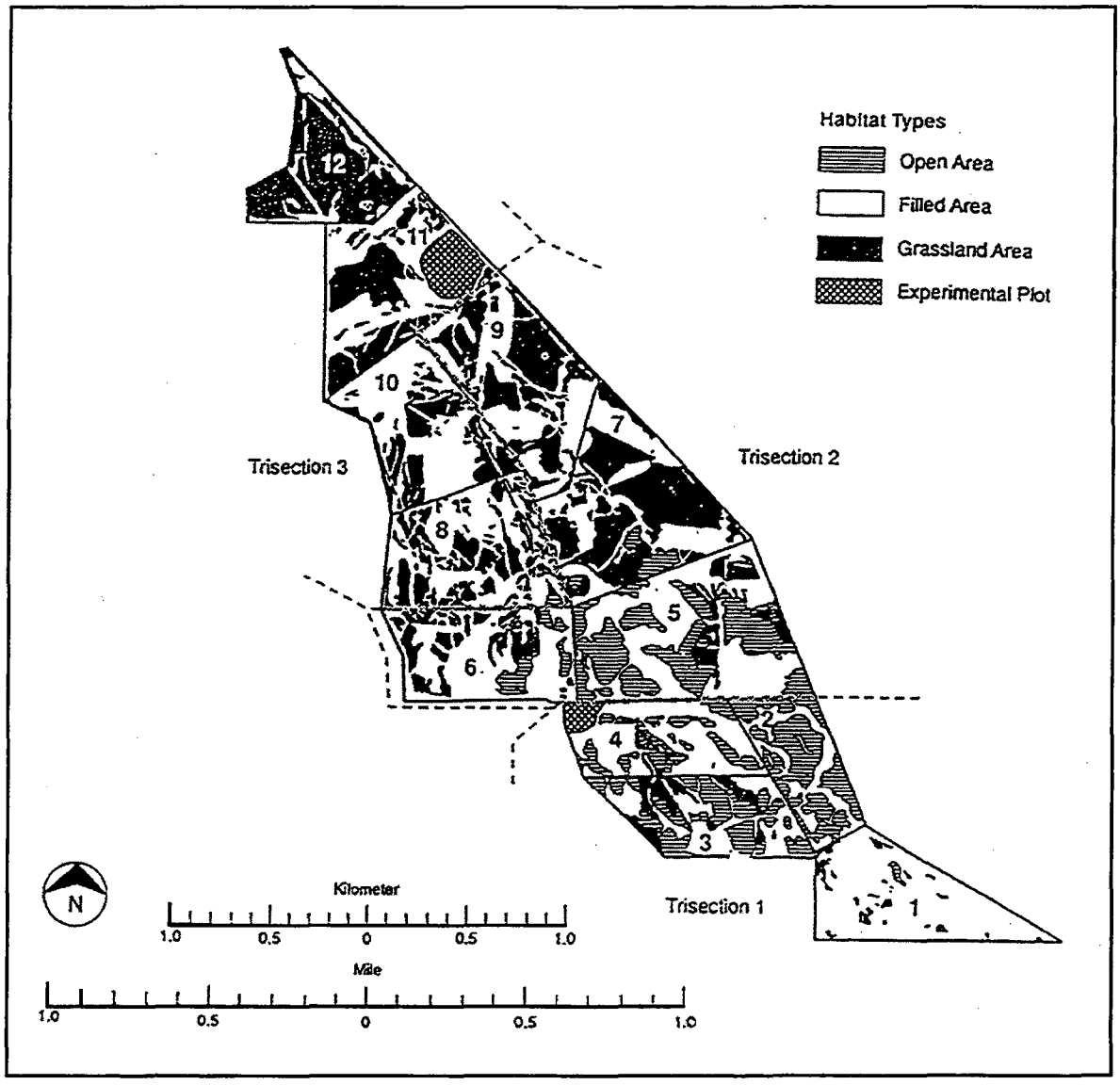

Figure 2.2.1. Map of habitat and trisection delineations at Kesterson Reservoir (CH2MHill, 1991).

Trisection 1 (T1) consists of the southern Ponds 1, 2, 3, and 4; Trisection 2 (T2) consists of the central Ponds (5, 6, 7, and 9); and Trisection 3 (T3) consists of the northern Ponds (8, 10, 11, and 12). Ponds 1 and 2 of T1 received the largest amounts of agricultural drainage water from the San Luis Drain during 1978-1986, as water flowed by gravity from south to north, with Ponds 1 through 5 being used most extensively. The ponds in this trisection have the highest reported soil selenium levels (LBL, 1990; CH2M Hill, 1991), and contained mostly open water and cattail areas in the past, and presently contain mostly open and fill habitats.

The ponds in T2 also received substantial amounts of drainwater in the past (LBL, 1990; CH2M Hill, 1991). However, these ponds generally have lower soil selenium levels than those in T1. Although only open water, and cattail areas were characteristic of T2 in the past, today open, grassland and fill habitats are all found in the trisection. Trisection 3 received the least amount of drainwater and ponds in this trisection have the lowest reported soil selenium levels (LBL, 1990; CH2M Hill, 1991). Trisection 3 is dominated by large areas of grassland and fill habitats.

2.2.2. Sampling, Extraction, and Analysis

Within each trisection, six sites of each habitat type were chosen for long-term monitoring of soils for a total of 54 sampling sites. Soil samples were collected by inserting a 2.54 cm diameter push-tube sampler to a depth of 15 cm from six stations in each habitat type of each trisection, for a total of 18 stations per trisection. The samples were collected at each site within a radius of about 1 m of the stations center. From 1989 through 1991, only the top 15 cm of soil was sampled. Beginning in 1992, samples were collected using a hydraulic drill rig at intervals of 0-15, 15-50, and 50-100 cm.

Soil samples were homogenized at field-moist conditions by hand chopping and passed through a 4.75-mm sieve. A known mass (between 20 and 30 g) of the homogenized subsample was then placed into an open stainless steel can and oven dried at 105°C for 24 hours to determine gravimetric moisture content. For the first 3 years, X-ray fluorescence (XRF) analysis was used to measure the total selenium concentrations of the sample (Giauque et al., 1976). Starting in 1992, hydride-generation atomic absorption spectroscopy (HGAAS) of an acid digest of dry soil was used instead (Zawislanski and Zavarin, 1996). This method has a much lower detection limit and can be used for both near-surface and sub-surface soils.

For the water-soluble selenium determination, a subsample of the homogenized soil (20 to 25 g) was used to prepare a 1:5 soil:water extract. Soil water extracts were analyzed for water-soluble selenium, water-soluble selenite; and two major anions: sulfate and chloride. Sulfate was analyzed using an Inductively Coupled Plasma Spectrophotometer (ICP) or ion chromatography (IC). Chloride was analyzed using either a Mohr titration, as described by Flaschka et al. (1969)

or IC. Water-extractable selenium was analyzed using atomic absorption spectroscopy (AAS) coupled with a hydride generator (see Section 8? of this report). In Kesterson Reservoir soils, water-extractable selenium includes selenate, selenite, and minor amounts of organically associated selenium (Weres et al., 1989; Long et al., 1990). All Se concentrations reported are in units of mg/kg or ppm on a dry weight basis.

2.2.3. Interpretation Methods and General Results

Analysis of Variance (ANOVA) was performed to determine if there were significant differences in soil selenium concentrations. Total selenium, water-extractable and phosphate-extractable selenium, water-extractable and phosphate-extractable selenite, and chloride data were determined to be log-normally distributed using the fractile method described in Warrick and Nielsen (1980). Sulfate concentrations were found to be normally distributed. Fisher's protected least significant difference (PLSD) method was used to determine significant differences in concentrations within year, trisection, habitat, and depth ($P<.05$) (Mead, 1988).

As presented in previous reports, near-surface total Se and water-soluble Se concentrations are highest in the Open habitat, followed by the Grassland habitat, and lowest in the Fill habitat. This pattern does not change from year to year. The Open habitat is also most saline, with the Grassland and Fill habitat salinities not significantly different from each other. Soils from T1 were found to be both highest in Se and salinity, while soils from T2 and T3 are not significantly different from each other. Se concentrations are strongly skewed toward the surface, with the mean total Se in the top 15 cm being an order of magnitude higher than Se in the 15-100 cm interval.

Because of the trends described above, the analysis presented herein will be split by habitat and depth. Based on previous experience, statistical analysis of Reservoir-wide Se levels is not particularly useful because time trends in each habitat tend to be different.

2.2.4. Se Trends in Surface (0-15 cm) Soils

Total and water-soluble Se concentrations in surface (0-15 cm) soils are presented by habitat in Table 2.2.1. The same data is presented graphically in Fig. 2.2.2 through 2.2.7. Total Se sample sets which are significantly different from each other within the 95% confidence interval are denoted in the figures in black lettering within the column for the given year.

There are no significant differences in total Se concentrations in the Fill habitat over any period of time (Fig. 2.2.2). The geometric mean for these measurements falls between 0.81 and 1.51 mg kg^{-1}. The water-soluble concentrations in the 0-15 cm interval in the Fill habitat (Fig. 2.2.3) show some fluctuations, most notably large increases in 1991 and 1994, but no consistent trend emerges.

Table 2.2.1. Soil Se concentrations in the top 15 cm of the soil profile over the seven-year sampling period. Values represent geometric mean concentrations* expressed in mg/kg•soil. Confidence intervals within the 95%-ile are indicated below geometric mean concentrations.

Habitat	1989	1990	1991	1992	1993	1994	1995
Total Se							
Fill	1.51 A (0.82-2.76)	1.05 A (0.65-1.69)	1.39 A (0.83-2.34)	0.82 A (0.47-1.43)	0.93 A (0.68-1.28)	0.81 A (0.47-1.38)	1.25 A (0.77-2.02)
Grass	3.62 A (2.04-6.42)	2.85 A,B (1.70-4.80)	2.30 A,B (1.45-3.65)	2.79 A,B (1.60-4.88)	3.18 A,B (1.80-5.59)	1.61 B (0.82-3.15)	3.62 A (2.14-6.11)
Open	9.23 A,B (6.44-13.24)	7.42 A (4.80-11.48)	7.14 A (4.31-11.83)	18.09 C (13.71-23.9)	14.92 B,C (10.84-20.52)	8.13 A (5.66-11.68)	22.23 C (14.10-35.05)
Water extractable Se							
Fill	0.07 A,B,C (0.03-0.17)	0.04 A (0.02-0.08)	0.08 B,C (0.03-0.21)	0.06 A,B,C (0.02-0.15)	0.06 A,B (0.03-0.10)	0.12 C (0.06-0..23)	0.08 B,C (0.05-0.14)
Grass	0.22 A (0.12-0.40)	0.15 A,B (0.10-0.24)	0.15 A,B (0.07-0.33)	0.11 B,C (0.07-0.17)	0.10 C (0.06-0.16)	0.14 A,B (0.08-0.26)	0.14 A,B (0.09-0.23)
Open	0.30 A, B,C (0.19-2.07)	0.27 B (0.15-0.49)	0.53 A,C (0.34-0.82)	0.25 B (0.18-0.35)	0.26 B (0.19-0.34)	0.38 A (0.28-0.50)	0.62 C (0.45-0.87)

* Geometric means *not* sharing the same letter within the same habitat are significantly different at a 95% confidence level.

Grassland habitat total Se concentrations are also fairly stable (Fig. 2.2.4). The only significantly different data set is in 1994, which is only lower than 1989 and 1995. Once more, no consistent trends emerge. The water-soluble Se concentrations in the same soils (Fig. 2.2.5) vary somewhat more, with highest values in 1989 and lowest in 1992 and 1993.

The distribution of average annual total Se concentrations in the Open habitat surface soils appears to fall into two ranges (Fig. 2.2.6). Mean total Se concentrations in 1989, 1990, 1991, and 1994 were around 7 to 9 mg kg^{-1}. Total Se levels in 1992, 1993, and 1995 were significantly higher, with mean values ranging from 15 to 22 mg kg^{-1}. This may be indicative of a net increasing trend, but more data are needed to confirm it. The very large +95% confidence interval for the water-soluble Se in 1989 is 2 to 6 times greater than during subsequent years. During the last four years (1992-1995) there appears to be a steady increase in soluble Se, suggesting a possible Se oxidation trend. However, total near-surface Se in 1995 was higher than in 1992 through 1994, so the relative percentage of water-soluble Se is actually *lower* in 1995 than in 1994 and about the same as in 1992 and 1993.

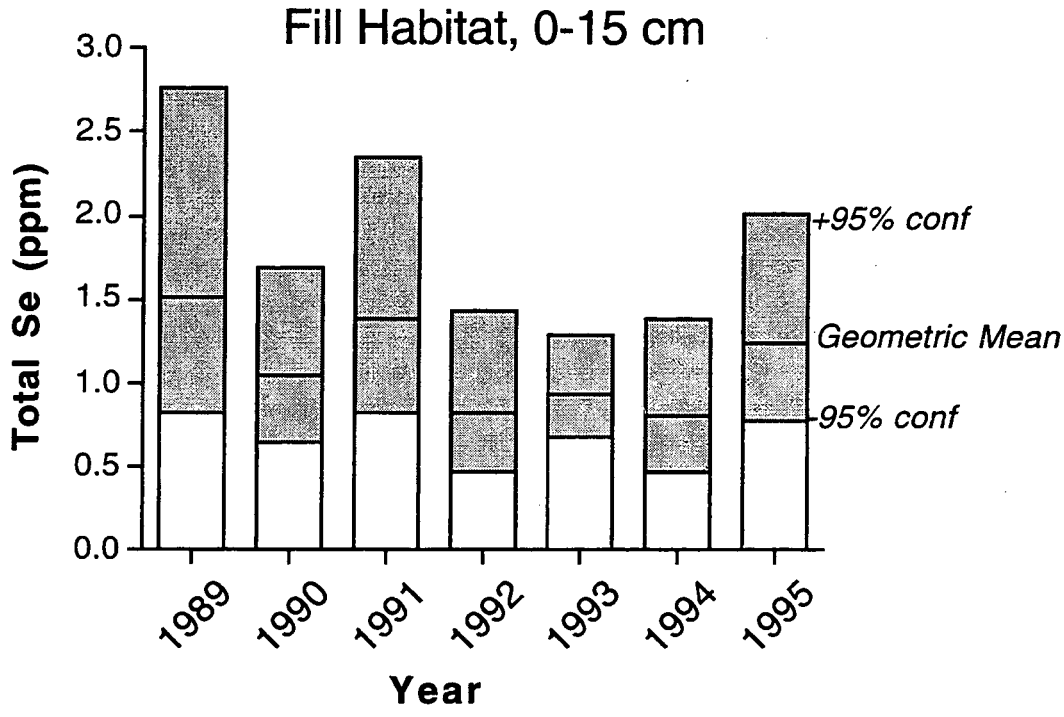

Figure 2.2.2. Total Se concentrations in the top 15 cm of soil in the Fill habitat. ANOVA showed no significant differences at the 95% confidence interval.

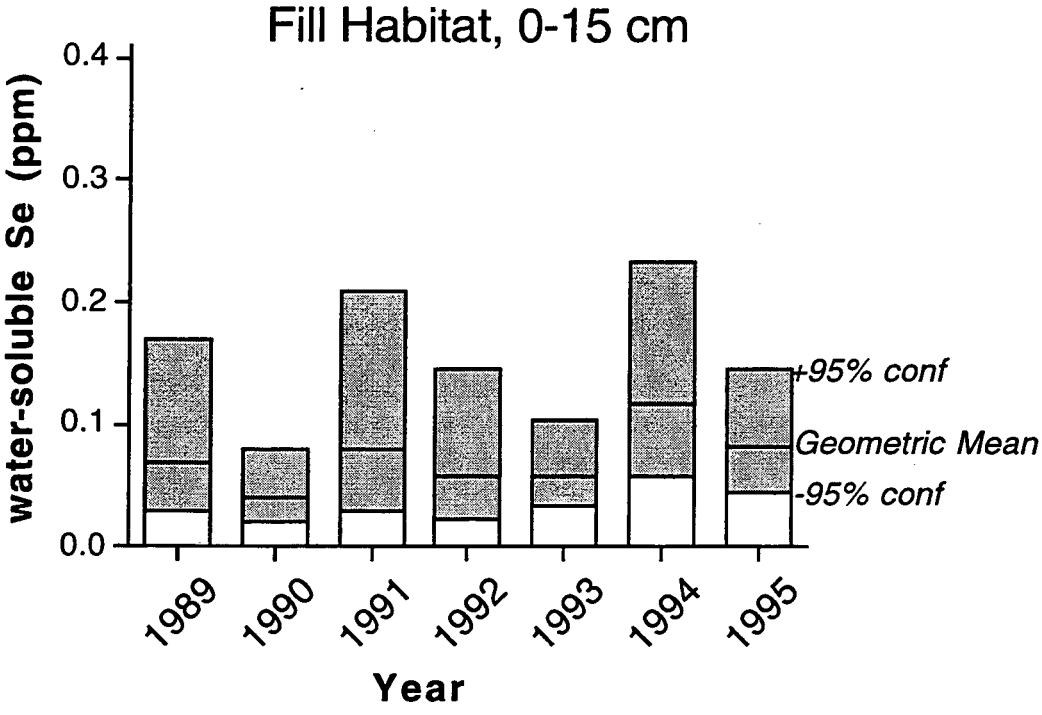

Figure 2.2.3. Water-soluble Se concentrations in the top 15 cm of soil in the Fill habitat. See Table 2.2.1 for ANOVA results.

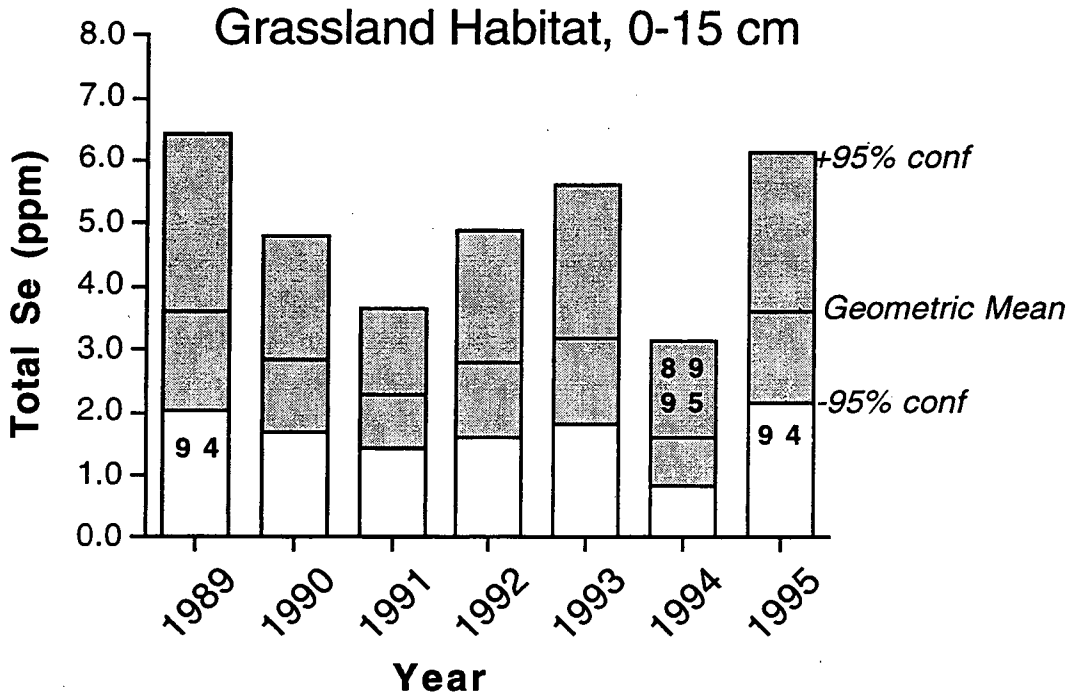

Figure 2.2.4. Total Se concentrations in the top 15 cm of soil in the Grassland habitat. Years which were significantly different at the 95% confidence interval shown for each year.

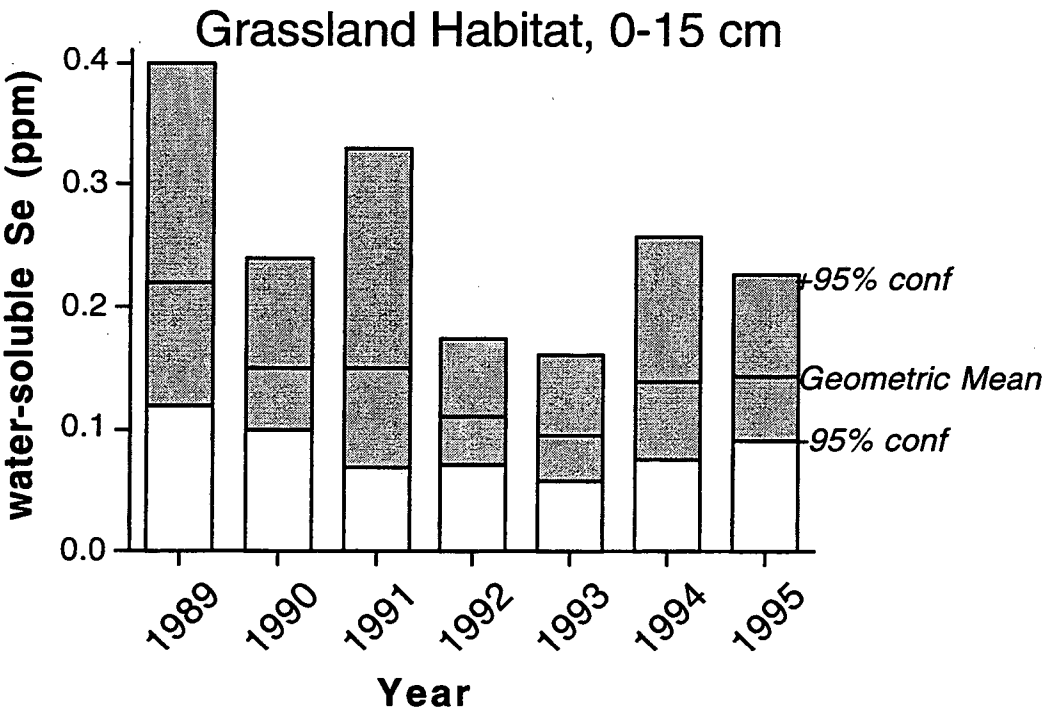

Figure 2.2.5. Water-soluble Se concentrations in the top 15 cm of soil in the Grassland habitat. See Table 2.2.1 for ANOVA results.

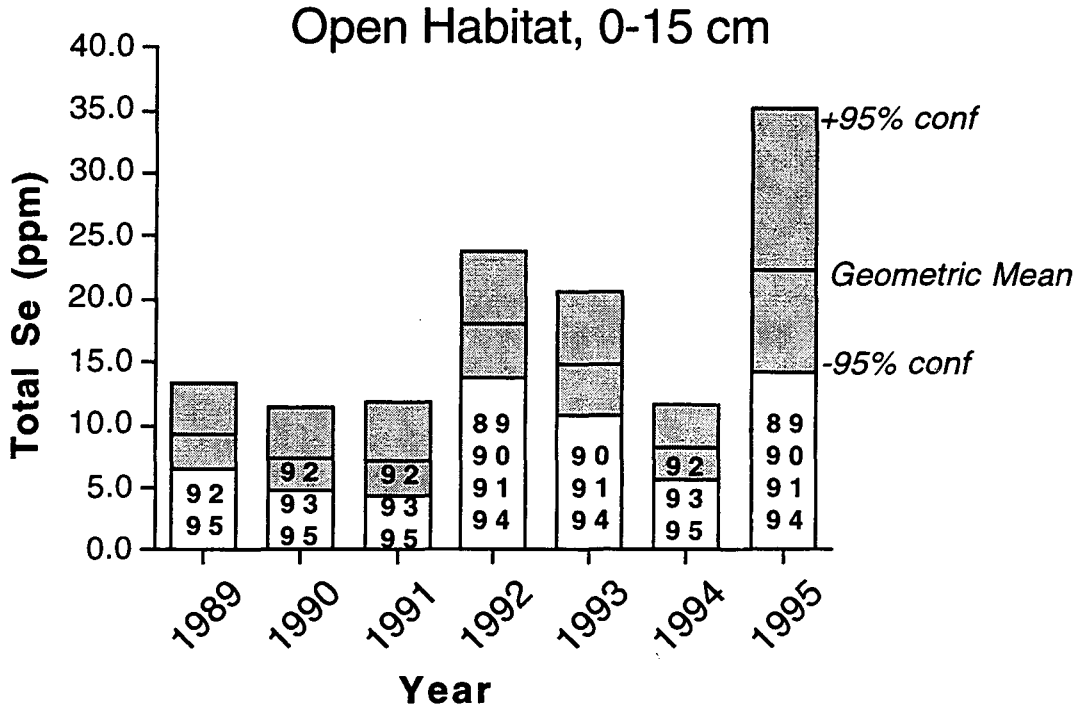

Figure 2.2.6. Total Se concentrations in the top 15 cm of soil in the Open habitat. Years which were significantly different at the 95% confidence interval shown for each year.

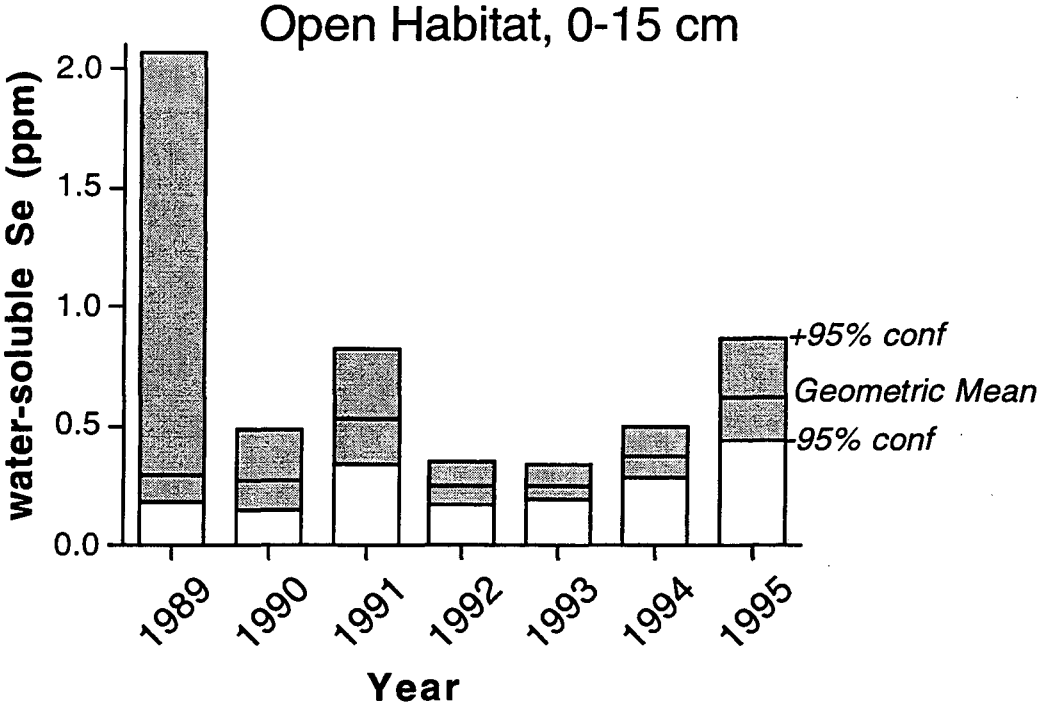

Figure 2.2.7. Water-soluble Se concentrations in the top 15 cm of soil in the Open habitat. See Table 2.2.1 for ANOVA results.

In order to better evaluate Se oxidation and solubilization rates, water-soluble Se concentrations were normalized to total Se concentrations for each given year and are shown as percentages of total Se in Fig. 2.2.8 through 2.2.10. Although it would be best to examine profile-wide trends, data below 15 cm was not collected prior to 1992. Therefore, only the fraction of soluble Se in the top 15 cm is shown. Trends differ from habitat to habitat. In the Fill habitat (Fig. 2.2.8), the soluble Se fraction in the top 15 cm has generally risen over the 7 year period, from around 4% to around 6%. A large increase in 1994, to 15%, is the only statistically significant ($P<0.05$) difference in this data set. In the Grassland habitat (Fig. 2.2.9), there has been a net decrease in the fraction of soluble Se in the top 15 cm, from 6% to around 4%, but similar to the Fill habitat, there was an increase in 1994, to almost 9%. However, none of the changes in this data set are significant ($P<0.05$). There are no consistent trends in the Open habitat data (Fig. 2.2.10) and there appears to be no net change in soluble Se fraction. A peak of soluble Se fraction was observed in 1991, at nearly 8%. Soluble Se percentage was significantly ($P<0.05$) lower in 1992 and 1993 than in 1991 and 1994. Otherwise, no significant changes were observed. The associated uncertainties in this data are large because they represent the combined uncertainties in the total Se and water-soluble Se data.

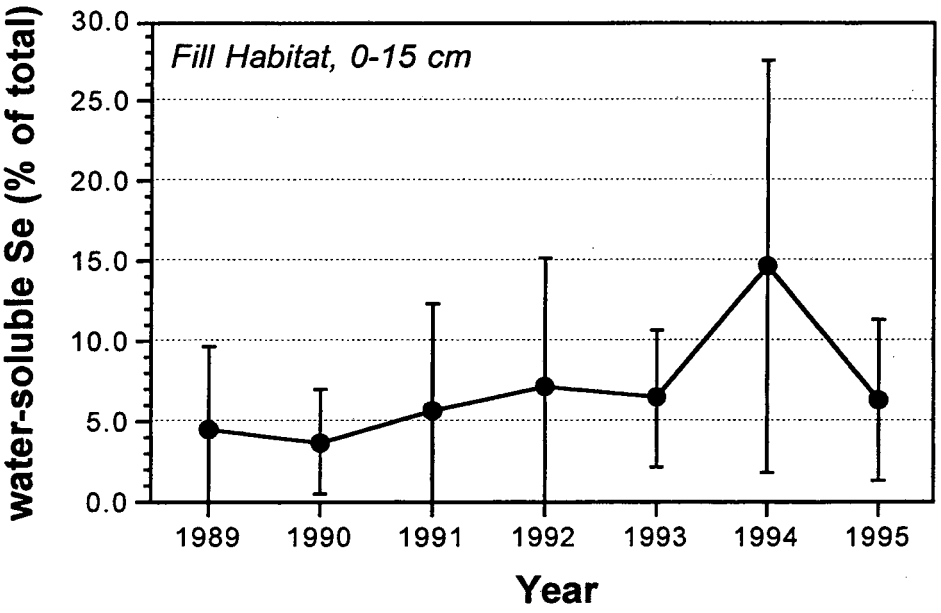

Figure 2.2.8. Water-soluble Se concentrations in the top 15 cm of Fill habitat soil, shown as percentage of total Se.

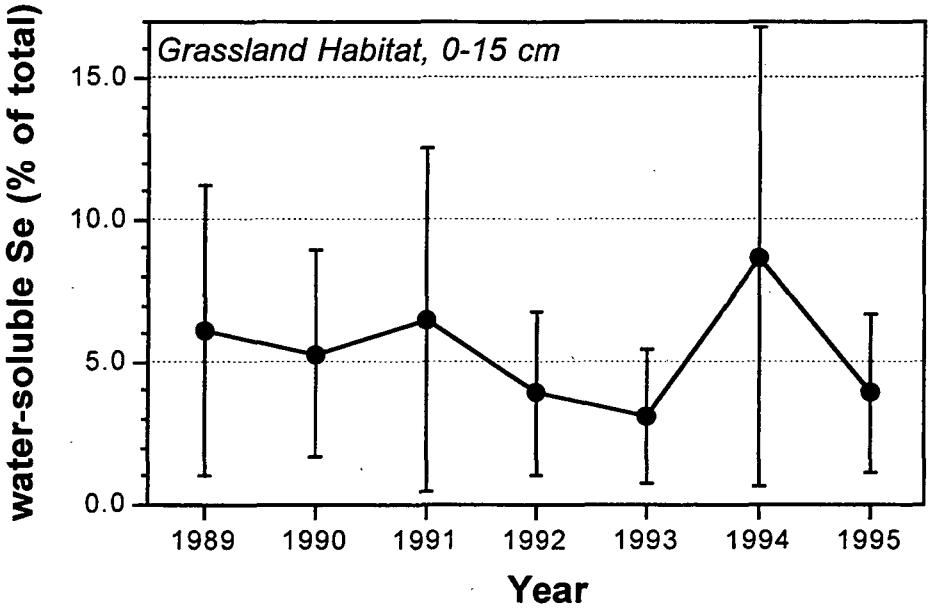

Figure 2.2.9. Water-soluble Se concentrations in the top 15 cm of Grassland habitat soil, shown as percentage of total Se.

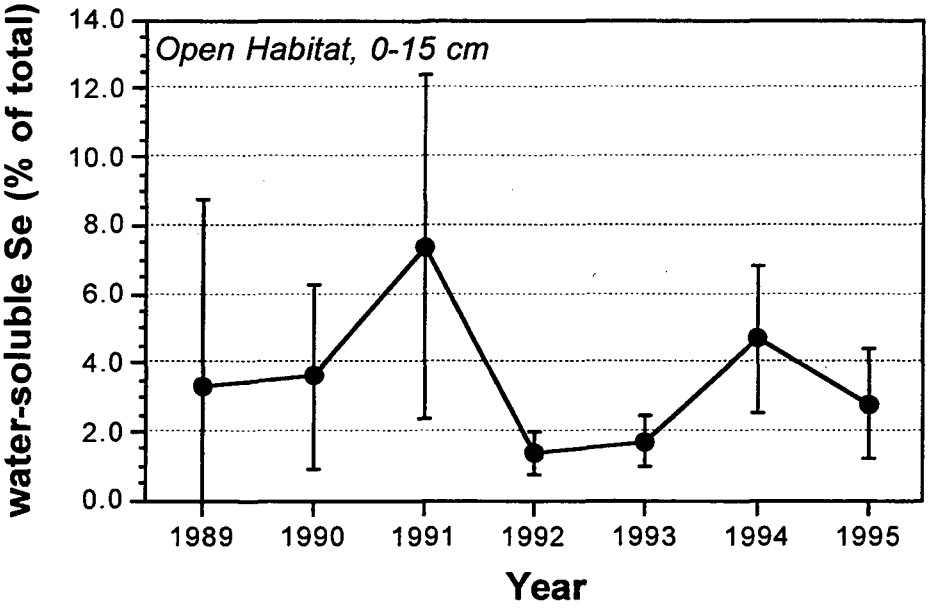

Figure 2.2.10. Water-soluble Se concentrations in the top 15 cm of Open habitat soil, shown as percentage of total Se.

2.2.5. Se Trends in Deeper (15-100 cm) Soils

Although surface soils are apparently the most direct source of Se to the biological system, deeper soils are an indirect but possibly equally important source via plant uptake. Total Se

concentrations in the 15-50 cm and 50-100 cm intervals have not changed over the studied period (1992-1995). In the 15-50 cm interval, total Se concentrations range from 1.7 to 3.1 ppm in the Fill habitat, 0.5 to 1 ppm in the Grassland habitat, and 0.8 to 1.8 ppm in the Open habitat. In the 50-100 cm interval, total Se levels range from 0.6 to 1.3 ppm in the Fill habitat, 0.5 to 1.0 ppm in the Grassland habitat, and 0.6 to 1.3 ppm in the Open habitat. Of greater importance from the perspective of plant-root uptake are water-soluble Se concentrations, since those represent the Se inventory which is more immediately available to plant roots. Water-soluble Se concentrations in the 50-100 cm interval did not vary and averaged around 0.2 ppm in all habitats. Data from the 15-50 cm interval is shown in Fig. 2.2.11 to 2.5.13. Recall that these samples were not collected prior to 1992.

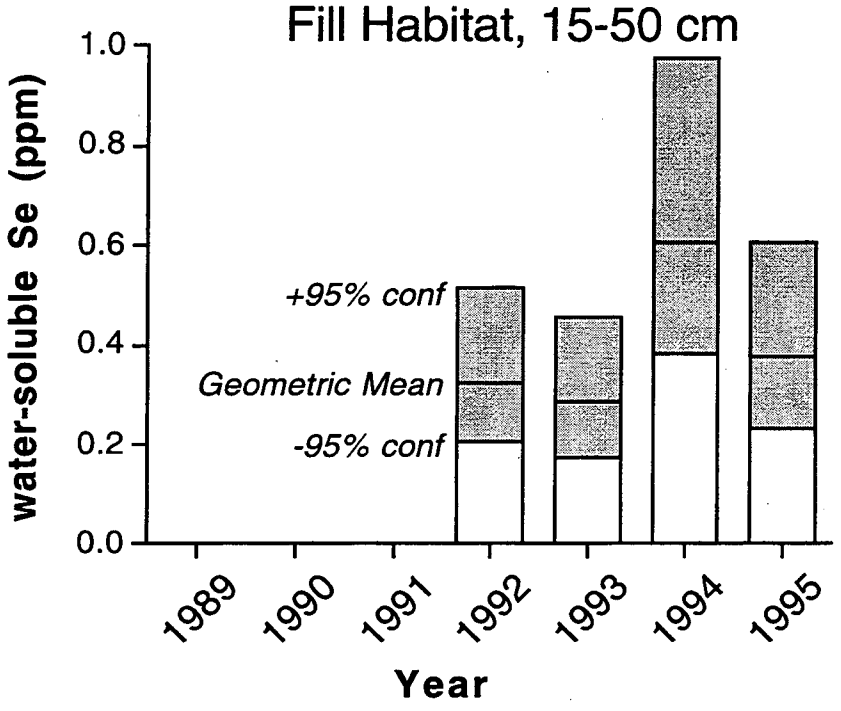

Figure 2.2.11. Water-soluble Se concentrations in the 15-50 cm soil interval in the Fill habitat.

Although there are some significant differences between soluble Se concentrations from year to year, there appear to be no net changes. Soluble Se in this depth interval was highest in 1994 for all habitats. The relatively higher concentrations in the Fill habitat (Fig. 2.2.11) are due to the fact that these are in what used to be contaminated surface soils, now covered by fill soils. Therefore, it may not be surprising to find deep-rooted plants growing in Fill areas with higher tissue-Se levels than those growing in Open or Grassland areas. However, these differences should be minor.

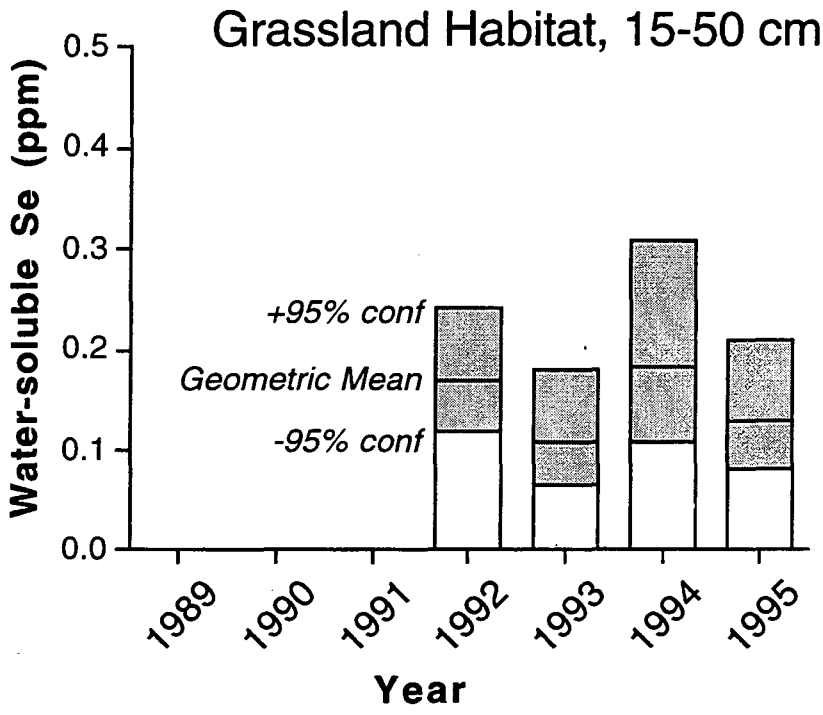

Figure 2.2.12. Water-soluble Se concentrations in the 15-50 cm soil interval in the Grassland habitat.

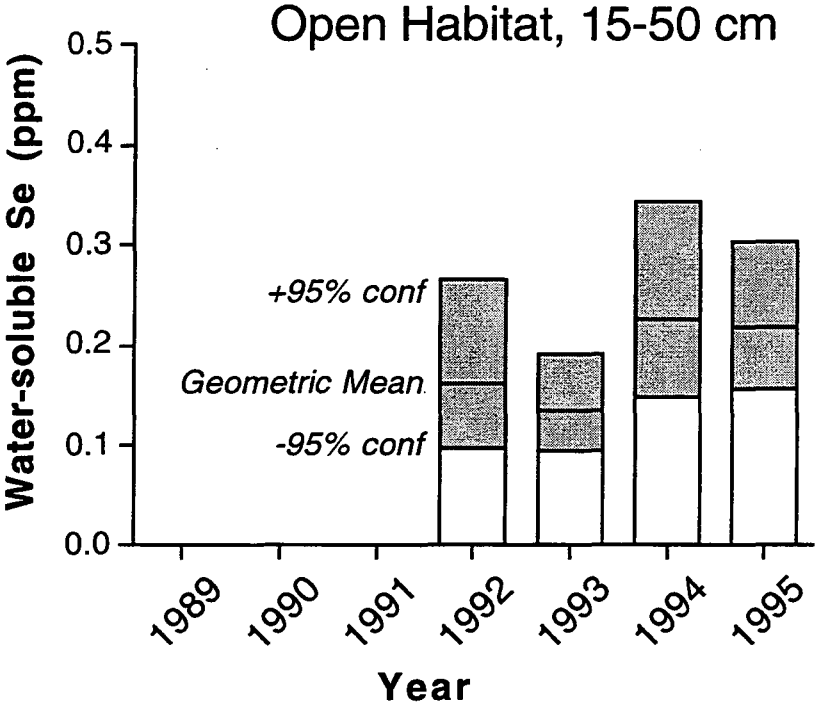

Figure 2.2.13. Water-soluble Se concentrations in the 15-50 cm soil interval in the Open habitat.

2.2.6. Se Concentrations Integrated Over All Intervals

Intensive process-oriented monitoring performed within small experimental plots throughout Kesterson has shown vertical displacement of soluble Se in the soil profile due to infiltration of rainwater or evapotranspirative fluxes (Zawislanski et al., 1992). These fluxes can often markedly affect the year-to-year distribution of Se within the soil profile. Therefore, it is important to account for Se throughout the profile in order to assess net Se losses due to volatilization or immobilization below the water table. Se concentrations were converted to Se mass per area and then integrated over the interval of 0-100 cm. The results are shown in Fig. 2.2.14 through 2.2.16. Because only the 0-15 cm interval was sampled through 1991, only 1992-1995 data can be included in this analysis.

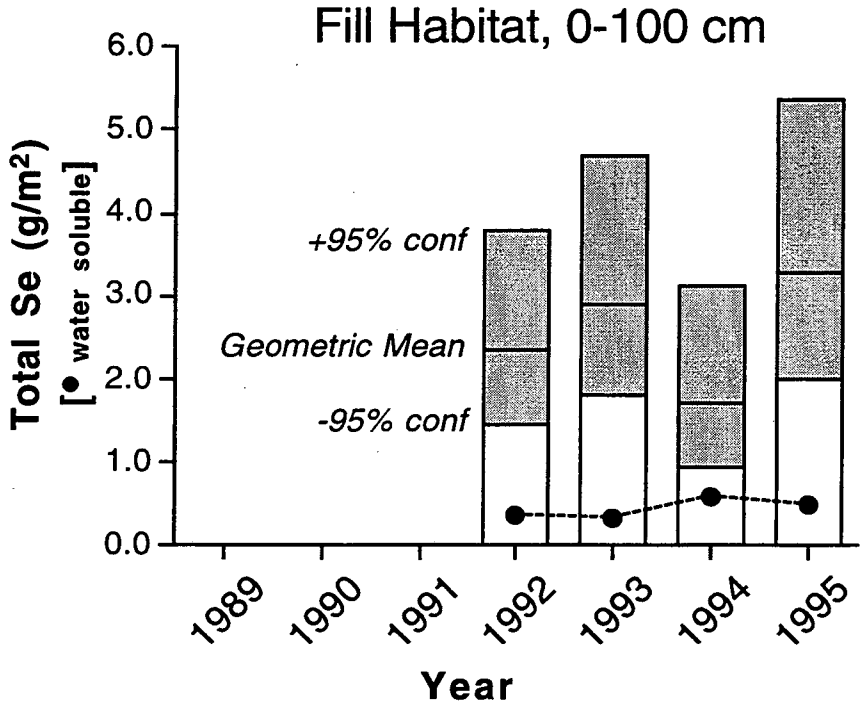

Figure 2.2.14. Total and water-soluble Se inventory in the top 100 cm of soil in the Fill habitat.

The overall total and soluble Se trends in the Fill and Grassland habitats are similar. Only a decrease in total Se in 1994 is significant at the 95% confidence interval. There was an increase in total Se from 1992 to 1993, a decrease from 1993 to 1994, and a marked increase from 1994 to 1995. There is not net change over the four years. Soluble Se trends are qualitatively opposite from total Se trends. A slight net increase is observed in the Fill habitat.

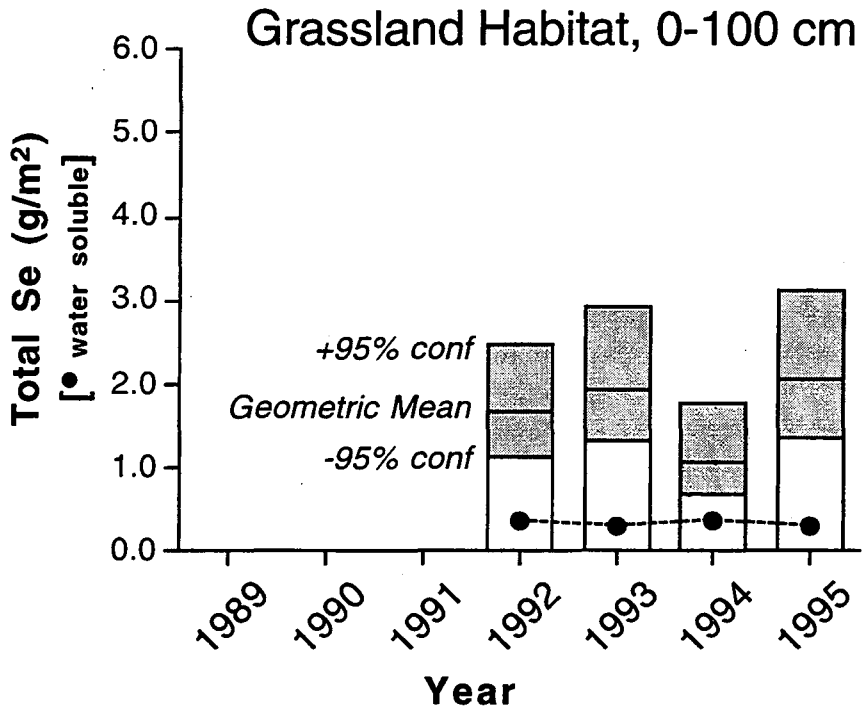

Figure 2.2.15. Total and water-soluble Se inventory in the top 100 cm of soil in the Grassland habitat.

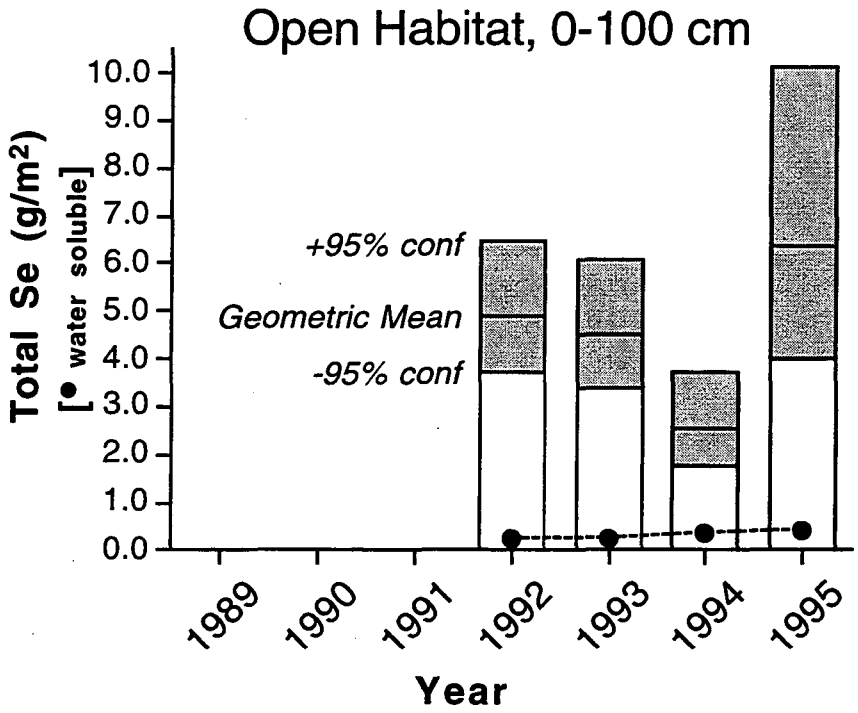

Figure 2.2.16. Total and water-soluble Se inventory in the top 100 cm of soil in the Open habitat.

In the Open habitat, there is no total Se change from 1992 to 1993, followed by a statistically significant decrease in 1994, followed by a marked increase in 1995. Water soluble Se mass steadily increases over the four-year period.

2.2.7. Discussion and Summary

The analysis of the data by habitat has helped identify trends, or lack thereof, which are habitat-specific and those which are more universal. The absence of any statistically-significant changes in the total Se measured in the surface soils of the Fill habitat is evidence for a lack of net enrichment of the fill soils with Se which may be moving upward in the profile due to evapotranspirative fluxes. Since samples are collected only once a year, it is impossible to say, based on this data alone, whether Se is moving up in the summer and vertically down in the winter due to infiltration, but other, more detailed studies have shown this to occur (Zawislanski et al., 1995, Section 2.5). Similarly, year-to-year changes in Se concentrations in the Grassland habitat are minor, with no long-term trends emerging. Open habitat total Se values seem to fluctuate much more than in the other habitats, although the reason for this is not clear. Leaching of the water-soluble Se fraction below the monitored interval, if it occurs, would be far too small to account for total Se changes observed between 1991 and 1992 or between 1993 and 1994, and again between 1994 and 1995. It is possible that the number of samples collected each year within this habitat is not large enough to adequately describe the statistical distribution of soil Se concentrations. Considering that caveat, it may not be possible to conclusively state that there are no consistent trends in total Se concentrations in the Open habitat, but the available data do support such a statement.

3 Ephemeral Pools: Selenium Levels, Distribution, and Transformations

Tetsu Tokunaga
Earth Sciences Division
Lawrence Berkeley Laboratory

Over the past 10 years, we have obtained water quality data from ephemeral pools formed under various conditions. Pools have formed from surface runoff originating from intentionally ponded areas, from water table rise into topographic depressions, and from rainfall ponding. Since drainage of ponds and filling of many of the topographically lower areas within Kesterson Reservoir in 1988, rainfall ponding has been the main cause of ephemeral pools. Data on selenium concentrations and salinities in ephemeral pools have been presented in previous LBNL and USBR reports. In this chapter, we present (1) a summary of ephemeral pool water quality data from the 1994-1995 and 1995-1996 wet seasons, (2) a method for estimating the time interval over which rainfall-generated ephemeral pools occur, and (3) results from laboratory studies on Se transfers from pool waters into sediments.

3.1 Summary of Wet Season Ephemeral Pools

This section updates observations reported previously up through the 1993-1994 wet season (Tokunaga, 1995). We include summaries of Se concentrations and salinity (electrical conductivity) of pool waters sampled during the 1994-95, and 1995-96 wet seasons.

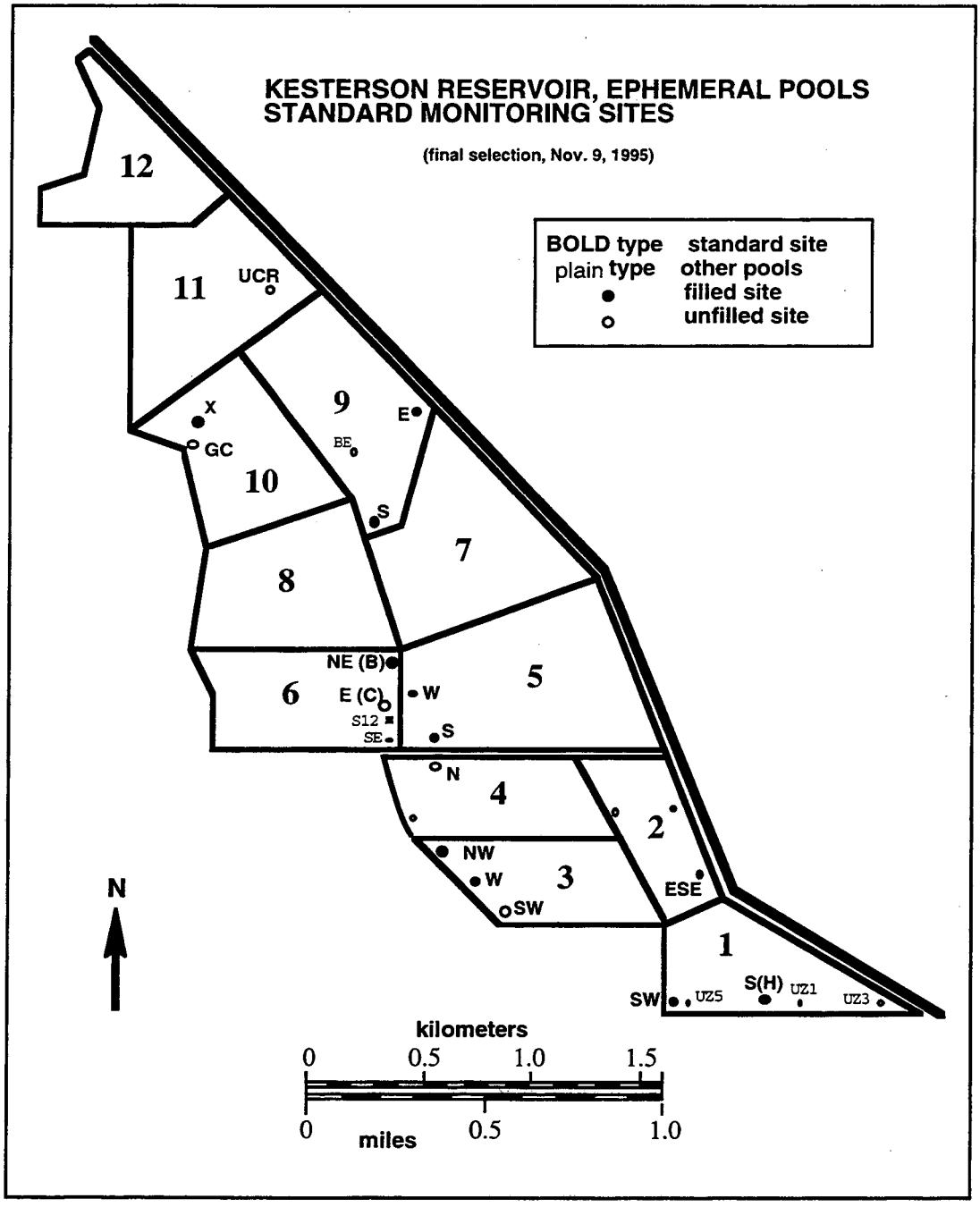

Figure 3.1.1. Map of Kesterson Reservoir showing locations of ephemeral pool sampling sites.

3.1.1 Site Descriptions and Sampling

During previous years, a wide variety of ephemeral pools have been sampled, with only a subset receiving relatively regular monitoring. In November of 1995, a set of 16 ephemeral pool sites was selected for such regular monitoring. The locations of these standard ephemeral pool sampling sites are shown in Fig. 3.1.1. The various surface soil conditions currently found at Kesterson Reservoir are included. Sites 2ESE, 4N, 6E, 10GC, and 11UCR are unfilled. Site 10GC, which is a saline surface depression and remnant tributary to Mud Slough, is known to flood by water table rise during the wet season. Sites 2ESE and 4N, which once contained cattails, have high Se concentrations in both surface soils and in the thick organic litter layers (partially decomposed cattail vegetation). Site 6E is at the center of a small topographic depression which floods by rainfall ponding rather than by water table rise. The vegetation in this undisturbed "upland" environment is dominated by annual grasses and some saltgrass. Site UCR is an extensive saline "playa" area which also formerly was part of a higher elevation tributary to Mud Slough. Sites 1S, 1SW, 3SW, 3W, 3NW, 5S, 5W, 6NE, 9S, 9E, and 10X are all filled areas. However, it should be noted that some of these areas include original Kesterson Reservoir soils as a significant part of the surface fill. These include sites 3W, 3NW, 5W, and 9S. Samples were collected by both the USBR and LBNL. The USBR-collected subsamples were split from their samples prior to filtration, and filtered (0.45 μm) later at LBNL. The LBNL-collected samples were either filtered at the time of sampling or prior to analysis at LBNL. All samples were refrigerated during storage.

3.1.2 Results

The data are presented as time trends for pool water Se and EC. In many cases, trends within a particular pool from previous years are plotted together for comparison. In addition, we have plotted time trends of the ratios of pool water Se concentrations to ECs, normalized to the value of this ratio at the first sampling of the season. These normalized Se/EC plots permit estimates of relative amounts of Se (relative to major soluble salts) transferred from pool waters into shallow sediments. Data presented here were collected by both the USBR and LBNL. Time trends for pool Se concentrations during early 1995 and 1996 are presented in Figs. 3.1.2a-3.1.2d. Information on distributions of major rainfall events subsequent to initial ponding is included in these figures. Comparisons of pool Se concentration trends from previous years, and for a limited set of data from the current wet season, are presented for a subset of pools in Figs. 3.1.3a-3.1.3f. Pool water salinities (ECs) are presented as time trends in Figs. 3.1.4a-3.1.4d.

Time trends in ratios of Se to EC in pool waters were also plotted, in order to qualitatively determine relative transfers of Se (versus major soluble salts) from pools back into sediments.

These plots (Figs. 3.1.5a-3.1.5d) are all normalized to the Se/EC ratio obtained in the initial sample from each site.

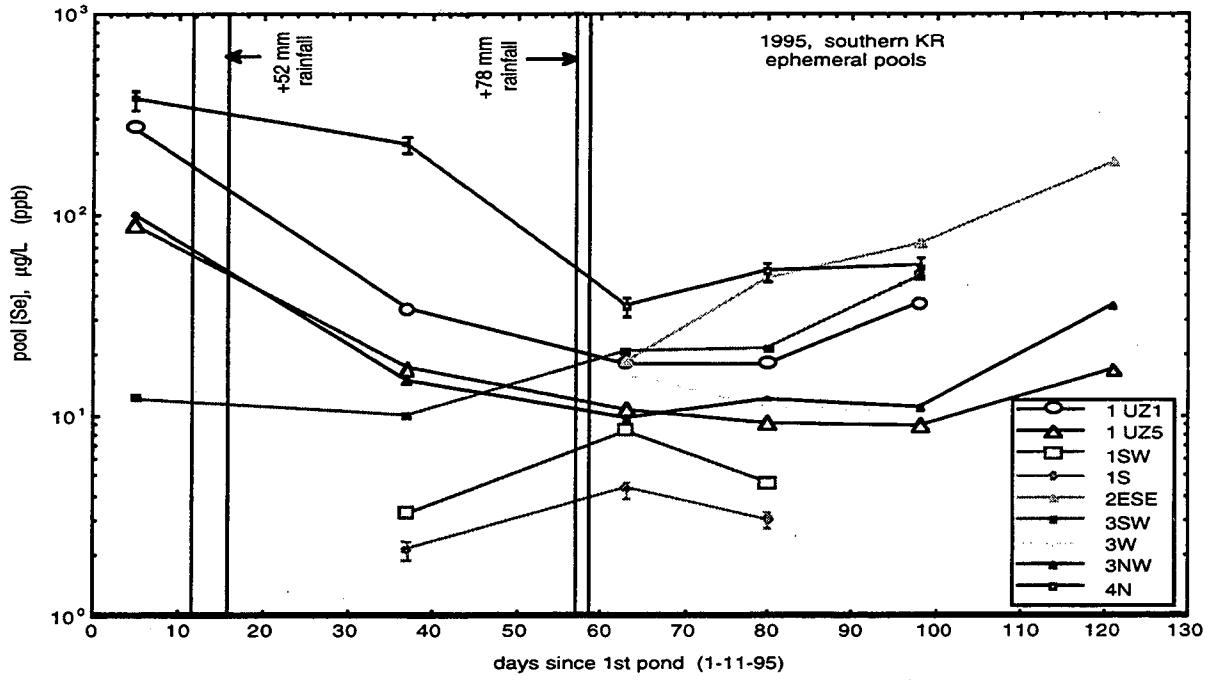

Figure 3.1.2a. Time trends in ephemeral pool Se concentrations. 1994-1995 wet season, southern pools.

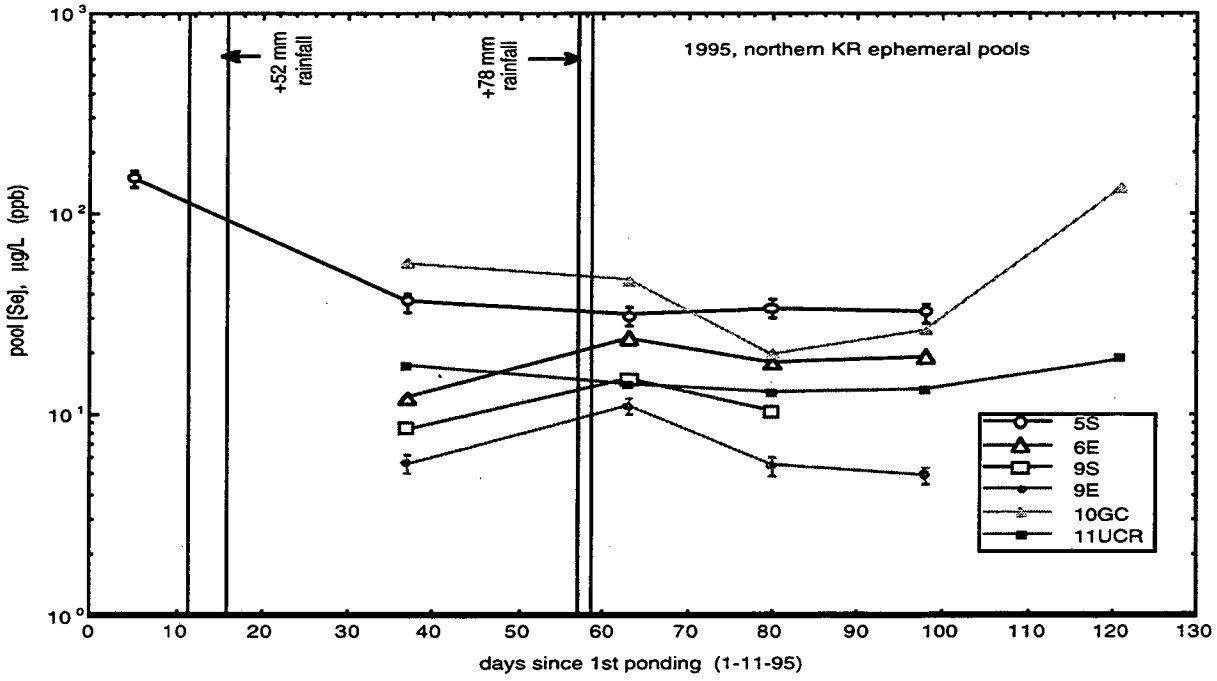

Figure 3.1.2b. Time trends in ephemeral pool Se concentrations. 1994-1995 wet season, northern pools.

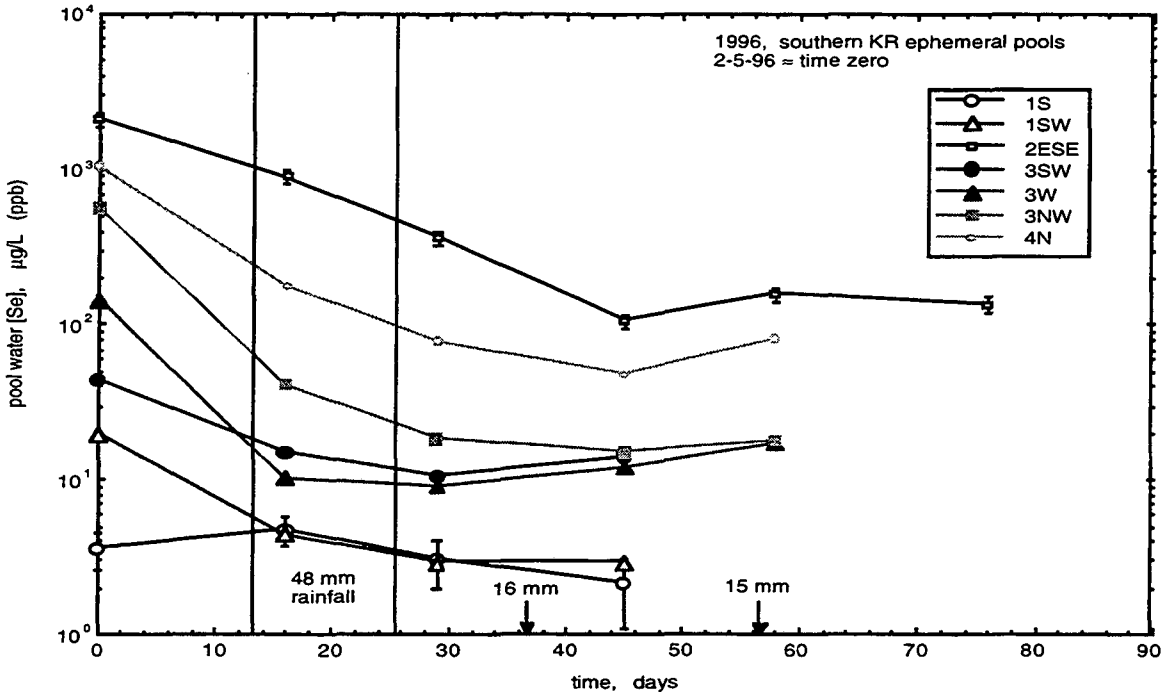

Figure 3.1.2c. Time trends in ephemeral pool Se concentrations. 1995-1996 wet season, southern pools.

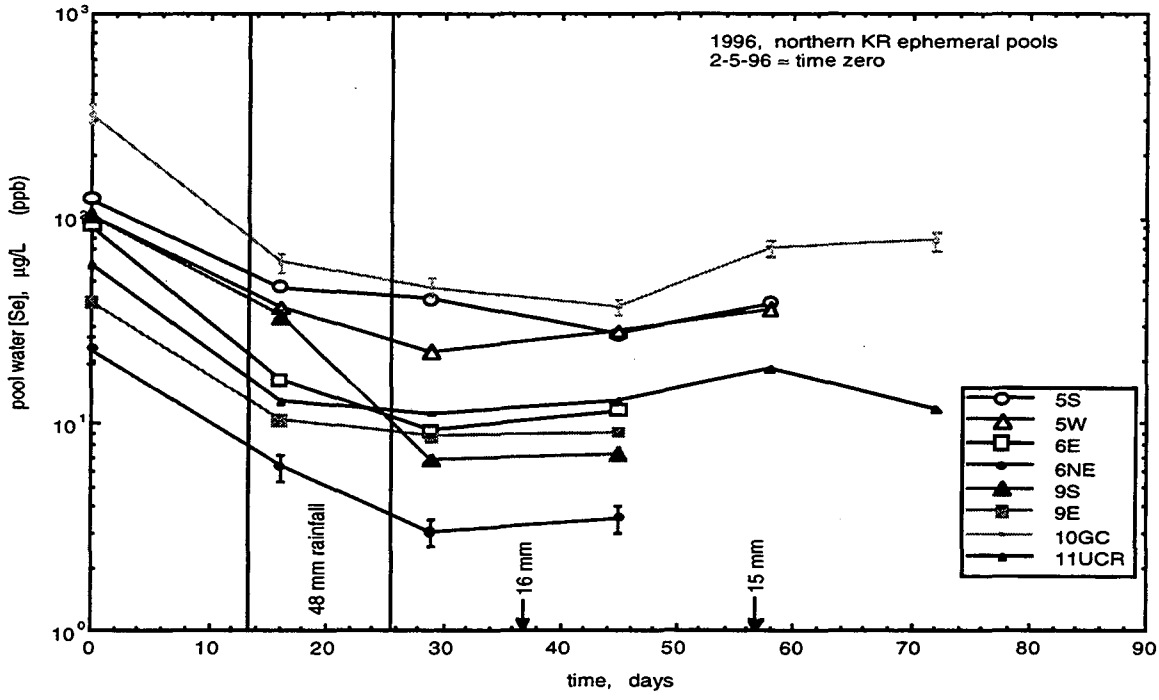

Figure 3.1.2d. Time trends in ephemeral pool Se concentrations. 1995-1996 wet season, northern pools.

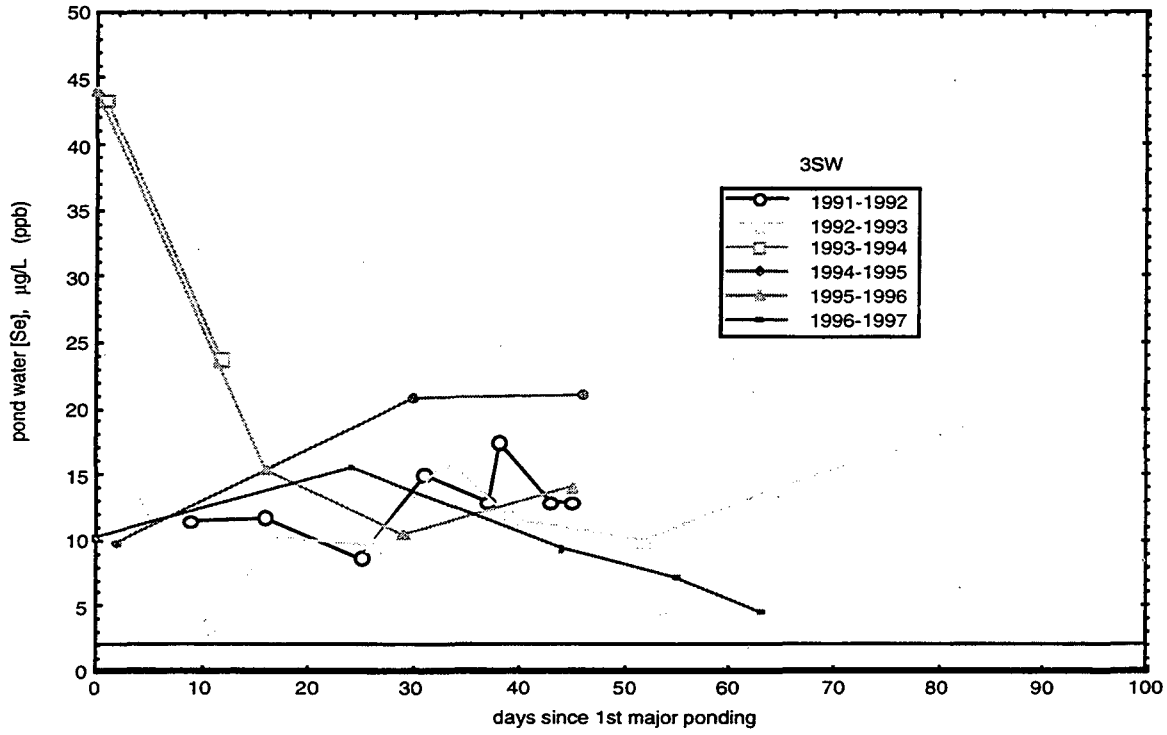

Figure 3.1.3a. Comparison of yearly trends in pool water Se concentrations at filled site 3SW. The horizontal line at 2 µg/L indicates the wetland surface water quality goal.

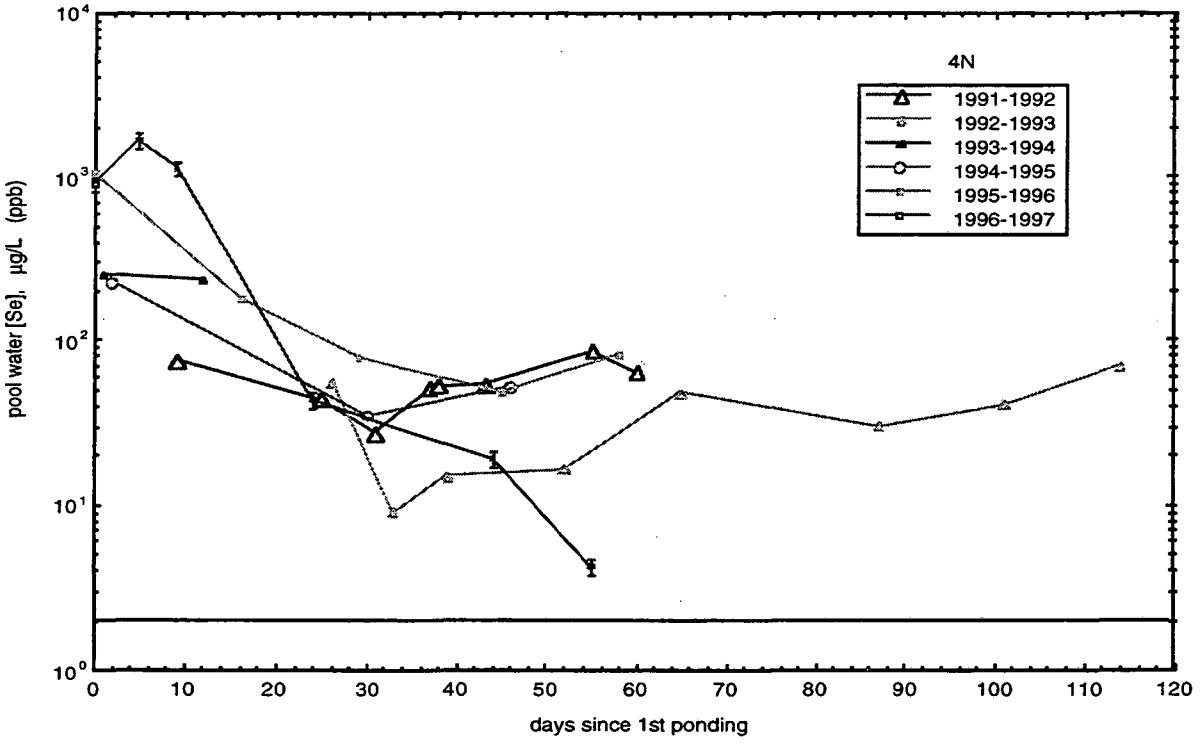

Figure 3.1.3b. Comparison of yearly trends in pool water Se concentrations at cattail site 4N. The horizontal line at 2 µg/L indicates the wetland surface water quality goal.

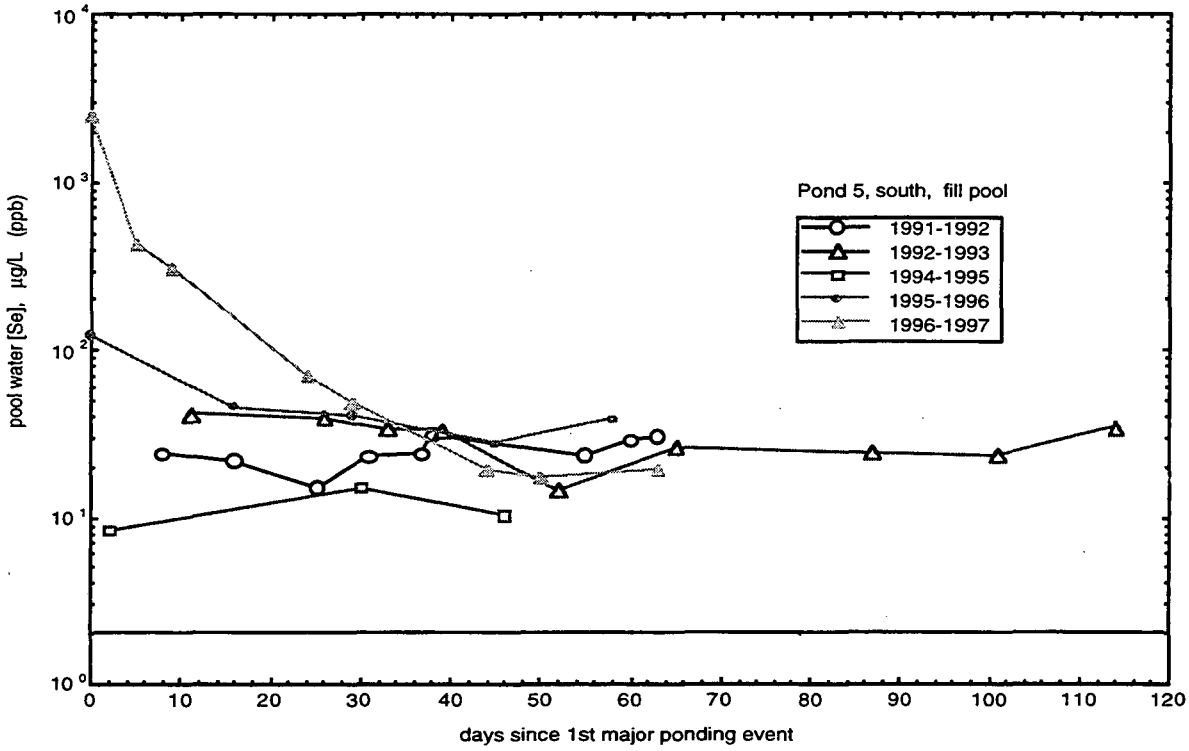

Figure 3.1.3c. Comparison of yearly trends in pool water Se concentrations at filled site 5S. The horizontal line at 2 µg/L indicates the wetland surface water quality goal.

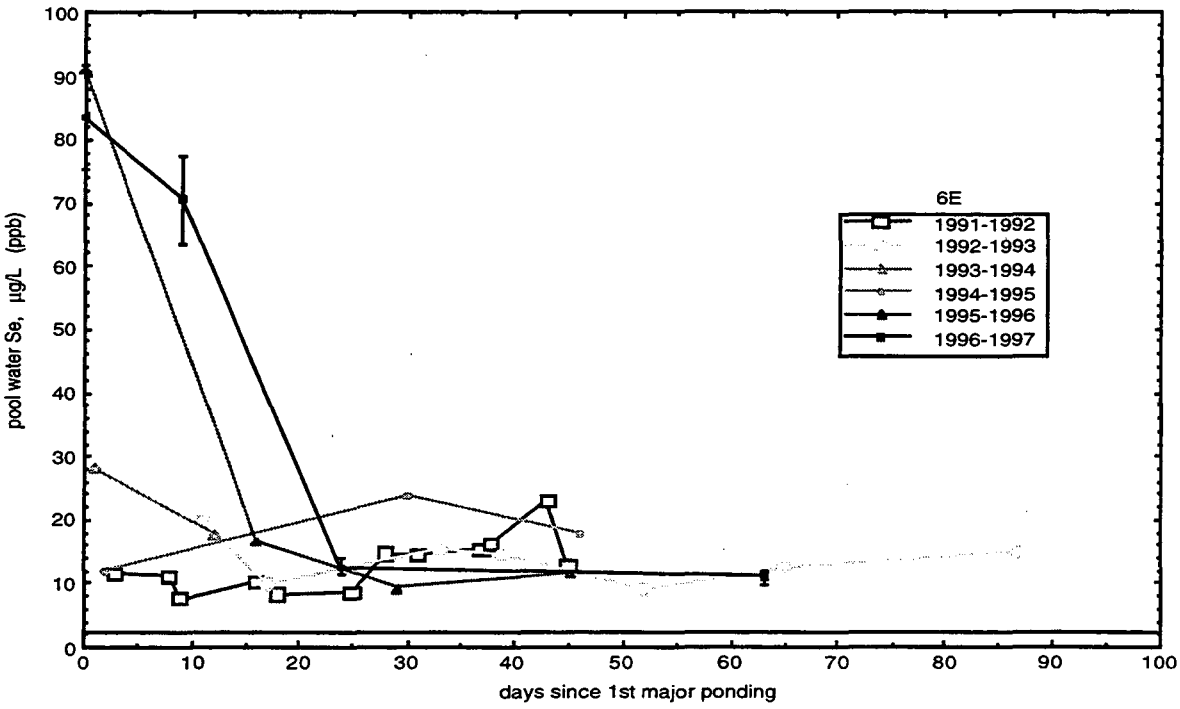

Figure 3.1.3d. Comparison of yearly trends in pool water Se concentrations at upland site 6E. The horizontal line at 2 µg/L indicates the wetland surface water quality goal.

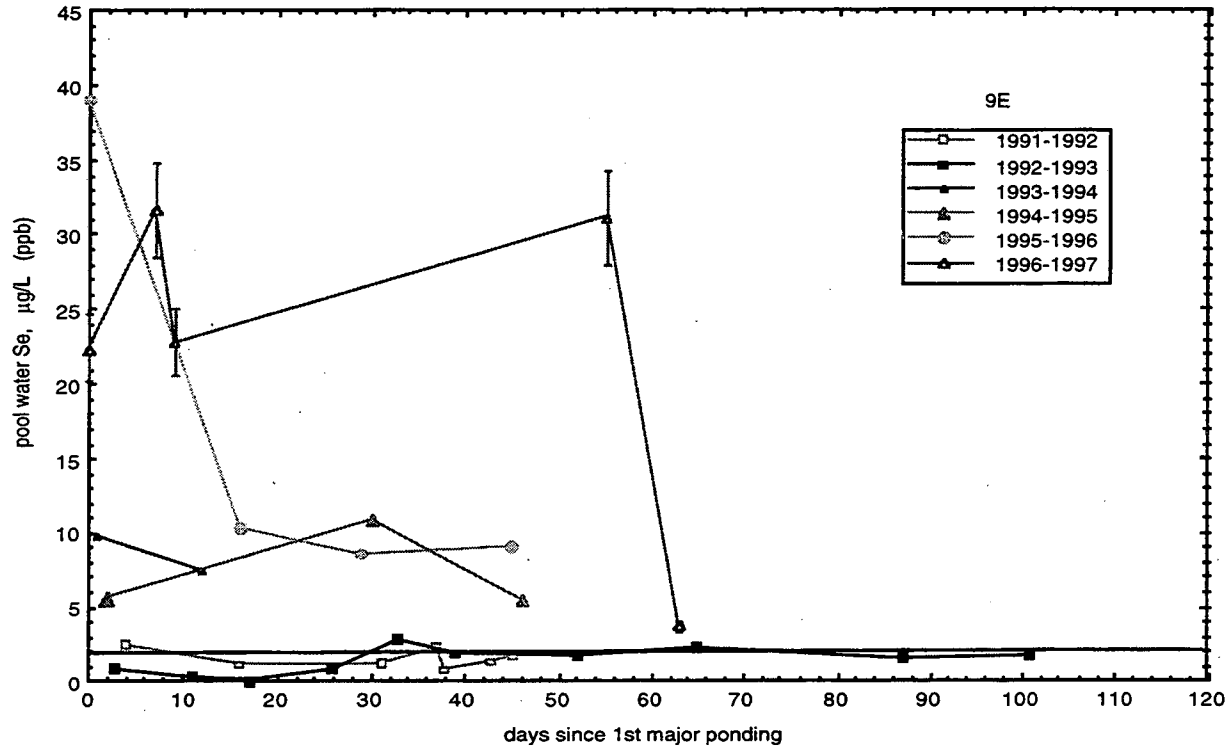

Figure 3.1.3e. Comparison of yearly trends in pool water Se concentrations at filled site 9E. The horizontal line at 2 µg/L indicates the wetland surface water quality goal.

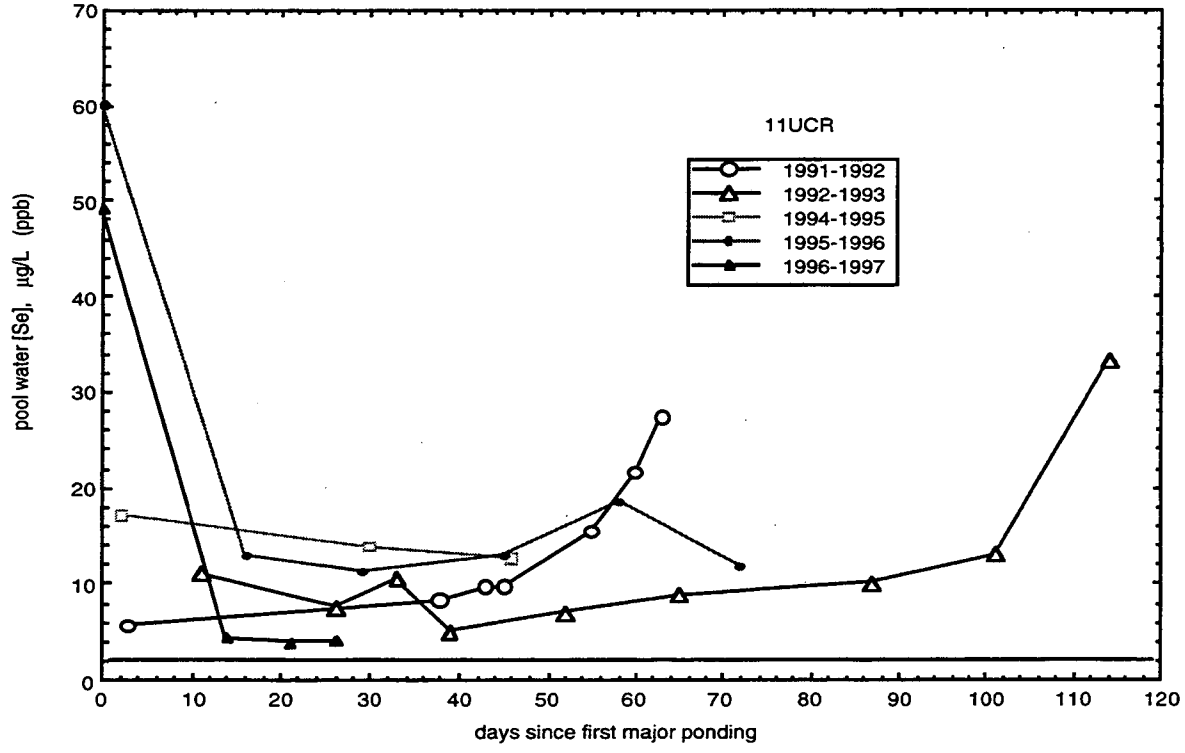

Figure 3.1.3f. Comparison of yearly trends in pool water Se concentrations at playa site 11UCR. The horizontal line at 2 µg/L indicates the wetland surface water quality goal.

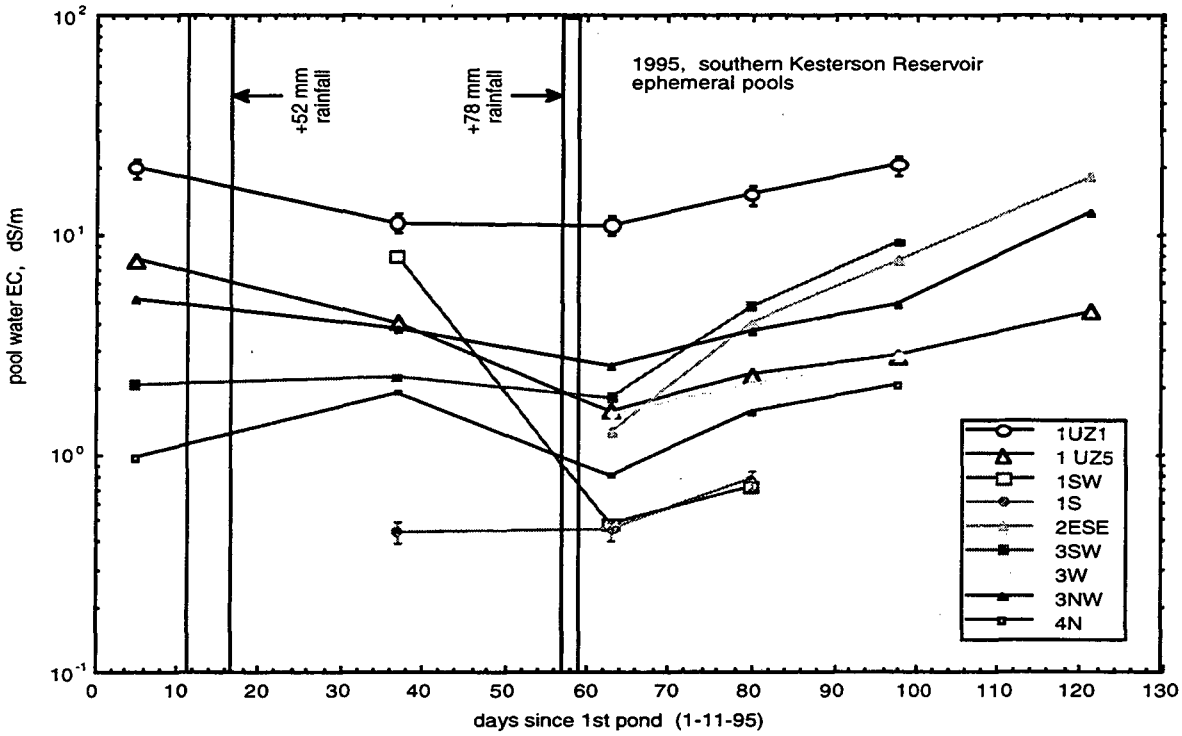

Figure 3.1.4a Time trends in 1995 ephemeral pool water salinities (southern KR pools).

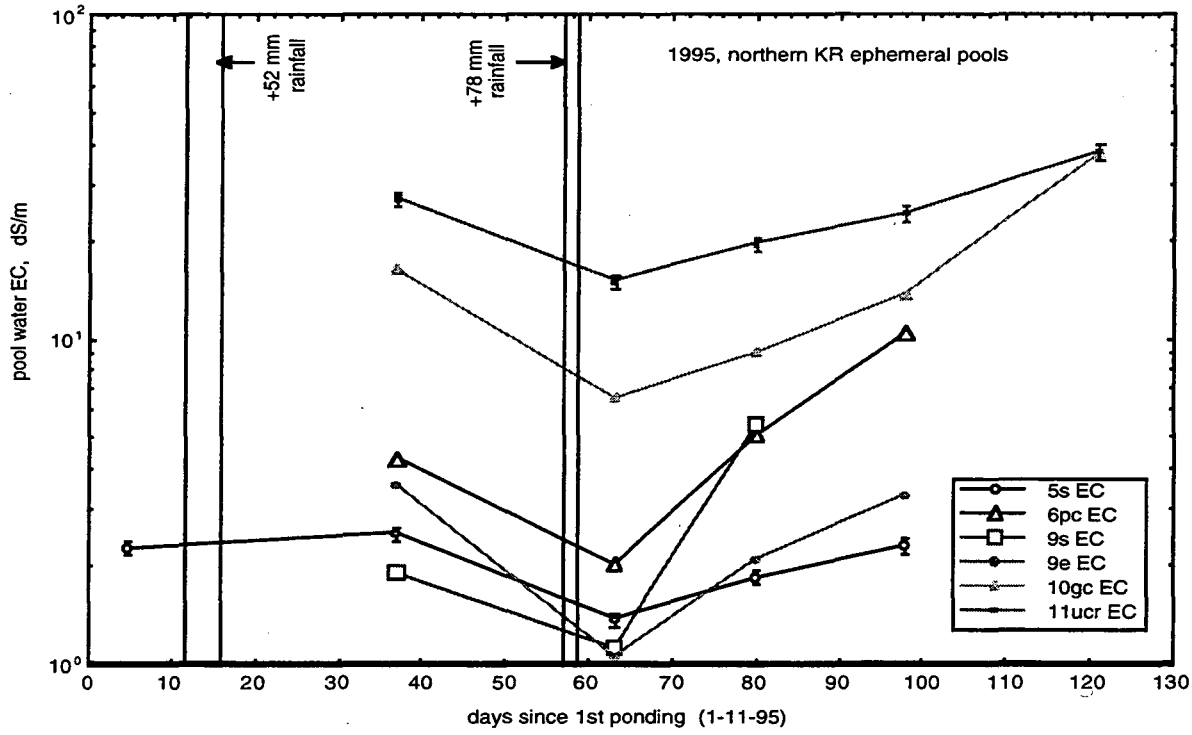

Figure 3.1.4b Time trends in 1995 ephemeral pool water salinities (northern KR pools).

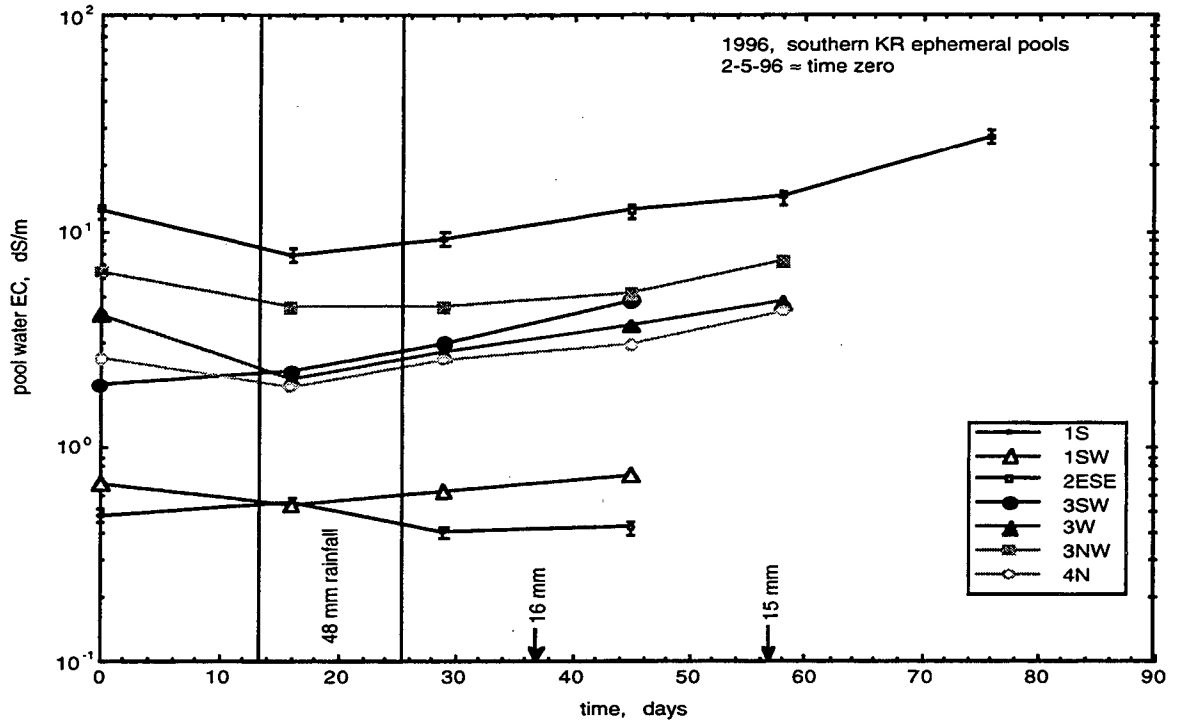

Figure 3.1.4c Time trends in 1996 ephemeral pool water salinities (southern KR pools).

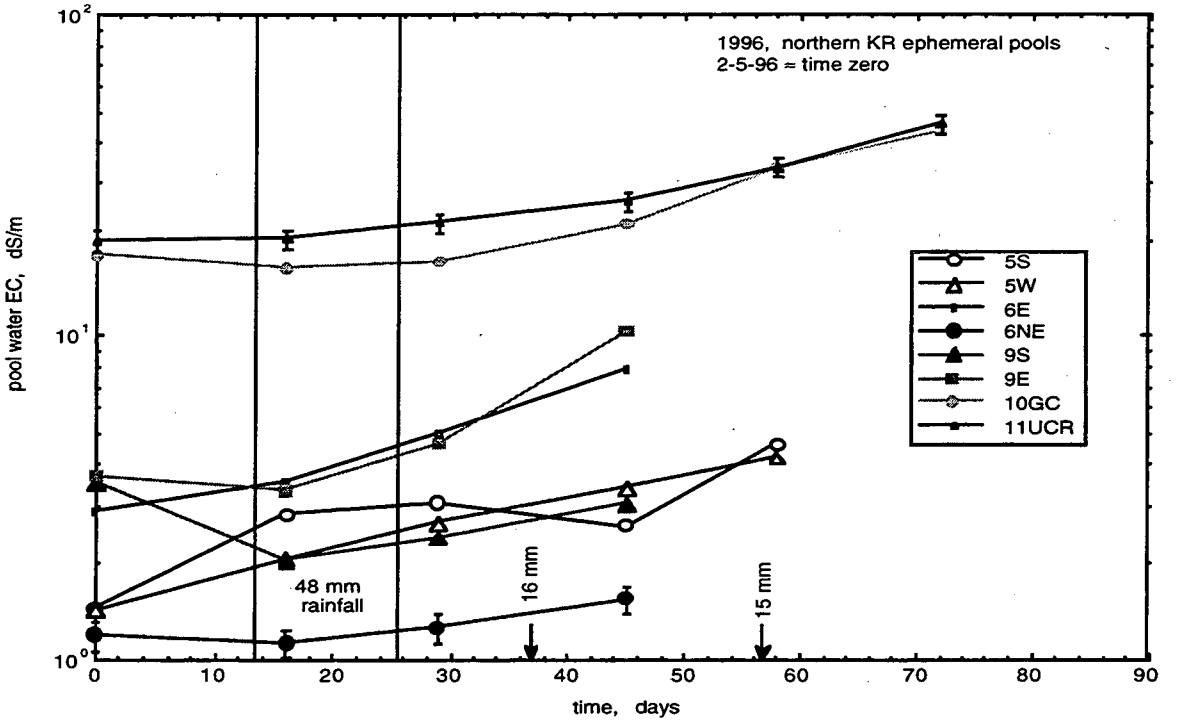

Figure 3.1.4d. Time trends in 1996 ephemeral pool water salinities (northern KR pools).

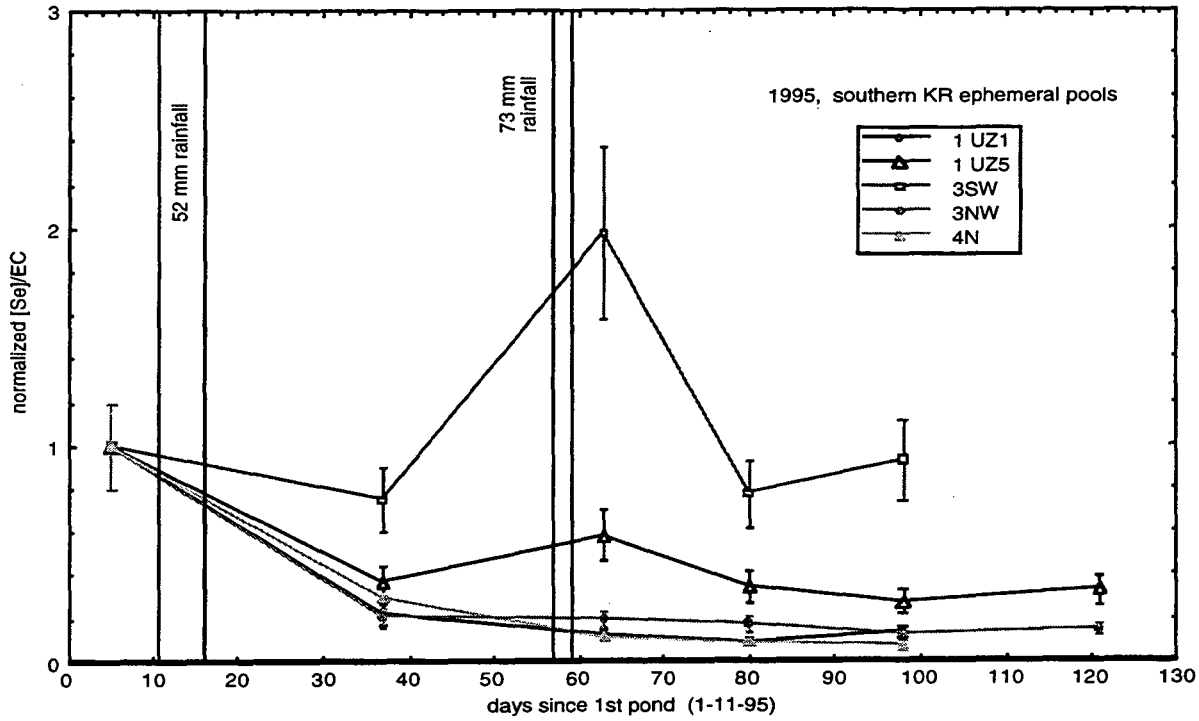

Figure 3.1.5a. Trends in ratios of pools Se to EC, normalized to values in initial samples. 1995, southern KR pools.

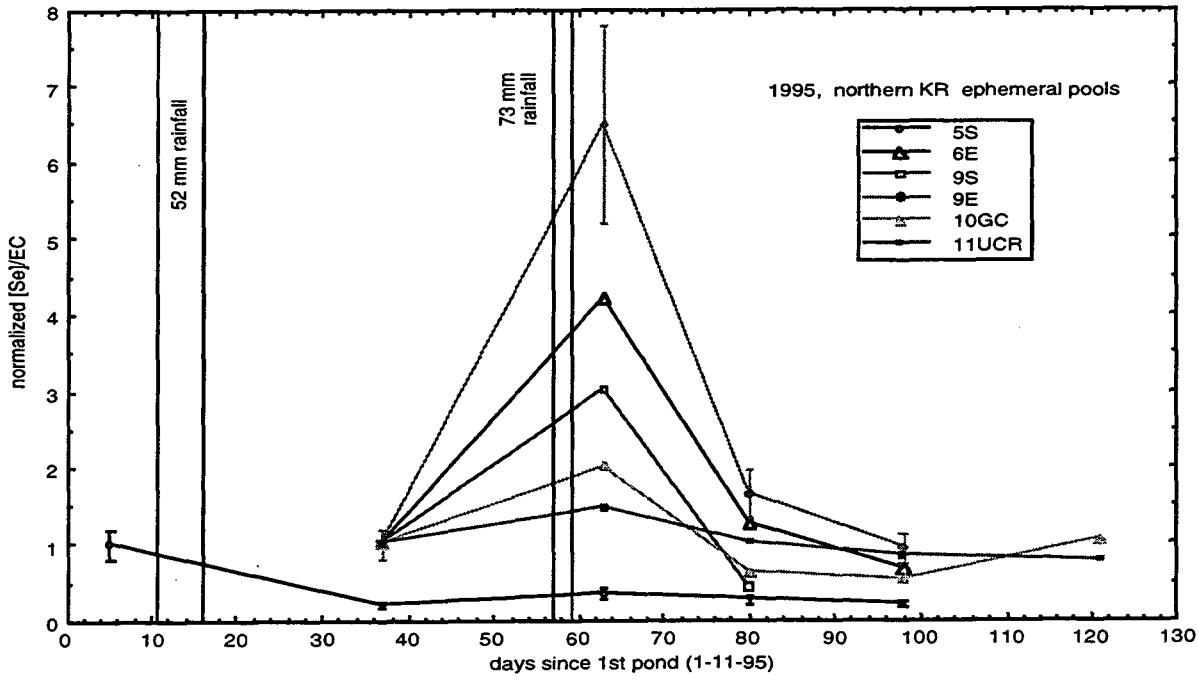

Figure 3.1.5b. Trends in ratios of pools Se to EC, normalized to values in initial samples. 1995, northern KR pools.

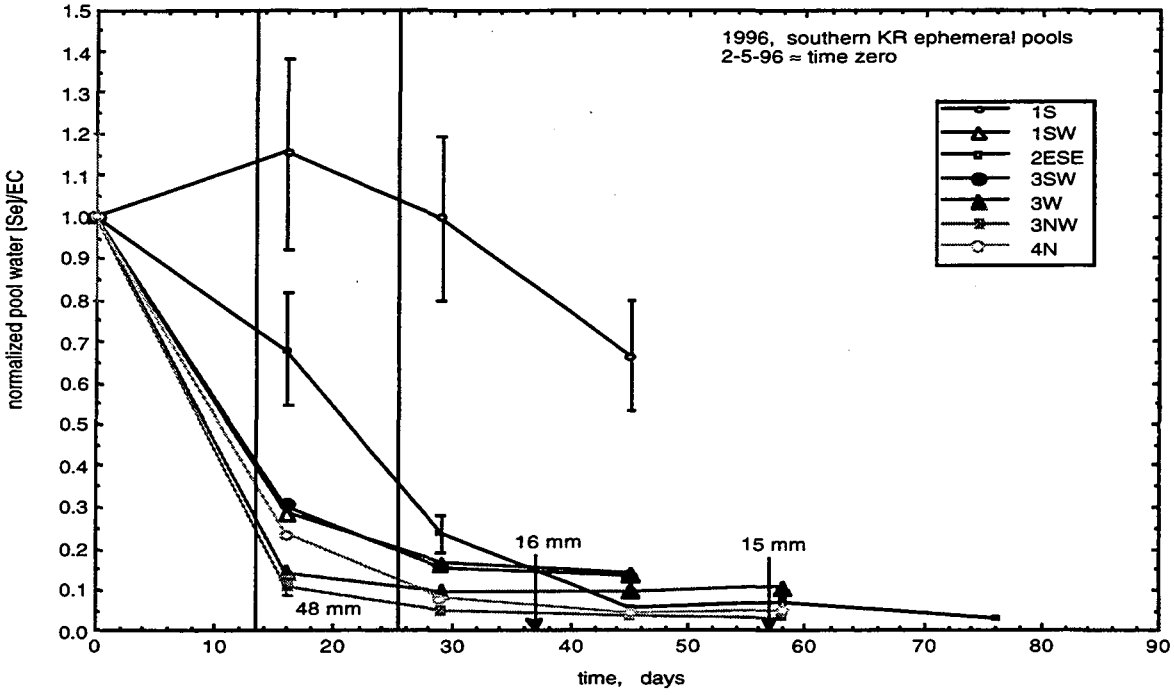

Figure 3.1.5c. Trends in ratios of pools Se to EC, normalized to values in initial samples.1996, southern KR pools.

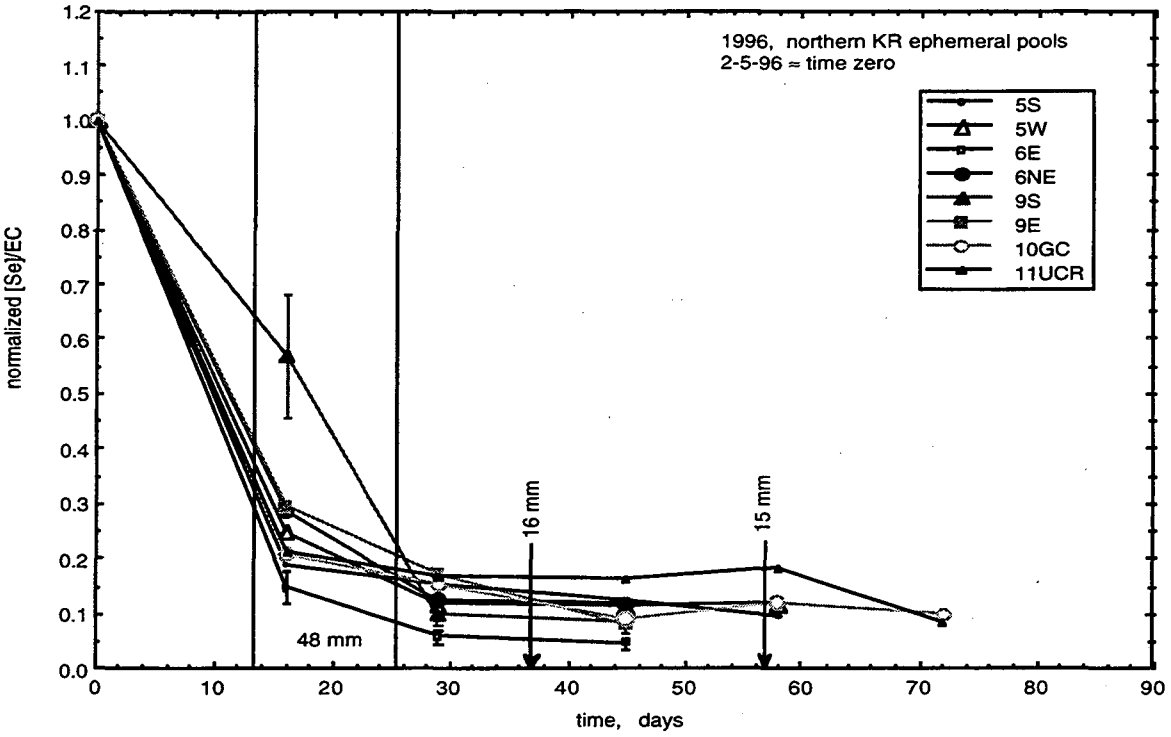

Figure 3.1.5d. Trends in ratios of pools Se to EC, normalized to values in initial samples. 1996, northern KR pools.

3.1.3 Discussion

As shown in Figs. 3.1.2a-3.1.2d, and 3.1.3a-3.1.3f, ephemeral pool concentrations typically start at relatively high values, decrease during the main ponding period, and increase to varying degrees towards the latter stages of ponding. Even at their lowest values, ephemeral pool Se concentrations commonly exceed the wetland surface water quality goal (2 ppb). Selenium in these pools occurs primarily as Se(VI), with up to about 30% as Se(IV). The decreases in pool Se concentrations during the initial stages of ponding result from transport into shallow sediments, in some cases also by dilution by additional rainfall, and a relatively smaller loss due to volatilization. The importance of pool to sediment Se transfers, and the minor role of volatilization are clearly demonstrated in a simple laboratory experiment described in Section 3.3. The influence of rainfall events on pool water quality, following the initial pool formation in a given season, is variable because it can bring in not only additional water for dilution, but also additional Se and salts in surface runoff from the surrounding areas. Pool Se concentrations are more generally determined by not only these rainfall influences, but also by water table rise which brings in the soluble Se inventory of the surface soil (including litter). In the few ephemeral pool areas now formed by water table rise (10GC, and a few other former LBNL monitoring soil sites), pool water Se concentrations start out at very high levels due to displacement of pore waters to the surface, and also sometimes due to large runoff contributions. Pools formed in unfilled, former cattail-vegetated areas (2ESE and 4N) also exhibit initially very high Se concentrations (sometimes exceeding 1000 ppb) as a result of the high soluble Se inventory available at the surface. The inclusion of some highly seleniferous cattail litter and associated soil in some filled areas result in high Se concentrations in their pools. This is clearly the case in site 5W. In areas covered largely with imported fill (such as 1S, 1SW, 6NE, 9E, 10X), pools form with much lower Se concentrations (typically < 50 ppb). Year-to-year comparisons in Se concentrations within individual pools reveal no obvious trends (Figs. 3.1.3a-3.1.3f).

The influence of evaporation on concentrating solutes within ephemeral pools is best identified by considering major soluble ions. Trends for pool water salinity generally increase with time due to evaporative concentration, with episodic dilutions due to rainfall (Figs. 3.1.4a-3.1.4d). The information on pool salinity trends is useful in assessing gains and losses of pool Se relative to major ions, thereby identifying the relative importance of other mechanisms such as Se oxidation-reduction and Se volatilization. In systems with minimal lateral inputs of Se and salts from surrounding soils, decreases in the Se/EC ratio indicate that Se is being removed from pools more efficiently than major ions. This ideal condition is compromised following the initial ponding whenever rainfall events occur with sufficient intensity to generate surface runoff. Plots of normalized pool Se/EC (Figs. 3.1.5a-3.1.5d) show that Se is preferentially removed from pool

waters relative to major ions. The 1995 data set (Figs. 3.1.5a, 5b) show large reversals in overall declining trends of Se/EC ratios, with reversals coinciding with the major rainfall event. The trends are most evident in the 1996 data set (Fig. 3.1.5c, 3.1.5d), since no large magnitude rainfall events occurred following the initial days of pool formation. By about 30 days into the pool cycle, the normalized Se/EC is in the range of 0.05 to 0.2. Assuming volatile Se losses were insignificant (supported in Section 3.3), these results show that roughly 80% to 95% of the initial pool Se inventory is transferred into the sediments. More quantitative assessment of this pool to sediment Se mass transfer requires information on major ion mass transfers. It is important to note that the initial stage of rapid Se transfers from pool waters into sediments is followed by an extended period where it is no longer exhibiting significant removal from pools. This is revealed in the relatively constant value of the normalized Se/EC ratio characteristic of this latter stage.

Two major features of the trends in Kesterson Reservoir ephemeral pool Se concentrations are important to recognize. First, initial pool Se concentrations can be extremely high (100's to 1,000's ppb). The extremely high Se concentrations diminish quickly. However, pools typically maintain lower Se concentrations over long periods of time which are usually still significantly above surface water quality goals.

3.1.4 Recommendations

1. The wildlife impacts of persistent ephemeral pools at Kesterson Reservoir need to be identified by wildlife biologists, in order to evaluate the need for developing alternative site management strategies during high rainfall years.

2. If wildlife impacts of persistent ephemeral pools warrant changes in site management, alternative strategies need to be identified, evaluated, and implemented. These could include surface or subsurface drainage and additional filling.

3. The remaining open areas which are susceptible to ponding by water table rise should be filled in. These are primarily associated with former soil profile monitoring and research sites.

3.2 Predicting Ephemeral Pool Formation and Duration

The formation of ephemeral pools during the wet season at Kesterson Reservoir remains a concern because of potential selenium uptake by wildlife attracted to these environments. The wet season in this region, characterized by a semi-arid Mediterranean climate, occurs largely during the months of November through April. Filling of low-elevation surfaces at Kesterson Reservoir has largely eliminated the occurrence of persistent highly seleniferous pools formed by shallow water table rise during the wet season (Tokunaga and Benson, 1992). However, rainfall ponding does occur, resulting in persistent ephemeral pools when a sufficient amount of precipitation is received. Soluble Se partitions into these rainfall-generated pools according to a complex array of processes which include dissolution and mixing of soluble Se contained in surface litter, diffusion from the underlying soil, and soluble Se transport from surrounding soil surfaces in surface runoff. Concentrations of Se in rainfall-generated ephemeral pools tend to be much lower than those previously formed by water table rise since the latter advection-dominated process is very efficient at displacing or redistributing soluble components from both the shallow soil and surface litter into pools (Tokunaga and Benson, 1992; Poister and Tokunaga, 1992). Nevertheless, adverse wildlife impacts of these rainfall-generated ephemeral pools remains a concern since their Se concentrations typically remain above wetland surface water quality goals of < 2 µg/L (Tokunaga, 1995). Given this outstanding concern, it would be useful to (1) predict the initiation and duration of rainfall-generated ephemeral pools, (2) predict time trends in ephemeral pool Se concentrations, and (3) quantify wildlife impacts of these pools. We present an approach for predicting pool formation and duration in this section. Aspects of predicting pool Se concentrations are presented in the next section. The important issue of wildlife impacts is beyond the scope of this study.

The following method for estimating ephemeral pool occurrence is restricted to ponding caused primarily by rainfall accumulation. In such cases, ponding will occur whenever the rainfall rate exceeds the combination of the evapotranspiration rate and the seepage rate. Accurate daily information on weather conditions at Kesterson Reservoir is therefore a primary need in predicting pool formation. The CIMIS (California Irrigation Management Information System) network of computerized weather stations is operated by the California Dept. of Water Resources (Sacramento, CA). These weather stations provide data on rainfall, and weather-based estimates of evapotranspiration from a standard vegetated surface (irrigated grass), denoted ET_o. The daily ET_o values are calculated from hourly data on net solar radiation, air temperature, wind speed and vapor pressure (Snyder and Pruitt, 1992). The CIMIS weather station at Kesterson Reservoir was installed in 1989, and has provided nearly continuous

meteorological data. In addition, U. S. Bureau of Reclamation (USBR) field staff collected pan evaporation rate data at Kesterson Reservoir from 1982 through 1987, and rainfall data from 1982 to 1996.

The general approach taken to estimate ephemeral pool formation and duration amounts to redistributing rainfall inputs into three compartments: shallow soil profile storage, evapotranspirative losses from soils, and ponding (including evaporation from pool surfaces). For each wet season, this rainfall mass balance is initiated on November 1st, based on the available rainfall data and field observations indicating that significant ponding at this time of the year is extremely unlikely. The CIMIS data provided daily measurements of rainfall, and daily estimates of ET_o. The ET_o values require re-scaling to account for the fact that evapotranspiration from soils vary, depending on vegetation type, the stage of the vegetation growth cycle, and surface soil moisture. In the CIMIS approach to estimating actual evapotranspiration from vegetated soil surfaces, the ET_o is multiplied by an empirical crop coefficient, k_c, which accounts for the vegetation type, growth stage, and local climate. Since available values of k_c are restricted to agricultural crops, an estimate of this factor suitable for the mixture of annual grasses and sparsely distributed forbs and shrubs found at Kesterson Reservoir is needed. Values of k_c for small grain crops in the San Joaquin Valley (late season) are in the range of 0.18 to 0.20 (Snyder et al., 1994). A k_c value of 0.10 was chosen for Kesterson Reservoir soils, since the majority of its annual grass and forb cover is dead during the late fall and winter months. Thus the daily evapotranspirative water loss from unponded Kesterson Reservoir soils was estimated by 0.1 ET_o, where ET_o is the corresponding Kesterson Reservoir CIMIS daily value. During periods of ponding, ET_o values must be re-scaled to account for evaporation from free water surfaces. An equivalent k_c value for ponded waters of 1.09 was obtained from correlating USBR monthly pan evaporation rates to CIMIS monthly cumulative ET_o values (November through April, Fig. 3.2.1). This value is in close agreement with a value of 1.10 suggested in Snyder et al. (1994) for free water surfaces. In our calculations, daily evaporation from ephemeral pool surfaces is estimated as 1.09 ET_o. During the very few periods when the Kesterson Reservoir CIMIS station was not recording precipitation, rain gauge data from the USBR Kesterson weather station and/or the nearby Los Banos CIMIS weather station were used. The CIMIS and USBR data provide the necessary information for estimating atmospheric exchanges of water from the ground surface. Thus, the only remaining unknowns are the seepage rate and shallow soil profile moisture storage.

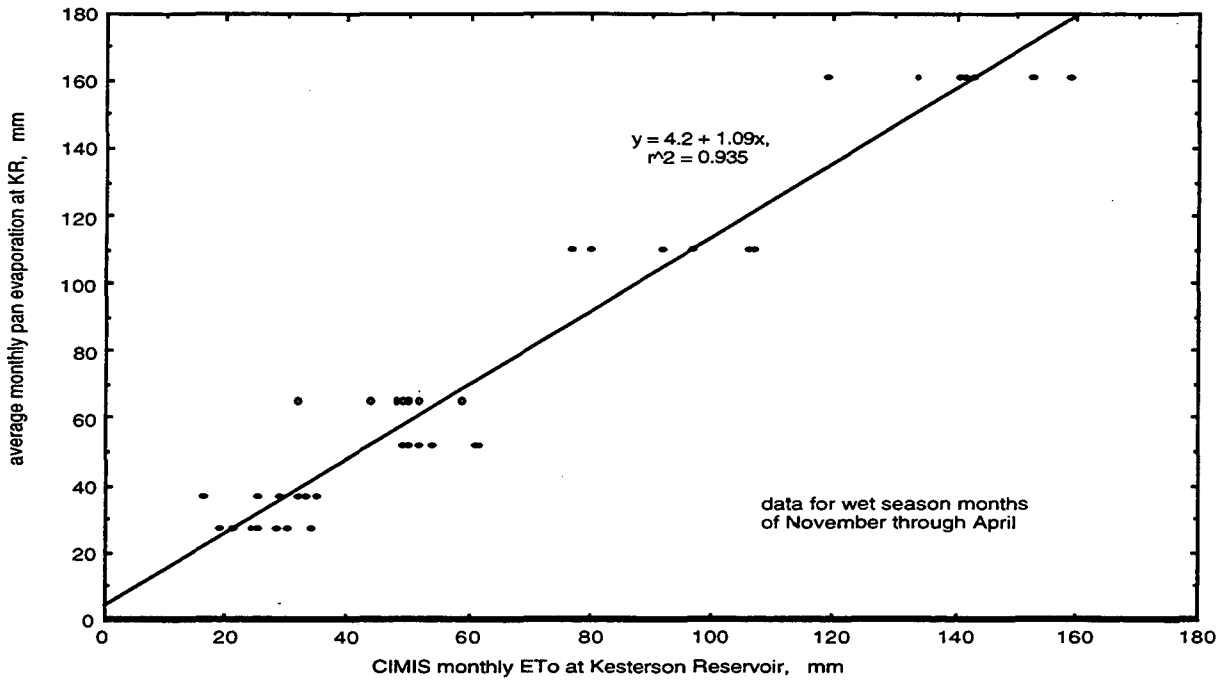

Figure 3.2.1. Estimating Kesterson Reservoir ephemeral pool water evaporation rates from CIMIS ET_o values through their correlation with pan evaporation rates.

Seepage rates can be constrained with information on Kesterson Reservoir soil hydraulic conductivity, hydraulic head gradients characteristic of soil profiles during the wet season, and available soil profile storage capacity. Measurements of field saturated hydraulic conductivity in several typical soil profiles at Kesterson Reservoir have been obtained using the Guelph Permeameter (Reynolds et al., 1983; Soilmoisture Equipment Corporation, Santa Barbara, CA). These essentially point measurements in soil profiles ranged from 0.5 up to 800 mm/d (Lawrence Berkeley Laboratory, 1987). For purposes of estimating seepage rates under effectively saturated conditions, the harmonic mean hydraulic conductivity of these profiles is more informative since is represents the effects of summing series hydraulic resistances and provides better estimates of influences of low permeability soil horizons. Harmonic mean values of soil profile hydraulic conductivity range from 2 to 44 mm/d, and the arithmetic mean of these 8 harmonically-averaged profile values is 12 mm/d. For comparison, surface soil hydraulic conductivity from 20 infiltrometer measurements performed on Waukena soils (now mapped as members of the Turlock soil series) at Kesterson ranged from 0.8 up to 42 mm/d, with an arithmetic average of 13 mm/d (Jackson, 1967; Table 3). Luthin (1966) reported a value of 30 mm/d from infiltrometer measurements at Kesterson, without mention of the number of measurements. Based on all of these sources, a characteristic surface soil hydraulic conductivity of 15 mm/d was assumed. It should be noted that there are locations within Kesterson Reservoir

where surface soils have higher than average clay and silt contents, and therefore have significantly lower saturated hydraulic conductivity. The harmonic mean profile averaged saturated hydraulic conductivity at one of these sites (P8EP) is 1 mm/d (Zawislanski, 1989).

Rainfall infiltration into soil profiles is typically described through analytical or numerical solutions of Richards' equation (e.g. Hillel, 1980; Campbell, 1985). Since a detailed description of successive rainfall infiltration events into soils is beyond the scope of the present analysis, a simpler algebraic approach was selected to estimate infiltration fluxes. This approach amounts to assuming daily steady-state infiltration rates, using 15 mm/d as the soil hydraulic conductivity, assuming a matric potential of zero at the soil surface during rainfall, and assuming no deep seepage. A reference soil profile depth of 1.00 m was selected since it corresponds to the approximate depth of the unsaturated zone during a "dry" wet season. The water table is assumed to be initially (Nov. 1st) located at the 1.00 m depth. An available, initially air-filled porosity of 0.10 is assumed, based on neutron probe data from Kesterson Reservoir soils (LBNL sites P5F, P6S12, P7F, P9C, P11C). Thus 100 mm of infiltration could be accommodated in the soil profile at time zero for a given wet season. Rainfall which infiltrates into the profile contributes directly to water table rise. The pressure head at the soil surface is set at zero during infiltration. The hydraulic head gradient used in estimating daily infiltration fluxes is evaluated over the 1.00 m reference depth, assuming a pressure head at the bottom of this profile equal to the hydrostatic value resulting from infiltrated water accumulation. In this approach, the hydraulic head gradient is initially equal to one, and decreases towards zero as the profile becomes saturated. Evaporative losses are accounted for by water table lowering, permitting increased hydraulic head gradients at the beginning of subsequent rainfall events. The daily amount of water allowed to infiltrate into the model profile is limited by the lesser of two quantities, daily profile infiltration capacity and available surface water. The daily profile infiltration capacity is the product of the profile hydraulic conductivity (15 mm/d) times the current estimated hydraulic head gradient. Available surface water is defined as the sum of daily rainfall plus current ponded water, minus daily pan evaporation. If the available water on a given day is less than or equal to the daily profile infiltration capacity, all available surface water is incorporated into the profile. On the other hand, if daily available water exceeds the infiltration capacity, the remaining difference accumulates as ponded water. In this model, ponding results from two different processes. The first is the case of daily rainfall rate exceeding daily infiltration rate just described. The second case is when the soil profile is fully water saturated.

It is recognized that seepage does in fact occur beyond the 1.00 m depth during the wet season. The chemical evidence for deep seepage comes from changes in deeper pore water Se concentrations and salinities during intense rainfall events, especially in areas underlying higher

permeability soils. Thus, the approximation of no seepage below the 1.00 m reference depth requires justification, especially during prolonged ponding. Measurements of vertical hydraulic head gradients within soil profiles under ephemeral pools at Kesterson Reservoir are scarce, since most of these sites are not instrumented with tensiometers and shallow piezometers. Measurements from tensiometers and shallow piezometers during ephemeral ponding at site P9L (Pond 9) have indicated hydraulic head gradients in the range of 0.00 to 0.03, ±0.02 m/m. Although hydraulic head gradients vary with time, a hydraulic head gradient of 0.02 will be used for purposes of estimating the magnitude of seepage fluxes. Combining this value for the gradient with a soil profile hydraulic conductivity of 15 mm/d yields a characteristic seepage rate of 0.3 mm/d. This value is small in comparison to typical pan evaporation rates (1 to 5 mm/d) during the wet season. Furthermore, the deeper profile in Kesterson Reservoir soils undergoes annual re-saturation from shallow water table rise due to flooding of surrounding wetlands. These considerations suggest that seepage losses are secondary to evaporation in dissipating ponded waters at Kesterson Reservoir.

Before presenting predictions of ephemeral pool formation and comparisons with field observations, the basic steps used in calculations will be reviewed. Using November 1st as the starting date for each wet season cycle, we assume a uniform soil profile with an impermeable boundary at a depth of 1.00 m (i.e., no seepage below this depth). This soil profile has an available air-filled porosity of 0.10, and a water table initially at the 1.00 m depth. Rainfall is allowed to infiltrate into the profile at a rate limited by the product of the soil hydraulic conductivity and estimated hydraulic head gradient. Ponding occurs when either the rainfall rate exceeds the sum of infiltration rates and pan evaporation rates, or when the soil profile becomes saturated. Evaporation from the unsaturated soil surface is estimated as 0.10 ET_o, while evaporation from ponded waters and saturated soil surfaces is estimated as 1.09ET_o.

CIMIS data are available for the last eight wet seasons at Kesterson Reservoir. Predictions of ephemeral pool formation based on this model are presented in Figs. 3.2.2a through 3.2.2h. Also included in each of these figures is information on the time span over which field observations of rainfall ponding were reported. The field observations come from sites which have been included in the yearly ephemeral pool water sampling effort. Note that overall, model predictions of ephemeral pool formation and duration come reasonably close to field observations. Field estimates of ponding intervals often have an uncertainty of about 15 to 20 days, since these are based on observations made during periodic field site visits. The dates of ponding resulting from episodic, large-magnitude rainfall events can generally be identified accurately since rainfall intensities which give rise to soil infiltration-limited ponding are easily identified. Correlations between predicted versus observed dates for major pool formation and depletion are summarized in Fig. 3.2.3. In this figure, predictions indicating ponding of

sufficient magnitude (> 10 mm) and duration (> 2 d) are used in defining the onset of ponding. Recall that reasonable values of soil hydraulic conductivity and available porosity were used in obtaining these results. The impermeable boundary approximation imposed at the 1.00 m depth is supported not only by the previous arguments relating to measured hydraulic head gradients during profile flooding, but now also by the reasonably accurate predictions of ponding duration. The primary simplification invoked in this approach is the method for estimating the hydraulic head gradient during infiltration. The reasonably close matches obtained in most cases, over a fairly wide range of rainfall distributions, indicate that the overall approach can be useful for predicting the onset and duration of rainfall-generated ephemeral pools.

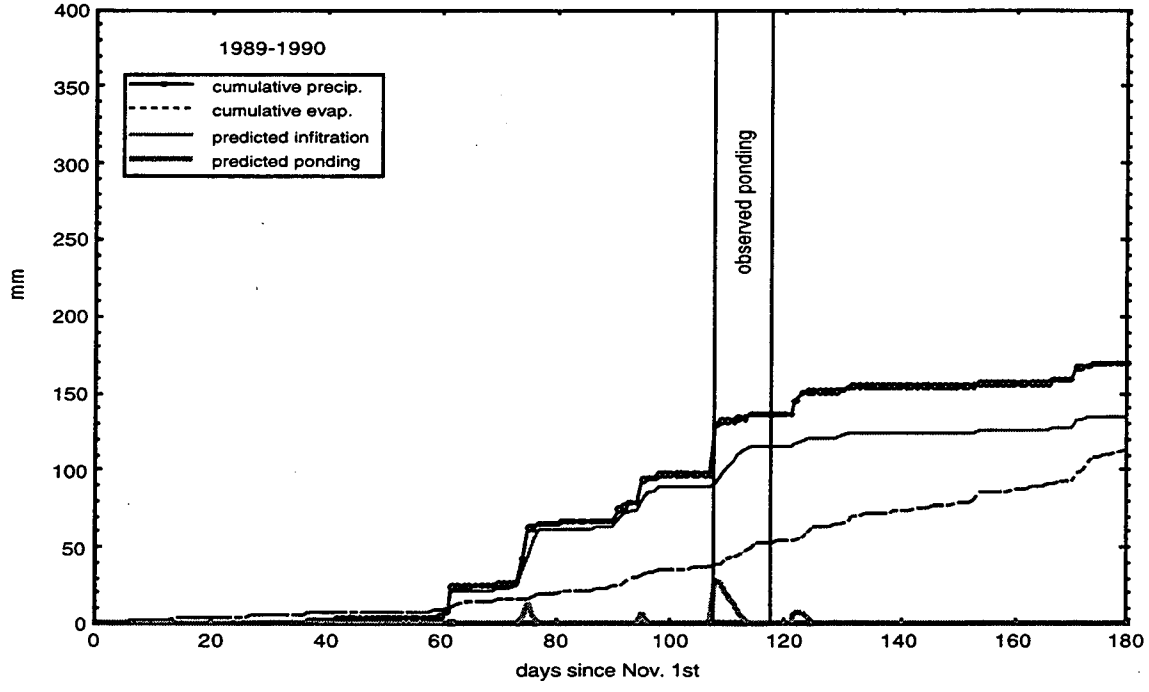

Figure 3.2.2a. Predicted versus observed duration of main ephemeral pools at Kesterson Reservoir during the 1989-90 wet season.

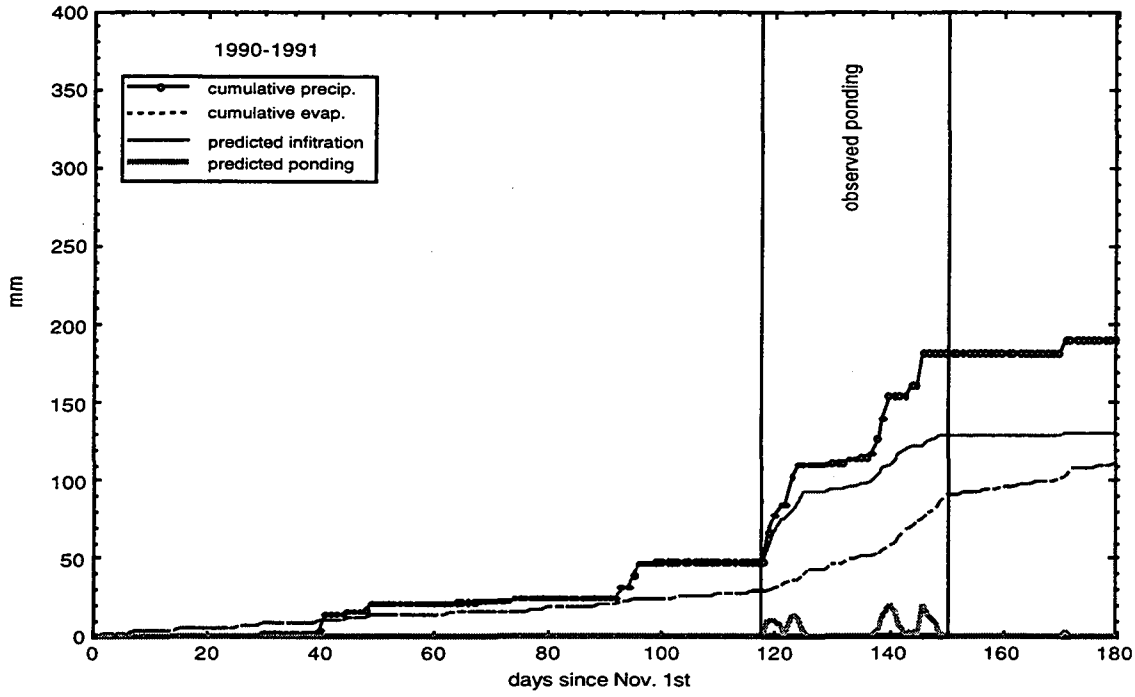

Figure 3.2.2b. Predicted versus observed duration of main ephemeral pools at Kesterson Reservoir during the 1990-91 wet season.

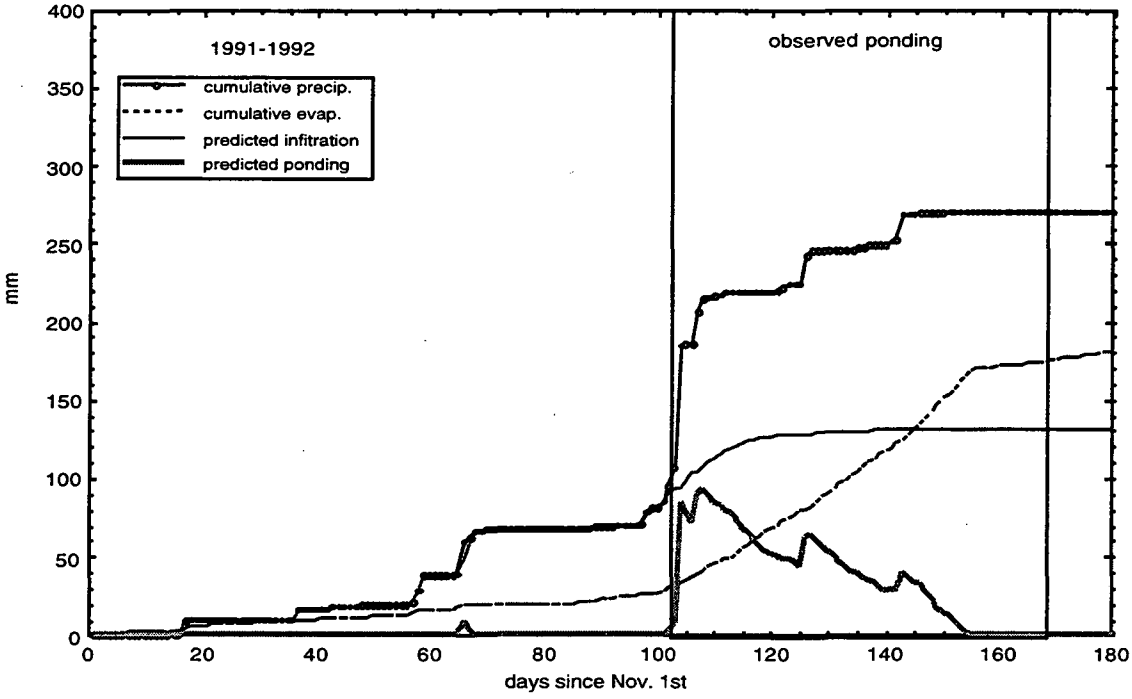

Figure 3.2.2c. Predicted versus observed duration of main ephemeral pools at Kesterson Reservoir during the 1991-92 wet season.

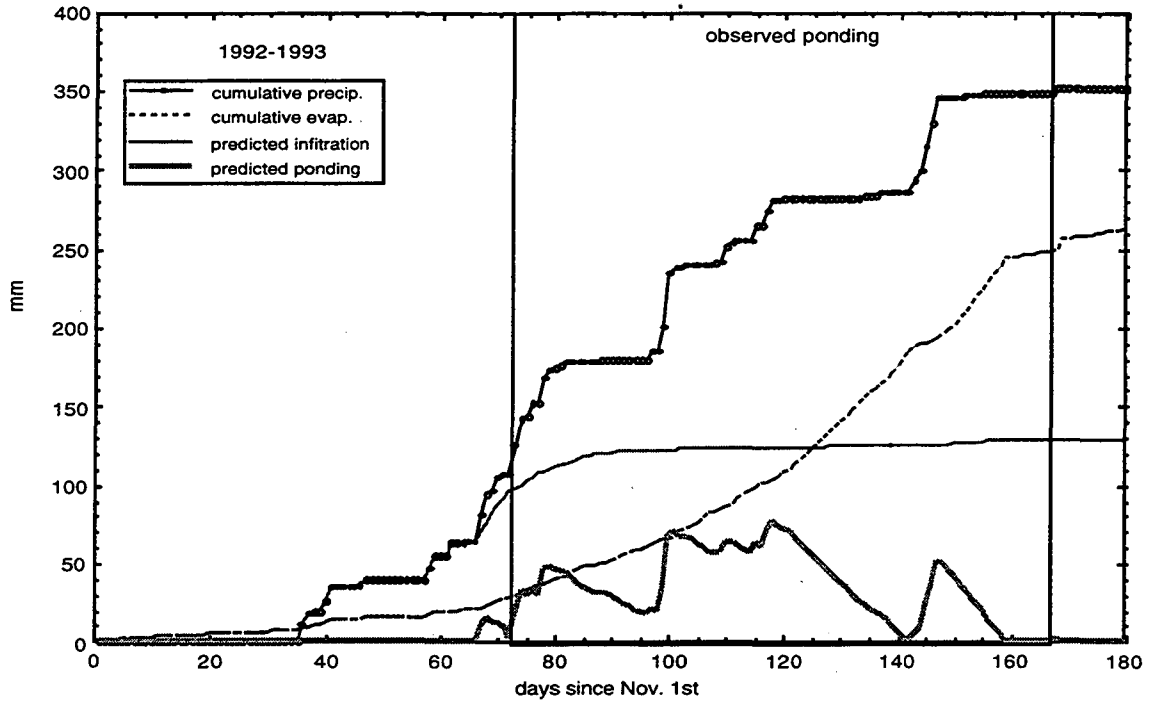

Figure 3.2.2d. Predicted versus observed duration of main ephemeral pools at Kesterson Reservoir during the 1992-93 wet season.

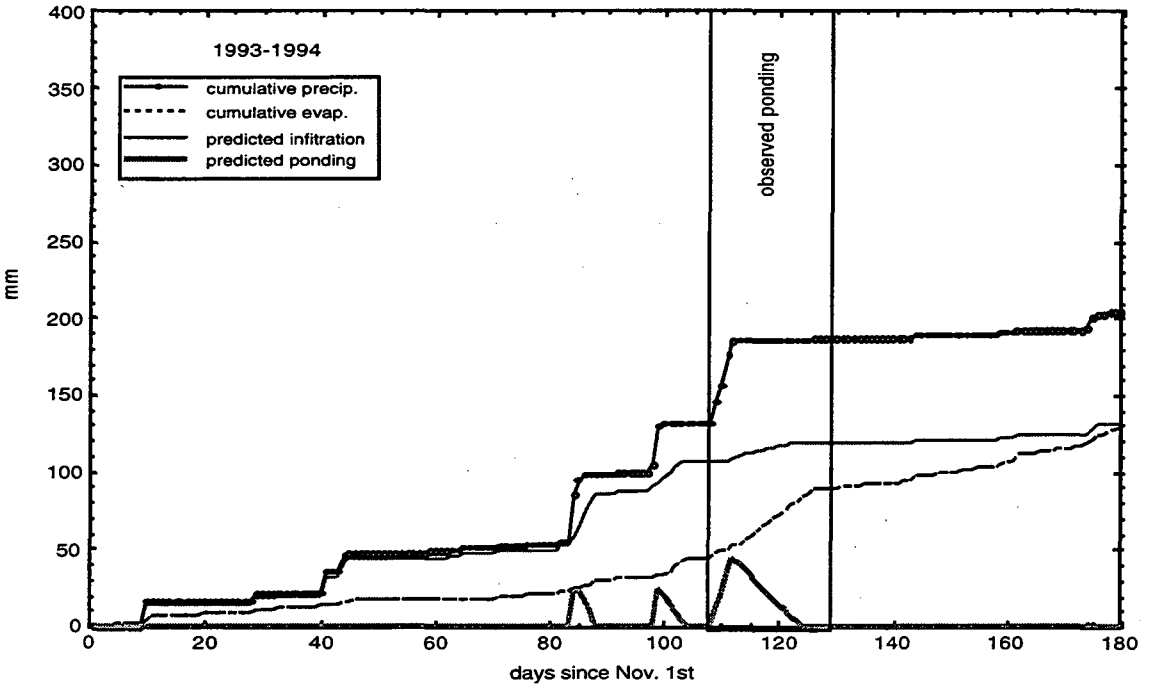

Figure 3.2.2e. Predicted versus observed duration of main ephemeral pools at Kesterson Reservoir during the 1993-94 wet season.

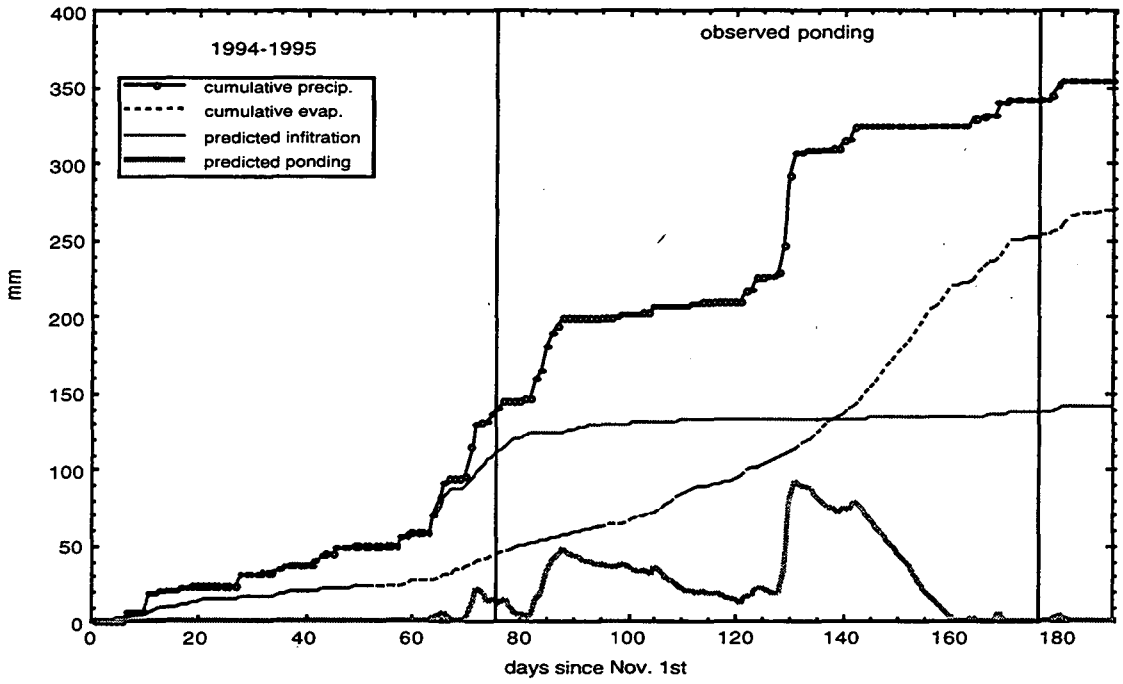

Figure 3.2.2f. Predicted versus observed duration of main ephemeral pools at Kesterson Reservoir during the 1994-95 wet season.

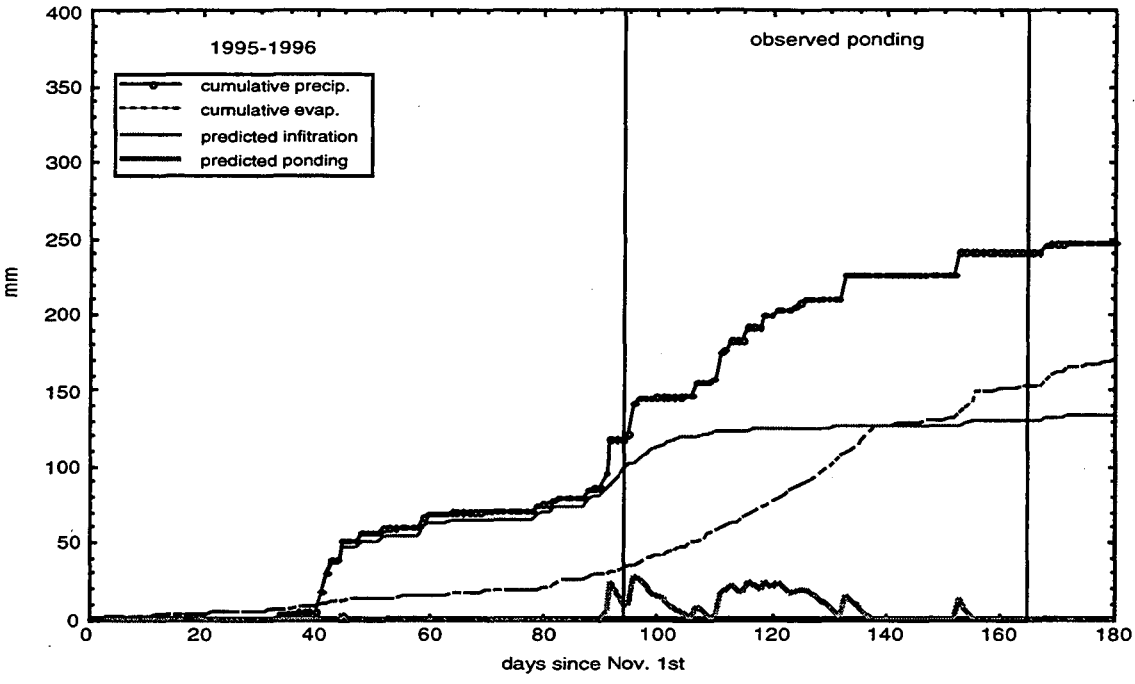

Figure 3.2.2g. Predicted versus observed duration of main ephemeral pools at Kesterson Reservoir during the 1995-96 wet season.

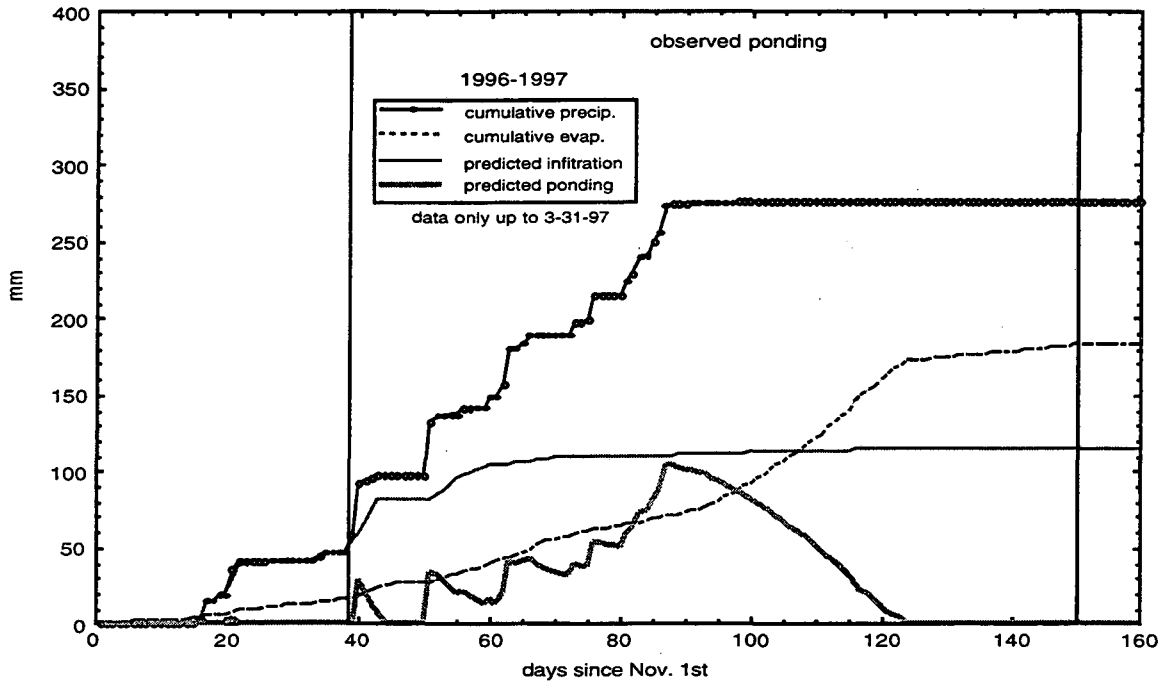

Figure 3.2.2h. Predicted versus observed duration of main ephemeral pools at Kesterson Reservoir during the 1996-97 wet season.

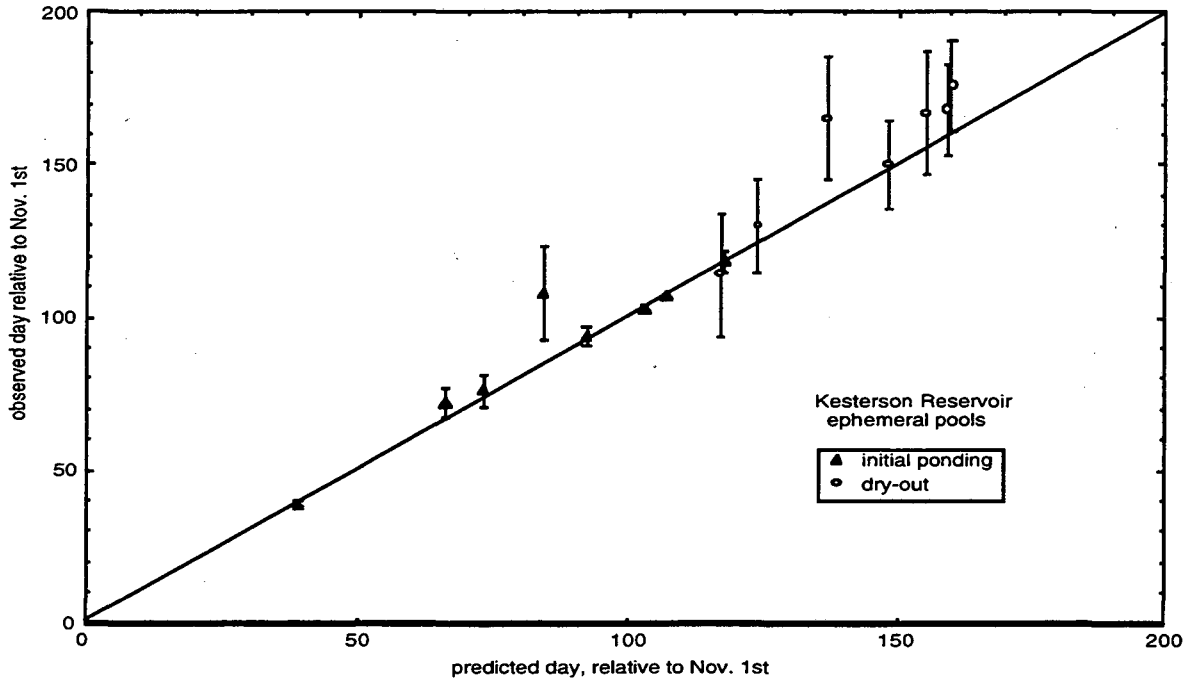

Figure 3.2.3. Comparisons between model-predictions and field observations for the formation and dissipation of ephemeral pools at Kesterson Reservoir.

It is worth noting that these results also reflect the fact that the timing of major rainfall events during the wet season is the primary factor in determining the duration of ponding. This is clearly revealed through comparisons of the 1991-1992 and 1996-1997 wet seasons. The approximately 270 mm of rainfall received early in the wet season (Dec. 1996 to Jan. 1997) results in significantly longer ponding periods than when the same amount of precipitation is received later in the season (Feb. to Mar. 1992). The shorter duration of pools formed from rainfall later in the season is due to the much higher potential evaporation rates during this stage. Typical pan evaporation rates during December and January are in the range of about 1 mm/d, compared to around 5 mm/d during March and April (Fig. 3.2.4). The proposition that rainfall quantities and distributions during the wet season almost exclusively account for differences observed between yearly ponding periods is strongly supported by the relative invariance of the ET_o from year to year. This is more clearly illustrated from records of cumulative ET_o during each wet season, which damp-out minor daily variations in ET_o. Plots of cumulative ET_o for 4 different wet seasons are shown in Fig. 3.2.5. Note that an average $ET_o(t)$ function could reasonably be used in place of any particular year's $ET_o(t)$. The ability to use a generic, site-specific $ET_o(t)$ function as input in this model will allow the approach presented here to be used fairly reliably in a more predictive mode.

One can now input various hypothetical temporal distributions of rainfall in combination with the site-specific average soil profile properties and average $ET_o(t)$ function, resulting in forecasts of the initiation and duration of ephemeral pools. The possibility of using this model in a predictive mode is potentially useful in at least two applications. Real time monitoring of rainfall and ET_o during the wet season would permit forecasting of the formation and duration of ephemeral pools. Such information would be useful in deciding whether or not surface water drainage control measures are warranted. By combining these types of predictions with estimates of Se concentrations in pools and with toxicity models, a clearer assessment of wildlife impacts might also be obtained.

It is emphasized that the approach presented here is intended only for estimating average aspects of rainfall-generated ephemeral pools. Important aspects of the field setting that are not accounted for here include the spatial variability of soil properties (primarily the saturated hydraulic conductivity and available porosity), and variable topography. The latter factor is very important for two reasons. First, it is related to variability in depths to the local water table. Second, and perhaps more important, topography allows for lateral runoff of rainfall into local depressions. The ponding depths predicted from the simple method presented here are equivalent to area-averaged depths, where averaging includes not only the variable-depth ponds but also the remaining air-filled porosity in surrounding unponded uplands.

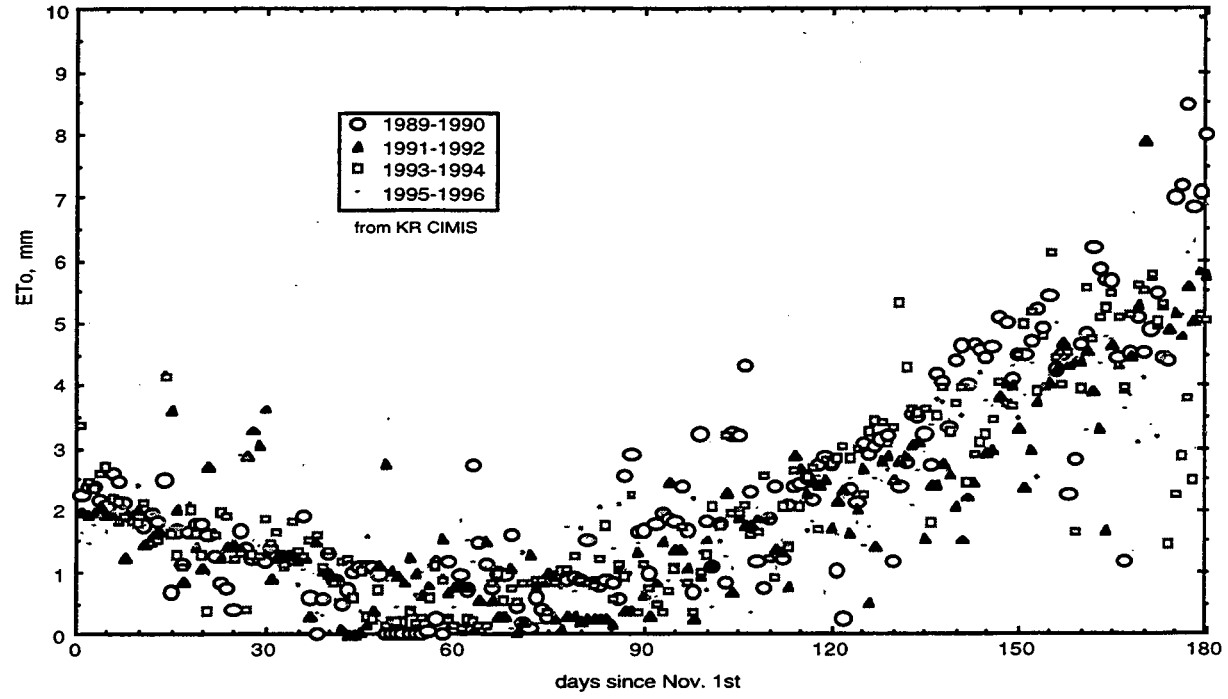

Figure 3.2.4. Daily ET_o values from the Kesterson Reservoir CIMIS station. Pan evaporation rates are equal to about 1.09 times these values. Note that evaporative losses in the later stages of the wet season are about 5 times greater than during December and November.

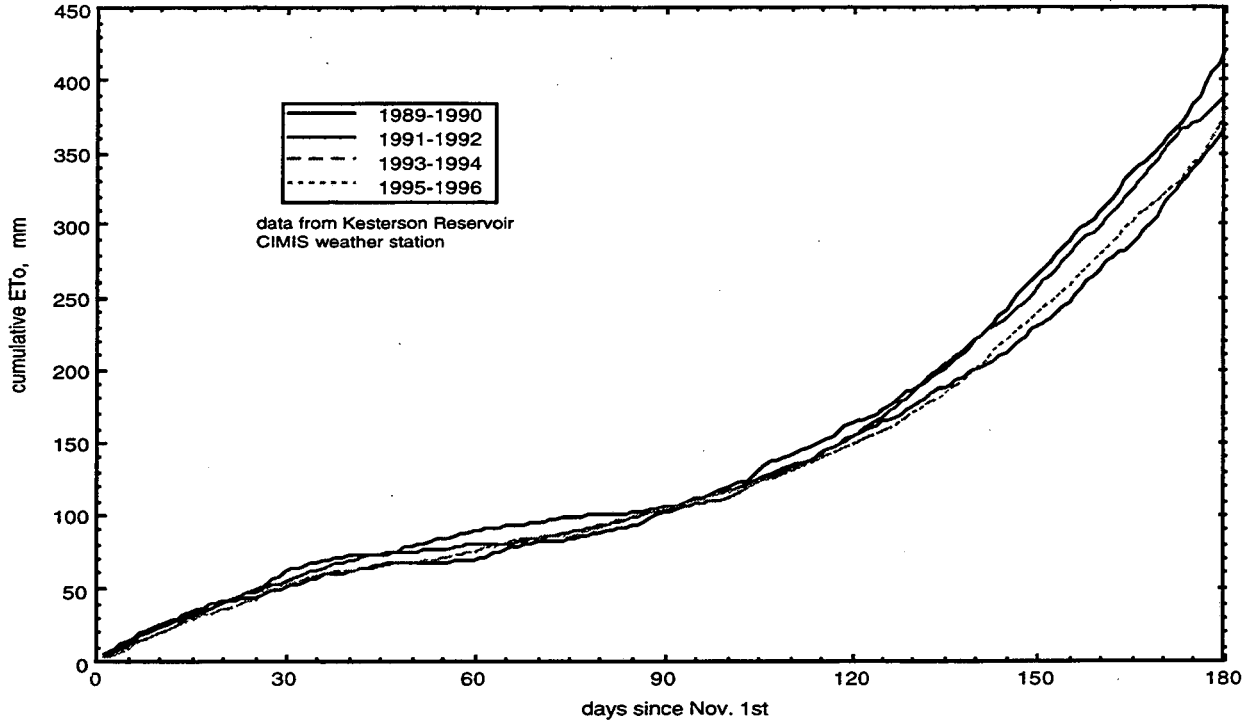

Figure 3.2.5. Cumulative ET_o (relative to Nov. 1st) for 4 different wet seasons. Note that the ET_o (t) functions from each year could be reasonably approximated by a single average ET_o (t).

3.3 Laboratory Ephemeral Pool Microcosm Experiment

Data from water samples collected in ephemeral pools provide information on Se concentrations and time trends characteristic of the field environment. However, accurate Se mass balances are difficult to perform in these field environments because of complex boundary conditions and limited spatial and temporal sampling. Thus the field-based results such as those presented in the previous section do not provide quantitative assessments of Se removal from pool waters. Furthermore, mechanisms responsible for Se removal are more difficult to isolate in the open field systems. These pathways include Se transport and reduction in sediments (Weres et al., 1989a; Tokunaga et al., 1996; Tokunaga et al., 1997), Se reduction within suspended organic matter, Se uptake by aquatic microorganisms, algae, and invertebrates (Besser et al., 1989, 1993; Saiki et al., 1993; Bowie et al., 1996), and volatilization of Se to the atmosphere (Cooke and Bruland, 1987; Thompson-Eagle and Frankenberger, 1990; Gao and Tanji, 1995; Zhang and Moore, 1997). Basic issues which have not been resolved in the many field measurements include (1) what fraction of the initially high pool Se inventory in a given pool is removed during the course of ponding?, and (2) what is the importance of pool to sediment transport and reduction of Se, relative to volatile Se losses, Se uptake by aquatic organisms, and conversion to reduced forms in suspended organic matter? In order to improve our understanding in these areas, a simple laboratory microcosm experiment was performed.

This study focused on quantifying basic influences of sediments on pool Se concentrations through comparing field-sampled pool waters which are incubated in the laboratory with and without their underlying sediments. Aspects of aqueous Se removal by volatilization and biological uptake are only indirectly addressed in this experiment. Features of the field environment make sediment-pool interactions difficult to isolate. Rainfall inputs into existing pools vary unpredictably, making it impractical to schedule long term sampling between significant precipitation events. Pool "edge effects" of shore regions are quite complex, and probably have important influences on bulk pool water quality. During more intense rainfall events, these regions probably provide surface runoff with highly variable concentrations of Se and major ions, depending on site characteristics and the temporal distribution of rainfall. Advective transport of solutes across the pool-sediment interface can also complicate mass balance analyses, although we showed in our analysis and model of pool formation (Section 3.2 in this report) that this is probably a secondary effect relative to evaporation. In order to isolate pool-sediment interactions in the absence of all of these complicating factors, pool waters were studied in laboratory beaker microcosms. The laboratory microcosms provided the following primary simplifications. First, water was exchanged to the atmosphere only by evaporation.

Second, "edge effects" of shore regions were eliminated since the walls were nearly vertical. Third, advection across the pool-sediment boundary was eliminated since flow was not permitted at the bottom of the beakers.

In addition to providing a general comparison of pool Se concentration time trends in systems with and without sediments, it is of interest of obtain information on the sediment depth interval most responsible for Se exchanges. Such information is important in understanding mechanisms behind Se transport at the pool-sediment boundary. For this purpose, data from the laboratory experiments will be compared with the simple pool-sediment Se transport model described below.

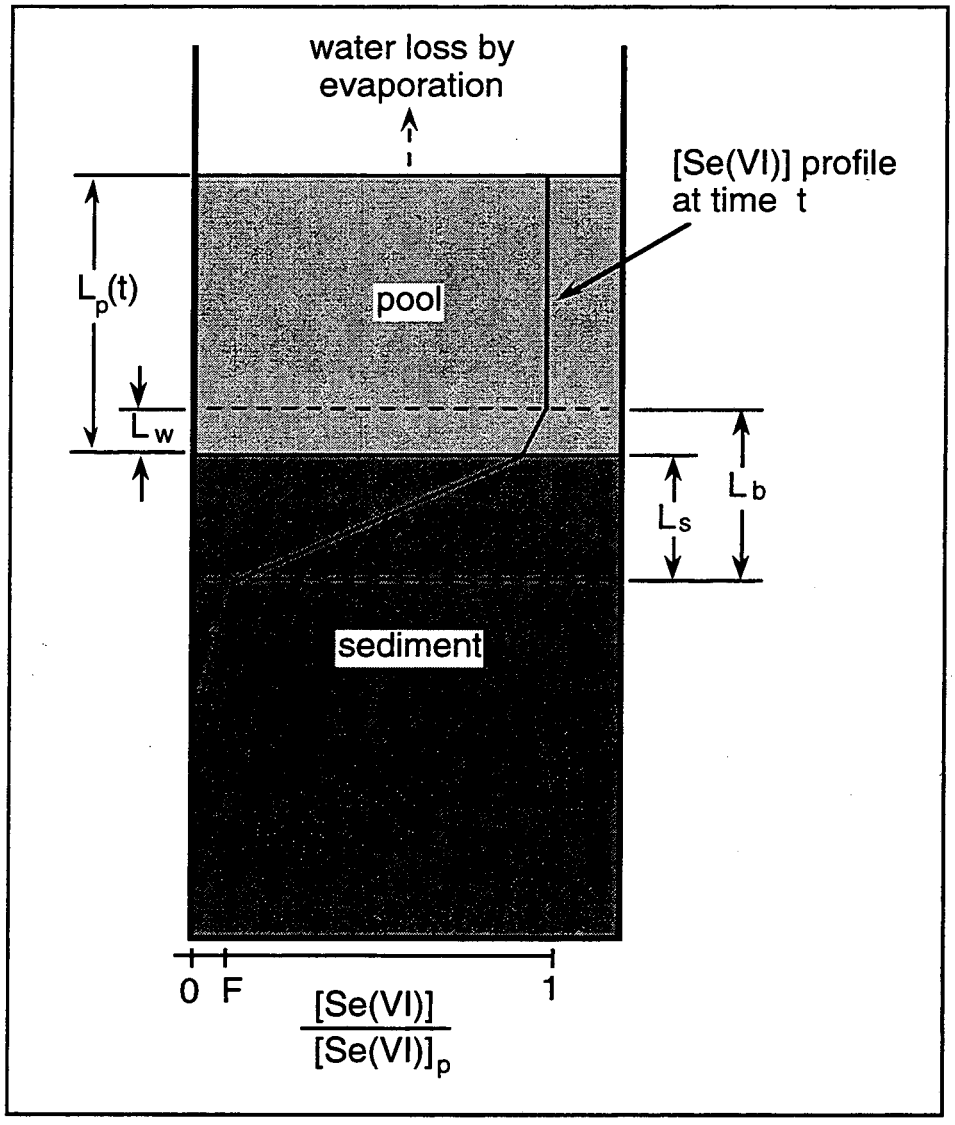

Figure 3.3.1. Conceptual model for estimating Se(VI) transport from pool waters into sediments. $L_p(t)$ is the pool depth at time t; K_w is the pool boundary layer thickness; L_s is the sediment boundary layer thickness; L_b is the composite boundary region thickness.

3.3.1 Pool-Sediment Se(VI) Mass Transfer Model

The main purpose for developing this model is to estimate the effective depth within sediments where Se reduction takes place. It will be shown that as this depth is varied within a very shallow region, pool Se concentrations will increase or decrease with time due to evaporation becoming either the primary or secondary influence. The approach developed here is similar to that presented in Tokunaga et al. (1997). It differs primarily in including evaporative concentration of solutes in pool waters, and in assuming that the Se(VI) concentration at the lower region of the diffusion boundary layer is equal to a fixed fraction, F, of the instantaneous Se(VI) concentration in overlying pool water. No Se volatilization or re-oxidation processes are included in this model. We start with considering the various major components responsible for changing pool Se concentrations, $[Se]_p$, where the oxidation state is understood to be +VI unless otherwise specified. In our simple laboratory system, diffusion, reduction, and evaporation contribute directly to changes in $[Se]_p$. Diffusion occurs at the pool-sediment boundary, and will be approximated as occurring through a fixed thickness boundary layer (Fig. 3.3.1). Reduction can occur within pool waters, and will be approximated as a first-order process. The reduction of Se which takes place within sediments is indirectly coupled to the pool Se inventory via diffusion, i.e., Se(VI) must diffuse into sediments prior to reduction. In the simple model presented here, the pore water inventory of Se(VI) is relatively small, so that changes in storage of Se(VI) in this compartment are minor. In this limit, the diffusive mass transfer rate becomes nearly equivalent to the mass transfer-limited overall Se(VI) reduction rate within the sediment. Evaporation of pool waters results in concentrating dissolved Se. The combined influences of these three processes on changing $[Se]_p$ will be approximated by

$$\frac{\partial}{\partial t}[Se]_p = -\frac{D_e}{L_p L_b}\left\{[Se]_p - [Se]_s\right\} - k_{r,p}[Se]_p - \frac{[Se]_p}{L_p}\frac{\partial}{\partial t}L_p \quad , \qquad [1]$$

where D_e is the effective diffusivity across the pool-sediment boundary layer, L_b is the diffusion boundary layer thickness, $[Se]_s$ is the Se(VI) concentration in sediment pore waters at the lower surface of the boundary region, L_p is the time-dependent pool depth, and $k_{r,p}$ is the apparent first order Se(VI) reduction rate constant. The diffusive mass transfer coefficient the pool-sediment boundary layer is approximated by

$$\frac{D_e}{L_b} = \frac{D_o}{L_w + \left[L_s(\alpha n)^{-1}\right]} \quad , \qquad (2)$$

where D_o is the diffusivity of SeO_4^{2-} in water, L_w is the thickness of the pool water boundary layer, L_s is the thickness of the surface sediment boundary layer, α is a proportionality factor accounting for tortuosity, and n is the surface sediment porosity (Tokunaga et al., 1997). We further define the location of the lower surface of the sediment boundary layer as the horizontal plane where $[Se]_s = F[Se]_p$. Incorporating these approximations into Eq.(1) results in

$$\frac{\partial}{\partial t}[Se]_p = -\frac{D_o}{L_w + \left[L_s(\alpha n)^{-1}\right]}\frac{(1-F)}{L_p}[Se]_p - k_{r,p}[Se]_p - \frac{[Se]_p}{L_p}\frac{\partial}{\partial t}L_p \quad . \qquad (3A)$$

Note that L_s is determined by the choice of F. The case of F = 0 is particularly interesting since it is associated with an L_s at which $[Se]_s$ goes to zero, thereby identifying the depth at which reducing conditions prevail. With F = 0, we have

$$\frac{\partial}{\partial t}[Se]_p = -\left\{\frac{1}{L_p(t)}\left[\frac{D_o}{L_w + \left[L_s(\alpha n)^{-1}\right]} - E(t)\right] + k_{r,p}\right\}[Se]_p \quad , \qquad (3B)$$

where E(t) is the pool water evaporation rate ($E(t) = -\frac{\partial}{\partial t}L_p$). In the laboratory pools, $L_p(t)$, D_o, α, n, E(t), L_w, and the initial $[Se]_p$ are known or at least very well-constrained. From previous work on similar types of laboratory columns, L_w was typically < 3 mm (Tokunaga et al., 1996). Circulation of pool waters in the field by wind and by thermal gradients would result in smaller values of L_w. Values of $k_{r,p}$ are obtainable from the systems without underlying sediments, since this term is associated with the depletion of $[Se]_p$ which is independent of the diffusive exchanges with sediment. Therefore only L_s remains to be determined. In a later section, Eq. (3) will be numerically integrated to obtain model $[Se]_p$ versus time relations for comparisons with experimental results. Values of L_s which provide best model fits to data will be discussed in terms of depths at which active Se(VI) reduction is inferred to occur.

An implication of Eq. (3B) and its underlying assumptions on time trends in pool Se concentrations is worth considering at this point. Here, we will identify the critical role which L_s has in determining whether $[Se]_p$ increases or decreases over time. Recall that diffusion and reduction lower $[Se]_p$ while evaporation results in its increase. A critical sediment depth, L_c, can be defined which distinguishes L_s values which lead to net increases and net decreases in $[Se]_p$. Thus, the dependence of L_c on E can be evaluated with the equation:

$$L_c = \alpha n\left(\frac{D_o}{E - k_{r,p}L_p} - L_w\right). \quad (4)$$

For a given ephemeral pool environment, D_o, α, n, and L_w are essentially fixed. At 20° C, D_o for SeO_4^{2-} is 89 $mm^2\ d^{-1}$ (Tokunaga et al., 1997). A value of α = 0.65 will be used, based on the study by Iversen and Jorgensen (1993). For an average E of 4 mm d^{-1} from pool waters overlying moderately high porosity surface sediment (n = 0.65), when the pool Se reduction term is insignificant, L_c will be in the range of 7 to 10 mm when L_w is set at 5 and 0 mm, respectively. This means that under these conditions, systems with L_s values smaller than these L_c will exhibit net decreases in $[Se]_p$ while systems with larger L_s will show increases in $[Se]_p$. When Se(VI) reduction within pool waters is significant, this process operates in combination with diffusion to decrease $[Se]_p$, thereby allowing larger values of L_c to balance evaporative increases in $[Se]_p$.

From the above analysis, it is clear that the depth at which Se(VI) reduction takes place is critical in determining rates of diffusive-reductive removal of Se(VI) from pool waters. Depths to reducing zones in natural surface water-sediment boundary regions vary considerably, sometime over very short distances (Jorgensen and Revsbech, 1985). The model presented here oversimplifies natural systems by identifying unique values of L_c, while a L_c probability distribution would be more realistic. Nevertheless, there is abundant evidence showing that reducing zones are commonly constrained to occur at very shallow depths within ponded sediments (e.g. Jorgensen and Revsbech, 1985; Santchi et al., 1990). The accumulation of Se species in very shallow reducing sediments has been demonstrated from analyses of core samples from Kesterson Reservoir ponds (Weres et al., 1989a), and in laboratory experiments (Tokunaga et al., 1996, 1997).

3.3.2 Materials and Methods

Shallow sediment samples and pool waters were collected from field sites 2ESE, 3NW, and 5S on Jan. 4, 1997. From sampling during previous years, these three sites were known to sustain different Se concentrations and salinities. During the 1996-1997 season, these sites became ponded on Dec. 10, 1996. Therefore the initial conditions for the laboratory experiment correspond to day 25 relative to the season's initial ponding event. Between Nov. 1, 1996, and Jan. 4, 1997, 183 mm of rainfall was recorded by the Kesterson CIMIS station, with 32 mm of rainfall deposited within 2 to 3 days prior to sampling. The sediment from site 2ESE is highly seleniferous, and includes partially decomposed cattail litter. The site 3NW and 5S sediments are both probably mixtures of fill and original Kesterson Reservoir soils. Decomposing vegetation (annual grasses and forbs) and some growing annual grasses were included in these

sediment samples. All sediments were sampled under about 0.15 m of ponded water, and transferred relatively intact, under water into the bottoms of 5.0 liter plastic beakers. The depth of sediment in these containers ranged from 50 to 70 mm. Surface water from each sampling site was ponded in the beaker to a depth of 117 ±2 mm over the corresponding sediment sample. At each site, a second 5.0 liter beaker was filled to a similar depth (110 to 117 mm) with surface water only (no sediment layer included). All pool waters contained a mixture of aquatic invertebrates, with Daphnia accounting for most (>90%) of the visible organisms. The beakers were incubated at laboratory room temperature (20° ±1° C), with continuous lighting, and with tops opened to permit evaporation. Pool water samples (5 mL) were collected in duplicate at 4 day intervals, filtered (0.45 μm), and diluted (to 10X). The small volumes of water collected during each sampling date amounted to less than 10% of the daily evaporative loss, and therefore were not considered to be significant perturbations in these systems. Analyses for Se(IV) and total Se were obtained on the diluted samples by hydride generation atomic absorption spectrometry (Weres et al, 1989b). Analyses for salinity were obtained from EC measurements on the diluted samples (adjusted to 25° C). The pool EC values reported here were obtained by linearly extrapolation of the readings in dilute solutions. The linear extrapolation was selected because this approach is proportional to the major ion concentrations of the waters over a moderate range in concentration. The actual pool water ECs are generally lower than the linearly extrapolated values, since total ionic concentrations become less than proportional to ECs at higher concentrations (Griffin and Jurinak, 1973; Marion and Babcock, 1976). Formation of ion pairs and complexes is more significant at higher concentrations, and this diminishes ideal independent ionic behavior.

3.3.3 Results and Discussion

All laboratory pools lost water through evaporation at similar rates during course of the experiment. Initial evaporation rates were 5 ±1 mm/d. Evaporation rates at the end of the 24 day experiment were 3 ±1 mm/d. For comparison, field pan evaporation rates during the months of January and February are typically in the 1 to 3 mm/d range. Another important factor which differed between field and laboratory conditions is the temperature. The average air and surface soil temperatures at Kesterson during this period (Jan.-Feb.) are 10°C and 12°C, respectively. Recall that the laboratory incubations were at 20° C. This temperature difference could have accelerated reaction rates by about two-fold, assuming commonly observed Q_{10} values of about 2, or activation energies of about 50 kJ/mol. The higher laboratory temperature also increases diffusion rates by about 36%, based on the Stokes-Einstein model. In both the field and laboratory systems, mass transfers of Se, other solutes, and suspended matter between ponded waters and sediments are further complicated by the presence of invertebrates which enhance

diffusion across this interface through bioturbation (Berner, 1980). Note that the reactions (precipitation of salts and Se, Se reduction) and mass transfer processes (evaporation of water, diffusion of Se and salts, bioturbation) occurring in these systems are coupled, and that their temperature-dependencies differ. This makes it difficult to accurately re-scale temperature-dependent temporal variations observed in these laboratory systems back to the colder field conditions. For the present purpose, it should simply be recognized that the laboratory experiments provided results characteristic of rates which were higher than those found in the field during winter months.

Increased concentrations of major dissolved ions in pool waters over time by evaporation is reflected in the EC time trends (Figs. 3.3.2a, 2b). These increases are typically greater in the pools without sediments since these systems lack sediment pore waters into which salts can diffuse. The salinities in the 2ESE and 3NW pools without sediments rise sharply in the last (day 24) measurement since less than 3% of the initial water volumes remained in each of these systems. A slightly larger initial pool volume and a slightly lower evaporation rate in the 5S pool left a volume equal to 18% of the initial water, hence a lower relative EC increase in the final sample. An estimate of changes in the major ion inventory within pools can be obtained by considering trends in the product of the pool EC and pool depth. Since the cross-sectional area of these beakers is nearly constant, the EC-depth product should remain nearly constant when there are no significant changes in the major ion inventory. Increases and decreases in this product would reflect net increases and decreases, respectively, of the dissolved ion inventory in the pools. The EC-depth products for pools without and with sediments are shown in Figs. 3.3.3a and 3.3.3b, where results have been normalized to their initial values. Normalized pool depths are also shown in these figures. The significant decreases in the EC-depth products at the end of the ponding period reflect a combination of ion pair formation, complexation, and evaporite precipitation. The latter process sequentially precipitates calcite, gypsum, thenardite, and halite (Hardie and Eugster, 1970; Eghbal et al., 1989).

Trends in pool water Se concentrations are shown in Figs. 3.3.4a and 3.3.4b, respectively. Selenium in pool waters remained primarily (> 90%) as Se(VI) throughout the experiment. Note that most of the systems exhibit increases in Se concentrations with time, indicating the importance of evaporative concentration. However, the 2ESE system with organic-rich sediment does show a significant decline in pool Se concentrations which is evident despite evaporation. Comparison of trends in systems with and without sediments show that sediments keep pool Se concentrations relatively lower. In the 2ESE-sediment system, pool Se concentrations actually decrease with time during the first half of the ponding period, despite evaporative concentration. The ability of the diffusion-evaporation-reduction model to match experimental results was tested using the data from Fig. 3.3.4b. These data are re-plotted as concentrations normalized to

initial pool concentration, along with best fit (minimized sums of squared differences) model results in Fig. 3.3.5. The model curves are numerical integrations of Eq. (3B), using 0.25 d time

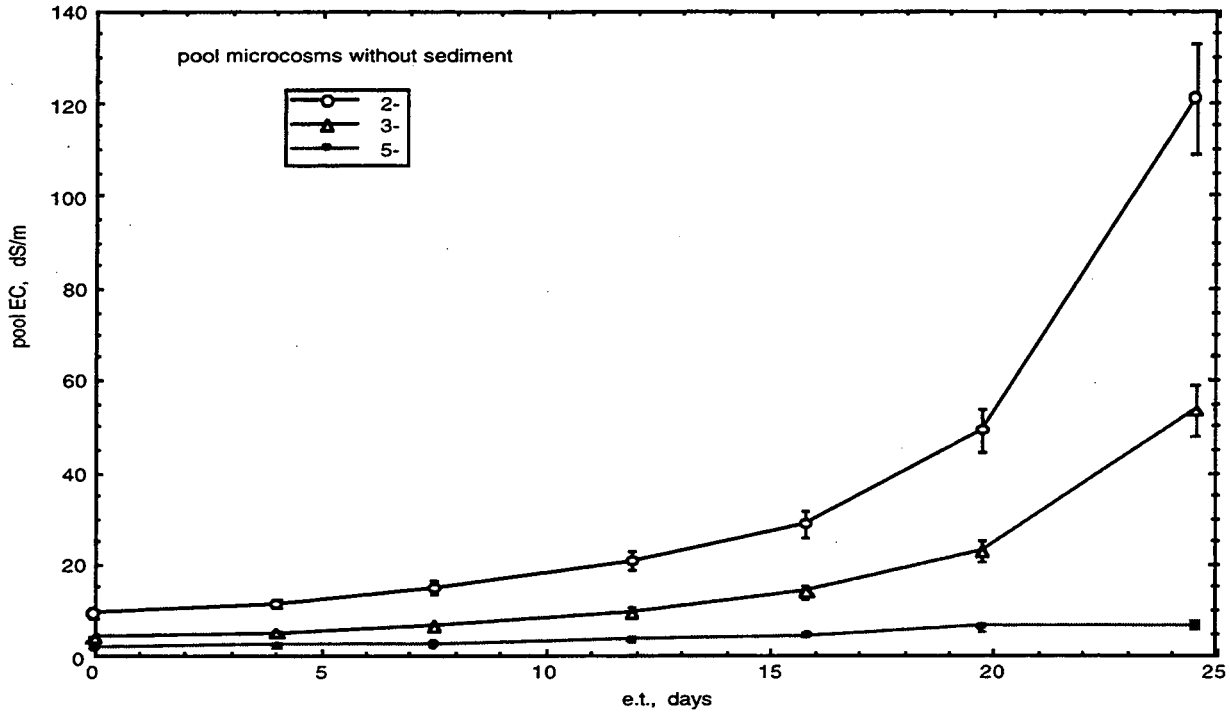

Figure 3.3.2a. Salinity (EC) increases during evaporation of pool waters without sediments. EC values are linearly scaled from measurements made on 10X diluted samples.

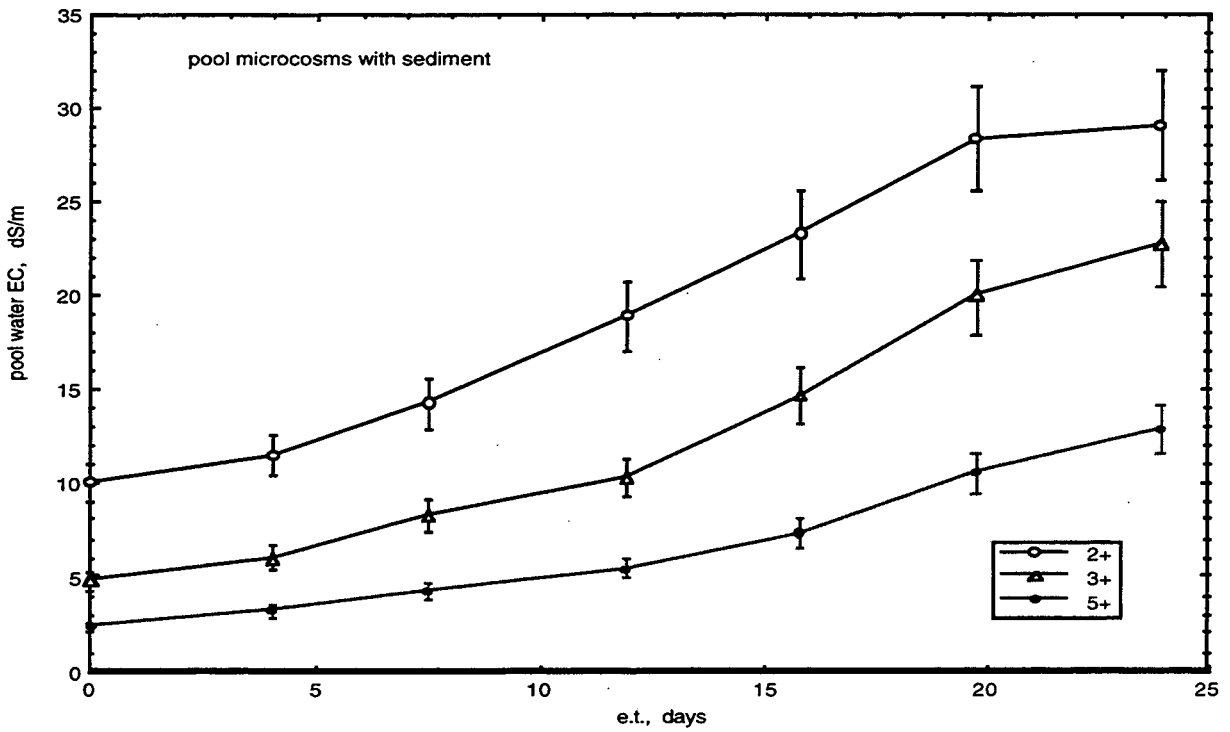

Figure 3.3.2b. Salinity (EC) increases during evaporation of pool waters with sediments. EC values are linearly scaled from measurements made on 10X diluted samples.

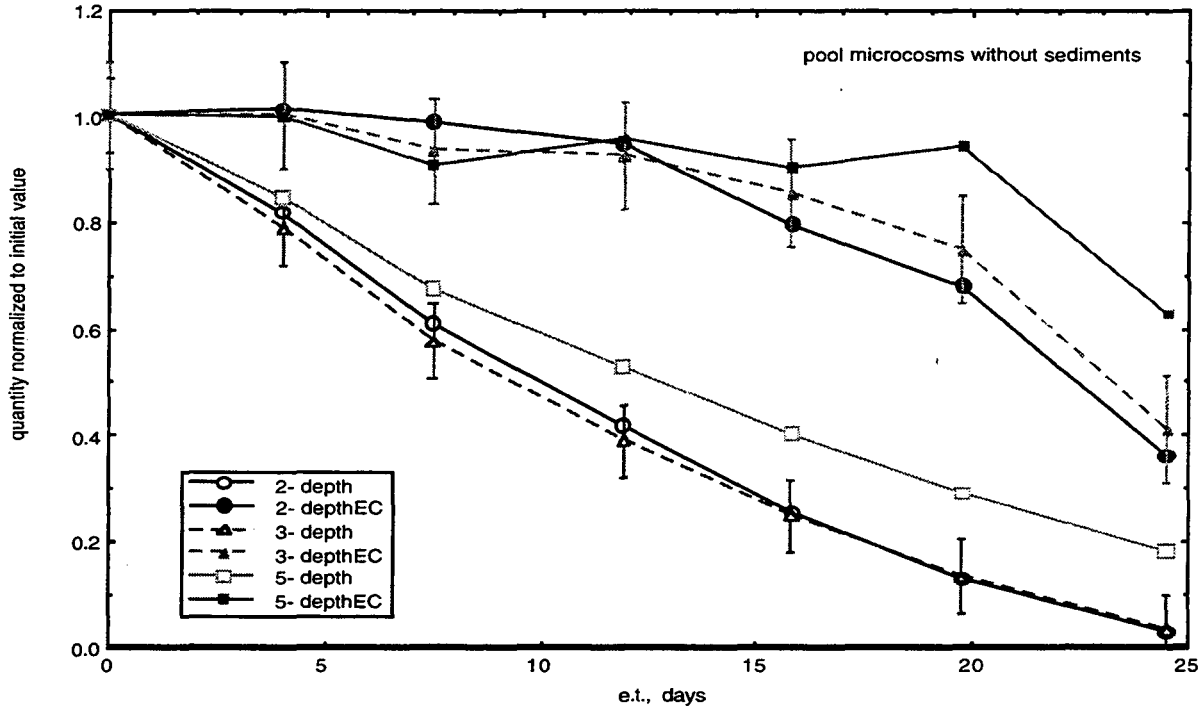

Figure 3.3.3a. Time trends in normalized pool depths (lower curves) and normalized ECxDepth (upper curves) in pools without sediments.

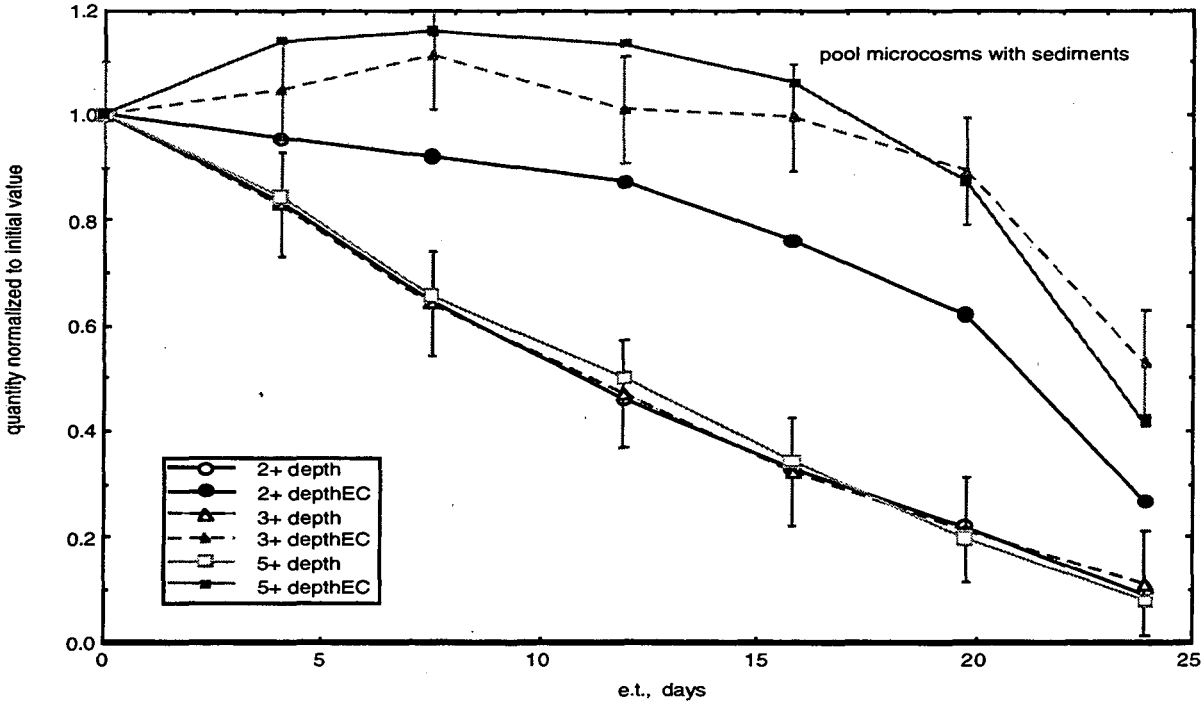

Figure 3.3.3b. Time trends in normalized pool depths (lower curves) and normalized ECxDepth (upper curves) in pools with sediments.

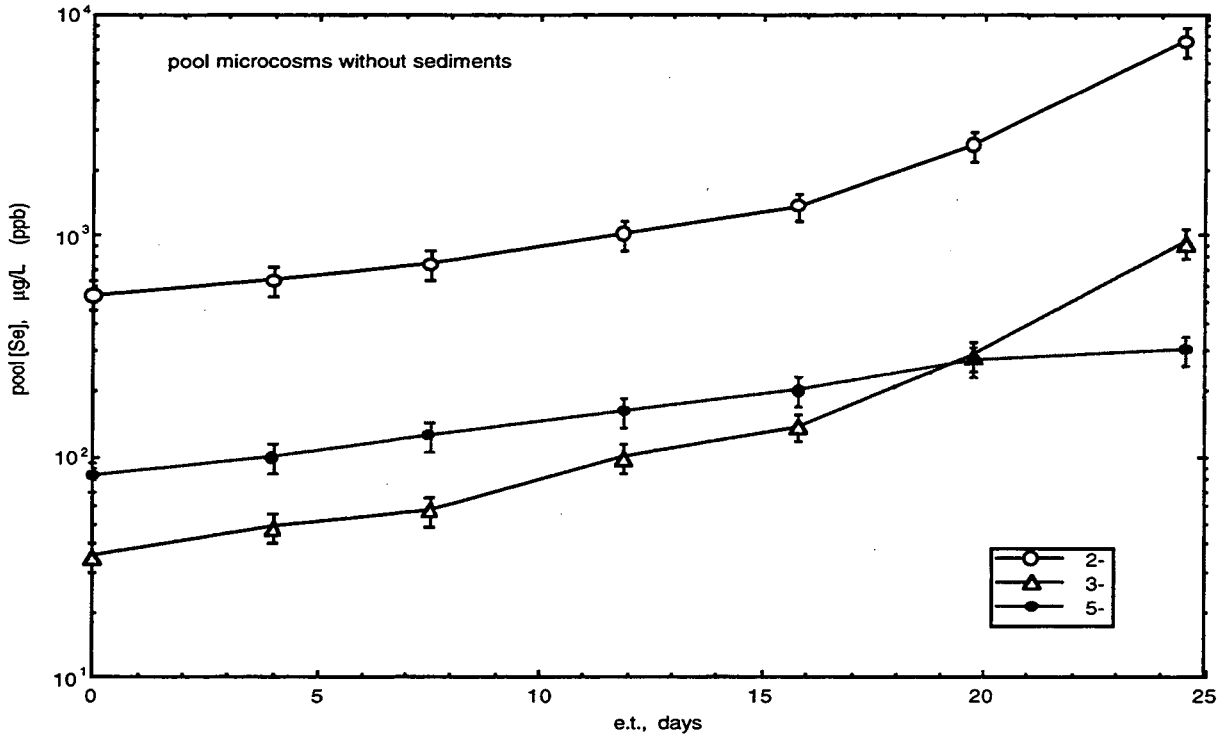

Figure 3.3.4a. Selenium concentrations in pool waters without sediments.

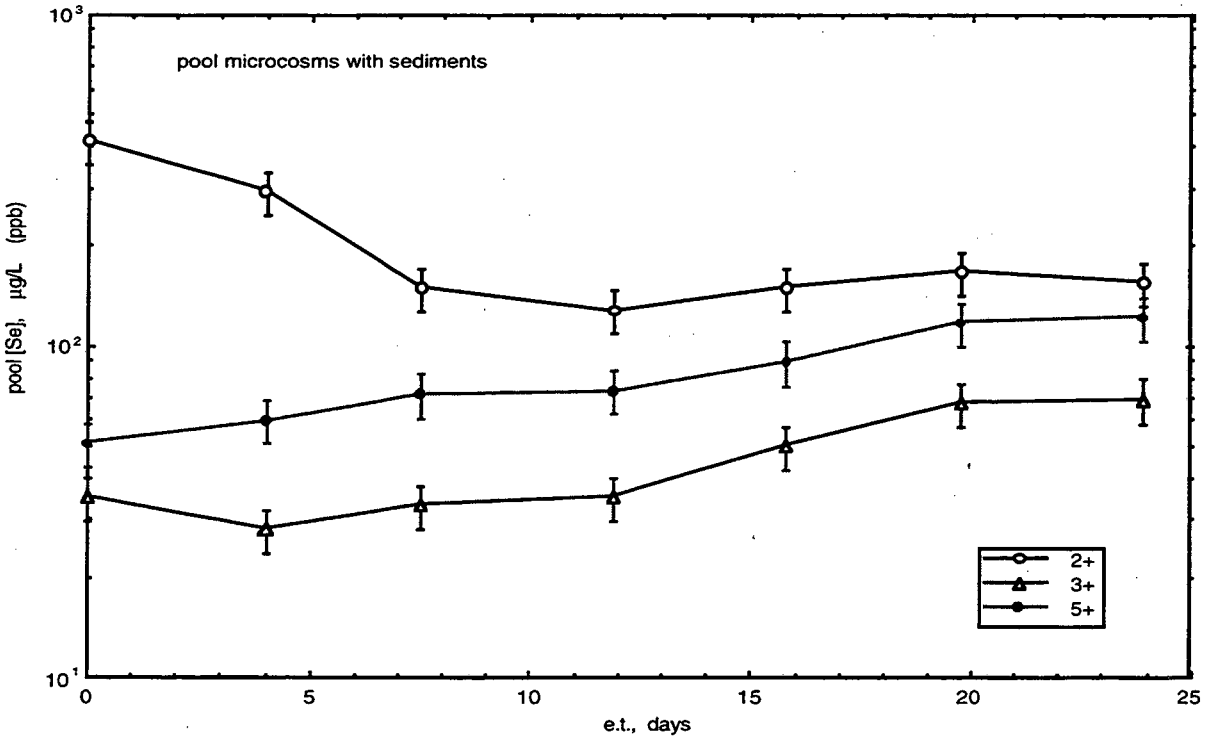

Figure 3.3.4b. Selenium concentrations in pool waters with sediments.

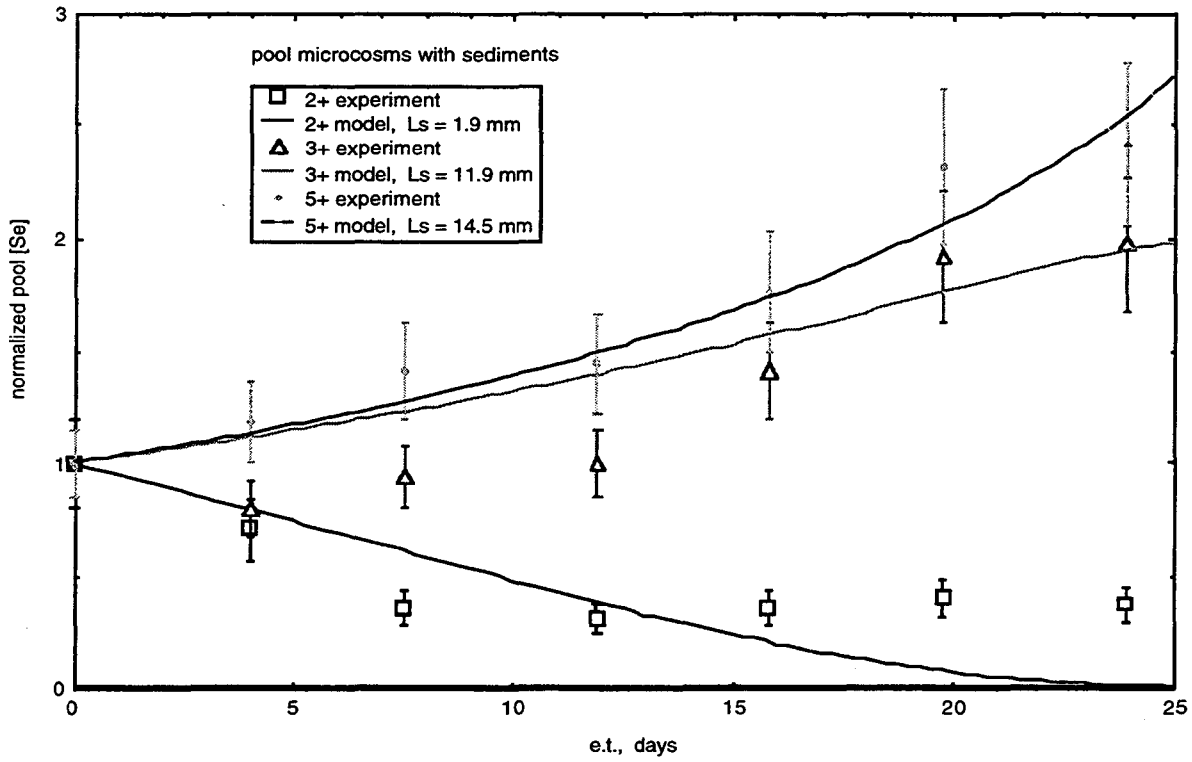

Figure 3.3.5. Comparison of Se(VI) concentrations (normalized to initial values) in pool waters with sediments with predictions from the diffusion-evaporation model. Model parameters are noted in the text.

intervals. The non-adjustable model input parameters were the measured pool depths and evaporation rates, D_o = 89 mm^2 d^{-1}, α = 0.65, n = 0.65, and $k_{r,p}$ = 0 (or 0.0023 d^{-1} as discussed later). The thickness of L_w was set at 3 mm, although variation of this value from 0 to 5 mm did not significantly affect the overall results. Thus the only adjustable parameter used for fitting the model to data was L_s. Best fit results were obtained with L_s equal to 1.9 mm (0.098), 11.9 mm (0.103), and 14.5 mm (0.056), in the 2ESE, 3NW, and 5S systems, respectively, with averages of model-data difference magnitudes indicated in parentheses. The selection of $k_{r,p}$ = 0 in the 3NW and 5S systems was based on lack of significant Se(VI) reduction in their corresponding laboratory systems without sediments. In the case of the 2ESE pool without sediments, Se(VI) removal was well matched by using a $k_{r,p}$ = 0.0023 d^{-1}, and therefore this rate term was included in the model fitting of its corresponding system with sediments. In the 2ESE system, changing $k_{r,p}$ from 0.0023 d^{-1} to 0 d^{-1} did not significantly change the modeled result, suggesting that diffusive removal of Se(VI) from pool waters into sediments was much more important than its reductive removal within pool waters. The relatively poor fits obtained in simulating the 2ESE and 3NW systems indicate that their Se mass transfer dynamics are significantly more complex than allowed for in the simple model. Note from Fig. 3.3.5 that in

both the 2ESE and 3NW systems, the model overestimates $[Se]_p$ at early stages and underestimates $[Se]_p$ at later stages. This discrepancy might have resulted from time-dependent migration of the active reducing zone in the experimental sediments, being initially located at shallower depths than the fitted L_s, and moving below this level at later stages. Such behavior would be consistent with initially higher microbial respiration rates within sediments, which gradually diminished during the course of the experiment. This in turn is an expected trend following ponding since easily available soil organic carbon sources are rapidly consumed at early stages of flooding, and would involve higher respiration rates. At later stages, the readily available carbon and other nutrients within the sediments would be smaller. Also, as a result of evaporative increases in salinity, osmotic stresses would be greater at later stages of the experiment. Both the depletion of available nutrients and increased osmotic stress at later stages of ponding would be reflected in lower respiration rates in these sediments. Measurements of respiration rates in such ponded sediment systems would be useful in future studies in order to test this possibility. In general, lower respiration rates would correspond to larger (deeper) L_s in this model. Note that the best model fit was obtained for the 5S pool-sediment, suggesting that temporal variations in relative respiration rates were smaller in this system which had the deepest calculated L_s (14.5 mm).

Net gains or losses of Se from pool waters can not be directly determined from concentration data such as those just discussed. In these open systems, additional information on the time dependence of the volume or mass of pool water is needed to obtain the pool Se mass balance. Two approaches were taken to determining whether or not Se is removed from pool waters during the course of ponding. The first approach relies on information on soluble Se concentrations and salinities within pool waters. It is an indirect indicator of pool Se inventories, but appears to be the only approach which is easily conducted in field studies. The second approach is a direct assessment of the soluble Se inventory, relying on measured Se concentrations and pool volumes in the laboratory microcosms. While having the advantage of being a direct measurement of the soluble Se inventory, this approach is much less practical in field environments since accurate surveys of pool volumes are required. These two approaches will be described in greater detail below, followed by a comparison of their respective predictions of trends in pool Se removal.

In the first approach, changes in the ratio of Se to major ions in pool waters were evaluated. This was done through examining trends in the pool water Se/EC ratios, normalized to their values at the beginning of the experiment (Figs. 3.3.6a and 3.3.6b). Trends in normalized pool Se/EC ratios reveal whether or not the inventories of soluble Se and major ions are changing in different proportions. This approach can only reveal changes in dissolved Se inventories when

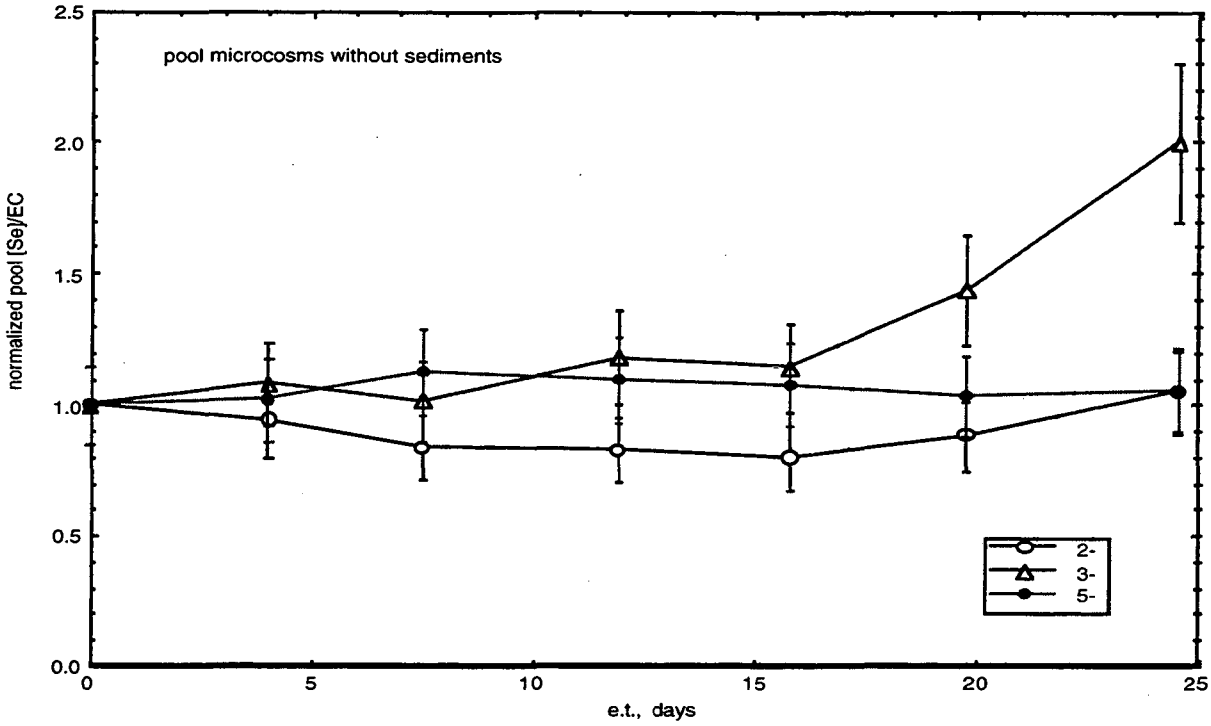

Figure 3.3.6a. Normalized pool water Se/EC ratios in waters without sediments.

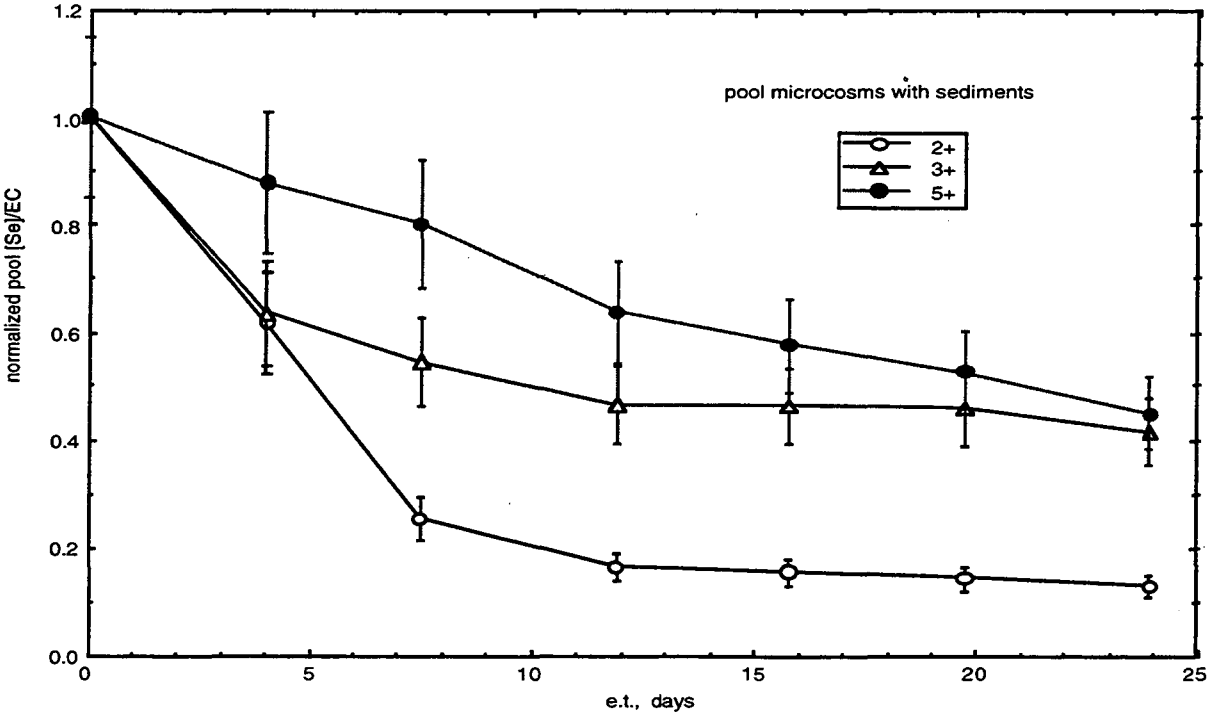

Figure 3.3.6b. Normalized pool water Se/EC ratios in waters with sediments.

the major ion inventory either remains constant (i.e., in the absence of precipitation losses) or changes in a quantified manner. With the exception of the 3NW system, the normalized Se/EC ratios in pool waters without sediments generally show no significant departures from initial values (Fig. 3.3.6a). The increase in normalized Se/EC ratios in the 3NW pool waters suggests that significant precipitation of certain major ions took place without incorporation of proportional amounts of Se. Evaporites which precipitate in this intermediate range of salinities in Kesterson soils are calcite and gypsum. Analyses of precipitates and major ions in solution have not been completed for this experiment. Data from pool waters ponded over sediments exhibit significant decreases in normalized Se/EC over time, in strong contrast to the systems without sediments. By the end of the experiment, the normalized Se/EC ratios in waters in contact with sediments where only 14% to 45% of initial values. It is worth noting that similar ranges in decreases in normalized Se/EC ratios have been observed in field pools (see Section 3.1). The primary limitation in the use of Se/EC trends to infer changes in the soluble Se inventory within a pool is that this approach assumes that the pool inventory of dissolved major ions remains constant, and furthermore that measured solutions are dilute enough to exhibit ideal EC readings. These conditions are never actually satisfied since mass transfers of major ions across the water-sediment boundary can be important, and since EC-concentration relations become nonlinear at and above intermediate ranges in salinities. Nevertheless, the use of normalized Se/EC ratios may still provide rough indications of changes in soluble Se inventories, as shown later.

The second approach to evaluating the pool Se data directly addresses the issue of changes in pool Se inventory. It is analogous to the previously described procedure for examining trends in pool EC-depth products. Since the cross-sectional area of the beakers are nearly constant, the product of pool depth times pool Se concentration is a measure of the pool Se inventory. The pool Se-depth products, normalized to initial values in each system, are shown in Figs. 3.3.7a and 3.3.7b. Note that in the pool waters from 3NW and 5S without sediments, the soluble Se inventory remains practically unchanged until the last stage of pool drying (Fig. 3.3.7a). Selenium concentrations in the 2ESE pool waters without sediments decrease steadily during the course of ponding. Trends in selenium concentrations in waters ponded over sediments showed greater rates of removal than their corresponding systems without sediments (Fig. 3.3.7b). The 2ESE waters showed the highest rates of Se removal, leaving less than 5% of the original Se inventory in solution at the end of the experiment. The other two systems (3NW and 5S, both with sediments) exhibited Se depletion as well, leaving about 20% of the original inventory in solution at the end of the 24 d experiment. Since the main difference between the systems shown in Figs. 3.3.7a and 3.3.7b is the absence and inclusion of sediment respectively, it is clear that the

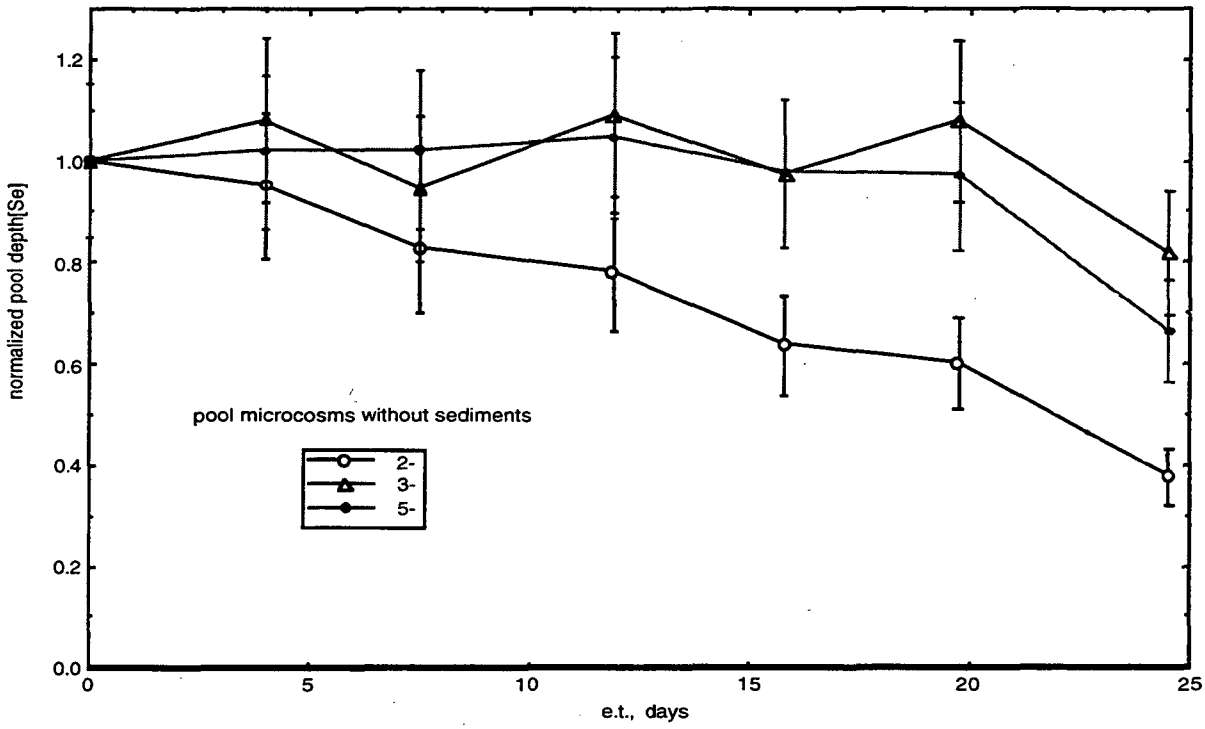

Figure 3.3.7a. Normalized pool Se inventories versus time, in pools without sediments.

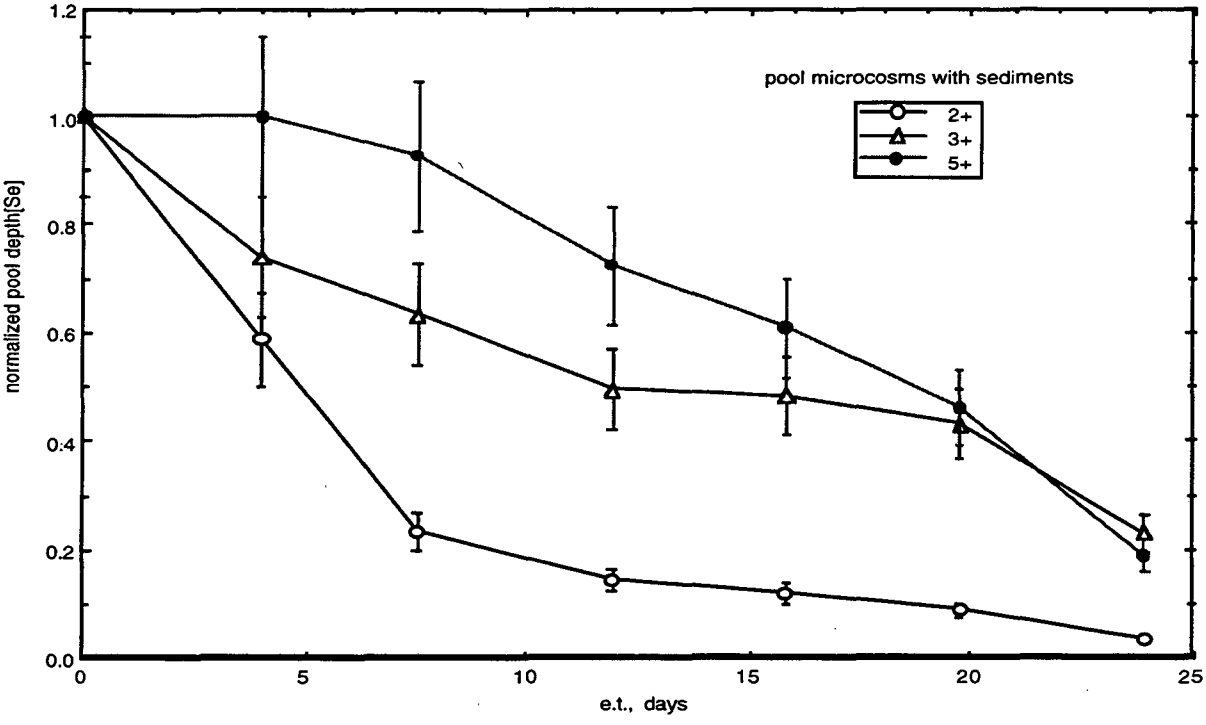

Figure 3.3.7b. Normalized pool Se inventories versus time, in pools with sediments.

sediment is the primary sink for Se in these simple pool environments. The gradual removal of Se from the 2ESE waters without sediments may have been due to Se reduction within suspended organic matter which was visibly abundant in that system and absent in the others without sediments, and also possibly due to Se volatilization.

The fact that the normalized Se-depth products for the 3NW and 5S pools without sediments remained about equal to 1 throughout most of the experiment may help constrain the magnitude of certain processes. The lack of measurable change in the dissolved Se inventory helps identify an upper limit on possible volatile Se losses from these systems. This upper limit is based on knowing the initial pool Se inventories, pool cross-sectional areas, and the fact that less than 5% of the initial soluble Se inventory was removed from the 3NW and 5S waters during the first 20 days. From this information, average volatile Se losses from the 3NW and 5S waters were < 10 and < 23 $\mu g\ m^{-2}\ d^{-1}$, respectively. Considerably lower Se volatilization rates (all < 4 $\mu g\ m^{-2}\ d^{-1}$) were obtained by Zhang and Moore (1997), in ponded laboratory microcosms containing much lower water (typically < 5 $\mu g\ L^{-1}$) and sediment (7.4 mg kg^{-1}) Se concentrations.

The relatively constant dissolved Se inventories in the 3NW and 5S waters (without sediments) also indicates that uptake of Se by microorganisms and invertebrates in these waters did not significantly deplete the soluble Se pool during this ponding period. However, this does not imply that biological uptake is not significant. The lack of observable Se removal in these two systems was probably due to biological uptake rates which were below detection based on solution analyses, or due to the systems already existing in quasi-steady-state with respect to Se partitioning at the time of field sampling. It is well known that Se accumulates in these organisms (Besser et al., 1989, 1993; Saiki et al., 1993; Bowie et al., 1996). In a laboratory microcosm study by Besser et al. (1989) zooplankton (primarily daphnids) bioconcentrated Se(VI), Se(IV), and Se-methionine by factors of 351 (±42), 1087 (±611), and 28870 (±9369), respectively over a 28 day period. The invertebrate population appeared relatively stable during the first 16 days of the experiment (≈100 L^{-1}). Their populations declined during the latter stages of the incubations. Assuming that stable populations (100 L^{-1}) bioconcentrated Se(VI) by the factor of 351, into 0.2 mg of tissue (dry mass) per daphnid, less than 1% of the initial soluble Se became incorporated into the collective invertebrate tissue. Combining initial pool Se concentrations from the 3NW and 5S laboratory systems with the bioconcentration factor indicates that daphnids in these two systems would have Se concentrations of 12 and 30 $\mu g\ g^{-1}$, respectively. These calculations show that very substantial bioconcentration of Se can occur without significantly depleting the soluble Se inventory in ephemeral pool waters.

We now compare calculations of soluble Se removal from pool waters resulting from the two different approaches, one based on Se/EC ratios and the other based on Se-depth products. In the indirect approach based on pool Se/EC ratios, the normalized net Se removed at any time

(relative to the initial soluble inventory) is obtained by subtracting the normalized Se/EC from unity. In the direct approach based on pool Se-depth products, the normalized net Se removed at any time is obtained by subtracting the normalized Se-depth product from unity. Comparisons of these two methods are shown in Figs. 3.3.8a and 3.3.8b, for the pools without and with sediments, respectively. These graphs again show that sediments are the primary sink for pool Se, with removal rates from pool waters being significantly faster with sediments. The two different approaches for calculating Se removal from pools are in fairly good agreement throughout the early and middle stages of the experiment. During the last stage of pool evaporation, the calculated Se removal based on these two approaches diverge significantly, especially in the waters without sediments. As previously mentioned, estimating pool Se inventory changes based on Se/EC ratios will be generally less reliable because of requiring the assumption of relatively constant major dissolved ion inventories. This assumption will generally be poor at the later stages of pool drying because of evaporite precipitation. When sediments are included, the assumption of constant major dissolved ion inventories in pools is further weakened by exchanges with underlying sediments. Nevertheless, it is worth noting that predictions of pool Se depletion based on normalized Se/EC ratios were relatively accurate in the three systems which included sediments, until relatively late in the ponding period (Fig. 3.3.8b). This good agreement is probably a result of the dominating influence of Se diffusion into and reduction within sediments, relative to diffusion of major ions across the water-sediment boundary. The good agreement obtained between the two methods for tracking the pool Se inventories in these simple laboratory pool-sediment systems provides support for use of the normalized Se/EC ratio in estimating changes in soluble Se inventories in field pools.

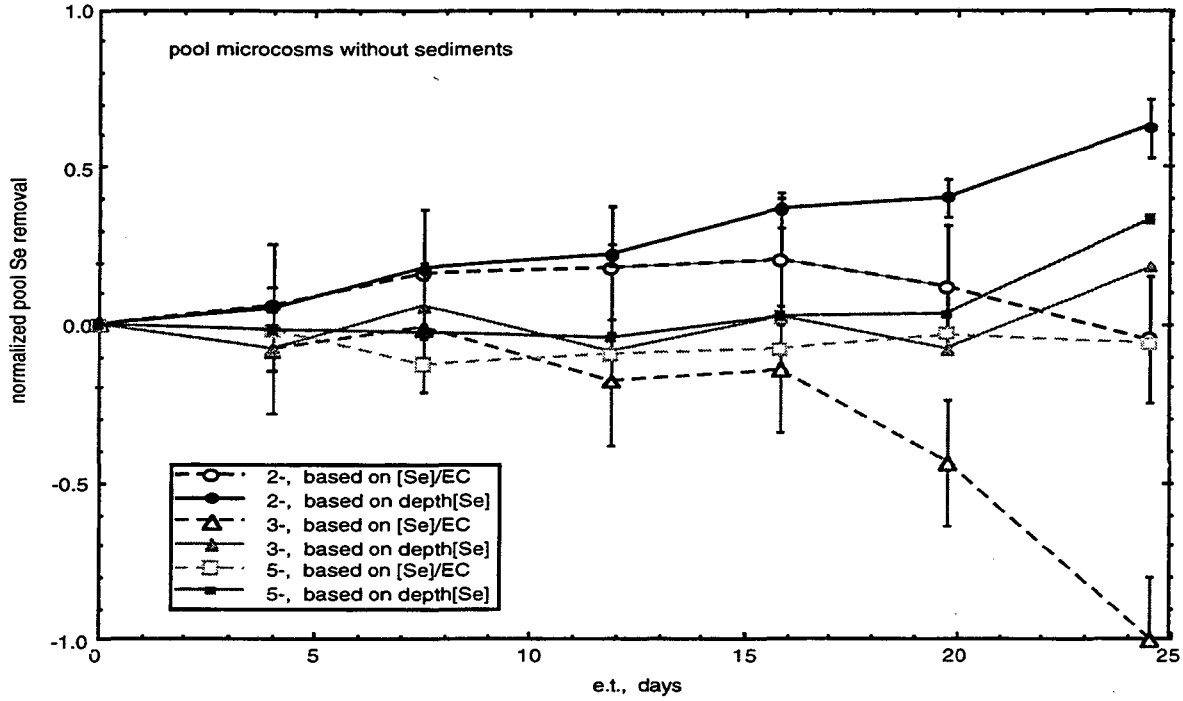

Figure 3.3.8a. Fraction of the initial pool water Se removed from solution during ponding without sediments. Calculations based on direct depth-concentration data and on Se/EC ratios are compared.

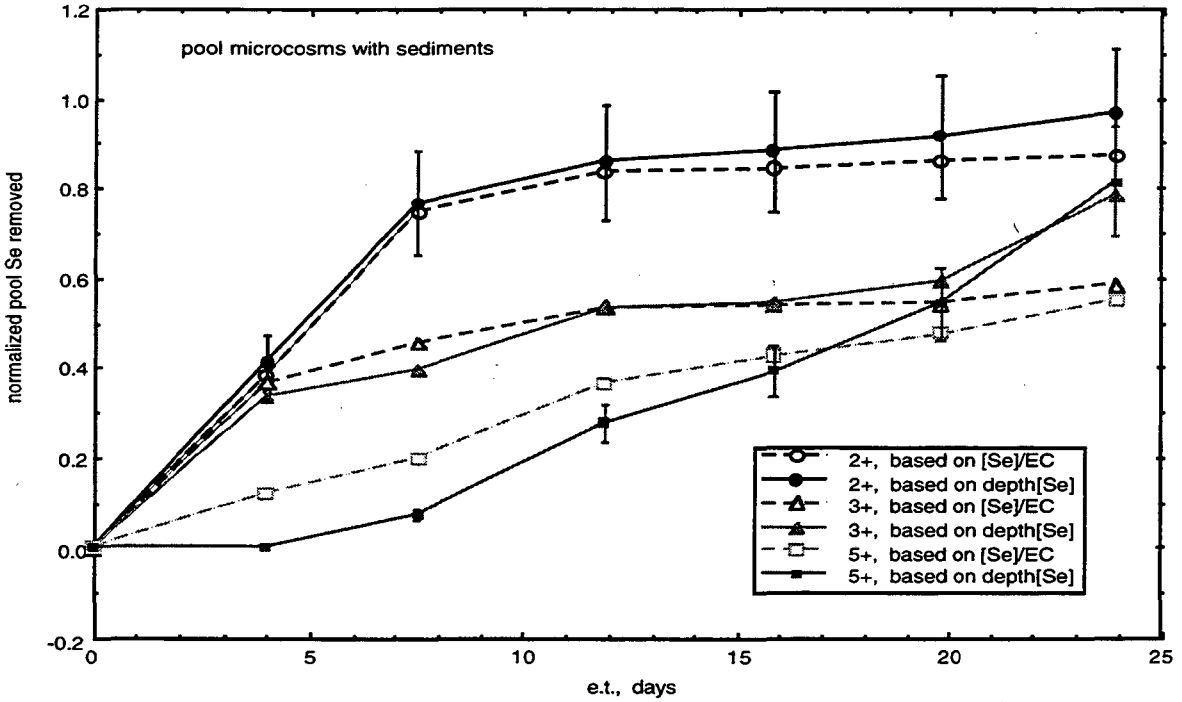

Figure 3.3.8b. Fraction of the initial pool water Se removed from solution during ponding with sediments. Calculations based on direct depth-concentration data and based on Se/EC ratios are compared.

4 Pond 2 Pilot Scale Microbial Volatilization Study

Peter Zawislanski
Earth Sciences Division
Lawrence Berkeley Laboratory

Microbial volatilization is being investigated as a potential remedial measure to decrease the selenium inventory at Kesterson Reservoir. In order to evaluate the effectiveness of this bioremediation method, a long-term field experiment is being conducted in Pond 2. The objectives of this study include the quantification of selenium losses and a test of a pilot-scale design which in the future may be used in other parts of the Reservoir. The rationale for and details of the design of this experiment have been extensively described in previous reports (Zawislanski et al., 1995) including a comprehensive summary of the project through 1995 (Zawislanski et al., February 1996). Therefore, only a brief summary of the field setup will precede an update of field data collected through 1996.

In 1989, the site for this study was chosen in the northern end of Pond 2 (Fig. 4.1), an area which was very frequently flooded during the operation of the Reservoir and supported primarily cattail vegetation. Preliminary soil sampling in this plot in November 1989 revealed some of the highest Se concentrations in the Reservoir: mean [Se] in the top 15 cm (5 samples) was 291 ppm; in the 15 to 30 cm interval it was 27.3 ppm. Furthermore, the same soil intervals were found to be less saline than average (1:10 soil:water extract electrical conductivity normalized to field water content ranged from 23 dS/m to 69 dS/m). In preparing this plot for the study, cattail remains on the soil surface were incorporated in 1990 into the top 20 cm or so of soil by repeated disking and rototilling. The plot was then divided into four subplots, each being reserved for a particular treatment: irrigation only (I), irrigation and disking (rototilling) (ID), disking (rototilling) only (D), and control or no treatment (C) (Fig. 4.2). An 11.6 meter buffer zone was set up between the irrigated and non-irrigated plots in order to prevent irrigation water from falling onto the disked plot. Losses of selenium in the soil are being monitored by annual sampling along selected transects and in randomly selected subplots as well as by direct measurement through charcoal trapping of dimethylselenide (UC Davis). Monitoring of the vadose zone for potential short-term and long-term leaching of selenium deeper into the profile is being conducted. In order to determine the amount of near-surface selenium lost to volatilization, selenium displaced by infiltrating water must be quantified. These efforts aid in constructing a selenium mass balance in the vadose zone and estimating selenium losses due to volatilization.

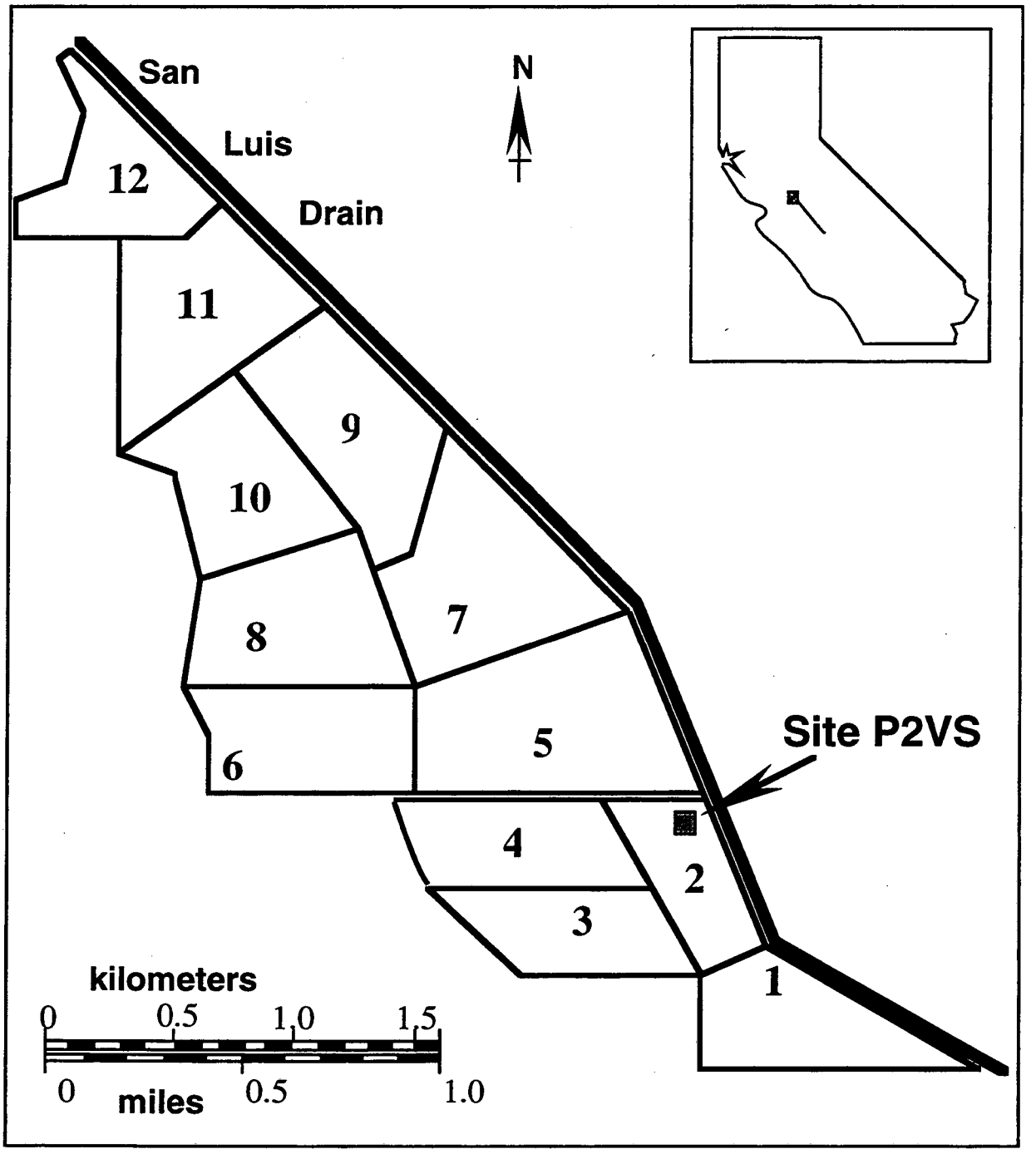

Figure 4.1 Location of experimental site within Kesterson Reservoir.

Figure 4.2 Site layout.

4.1 Moisture and Solute Monitoring

The design and operation of the vadose zone monitoring system are described in Benson et. al. (1992). General long-term trends in soil moisture content are shown in Fig. 4.3 and 5.4. These data are based on neutron probe readings obtained in PVC wells and integrated over a depth of 1 m. Moisture content is inversely proportional to the amount of vegetation within the plot. As there is no vegetation in the rototilled treatments (ID and D), and the soil is mulched, evapotranspiration is minimized and the soil profile retains moisture throughout the year. On the other hand, plants in the non-rototilled treatments remove water via transpiration, resulting in a dry soil profile during summer months. All treatments are affected by winter and spring rainfall, which in the case of treatment I can result in as much as a tripling of moisture content. The vast and rapid changes in moisture content following major rainfall events have great significance in terms of solute transport into the soil profile. Rapid changes in soil moisture content due infiltration of rainwater are observed and have been analyzed in detail by Zawislanski et al. (1996).

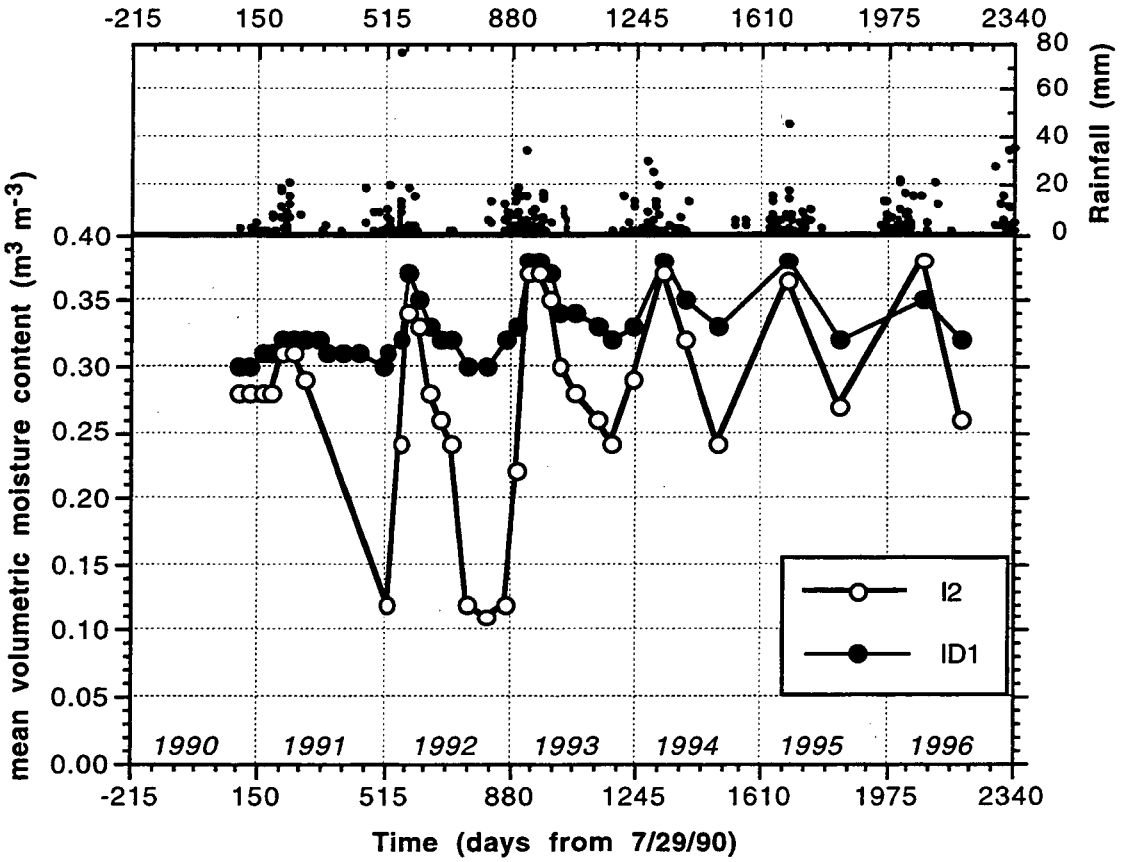

Figure 4.3. Changes in mean moisture content over the top 1 m of soil in treatments I and ID, estimated from neutron probe readings.

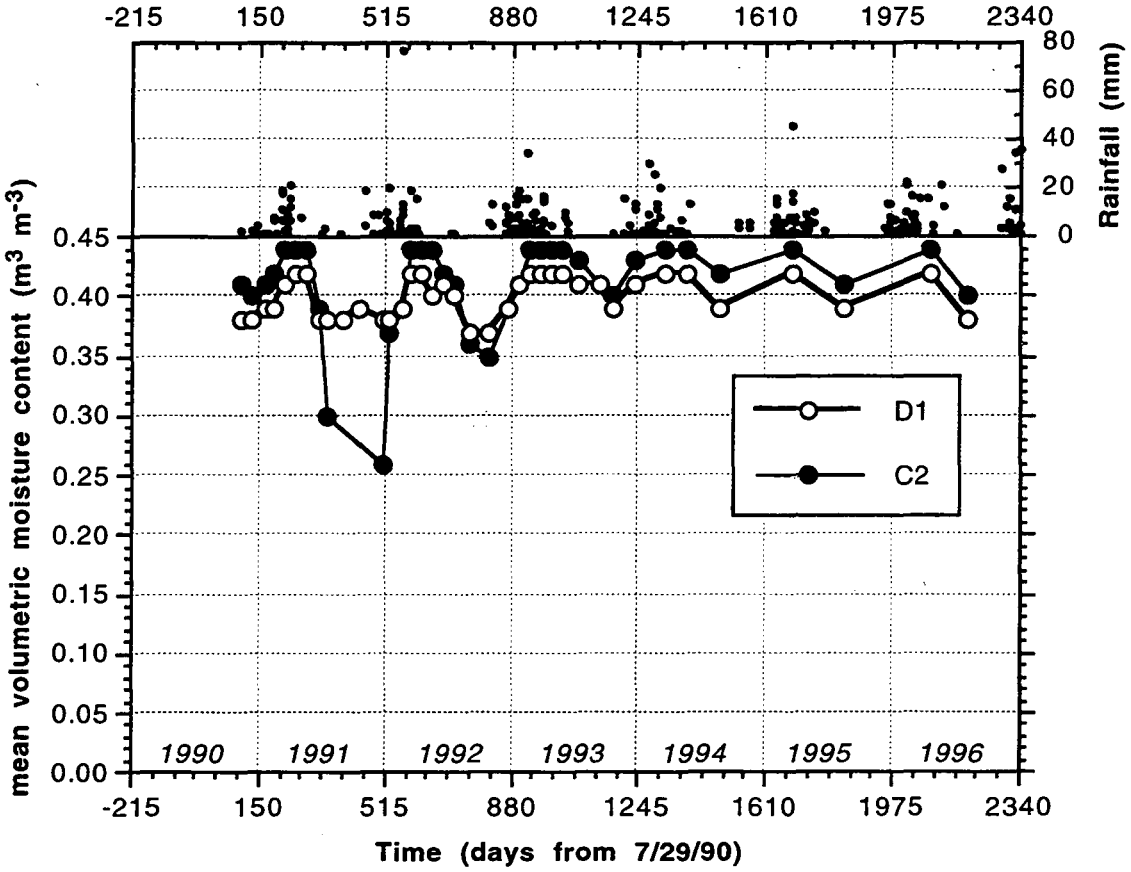

Figure 4.4. Changes in mean moisture content over the top 1 m of soil in treatments D and C, estimated from neutron probe readings.

The degree to which solute movement is affected by rainfall infiltration is demonstrated by changes in soil-water Se and Cl concentrations. These data, which are depth-integrated between 0.425 and 1.00 m, are shown in Fig. 4.5 through 4.8 and are expressed as mass per area in order to be comparable with soil Se data, presented in the following subsection. In treatment I (Fig. 4.5), both Se and Cl concentrations have increased significantly in this interval over the last 6 years. This is primarily due to the high density of plants growing in this plot. Plant transpiration results in the concentration of solutes in the root zone and the effect of rainfall events is diffused. On the other hand, in treatments ID and D (Fig. 4.6, 4.7), the effect of rainfall is apparent and results in large fluxes of Se into the soil profile. Because of its more even depth-distribution, Cl concentrations do not vary greatly in these plots. In the control treatment (Fig. 4.8), Cl concentrations increase as they do in treatment I, but Se concentration changes are much smaller in magnitude, probably because of the relatively high groundwater table in this area, which limits the downward movement of Se due to rapid chemical reduction. This effect is observed at the peak of the wet season in 1992 and 1993, when Se concentrations drop to close to zero. A

common feature observed in all treatments, though less markedly in treatment D, is the net increase in pore-water Se and Cl in 1995 and 1996. This may be a result of either of two scenarios: a) more Se than before is being flushed out of the near-surface soil into the root zone, or b) Se deeper in the profile is being oxidized, mobilized and transported along an evapotranspirative gradient toward the surface. Soil-Se data presented in the following section support the latter scenario.

It should be noted that the frequency of sample collection in 1995 and 1996 was reduced relative to previous years, resulting in diminished data resolution. Therefore, the interpretation of this data needs to be made alongside the interpretation of soil-Se data.

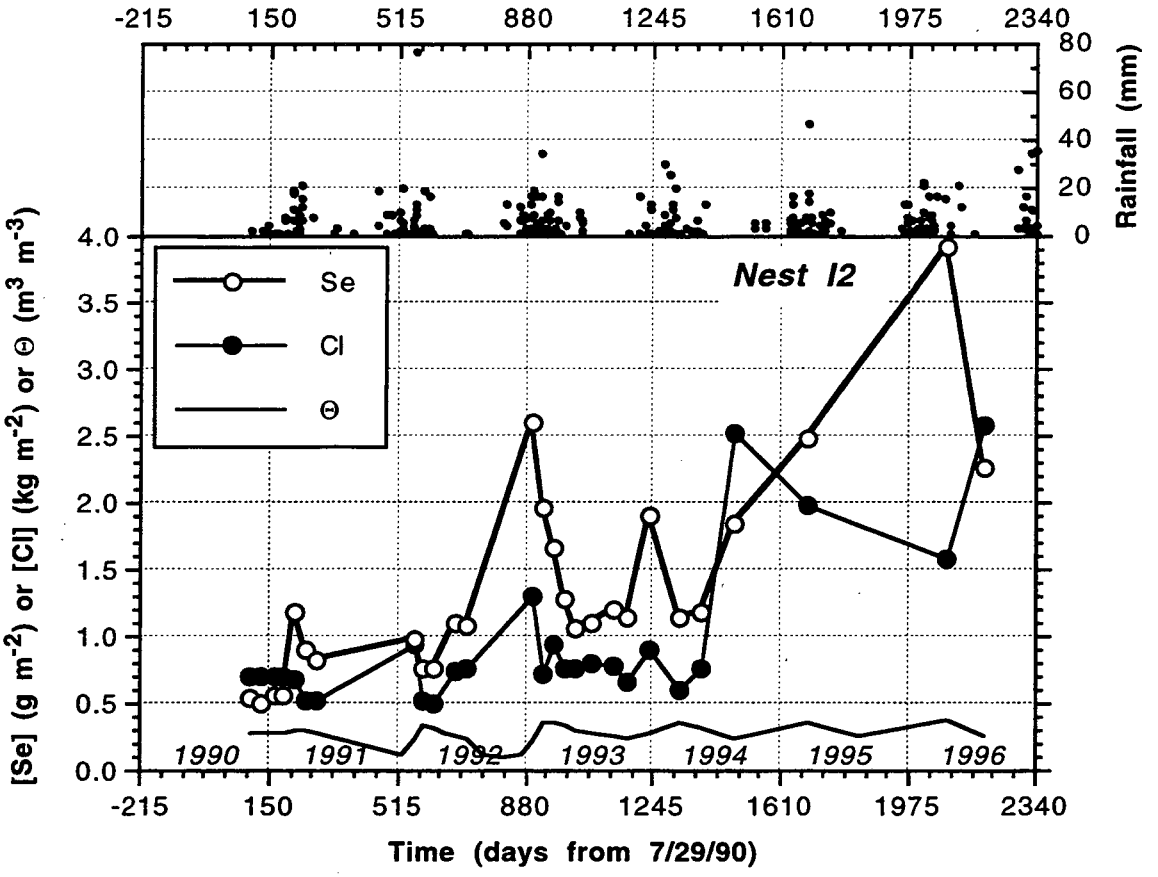

Figure 4.5. Mass of Se and Cl, and volumetric moisture content over the depth of 0.4 m to 1.00 m in treatment I, based on data from soil water samplers and neutron probe measurements at nest I2.

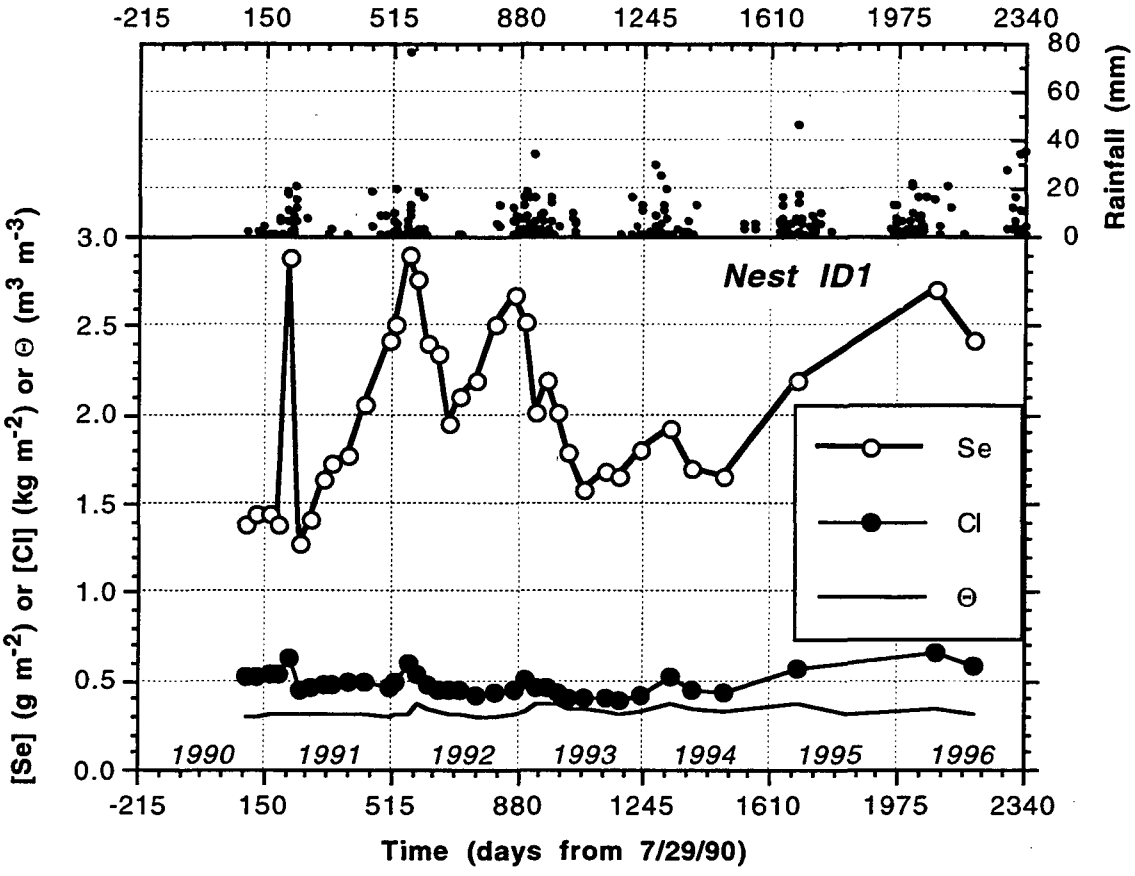

Figure 4.6. Mass of Se and Cl, and volumetric moisture content over the depth of 0.4 m to 1.00 m in treatment ID, based on data from soil water samplers and neutron probe measurements at nest ID1.

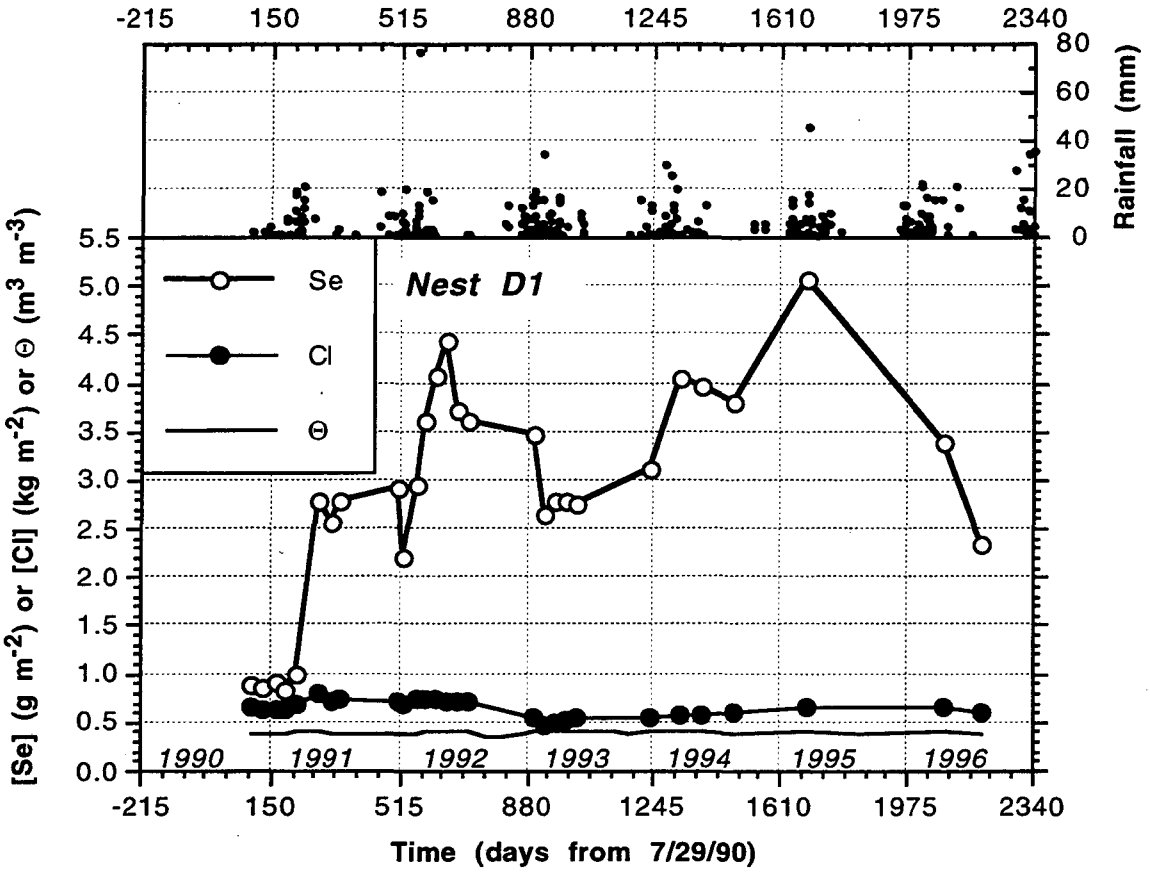

Figure 4.7. Mass of Se and Cl, and volumetric moisture content over the depth of 0.4 m to 1.00 m in treatment D, based on data from soil water samplers and neutron probe measurements at nest D1.

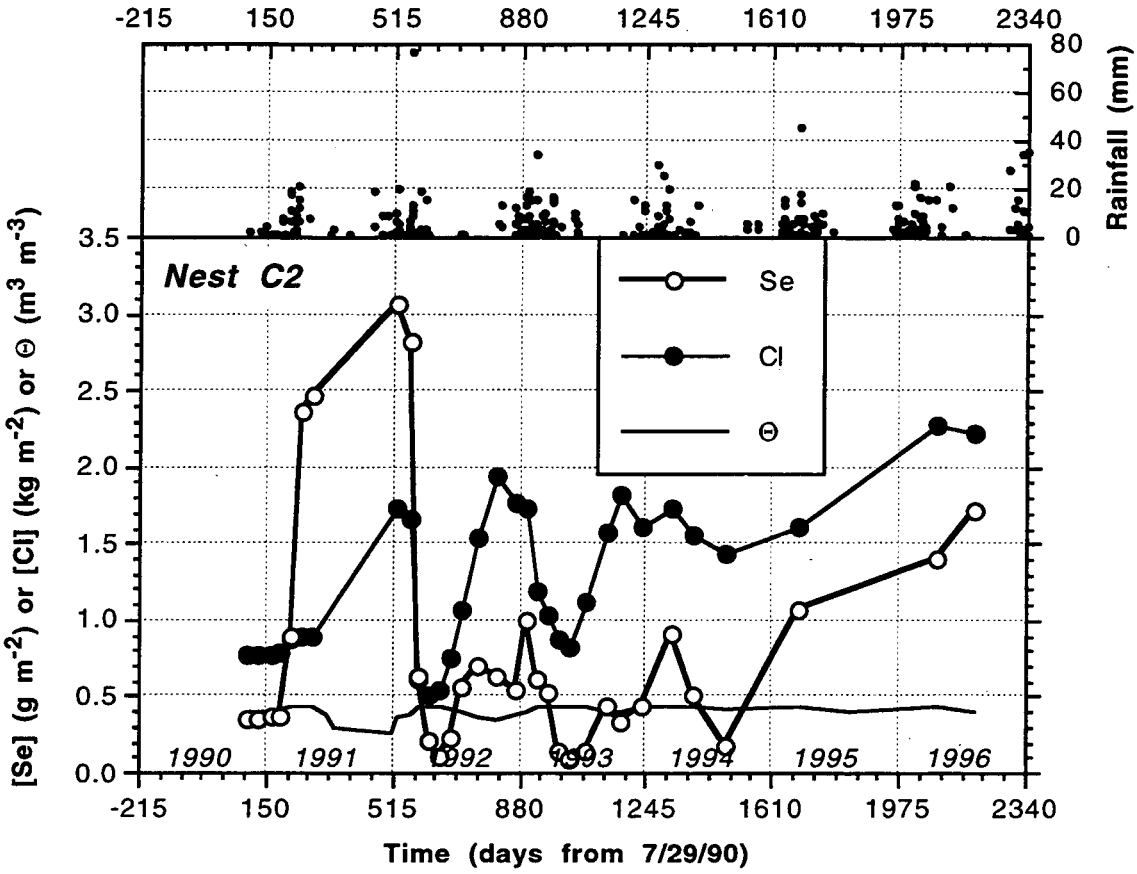

Figure 4.8. Mass of Se and Cl, and volumetric moisture content over the depth of 0.4 m to 1.00 m in treatment C, based on data from soil water samplers and neutron probe measurements at nest C2.

4.2 Soil Monitoring

Soil samples down to a depth of 60 cm are collected along a N-S transect through the middle of each treatment in July. In 1990 through 1992 cores were collected every 3 m along these lines. In 1993 and 1994 cores from transects D and C were collected every 6 m. In 1995 and 1996 cores from all transects were collected every 10 m. Soil from the transects is extracted using a 1:5 soil:water extract and extracts are analyzed for total soluble selenium via HGAAS. All soil samples are extracted for total Se via an acid digest and analyzed via HGAAS. See Figure 4.2 for sampling locations.

4.2.1 Depth-Distribution of Soil-Se

Total Se concentrations in each treatment were averaged by depth and are shown in Fig. 4.9-4.12. The error bars, representing one standard deviation from an arithmetic mean, are indicative

of the spatial variability observed in the field. Such variability makes it difficult to discern temporal trends and necessitates the collection of many data sets in time. Currently, with seven years of data available, it is apparent that there are no net decreases in any of the treatments, except possibly ID. All treatments exhibit a trend of decreasing Se in the top 30 cm with slight increases in the 30-60 cm interval from 1990 to 1993, followed by a negligible decrease in Se in the 0-15 cm interval and increases in Se in deeper intervals between 1993 and 1994, followed by increases in Se in 1995 and 1996. This commonality among the different treatments suggest that Se movement is being controlled by common external factors, i.e., rainfall, water table fluctuations, and evapotranspirative flux, while the slight differences are probably the result of the different treatments and the resultant soil conditions (i.e., varying moisture content, presence/absence of plants, differences in soil bulk density). Given the large fluctuations observed in the near-surface Se concentrations, it may be difficult to assess the effectiveness of microbial volatilization, unless it results in a loss of at least 10% of the Se inventory per annum.

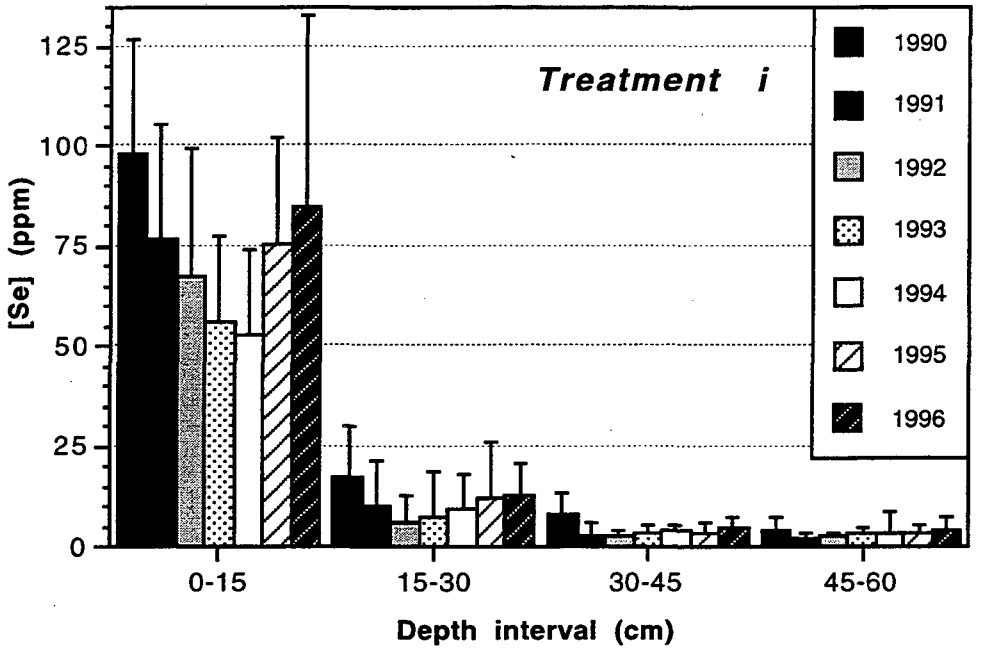

Figure 4.9. Mean total Se concentrations in 15-cm intervals of the top 60 cm of the soil profile along the N-S transect of treatment I. Error bars represent one standard deviation from the arithmetic mean.

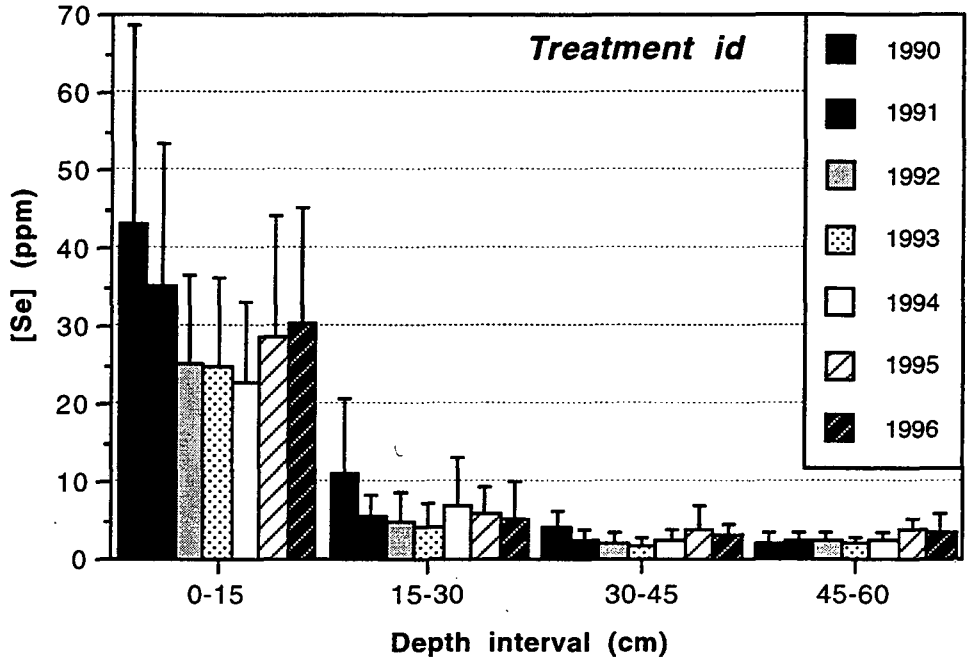

Figure 4.10. Mean total Se concentrations in 15-cm intervals of the top 60 cm of the soil profile along the N-S transect of treatment ID. Error bars represent one standard deviation from the arithmetic mean.

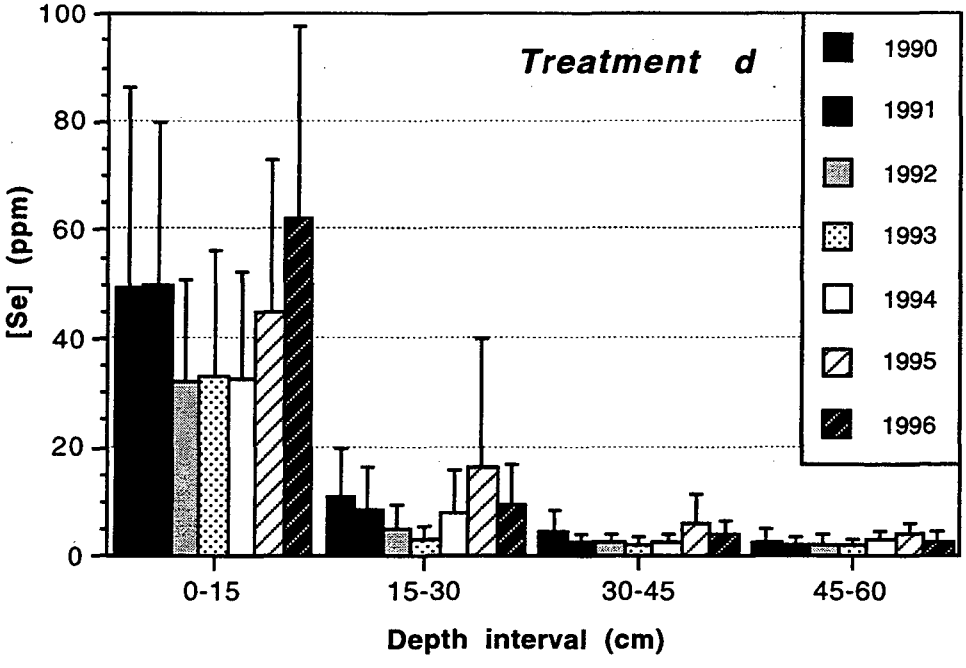

Figure 4.11. Mean total Se concentrations in 15-cm intervals of the top 60 cm of the soil profile along the N-S transect of treatment D. Error bars represent one standard deviation from the arithmetic mean.

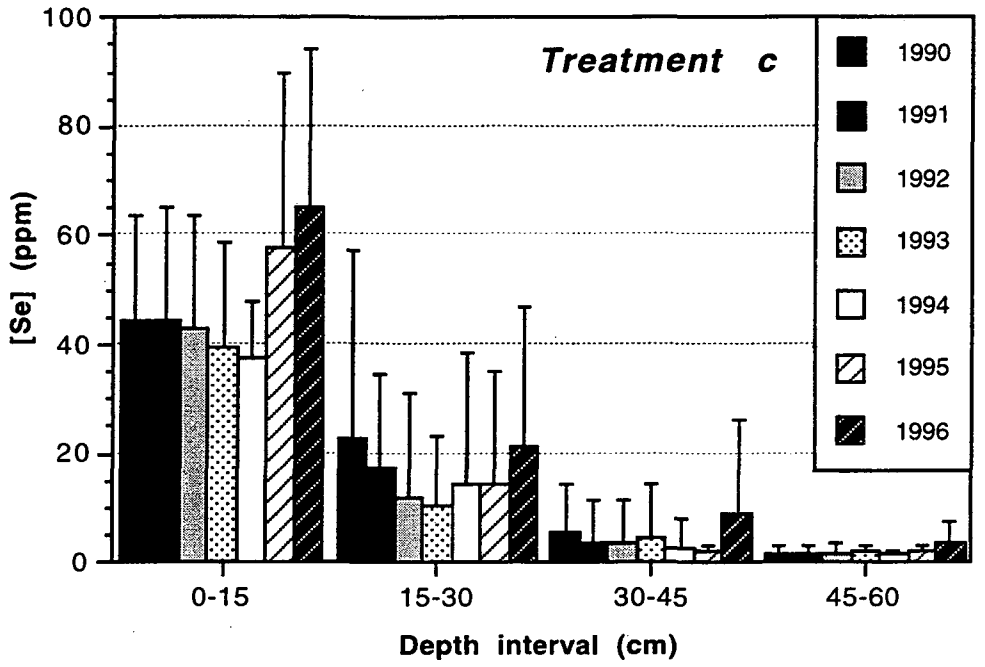

Figure 4.12. Mean total Se concentrations in 15-cm intervals of the top 60 cm of the soil profile along the N-S transect of treatment C. Error bars represent one standard deviation from the arithmetic mean.

4.2.2 Depth-Distribution of Soluble-Se

Water-soluble Se extracted from the same soil samples is indicative of the potentially mobile Se fraction. This data, normalized as a percentage of total Se, is shown in Fig. 4.13-4.16. Water-soluble Se in the 0-15 cm interval generally ranges from 10 to 20% of total, except in treatment I (Fig. 4.13) where soluble Se was only 5% of total during the period 1990-1993, and then rose to the 10 to 20% range in subsequent years. The percentage of soluble Se increases with depth, with values up to near 100% in the 45-60 cm interval. This finding is very important in that it shows the great potential for Se displacement in the profile, whether it be due to infiltration, diffusion, or evapotranspirative fluxes. It should be noted that samples were collected in July, whereas annual peaks of Se oxidation and solubilization are generally observed in late summer (Zawislanski et al., 1995, Ch.2), which means that even more of the Se inventory may be soluble during times of late fall, early winter rains. There is an overall net increase in soluble Se in the average profile in all treatments from 1990 through 1992 with either a leveling off or slight decline in subsequent years. This corresponds with increases in average moisture

content observed in these soil profiles during the period of 1993-1996, as seen in Figs. 4.3 and 4.4.

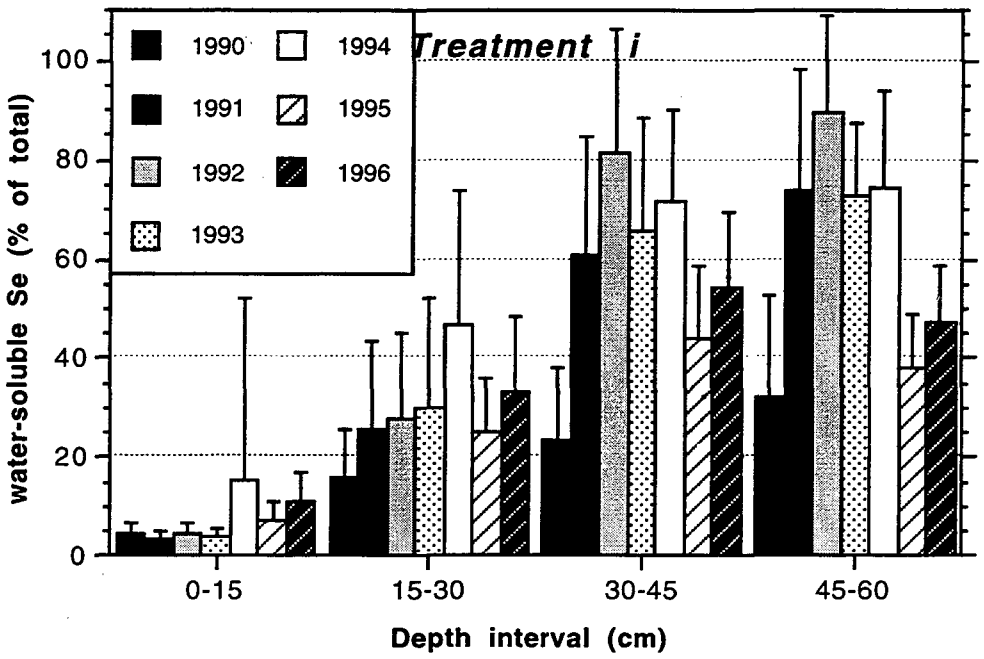

Figure 4.13. Mean water-soluble Se, as percentage of total, in 15-cm intervals of the top 60 cm of the soil profile along the N-S transect of treatment I. Error bars represent one standard deviation from the arithmetic mean.

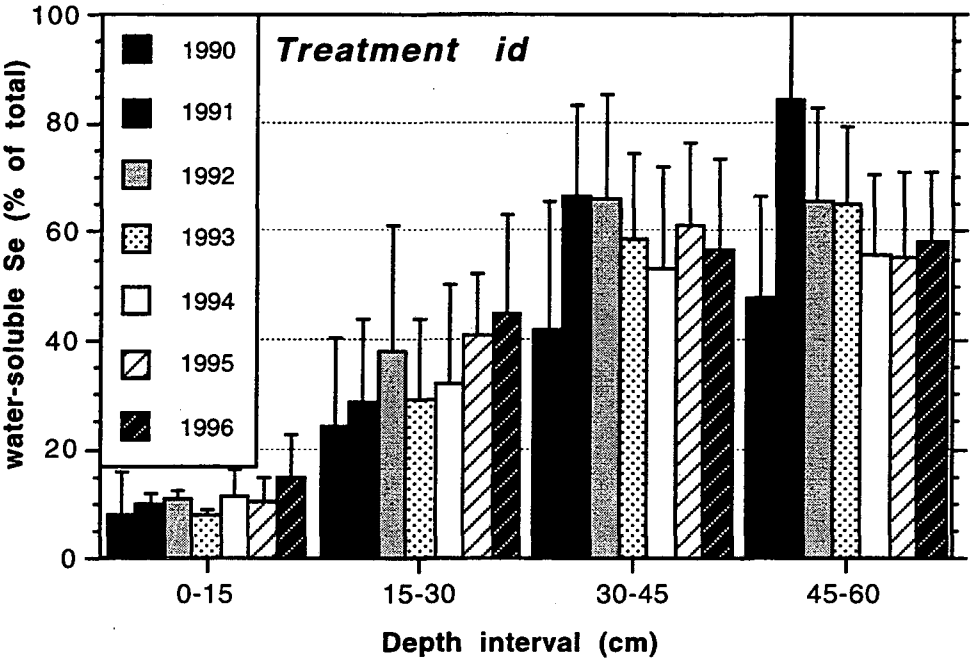

Figure 4.14. Mean water-soluble Se, as percentage of total, in 15-cm intervals of the top 60 cm of the soil profile along the N-S transect of treatment ID. Error bars represent one standard deviation from the arithmetic mean.

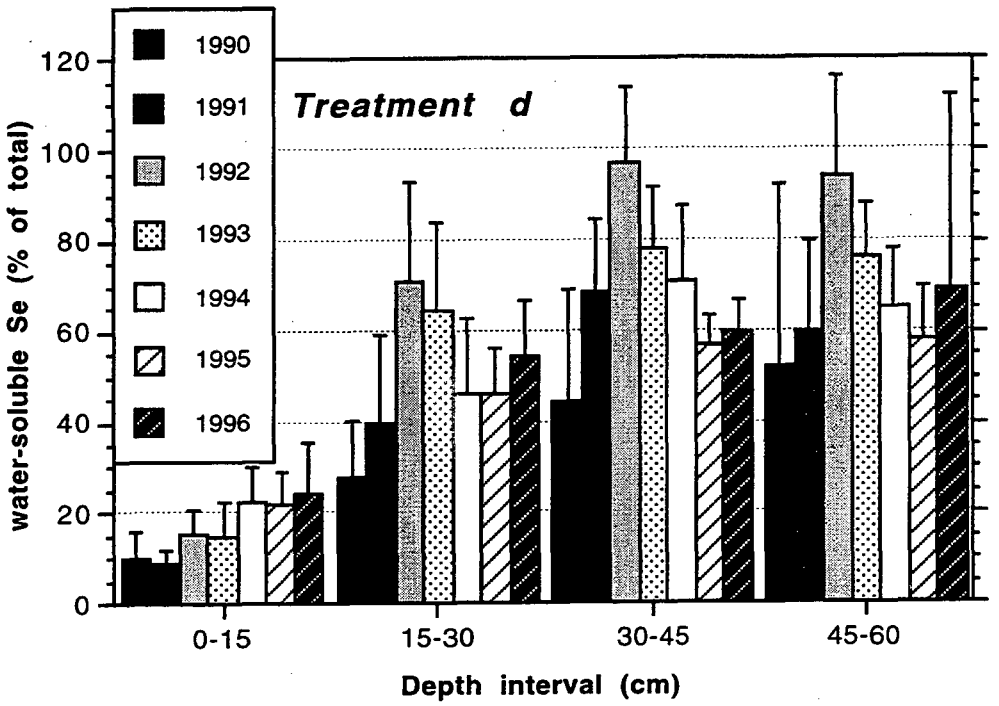

Figure 4.15. Mean water-soluble Se, as percentage of total, in 15-cm intervals of the top 60 cm of the soil profile along the N-S transect of treatment D. Error bars represent one standard deviation from the arithmetic mean.

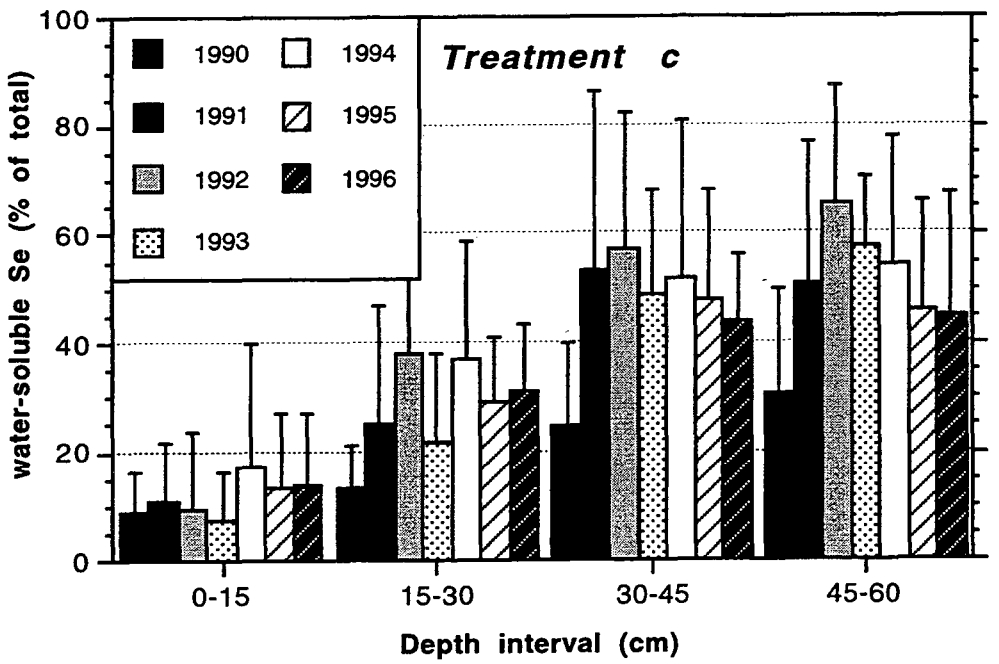

Figure 4.16. Mean water-soluble Se, as percentage of total, in 15-cm intervals of the top 60 cm of the soil profile along the N-S transect of treatment C. Error bars represent one standard deviation from the arithmetic mean.

4.2.3 Depth-Distribution of Salinity

Electrical conductivity (EC) was measured in the 1:5 soil:water extracts as an estimate of salinity. Salinity can be used to monitor the movement of solutes in the soil profile. Although EC is affected by all dissolved solids, it is considered an indicator for the more soluble species, primarily Na, Cl, and SO_4. Mean EC data for all four treatments is shown in Fig. 4.17-4.20.

The trends in EC are similar to total Se trends (cf. Fig. 4.9-4.12) and are indicative of the displacement of solutes out of the 0-15 cm interval and deeper into the profile during the period of 1990-1993, followed by an upward flux of solutes into the 0-15 cm interval through 1996. There are differences between the vegetated treatments (I and C) and the non-vegetated treatments (ID and D). In I and C there was a net increase in salinity in the 15-60 cm interval, caused by plant-root extraction of soil water. This effect is not observed in ID or D, where the net salinity did not change significantly over the course of the experiment.

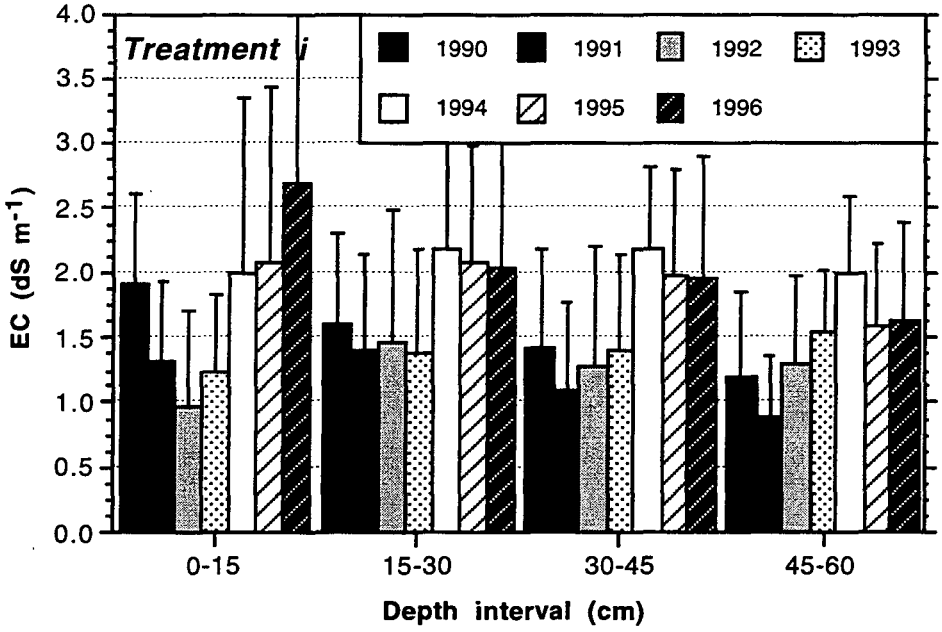

Figure 4.17. Mean electrical conductivity, as measured in a 1:5 soil:water extract, in 15-cm intervals of the top 60 cm of the soil profile along the N-S transect of treatment I. Error bars represent one standard deviation from the arithmetic mean.

There is little correlation between EC changes and trends in soluble Se (cf. Fig. 4.13-4.16). This may be indicative of soluble Se concentrations being driven by annual re-oxidation rates. Although both salts and Se will be displaced with infiltrating rainwater, at some point in the profile Se will become chemically reduced and immobilized under saturated conditions, while salts will remain soluble. Therefore, soluble Se concentrations will at first increase at depth due

to physical transport, then over the course of the wet season will decline due to chemical reduction, and over the summer increase due to re-oxidation.

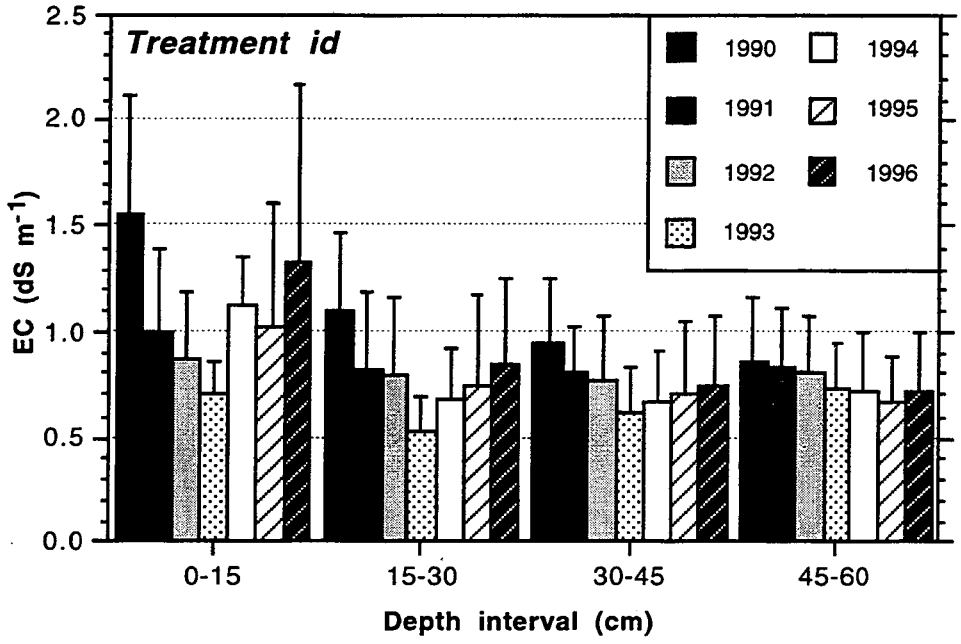

Figure 4.18. Mean electrical conductivity, as measured in a 1:5 soil:water extract, in 15-cm intervals of the top 60 cm of the soil profile along the N-S transect of treatment ID. Error bars represent one standard deviation from the arithmetic mean.

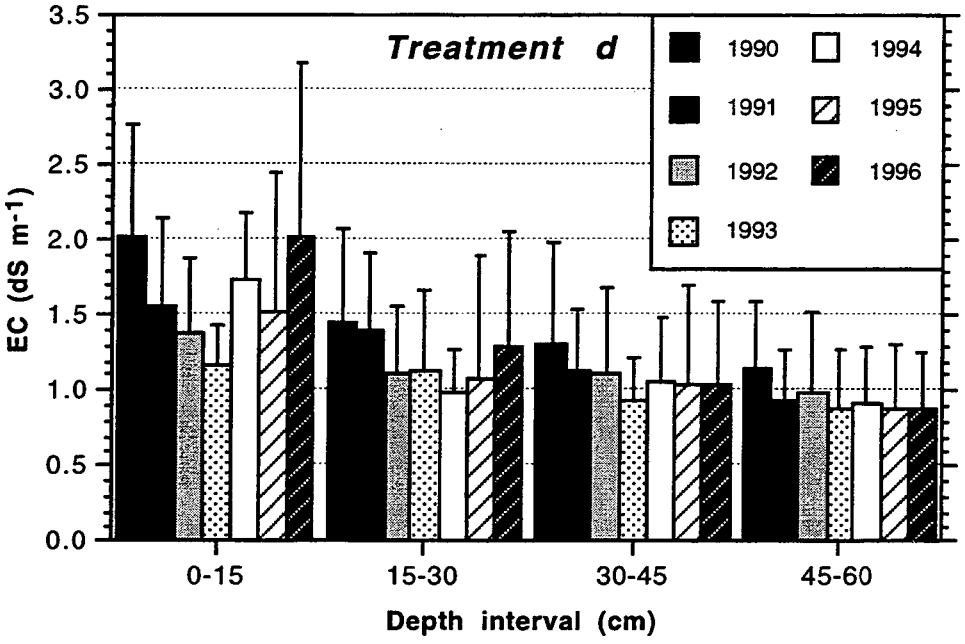

Figure 4.19. Mean electrical conductivity, as measured in a 1:5 soil:water extract, in 15-cm intervals of the top 60 cm of the soil profile along the N-S transect of treatment D. Error bars represent one standard deviation from the arithmetic mean.

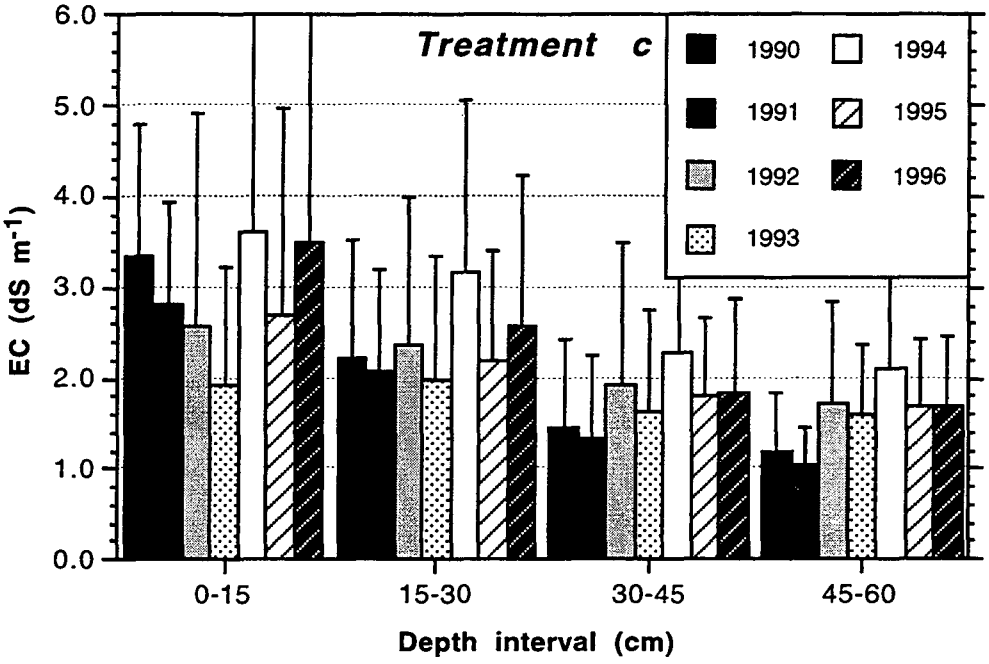

Figure 4.20. Mean electrical conductivity, as measured in a 1:5 soil:water extract, in 15-cm intervals of the top 60 cm of the soil profile along the N-S transect of treatment C. Error bars represent one standard deviation from the arithmetic mean.

4.2.3 Depth-Integrated Se Inventory

All total Se data from transect soils was integrated over the sampled depth of 0.0 to 0.60 m (Fig. 4.21 through 4.24). This representation accounts for Se which may have been flushed out of the top 0.15 m but was not displaced below 0.60 m. Any Se displaced below the depth of 60 cm would not be accounted for. The Se inventory is presented as mass per area (g m^{-2}). Analysis of Variance (ANOVA) was performed to determine if there were significant differences in soil selenium concentrations between years. The Fisher's protected least significant difference (PLSD) method was used to determine significant differences in concentrations (95% confidence interval; $P<.05$) (Mead, 1988). Those sample sets which were significantly different from each other are shown in white lettering within each column.

The most prominent trend observed in all treatments is the decline in Se from 1990 to 1993, followed by an increase from 1993 to 1996. Only within treatment I was there a significant net difference (decrease) in Se between 1990 and 1996. In treatments D and C, 1996 Se levels were actually higher than in 1990, but not at the tested level of significance. The inter-treatment

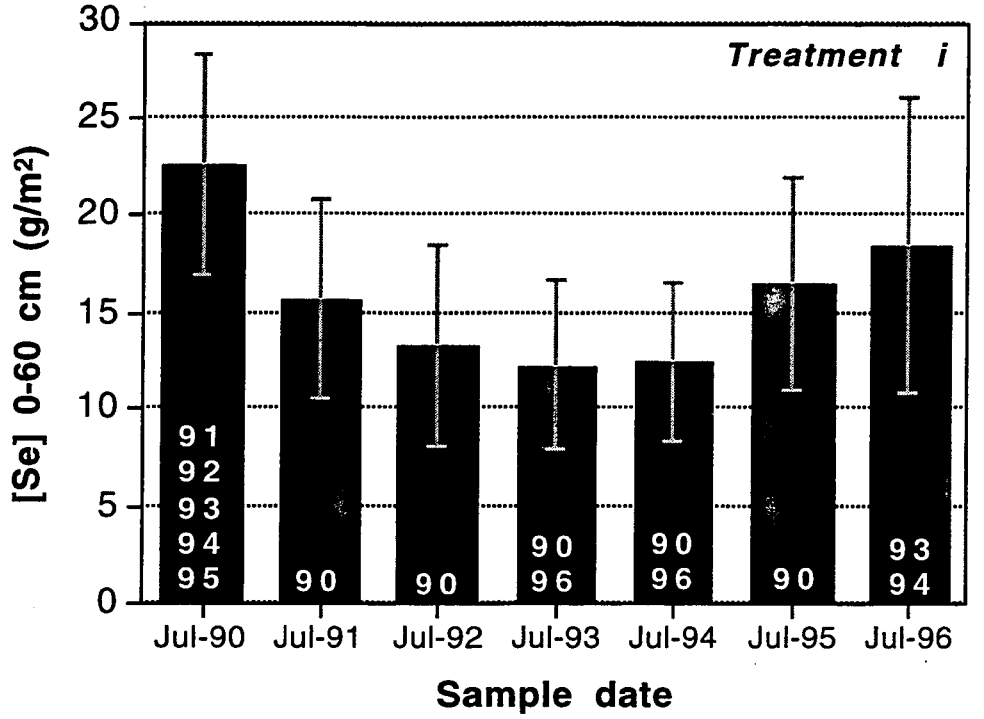

Figure 4.21. Cumulative total Se in treatment I, over the interval of 0 to 60 cm. Sample sets which are significantly different from each other within the 95% confidence interval are denoted in white lettering.

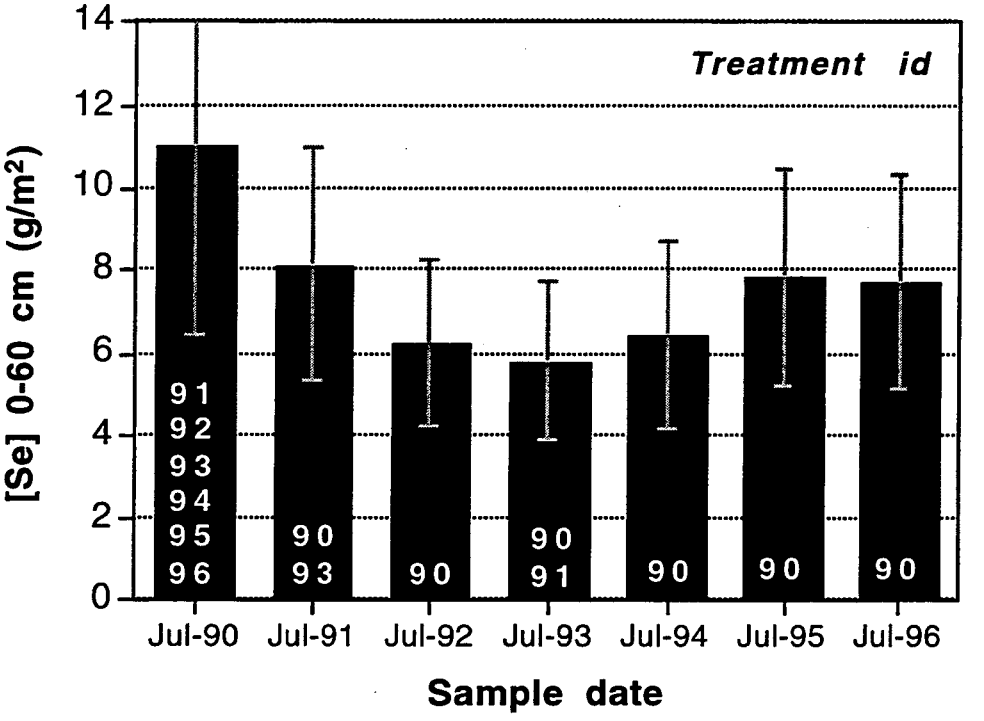

Figure 4.22. Cumulative total Se in treatment ID, over the interval of 0 to 60 cm. Sample sets which are significantly different from each other within the 95% confidence interval are denoted in white lettering.

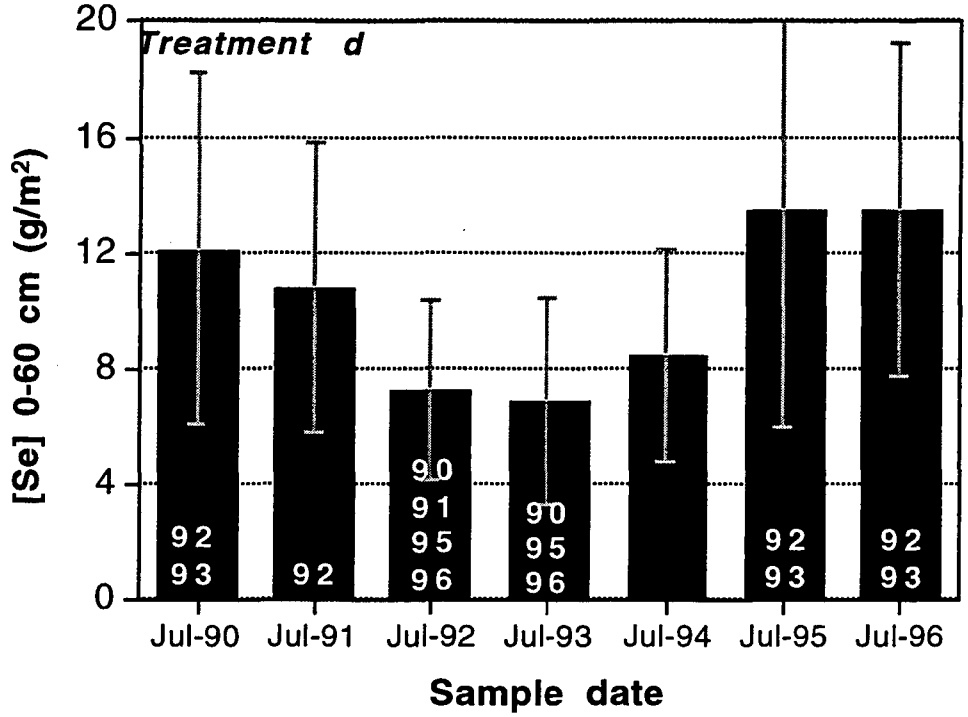

Figure 4.23. Cumulative total Se in treatment D, over the interval of 0 to 60 cm. Sample sets which are significantly different from each other within the 95% confidence interval are denoted in white lettering.

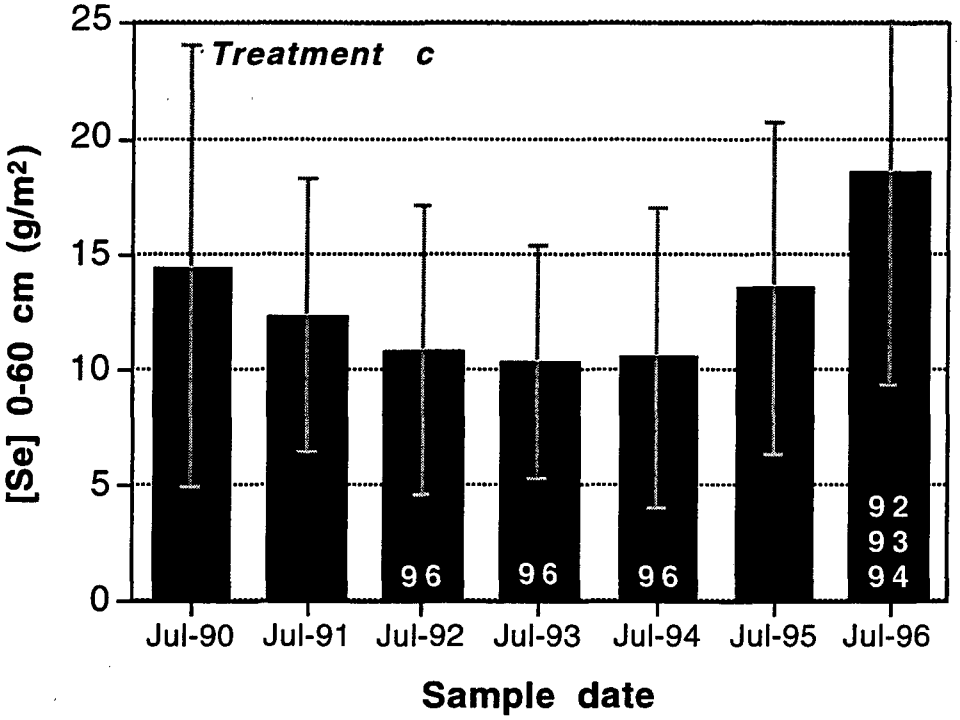

Figure 4.24. Cumulative total Se in treatment C, over the interval of 0 to 60 cm. Sample sets which are significantly different from each other within the 95% confidence interval are denoted in white lettering.

commonality of the observed pattern, as discussed in Section 4.2.1, suggests that Se movement is being controlled by common external factors. Increases observed after several years of decreases in Se concentrations, show that volatilization is a minor flux compared to the fluxes which physically redistribute Se within the soil profile.

4.3 Conclusions

Trends in Se and salinity observed over the course of this experiment are a testament to the need for long-term monitoring in order to resolve the influence of various fluxes on Se levels in soil. Future monitoring of this site may be useful in that it will show the bio-availability of Se based on the concentrations of soluble Se. It is not likely that continued soil monitoring of the kind performed to date will shed any further light on rates of and variables affecting microbial volatilization of Se in the field setting. Given the results presented herein, the effect of microbial volatilization on the Se inventory in Pond 2 is minor.

5 Analytical Quality Control

H. Scott Mountford
Earth Sciences Division
Lawrence Berkeley Laboratory

The Geochemistry Group has had a quality assurance program in operation for ten years, covering chemical analysis for selenium in samples collected from the Kesterson Reservoir. The performance of the analytical program as monitored via quality assurance is presented herein.

5.1 Measurement Statistics

Analytical chemistry has a number of means to judge the quality of the measurements made. Here we are considering the entire measurement process which includes the performance of the analyst and preparation of samples prior to measurement. This means that blind quality control samples must be placed in the sample preparation process. We use standard solutions to gauge accuracy and precision, duplicates to gauge precision with the natural matrix, blanks to gauge contamination and spiked samples or known addition to gauge interference.

5.2 Analytic Technique

Se analyses are performed on a Perkin-Elmer 3030 Atomic Absorption Spectrophotometer with a Varian Hydride Generator (HG-AAS). Selenite is analyzed by introducing the sample directly into the hydride generator. Total selenium is prepared for analysis by mixing 5.0 mL of a sample with an equal volume of concentrated (~37%) hydrochloric acid and between 0.2 and 0.5 mL of a 2% ammonium persulfate solution to oxidize any organic selenium compounds and other potentially interfering organic compounds. The mixture is heated at 98°C for 10 minutes to reduce all selenate to selenite, then allowed to cool and is introduced into the hydride generator for reading. The values reported to investigators are selenite and total selenium concentrations. Selenate concentration may be calculated from these values but is itself not directly subject to quality control because it is a derived quantity.

5.3 The Quality Control Process

Sample sets are assigned set numbers and tend to have 20 - 80 samples per set. Every seventh sample is a quality control, QC, sample. The QC coordinator will prepare the QC samples. The QC samples are used to track different aspects of the analysis. Once the sample set has been

considered in control the results are sent to the analyst and requester. After this the sample sheets are stored in a binder for reference at a later date.

The different types of QC samples are a Blank, Matrix Spike, Standard and Duplicate. The blank represents any type of contamination that may occur during analysis. These can include: carry over on the instrument, contaminated reagents, contaminated glassware or pipettors, or improper hydride generation. The QC limit for blanks is the value must be less than the practical quantitation limit, PQL. Therefore if the samples are analyzed for selenite the blank must be less than 0.32 $\mu g\ L^{-1}$ if the samples were total acid digests (TAD), which are diluted 10.2 times, the blank must be less than 3.2 $\mu g\ L^{-1}$. Blanks are prepared by adding Nanopure water to an empty QC bottle.

Matrix spikes are used to determine if there is something in the sample suppressing or enhancing the results for the selenium analysis. The quality control limits for acceptance for matrix spikes is ± 25% or 75 to 125% recovery of the matrix spike. A matrix spike may be considered, "not statistically meaningful", NSM, if the sample is greater than three times the spike of selenium. The spiking solution contains both selenite and selenate. Since the main objective is to speciate the selenate and selenite the recovery of both of these compounds is tracked. There are two different spiking solutions. One is a high level solution, primarily meant for TADs. The second is for all other extraction methods and is at a much lower concentration. The high level spike contains 3030 $\mu g\ L^{-1}$ total selenium, presently, with 46% being selenite. The low-level spike contains 710 $\mu g\ L^{-1}$ total selenium, presently, with 29% being selenite. Matrix spikes are prepared by adding a known amount of the research sample to an empty QC bottle and spiking the solution with a know amount of selenium standard.

Standards are meant to serve as a secondary check to verify the calibration curve, conversion of selenate to selenite, and technique of the analyst. A standard has a much tighter control limit of ± 15% or 85 - 115% recovery. The same spiking solution used for the matrix spike is used for the standard QC sample. Standards are prepared by adding Nanopure water and spiking the water with a known amount of selenium standard.

Duplicates are used to verify sample homogeneity, analyst technique, and instrument stability. A duplicate is considered in control when the relative percent difference, RPD, between the two samples are within 20 %. Where RPD is defined as

$$\frac{200 * |C_1 - C_2|}{(C_1 + C_2)}$$

C_1 and C_2 are the sample values. If the samples are below the lowest point of the calibration curve then the samples are considered NSM. Duplicate samples are prepared by pouring from the research sample bottle into a provided empty QC sample bottle.

5.4 Measurements

A total of 886 research samples were analyzed for total selenium with a QC load of 15.0%. Therefore, 1042 samples were analyzed for total selenium. There were a total of 248 research samples submitted for selenite with a QC load of 14.8 %. Therefore a total of 291 samples were analyzed for selenite.

5.4.1 Blanks

The practical quantitation limit, PQL, is a control limit for blanks. For total selenium this is presently 1.02 µg/L and for selenite is 0.50 µg/L. Looking at the concentrations of total selenium plotted vs. number of analysis (Fig. 5.1) we can see that on two occasions the blank would appear out of control out of a total of 18 blank QC samples. In both cases, the sample sets were diluted by a factor of 10.2 because of high selenium levels. The dilution factor therefore took the blank above the typical PQL. When examining the selenite data, the blank ranged from -0.04 to 0.15 ppb Se for a total of five blank QC samples.

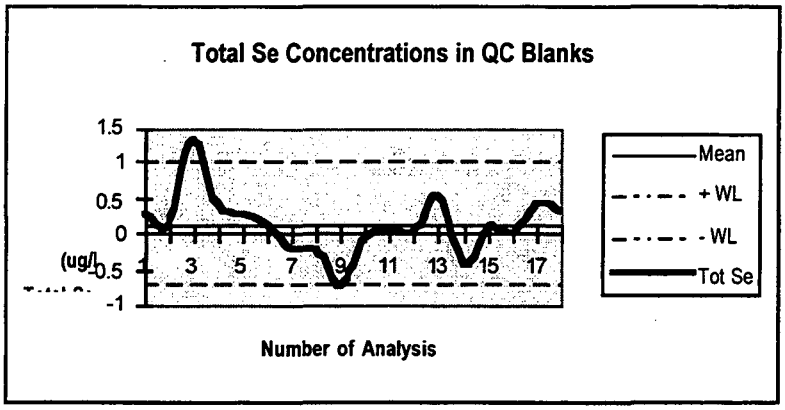

Figure 5.1. Total selenium concentrations for Blank QC samples.

5.4.2 Matrix Spikes

A warning limit, WL, is considered to be two standard deviations from the mean value. In this case the warning limit range is 71 - 115 % recovery, whereas the QC range is 75 - 125 % recovery. In Fig. 5.2, we can see that the data, with the exception of four points is within the

warning limits. In the case or the four outliers, the samples were reanalyzed and were in control after the second analysis. The selenite samples were within the range of 18 - 104 percent recovery. There were 3 outliers for a total of 15 samples. Selenite samples are not typically reanalyzed because the high level of organic matter in the sample is usually the cause of the suppressed selenium recovery. These outliers are noted for the researchers in the case narrative.

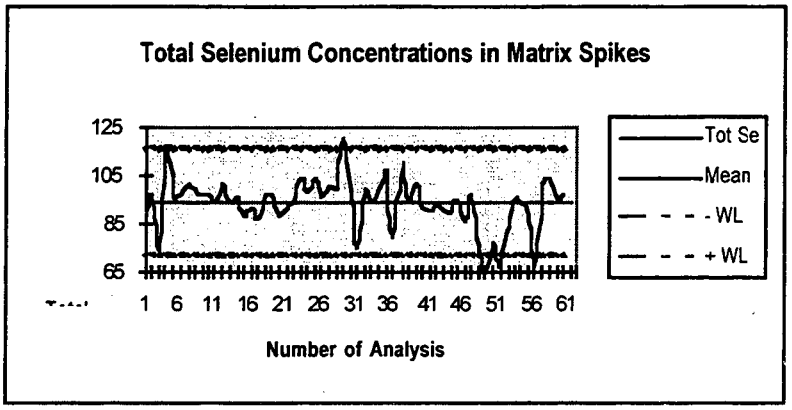

Figure 5.2. Total selenium concentrations for Matrix Spike QC samples.

5.4.3 Standards

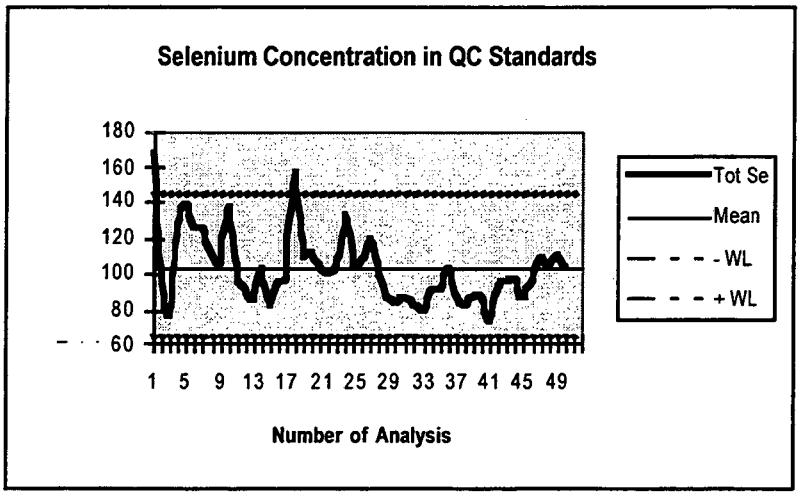

Figure 5.3 Total selenium concentration for Standard QC samples

Standards tend to have a much tighter QC limit than matrix spikes because of the lack of matrix interference. In Fig. 5.3, we can see that 50 standard QC samples were analyzed this year for total selenium. There were two samples outside of the warning limits. Both of these samples were at very low levels. Therefore, the recovery of these samples will fluctuate significantly

with small changes. Otherwise the data reflects that the standards behaved as expected to validate the data represented by the researchers in this report. There were 11 selenite standards analyzed with a recovery range of 96 -113%. None of the selenite standards were out of the warning or QC limits.

5.4.4 Duplicates

A total of 42 total selenium duplicate QC samples were analyzed. The range of RPD was from 0 to 27%, with two samples being reanalyzed because they were above 20%. There were a total of 12 selenite duplicate QC samples analyzed. The RPD range was 0 - 12%.

6 References

Benson, S.M., A.F. White, S. Halfman, S. Flexser, and M. Alavi. 1991. Groundwater contamination at Kesterson Reservoir, California 1. Hydrogeologic setting and conservative solute transport. Water Resour. Res. 27:1071-1084.

Benson, S.M., T. Tokunaga, P. Zawislanski, C. Wahl, P. Johannis, M. Zavarin, A. Yee, D. Phillips, and S. Ita. 1992. Hydrological and geochemical investigations of selenium behavior at Kesterson Reservoir. Lawrence Berkeley Laboratory report LBL-33532, Berkeley, CA.

Berner, R.A. 1980. Early Diagenesis, A Theoretical Approach. Princeton University Press, Princeton, NJ, 241 pp.

Besser, J.M., J.N. Huckins, E.E. Little, and T.W. La Point. 1989. Distribution and bioaccumulation of selenium in aquatic microcosms. Environ. Pollut. 62, 1-12.

Besser, J.M., T.J. Canfield, and T.W. LaPoint. 1993. Bioaccumulation of organic and inorganic selenium in a laboratory food chain. Environ. Toxicology Chem. 12, 57-72.

Bowie, G.L., J.G. Sanders, G.F. Reidel, C.C. Gilmour, D.L. Breitburg, G.A. Cutter, and D.B. Porcella. 1996. Assessing selenium cycling and accumulation in aquatic ecosystems, Water Air Soil Pollut. 90, 93-104.

Campbell, G.S. 1985. Soil Physics with Basic. Developments in Soil Sci. 14, Elsevier, Amsterdam.

CH2M Hill. 1991. Kesterson Reservoir Biological Report (Draft). U.S. Bureau of Reclamation Mid Pacific Region.

Cooke, T.D., and K.W. Bruland. 1987. Aquatic chemistry of selenium: Evidence of biomethylation. Environ. Sci. Technol. 21, 1214-1219.

Eghbal, M.K., R.J. Southard, and L.D. Whittig. 1989. Dynamics of evaporite distributions in soils on a fan-playa transect in the Carrizo Plain, California. Soil Sci. Soc. Am. J. 53, 898-903.

Flaschka, H.A., Barnard, A.J., and P.E. Storrock. 1969. Quantitative Analytical Chemistry Vol. 1, Barnes and Noble. New York.

Gao, S., and K.K. Tanji. 1995. Model for biomethylation and volatilization of selenium from agricultural evaporation ponds. J. Environ. Qual. 24, 191-197.

Giauque, R.D., R.B. Garrett, and L.Y. Goda. 1977. Determination of forty elements in geochemical samples and coal fly ash by x-ray fluorescence spectrometry. Anal. Chem. 49:1012-1017.

Griffin, R.A., and J.J. Jurinak. 1973. Estimation of activity coefficients from the electrical conductivity of natural aquatic systems and soil extracts. Soil Sci. 116, 26-30.

Hardie, L.A., and H.P. Eugster. 1970. The evolution of closed-basin brines. Mineral. Soc. Am. Spec. Paper 3, 273-290.

Hillel, D. 1980. Fundamentals of Soil Physics. Academic Press, New York.

Iversen, N., and B.B. Jorgensen. 1993. Diffusion coefficients of sulfate and methane in marine sediments: Influence of porosity. Geochim. Cosmochim. Acta 57:571-578.

Jackson, J. L. 1967. Kesterson Reservoir Site Summary of Geologic Data, U. S. Dept. Interior, Bureau of Reclamation, San Luis Unit, Central Valley Project, California, Sacramento, CA, Aug. 1, 1967.

Jorgensen, B.B., and N.P. Revsbech. 1985. Diffusion boundary layers and the oxygen uptake of sediments and detritus. Limnol. Oceanogr. 30, 111-122.

Lakin, H.W. 1961. In Selenium in Agriculture. Agricultural Handbook No. 200. Anderson, M.S., H.W. Lakin, K.C. Beeson, F.F. Smith, and E. Thacker. U.S. Dept. Agric., U.S. Government Printing Office.

Lawrence Berkeley Laboratory. 1987. Hydrological, geochemical, and ecological characterization of Kesterson Reservoir. 5th progress report, January 1987 through March 1987. LBID 1291. Berkeley, CA.

Lawrence Berkeley Laboratory. 1987. Kesterson Reservoir Annual Report. LBL-24250. Berkeley, CA.

Lawrence Berkeley Laboratory. 1988. Hydrological, Geochemical, and Ecological Characterization of Kesterson Reservoir. Annual Report. LBL-26438. Berkeley, CA.

Lawrence Berkeley Laboratory. 1990a. Hydrological, Geochemical, and Ecological Characterization of Kesterson Reservoir. Annual Report. October 1, 1988-September 30th, 1989. LBL-27993. Berkeley, CA.

Lawrence Berkeley Laboratory. 1990b. Hydrological and Geochemical Investigations of Selenium Behavior at Kesterson Reservoir. Annual Report. October 1, 1989-September 30th, 1990. LBL-29689. Berkeley, CA.

Lawrence Berkeley Laboratory. 1992. Hydrological and Geochemical Investigations of Selenium Behavior at Kesterson Reservoir. Annual Report. October 1, 1990-September 30th, 1992. LBL-33532. Berkeley, CA.

Long, R.H.B., S.M. Benson, T.K. Tokunaga, and A. Yee. 1990. Selenium immobilization in a pond sediment at Kesterson Reservoir. J. Environ. Qual. 19:302-311.
Luthin, J. N. 1966. Final Report on Seepage from Reservoir Sites in the Dos Palos and Kesterson Areas, Western Merced County. California Dept. Water Resour. June 8, 1966.
Marion, G.M., and K.L. Babcock. 1976. Predicting specific conductance and salt concentration in dilute aqueous solutions. Soil Sci. 122, 181-187.
Mead, R. 1988. The Design of Experiments: Statistical Principles for Practical Applications. Cambridge University Press. New York.
Nazar, P.G. 1990. Soil Survey of Merced County, California, Western Part. U.S. Dept. Agriculture, Soil Conservation Service. U.S. Government Printing Office.
Pickering, I.J., G.E. Brown, Jr., and T.K. Tokunaga. 1995. Quantitative speciation of selenium in soils using x-ray absorption spectroscopy. Environ. Sci. Technol., 29:2456-2459.
Poister, D., and T.K. Tokunaga. 1992. Selenium in Kesterson Reservoir ephemeral pools formed by groundwater rise: II. Laboratory experiments. J. Environ. Qual. 21:252-258.
Reynolds, W. D., D. E. Elrick, and G. C. Topp. 1983. A reexamination of the constant head well permeameter method for measuring saturated hydraulic conductivity above the water table. Soil Sci. 136:250-268.
Runnells, D.D., and R.G. Lindberg. 1990. Selenium in aqueous solutions: The impossibility of obtaining meaningful Eh using a platinum electrode, with implications for modeling natural waters. Geology 18, 212-215.
Saiki, M.K., M.R. Jennings, and W.G. Brumbaugh. 1993. Boron, molybdenum, and selenium in aquatic food chains from the lower San Joaquin River and its tributaries, California. Arch. Environ. Contam. Toxicol. 24, 307-319.
Santschi, P., P. Hohener, G. Benoit, and M. Buchholtz-ten Brink. 1990. Chemical processes at the sediment-water interface. Marine Chem. 30, 269-315.
Snyder, R.L., and W.O. Pruitt. 1992. Evapotranspiration management in California. Proc. Am. Soc. Civil Eng., Water Forum. Baltimore, MD, Aug. 2-6, 1992.
Snyder, R.L., B.J. Lanini, D.A. Shaw, and W.O. Pruitt. 1994. Using reference evapotranspiration (ETo) and crop coefficients to estimate crop evapotranspiration (ETc) for agronomic crops, grasses, and vegetable crops, Cooperative Extension, Leaflet 21427, University of California, Division of Agriculture and Natural Resources, Oakland, CA.
Thompson-Eagle, E.T., and W.T. Frankenberger. 1990. Volatilization of selenium from agricultural pond water. J. Environ. Qual. 19:125-131.
Tokunaga, T.K. 1992. The pressure response of the soil water sampler and possibilities for simultaneous soil solution sampling and tensiometry. Soil Sci. 154:171-183.
Tokunaga, T.K., and S.M. Benson. 1992. Selenium in Kesterson Reservoir ephemeral pools formed by groundwater rise: 1. Field studies. J. Environ. Qual. 21:246-251.
Tokunaga, T. 1995. Ephemeral pools: Summary of 1992 to 1994 water quality. In P. T. Zawislanski, T. K. Tokunaga, S. M. Benson, P. W. Johannis, M. Zavarin, C. Wahl, T. Sears, J. Kengsoontra, L. Tsao, J. Oldfather, A. W. Yee, Hydrological and Geochemical Investigations of Selenium Behavior at Kesterson Reservoir. LBNL-39518, UC-000. Lawrence Berkeley National Laboratory, Berkeley, CA.
Tokunaga, T.K., I.J. Pickering, and G.E. Brown, Jr. 1996. Selenium transformations in ponded sediments. Soil Sci. Soc. Am. J. 60, 781-790.
Tokunaga, T.K., G.E. Brown, Jr., I.J. Pickering, S.R. Sutton, and S. Bajt. 1997. Selenium redox reactions and transport between ponded waters and sediments. Environ. Sci. Technol., in press.
Tu, Q., X.-Q. Shan, and Z.-M. Ni. 1994. Evaluation of a sequential extraction procedure for the fractionation of amorphous iron and manganese oxides and organic matter in soils. Sci. Total Environ. 151:159-165.
USBR (United States Bureau of Reclamation) 1986. Final Environmental Impact Statement. Volume 2. Kesterson Program, Sacramento, Ca.
USBR. 1996. Revised monitoring and reporting program number 87-149 for the US Dept. of Interior, Bureau of Reclamation, Kesterson Reservoir, Merced County. USBR. Sacramento, CA.
Warrick, A.W and D.R. Nielsen. 1980. Application of Soil Physics. Academic Press. NY.
Weres, O., A.-R. Jaouni, and L. Tsao. 1989a. The distribution, speciation and geochemical cycling of selenium in a sedimentary environment, Kesterson Reservoir, California, U.S.A. Applied Geochemistry 4:543-563.
Weres, O., G.A. Cutter, A. Yee, R. Neal, H. Moehser, and L. Tsao. 1989b. Section 3500-Se. pp. 3-128 to 3-141. In L.S. Clesceri et al. (ed.0 Standard Methods for the Examination of Water and Wastewater. 17th ed. Am. Public Health Assoc., Washington, D.C.
Weres, O., H.R. Bowman, A. Goldstein, E.C. Taylor, and L. Tsao. 1990. The effect of nitrate and organic matter upon mobility of selenium in groundwater and in a water treatment process. Water Air Soil Pollut. 49, 251-272.

White, A.F., S.M. Benson, A.W. Yee, H.A. Wollenberg, and S. Flexser. 1991. Groundwater contamination at Kesterson Reservoir, California, Part 2. Geochemical parameters influencing selenium mobility. Water Resour. Res. 27:1085-1098.

Ylaranta, T. 1983. Sorption of selenite and selenate in the soil. Annales Agric. Fenniae 22, 29-39.

Zawislanski, P.T. 1989. Bare Soil Evaporation at Kesterson Reservoir, Merced County, California: Estimation by Physical and Chemical Methods. Thesis, University of California, Berkeley, CA.

Zawislanski, P.T., T.K. Tokunaga, S.M. Benson, J.M. Oldfather, and T.N. Narasimhan. 1992. Bare soil evaporation and solute movement of selenium in contaminated soils at Kesterson Reservoir. J. Environ. Qual. 21:447-457.

Zawislanski, P.T., T.K. Tokunaga, S.M. Benson, P.W. Johannis, M. Zavarin, C. Wahl, T. Sears, J. Kengsoontra, L. Tsao, J. Oldfather, and A.W. Yee. 1995. Hydrological and Geochemical Investigations of Selenium Behavior at Kesterson Reservoir. E.O. Lawrence Berkeley National Laboratory report LBNL-39518. Berkeley, CA.

Zhang, Y., and J.N. Moore. 1997. Environmental conditions controlling selenium volatilization from a wetland system. Environ. Sci. Technol. 31, 511-517.

Ernest Orlando Lawrence Berkeley National Laboratory
One Cyclotron Road | Berkeley, California 94720

Prepared for the U.S. Department of Energy under Contract No. DE-AC03-76SF00098